CLINICAL ANATOMY OF THE EUROPEAN HAMSTER

CRICETUS CRICETUS, L.

CLINICAL ANATOMY OF THE EUROPEAN HAMSTER

CRICETUS CRICETUS, L.

LIBRARY
JUN 1 6 1993
National Institutes of Health

For sale by the Superintendent of Documents, U.S. Government Printing Office
Washington, D.C. 20402
Stock Number 017-042-00122-6

CLINICAL ANATOMY OF THE EUROPEAN HAMSTER

Cricetus cricetus, L.

By

Gerd Reznik, D.V.M.
Hildegard Reznik-Schüller, D.V.M.
Ulrich Mohr, M.D.

Abteilung für Experimentelle Pathologie
Medizinische Hochschule Hannover
Hannover, West Germany

Prepared For The
Carcinogenesis Program
Division Of Cancer Cause And Prevention
National Cancer Institute
Under Contract No. N01-CP-55687

Edited by

Peter Dodson, Ph.D.

School of Veterinary Medicine
University of Pennsylvania
Philadelphia, Penna. 19174

With Editorial Assistance From

Paul C. Walter, M.D.
Ronald B. Levine

Science Information Services Department
The Franklin Institute
Philadelphia, Penna. 19103

1979

FOREWORD

The European hamster has proved to be a very useful animal for research in pulmonary carcinogenesis. However, prior to the publication of this handbook there has been little useful anatomical information on the animal. In 1974, Drs. Mohr, Reznik and Reznik-Schüller of the Medizinische Hochschule Anatomical of Hannover produced an illustrated manuscript entitled "The European Hamster, An Anatomical Atlas." The manuscript was reviewed by Drs. Robert E. Habel and Howard E. Evans of the Cornell University Veterinary School, and in 1975 a contract was awarded by the National Cancer Institute to the Franklin Institute Research Laboratories (FIRL) for publication of the manuscript. Dr. Stephen Tauber of FIRL directed this project, with Dr. Paul Walter of FIRL editing the publication and Dr. Peter Dodson of the University of Pennsylvania School of Veterinary Medicine acting as anatomical consultant.

This volume is not an all-inclusive atlas. Clinically relevant systems such as the respiratory system are emphasized and the anatomical orientation is focused on regions rather than systems. Details of the anatomy of the appendages or of other regions not covered in this volume may be obtained by writing to the authors.

Likewise, emphasis is not given to microanatomy; however, when the histology of structures is described, it is noted in smaller typeface to alert the reader.

Nomenclature was standardized by using the *Nomina Anatomica Veterinaria* (N.A.V. 1968, 1973) as an authority, except insofar as it failed to denote structures unique either to rodents or hamsters (i.e., *bursa buccalis*). Each anatomical structure is introduced with its Latin (N.A.V.) term but the English term is used subsequently throughout the text.

The German manuscript was translated in the authors' laboratory and edited by Dr. Walter and Dr. Dodson and Mr. Ronald Levine of FIRL. Dr. Walter also contributed significant segments of original text, especially with regard to limits and landmarks of thoracic and abdominal cavities, peritoneal relationships, and clinical considerations. Any editorial addition was read and approved by the authors who accept full responsibility for the text.

The typing help of Francine Davis, Barbara Knox, Brenda Allen, and Clare M. Byrnes is most gratefully acknowledged.

This monograph is part of Contract No. N01-CP-55687 awarded by the National Cancer Institute, Division of Cancer Cause and Prevention, Dr. Thomas P. Cameron, Project Officer.

ERRATA

P 38	Figure 2-33 Figure 2-34	Upside down
P 41	Figure 2-40	Upside down
P 42	Figure 2-42	Upside down
P 147	Figure 5-11	Upside down
P 159	Figure 5-32	Upside down

PREFACE

Since our research has been oriented for many years towards lung cancer, especially studies in etiology, we have been consistently seeking sensitive experimental animals. Such models should fulfill the following stipulations: 1. that lesions be induced within a surveyable time period after administration of known carcinogens; 2. that well-differentiated tumor types (adeno- and squamous cell carcinomata) should originate in the respiratory tract; and 3. that no infectious diseases of the respiratory tract should interfere with the experimental results.

About 10 years ago, our work was confined to the use of the Syrian golden hamster (*Mesocricetus auratus*) which had been recognized as the model for respiratory tract carcinogenesis (Saffiotti 1969, 1974; Saffiotti, *et al.,* 1968; Althoff, *et al.,* 1971a, b; Nettesheim, 1972; Laskin and Sellakumar, 1975; Wynder and Hoffman, 1964, 1967; Della Porta, *et al.,* 1958; Dontenwill and Mohr, 1961; Montesano and Saffiotti, 1968, 1970). This animal, however, frequently presented with early tracheal papillomata, resulting in premature death by asphyxiation; consequently, the time required for induction of lung carcinomata, whose histopathology would be significantly differential (adenocarcinoma, squamous cell carcinoma) could not be realized (Feron, *et al.,* 1972; Montesano, 1970; Lijinsky, *et al.,* 1970; Haas, *et al.,* 1973; Herrold and Dunham, 1963). Moreover, the pulmonary tumors in this experimental animal have been suspected as originating from parts of tracheal papillomata "transplanted" to the lungs (Spit and Feron, 1975; Stenbäck, *et al.,* 1973; Creasia and Nettesheim, 1974). Studies on respiratory tract sensitivity to known carcinogens in Chinese hamsters led to mainly negative results, so that this animal species had to be rejected (Mohr, *et al.,* 1966, 1967, 1970; Althoff, *et al.,* 1971b; Reznik, *et al.,* 1976a, b, c).

We have finally verified that the European hamster, which lives wild in West Germany, fulfills the set stipulations for an animal model and that, in comparison to the Syrian golden hamster (Fig. 0–1), offers additional advantages. With known nitroso- compounds, respiratory tract tumors have developed within a relatively short time of 13 weeks (Mohr, *et al.,* 1972); moreover, these tumors are for the most part well-differentiated. With corresponding doses of carcinogens, tumors are produced in all animals (100%) (Mohr, *et al.,* 1972, 1973, 1974a, b; Reznik-Schüller and Mohr, 1975; Reznik, *et al.,* 1977).

The European hamster is comparable in size to the guinea pig and therefore offers sufficiently large anatomical dimensions for the execution of clinical test procedures (radiology, bronchography, cytology) throughout the period of tumor development (Freyschmidt, *et al.,* 1975; Reznik, *et al.,* 1975a; Eckel, *et al.,* 1973, 1974a, b, 1975). The value of such studies in determining early tumor recognition cannot be under-estimated. Moreover, *Cricetus cricetus* is quite appropriate for special treatment techniques such as intratracheal and intrabronchial instillation of a carcinogen; this procedure can be performed without difficulty and much more easily than in other rodents. It also appears that the European hamster will prove to be better for studies on inhalation because its tidal volume is larger than that of the Syrian golden hamster (Kmoch, *et al.,* 1975; Reznik, *et al.,* 1975b, c; Kmoch, *et al.,* 1976). Moreover, it has been demonstrated in inhalation experiments with labelled cigarette smoke that about 30% more particulate matter is deposited in the lungs of the European hamster than in the Syrian golden hamster

(Kmoch, *et al.,* 1975; Reznik, *et al.,* 1975b; Kmoch, *et al.,* 1976). Its size also means that biochemical studies to establish metabolites of carcinogens in the larynx, trachea and lungs are likely to be more successful than similar studies in the Syrian golden hamster, since the experimenter has significantly more tissue at his disposal.

As is well known, *C. cricetus* is a hibernator (Fig. 0–2) (Kayser, 1961; Precht, *et al.,* 1973) and, according to the reports of zoologists, should live up to 8 years of age (Gaffrey, 1961; Zimmermann, 1965). Accordingly, we attempted to establish a breeding colony under laboratory conditions (Mohr, *et al.,* 1973; Reznik-Schüller, *et al.,* 1974a). The problem of breeding has now been solved and we presently have a well established colony of seven generations with sufficient numbers of animals for experimental use. From all observations, the European hamster has adapted quite well to laboratory life and, under standard conditions, the animals demonstrate no inclination toward hibernation. However, in the absence of hibernation, the lifespan of the hamsters may be shortened from the reported 8 years to 5 years. Nevertheless, this survival time still doubles the average span of the Syrian golden hamster. Of course, a longer survival time is a definite advantage for inhalation studies in carcinogenesis of the nasal and paranasal spaces, larynx, trachea and lungs.

Thus, our experimental animal has higher sensitivity to already known carcinogens and lives substantially longer than conventional laboratory rodents such as the mouse, rat and Syrian golden hamster. In addition, the European hamster, similar to the Syrian golden hamster, is free of infectious diseases of the respiratory tract. It is clear, then, that the European hamster is the animal of choice for studies in chemical carcinogenesis. Accordingly, we are engaged in enlarging our breeding colony and maintain the hope that other scientists will also use this species in their investigations. We are making every effort to place enough breeding pairs at the disposal of others.

For studies in experimental carcinogenesis, it became apparent that a knowledge of the anatomy of *C. cricetus* would be especially useful. It must be possible to detail exactly the location of lesions to establish higher confirmation of species sensitivity to carcinogenic challenge. For this reason the present work on the anatomy of the European hamster has been compiled. The reader should bear in mind that we have placed special importance upon the respiratory tract. Moreover, the conventional systemic treatment of anatomical structure has been replaced in favor of topical regionalization, compatible with the purpose of a work designed especially for the non-anatomist in experimental pathology. Accordingly, attention is given to traditional mammalian body regions, including sections of all relevant organ systems and their relations, rather than exhaustive and exclusive treatment of single systems independent of region.

[Figures 0–1 and 0–2 are located on pp. 4 and 5, respectively.]

ACKNOWLEDGMENTS

Finally, it is appropriate to extend our deep appreciation to Mr. E. Theel and Mr. K. Fischer for their meticulous draftsmanship and their ability to comprehend the scientific intent of projected illustrations in preparing the anatomical drawings. Also especially deserving of our indebtedness are Mr. W. Fischer and Mrs. A. Boysen for assistance in obtaining optimal macroscopic pictures and for making slides and prints. We are also grateful to Naoma Crisp-Lindgren who has translated the text. To our many colleagues of the Abteilung für Experimentelle Pathologie who critically advised and supported the production of this work, as well as having helped sustain our enthusiasm, we remain profoundly grateful.

Gerd Reznik, D.V.M.
Hildegard Reznik-Schüller, D.V.M.
Ulrich Mohr, M.D.

Hannover
May 1, 1976

TABLE OF CONTENTS

		Page
	Foreword	iii
	Preface	v
	Chapter 1: External Anatomy, Reproduction and Distribution	
1.1	External Features	1
1.2	Physiology of Reproduction	2
1.3	Present Distribution of European Hamsters in Europe	2
	Chapter 2: Anatomy of the Head	
2.1	Bones of the Skull	17
2.2	Facial Skeleton	17
2.3	Nasal Cavity	17
2.4	Nasopharynx	18
2.5	Vomeronasal Organs	18
2.6	Paranasal Cavity	19
2.7	Oral Cavity	19
2.8	Lips	19
2.9	Cheeks	20
2.10	Palate	20
2.11	Gums and Tongue	20
2.12	Teeth	21
2.13	Salivary Glands	21
2.14	Mandibular Gland	22
2.15	Sublingual Gland	22
2.16	Parotid Gland	22
2.17	Zygomatic Gland	23
2.18	Neurocranium and Brain	23
2.19	Hypophysis	23
2.20	Orbital Adipose Tissue	24
2.21	Lacrimal Apparatus	24
2.22	Lacrimal Gland	24
2.23	Accessory Lacrimal Gland	24
2.24	Nasolacrimal Duct	25
2.25	Cranial and Facial Vascularization	25
2.25.1	Arteries	25
2.25.2	Venous Drainage of the Skull and the Ophthalmic Plexus	25
	Chapter 3: Cervical Region	
3.1	Cervical Skeleton	65
3.2	Topography of the Ventral Cervical Region	65
3.3	Pharynx	66

		Page
3.4	Lymphatic System of Neck and Adjacent Thoracic Region	66
3.5	Larynx	67
3.5.1	Ligaments of the Larynx	68
3.5.2	Muscles of the Larynx	68
3.6	Trachea	68
3.7	Thyroid and Parathyroid Gland	69
	Chapter 4: Thorax	
4.1	Bony Thorax	85
4.2	Thoracic Musculature	86
4.3	The Diaphragm	86
4.4	Thoracic Cavity	87
4.4.1	Pleura and Pleural Sinuses	87
4.4.2	The Mediastinum	88
4.4.2.1	The Ventral Mediastinum	88
4.4.2.1.1	Heart	89
4.4.2.1.2	The Great Vessels	90
4.4.2.1.3	Thymus and Lymphatic Tissue	91
4.4.2.1.4	Nerves	92
4.4.2.2	The Dorsal Mediastinum	92
4.4.2.2.1	Lymphatic Tissue	92
4.4.2.2.2	The Esophagus	93
4.5	Respiratory System	93
4.5.1	Trachea and Extrapulmonary Bronchi	93
4.5.2	The Intrapulmonary System	94
4.5.3	Lungs and Pulmonary Topography	95
	Chapter 5: Abdomen and Pelvis	
5.1	Limits and Landmarks	121
5.2	Bony Skeleton of the Abdomen and Pelvis	121
5.3	Abdomen and Peritoneum	122
5.4	Segmental Topography of the Abdomen	122
5.5	Craniomesocolic Region	122
5.5.1	Craniomesocolic Peritoneum	122
5.5.2	Craniomesocolic Viscera and Relations	124
5.5.2.1	Esophagus	124
5.5.2.2	Stomach	124
5.5.2.3	Proximal Duodenum	125
5.5.2.4	Liver	125
5.5.2.5	Pancreas	127
5.5.2.6	Spleen	127
5.5.3	Craniomesocolic Vascularization and Innervation	127
5.5.4	Greater Nerves of the Abdominal Cavity	128
5.6	Caudomesocolic Region	128

		Page
5.6.1	Caudomesocolic Peritoneum	128
5.6.2	Caudomesocolic Viscera and Relations	129
5.6.2.1	Structure of the Small Intestine	129
5.6.2.2	Duodenum	129
5.6.2.3	Jejunum	129
5.6.2.4	Ileum	129
5.6.2.5	Structure of the Large Intestine	130
5.6.2.6	Caecum	130
5.6.2.7	Colon	130
5.6.3	Retroperitoneal Viscera and Relations	131
5.6.3.1	Rectum	131
5.6.3.2	Urinary Organs	131
5.6.3.2.1	Kidney	131
5.6.3.2.2	Ureter	132
5.6.3.2.3	Urinary Bladder	132
5.6.4	Adrenal Gland	132
5.6.5	Caudomesocolic and Retroperitoneal Vascularization	133
5.6.5.1	Arteries	133
5.6.5.2	Veins	133
5.6.5.3	Portal Circulation	134
5.7	Lymphatic System of the Abdomen and Pelvis	134
5.7.1	Lymph Nodes of the Gastrointestinal Tract	134
5.7.1.1	Coeliac Lymph Center	134
5.7.1.2	Cranial Mesenteric Lymph Center	134
5.7.2	Lumbar Lymph Center	135
5.7.3	Lymph Nodes of the Pelvis and Hind Limb	135
5.8	Male Genital Organs	135
5.8.1	Testis	136
5.8.2	Epididymis	136
5.8.3	Accessory Genital Glands	136
5.8.3.1	Vesicular Gland	136
5.8.3.2	Prostate Gland	137
5.8.3.3	Bulbourethral Gland	137
5.8.4	Penis	137
5.9	Female Genital Organs	138
5.9.1	Ovary	138
5.9.2	Oviduct	138
5.9.3	Uterus	138
5.9.4	Vagina	139

CHAPTER ONE
EXTERNAL ANATOMY, REPRODUCTION AND DISTRIBUTION

The European hamster, *Cricetus cricetus Lineé*, belongs to the family Cricetidae and the subfamily Cricetinae of the order Rodentia.

1.1 EXTERNAL FEATURES

When kept under laboratory conditions, adult male European hamsters have an average body weight of 451 ± 49 g in summer and 245 ± 92 g in winter; while the adult females weigh an average of 359 ± 63 g in summer and 174 ± 49 g in winter. Under cold laboratory conditions (4°C; 90% relative humidity) hibernating males and females have average body weights of 245 ± 92 g and 174 ± 49 g, respectively (Reznik, *et al.,* 1973); the weight loss during winter is dependent upon hibernation (Fig. 0–2). Adult males have a mean length of 241 ± 9 mm and adult females of 237 ± 12 mm (Figs. 1–1, 1–2; Table 1).

The full-grown body is stocky, has a short tail (⅙ of body length, or 3–6 cm) and the fur of the dorsal and lateral surfaces is yellow reddish-brown to grayish-brown in color (Figs. 1–1, 1–2). The tip of the snout, lips, throat and feet are white to yellowish-white, while the ventral surface is black (Fig. 1–1). Throughout summer, the dorsal surface is lighter in color than during winter (Kourist, 1957). The hairs (*pili*) of the tail and the scrotum are much shorter than those on the rest of the body (Figs. 1–1, 1–2). During late summer and autumn, the animals have large subcutaneous fat deposits in preparation for hibernation (Fig. 1–3).

On the head of the living European hamster, the black, round protruding eyes (*oculi*) are striking characteristics (Figs. 1–4, 1–5). Their deep black color is the result of very marked pigmentation, especially of the iris. A prominent *planum nasale* is formed by the epidermis. The nostrils (*nares*) are more broad than long and run obliquely caudally. A *philtrum,* which begins at the upper lip and extends dorsally, is located in the mid-line between the two nostrils (Fig. 1–4, 2–9). No hair follicles can be seen around the nares; this portion of the *planum nasale* has a whitish-gray color.

The facial whiskers or *vibrissae* are especially noticeable laterally on the upper lip of both male and female European hamsters. They are straight stiff hairs mainly occurring in two main colors, white and brown. They appear in four or five distinct rows and consist of up to 30 hairs on each side (Figs. 1–4, 1–5). The length of the dark hairs is 32 to 39 mm with root lengths of 0.585–0.730 mm. The maximal width is 0.166–0.191 mm above the root, narrowing towards the apex, which has a width of 0.005 mm. The measurements for the lighter-colored hairs are the following: length 7.5–25.1 mm, breadth 0.074–0.136 mm, root length, 0.292–0.542 mm (Kourist, 1957).

The prominent external ears, (*auris externa*), 2.3–3.2 cm long in the adult (Figs. 1–4, 1–5), are translucent and relatively avascular in bright light. They are directed dorsomedially and appear shorter than they actually are due to the long body hairs.

The soles of the hands and feet (*palma manus, planta*) demonstrate no sex differences (Figs. 1–6, 1–7). The soles of the forefeet have five pads (*tori*). The hindpaws are very long (3.0–4.0 cm), with six pads on each paw. The arrangement of the pads is less symmetrical than that of the forefeet (Fig. 1–7). The pads vary in size on the hindfeet and the forefeet, with the size increasing from the digits to the metapoidal joint in the forefeet, and decreasing in the hindfeet.

When hibernating, it is difficult to distinguish the sex of the animals, as the testes lie intrapelvically during this period of sexual inactivity. This does not occur in laboratory bred animals when kept under standard laboratory conditions throughout the year.

Other characteristics which differentiate the sexes are the round preputial opening (*ostium praeputiale*) and the space, about 2 cm. long, between the *anus* and prepuce (*praeputium*) in the male. (Figs. 1–8, 1–9, 1–10). In the female, the distance between the *clitoris* and anus is only about one cm. When the females are about 10 to 14 days old, eight teats (*papillae mammae*) (one cranial thoracic pair, one caudal thoracic pair, one abdominal pair,

one inguinal pair) become prominent (Figs. 1–10, 1–11) (Nehring, 1901). Furthermore, in contrast to the relatively large round prepuce of the males, the clitoris has a pointed shape with only a very small urinary opening (*orificium urethrae externum*). Before sexual maturity as well as during hibernation, the *vagina* is closed by a layer of squamous epithelium in both wild and laboratory bred hamsters (Illman, 1968; Kayser and Aron, 1938; Jahn, 1968).

Males and females have a sac-like cutaneous organ in the umbilical region, the umbilical glandular organ (Fig. 1–12, 1–13).

It consists of compound sebaceous glands covered with a very thick epidermis (Vrtiš, 1932).

Bilaterally, at the level of the anterior process of ilium, the European hamster has dark cutaneous stripes 2 cm long and 2 mm wide (Vrtis, 1930), the so-called flank organs (Fig. 1–14).

On their surfaces, the flank organs have a thin epidermis under which compound sebaceous cells are located. These cells, especially active in sexually mature males, produce a secretion by which the hamsters mark their territories (Petzsch, 1943; Eibl-Eibesfeld, 1953; Petzsch and Petzsch, 1968; Sulzer, 1974; Pidoplička, 1928; Kristal, 1929).

Beneath the epidermis of the umbilical glandular and the flank organs, as well as between the glands, is abundant melanin which, because of its dark brown color, may be externally identified from earliest youth (Fig. 1–17).

1.2 PHYSIOLOGY OF REPRODUCTION

Wild European hamsters observe a seasonal sexual cycle. Their mating season begins around the end of April and ceases in the first weeks of August (Petzsch, 1937). During this time, the females demonstrate a regular estrus cycle consisting of the following four stages: proestrus (a few hours), estrus (1 to 2 days), metestrus (a few hours) and diestrus (4 to 6 days) (Reznik-Schüller, *et al.*, 1974a). The females are willing to mate only during estrus, since they demonstrate marked aggressive behavior towards males in the other three stages. The European hamster has a distinctive mating behavior. The pronounced foreplay is quite extensive and requires a great deal of space. During foreplay, the female runs in a figure eight while the male follows closely behind, uttering a mating call which increases in loudness with the female's readiness to mate. Finally, the hamsters copulate several times before mating is completed.

Pregnancy lasts from 18 to 21 days and the young remain sucklings for about 30 days. Depending upon the annual variation of temperature, the European hamster hibernates from about the middle of October to the middle of March. Breeding of the European hamster (Fig. 1–15) has been undertaken to obtain animals of a defined age and pedigree for experimental purposes (Mohr, *et al.*, 1973; Reznick–Schüller, *et al.*, 1974a).

The variation in aggressiveness of the females during their estrus cycles and the great demand for space throughout foreplay and actual mating has been considered in developing a breeding method. Laboratory-bred hamsters have gradually lost their seasonal sexual cycles and observe no hibernation when kept under standard laboratory conditions. Pregnancy has shortened to only 15.5 to 17 days. The females deliver young from 2 to 5 times per year and litters are born in each month of the year. In addition, the laboratory-bred European hamster shows neither aggressiveness towards man nor members of its own species. Contrary to wild European hamsters which are reported to live only solitarily (Petzsch, 1937; Eibl-Eibesfeld, 1953), the laboratory bred animals can be kept in groups (Fig. 1–16) and develop a social order with the largest male dominant (Fig. 1–17).

1.3 PRESENT DISTRIBUTION OF EUROPEAN HAMSTERS IN EUROPE

The European hamster, an animal species which had been recognized as a pest by the agricultural community, was a menace especially around the turn of the century. However, today we know of only a few small areas where this animal has not yet been exterminated and where it can, at definite periods of time, be found in great numbers.

The results of a general inquiry concerning the presence of European hamsters in Germany, which was distributed throughout the entire Federal Republic by a questionnaire in a specialty magazine for hunters, are pictorially represented on the following geographic map (Fig. 1–18). Within the boundaries of the Democratic Republic of Germany, the European hamster is found in the regions es-

pecially surrounding Halle, Saale, Jena, Weimar and Erfurt. It can also be found in smaller numbers in Western Europe (particularly in parts of France, Belgium and The Netherlands). This species is also scattered in the Ukraine, Rumania and southern Czechoslovakia. The most northern limit of its occurrence, which appears to be at a latitude of about 60 degrees, is in the U.S.S.R. (Serebrennikov, 1930; Saint Girons, *et al.*, 1968; Hannoun, 1974; Vohralik, 1974). In its western ranges, it is limited strictly to rural districts with loess soil. In addition to the typically colored European hamster, albino, black and transitionally colored animals can also be found, though only rarely (Petzsch and Petzsch, 1970). Petzsch and Petzsch (1956) reported that black hamsters are dominant over non-black animals; this fact explains the increase in number of these hamsters in some areas around Thüringen (Zimmermann, 1969). *C. cricetus* lives only in small well-defined areas (Fig. 1–18) within these regions; however, the incidence of the species is high.

Annually, variations in the number of these hamsters are observed and presumed to be seasonally dependent; sometimes the animals become so numerous that they are a scourge to the land. Geographically, they are abundant in rural areas bordering highly industrialized regions, especially those where predominately summer and winter grains as well as root crops are planted. The European hamster prefers ground that is heavy, clayish, and not too damp—ground appropriate for building burrows with depths varying from 30–60 cm in summer to more than 2 m in winter. Each burrow has several exits with tunnel diameters approximately 8–9 cm. This species lives primarily on plains not more than 400 m above sea level (Petzsch, 1936, 1937).

Due to the proximity of heavily industrialized, thickly populated districts with relatively high environmental pollution, wild European hamsters from these areas have special interest for research on "spontaneous" cancer and respiratory diseases.

Figure 0-1: Comparison of 1-year-old male European and Syrian golden hamsters.

Figure 0-2: Adult European hamster hibernating under artificially induced hibernating conditions (+4°C, 90% relative humidity). Note typical curled posture with outstretched forelegs.

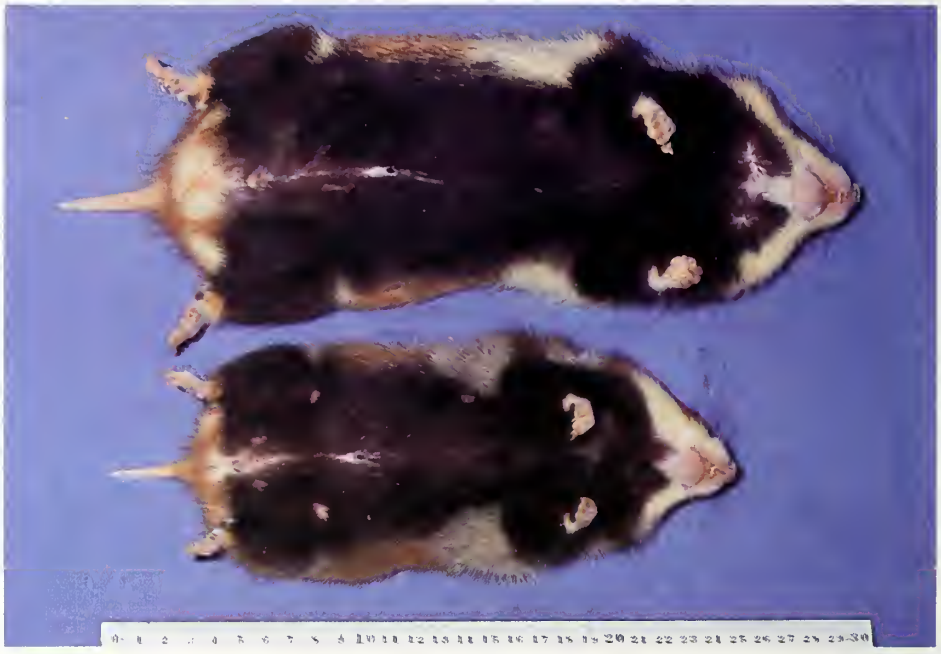

Figure 1-1: Anesthetized adult male and female hamsters in supine position. Note larger size of male as compared to female, and black color of their ventral fur.

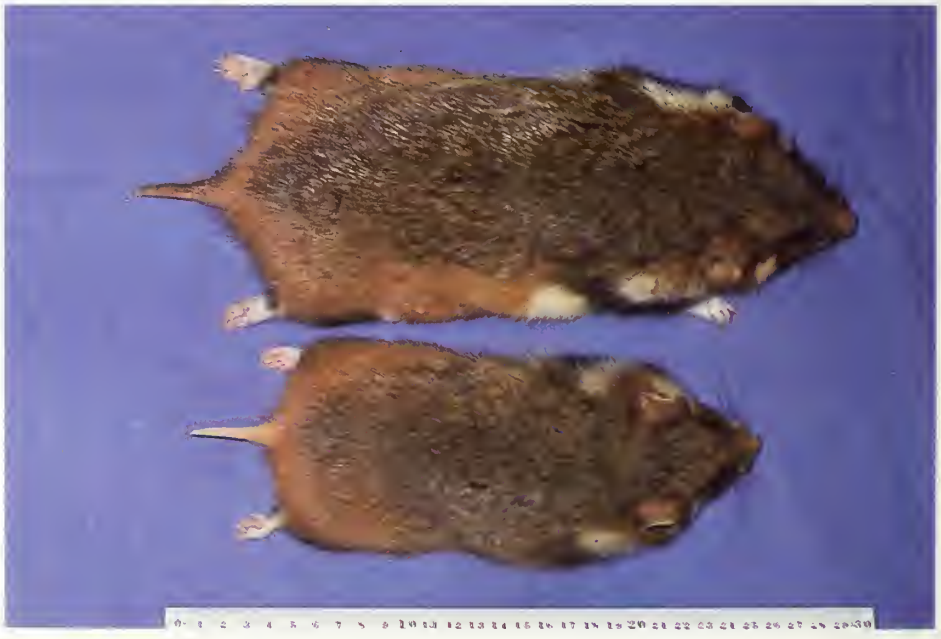

Figure 1-2: Adult hamsters in prone position; note short tails of both animals in comparison to length of whole body.

Figure 1-3: Adult hamster sacrificed in autumn. Note large subcutaneous fat deposits, especially in thoracic and lumbar regions.

Figure 1-4: External features of head, rostral view. 1=dorsum nasi; 2=vibrissae; 3=naris; 4=philtrum; 5=auris externa; 6=bulbus oculi.

Figure 1-5: External features of head, lateral view. 1=meatus acusticus externus; 2=palpebra; 3=vibrissae.

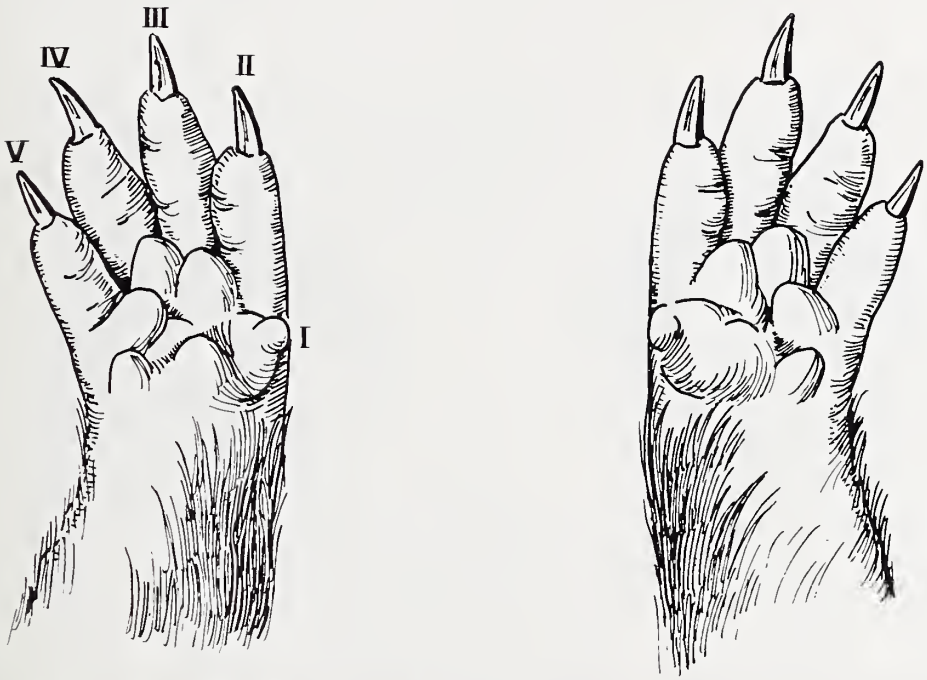

Figure 1-6: External features of palmar aspect of forefeet. Note strongly reduced first digit. I–V=digiti.

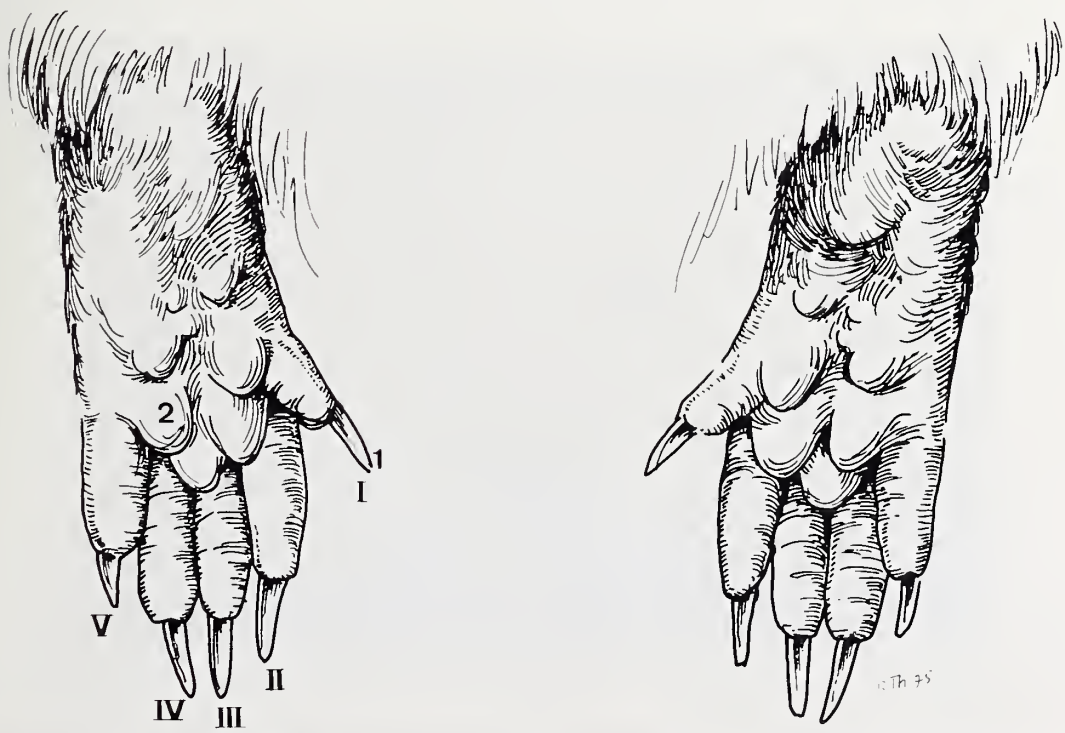

Figure 1-7: External features of plantar aspect of hind feet. I–V=digiti; 1=unguis; 2=torus.

Figure 1-8: Sketch demonstrating ventral aspects of perineal regions of both sexes. Note location of caudal, inguinal pair of teats in female.

Figure 1-9: Ventral aspect of perineal regions of adult male and female hamsters; sexes are well differentiated.

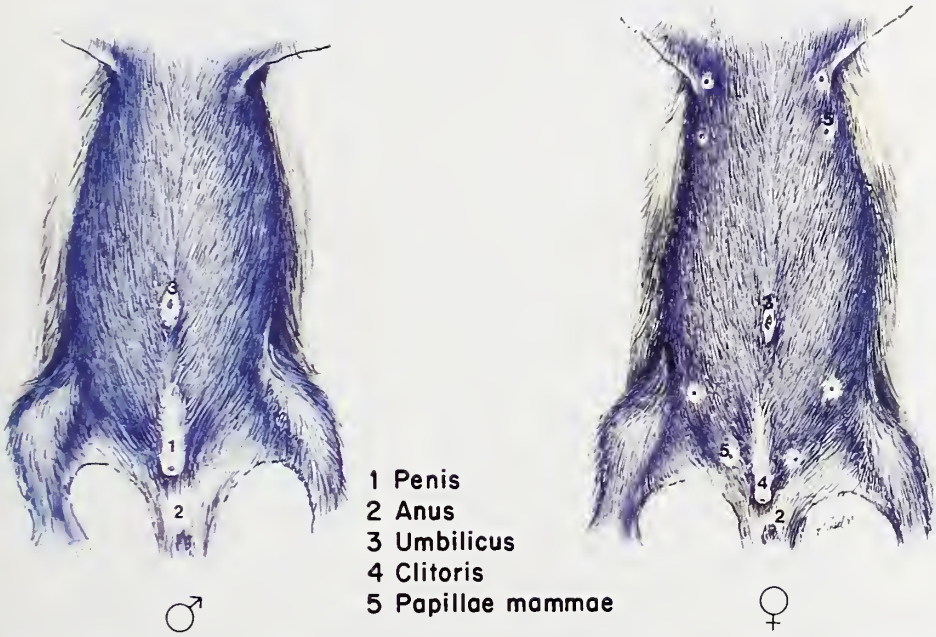

Figure 1-10: Drawing of ventral view of two litter mates, 14 days old, demonstrating sex differences. Note larger urogenital orifice of male and smaller one of female. Preputial opening of male is circular or slightly oval; it has pointed form in female. Note longer space between urogenital opening and anus in male, and teats in female.

Figure 1-11: Ventral view of adult female during lactation, which causes teats to become prominent.

Figure 1-12: Ventral view of part of abdomen of adult male shaved to demonstrate well-developed umbilical glandular organ.

Figure 1-13: Umbilical glandular organ after removal of skin; the sac-like organ has opening at ventral surface that is occupied by fatty secretion of the sebaceous glands.

Figure 1-14: Dorsolateral aspect of two litter mates, 8 days old, demonstrating flank organs.

Figure 1-15: Litter of laboratory-bred European hamsters, 12 days old, with mother.

Figure 1-16: Litter of laboratory-bred European hamsters demonstrating group living.

Figure 1-17: Adult male, dominant animal of one-year-old litter.

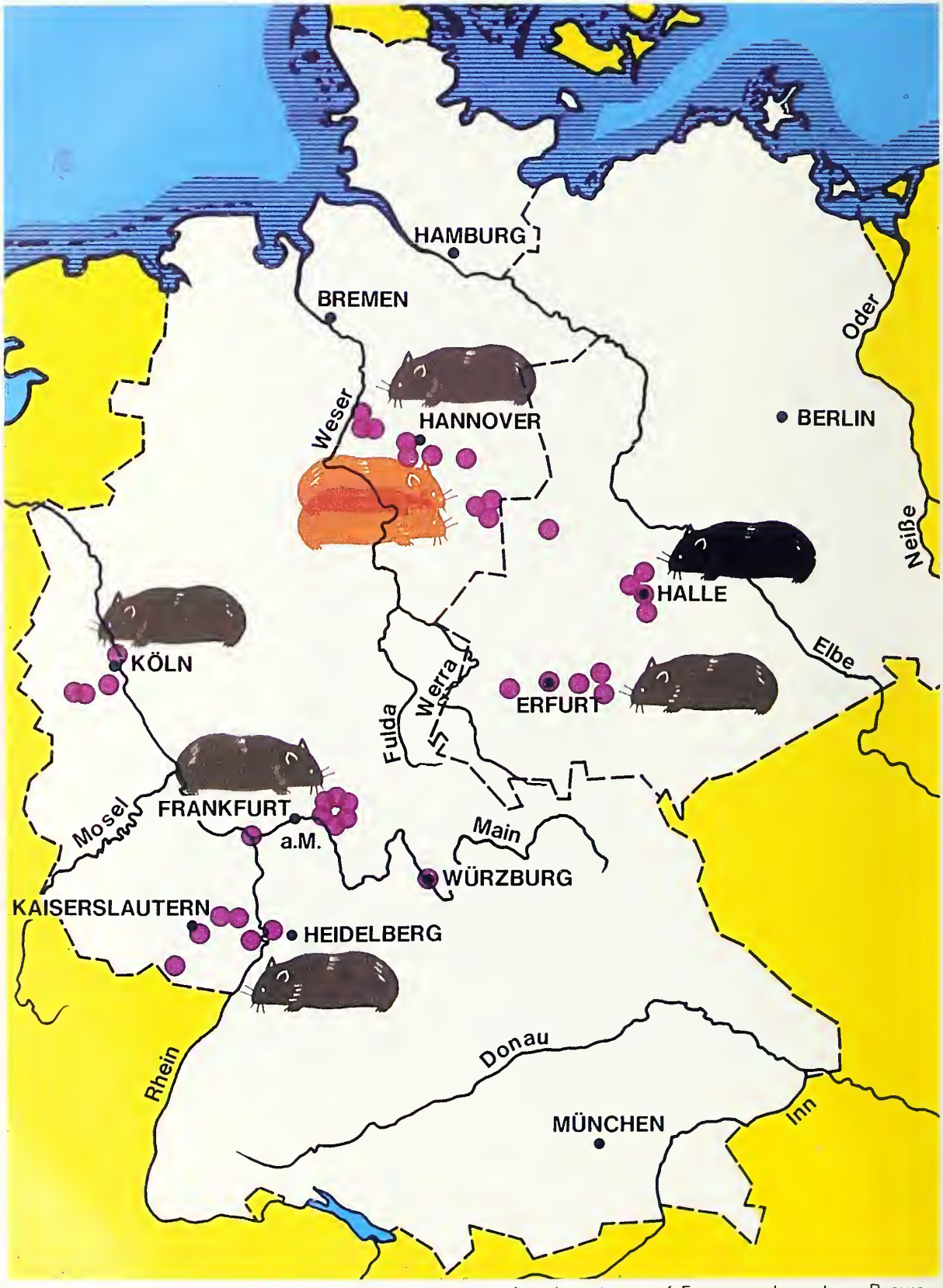

Figure 1-18: Map of Germany showing distribution of various types of European hamsters. Brown color represents normally occurring animal; black, orange, and purple colors represent rare, transitionally colored animal.

CHAPTER TWO
ANATOMY OF THE HEAD

2.1 BONES OF THE SKULL

The skull of the European hamster accounts for approximately a fifth of the length of the body (Fig. 2–1). The skull includes two bone assemblies, neurocranial and facial, which partly overlap. The neurocranium (*cranium*) encloses the brain, while the facial skeleton (*facies*) encloses the nasal, paranasal and oral cavities, including the mandible.

The soft tissue over the neurocranium, includes the skin, superficial fascia and *m. cervicoauricularis* with its aponeurosis. The skin is among the deepest in the body and attaches firmly to the aponeurosis via the superficial fascia, the freely movable skin carrying the aponeurosis with it. The loose subaponeurotic connective tissue and the periosteum to which it attaches underneath are easily torn from the skull, except at the sutures, and are sites of freely spreading effusions, sometimes indicative of subcranial or submeningeal neoplasms.

2.2 FACIAL SKELETON

The facial skeleton (Fig. 2–2) invests the nasal and paranasal cavities (*cavum nasi, sinus paranasales*) as far as the nasopharynx (*pharynx, pars nasalis*), extending between the *choanae* and the *epiglottis,* and the oral cavity (*cavum oris*) as far as the oropharynx (*pharynx, pars oralis*), extending between the soft palate (*palatum molle*) and the hyoid bone (*os hyoideum*) (Figs. 2–3, 2–4, 2–5).

2.3 NASAL CAVITY

The nasal cavity (*cavum nasi*) is separated from the braincase by the ethmoid bone (*os ethmoides*) (Fig. 2–6). The roof of the nasal cavity (*dorsum nasi*) includes the paired nasal (*os nasale*) and frontal (*os frontale*) bones (Figs. 2–2, 2–6, 2–7). The lateral wall is composed of incisive or premaxillary (*os incisivum*), maxillary (*maxilla*) and caudally the palatine (*os palatinum*) bones (Figs. 2–2, 2–7). The base of the nasal cavity, the ventral surface of which is the bony roof of the oral cavity, is formed by the horizontal laminae of the incisive, maxillary and palatine bones (Figs. 2–6, 2–8). The incisive duct (*ductus incisivus*) perforates the bony base of the nasal cavity through the palatine fissure (*fissura palatina*) in the incisive and maxillary bones (Fig. 2–8.).

The interior of the nasal cavity is best studied in serial section (Figs. 2–9 to 2–37). The nasal cavity extends from the nostrils to the choanae and is bisected by a principally cartilaginous median septum (*septum nasi*) (Figs. 2–9 to 2–20, 2–29 to 2–33) (Reznik and Reznik-Schüller, 1974). The cavity is filled with epithelium disposed in a highly elaborated pattern, borne by thin bony processes, the turbinal scrolls (*turbinalia*) or nasal conchae (Figs. 2–10 to 2–20, 2–29, 2–33). Dorsal and ventral nasal conchae are attached to the lateral walls of the nasal cavity (Figs. 2–3, 2–4). The dorsal nasal concha (*concha nasalis dorsalis*) (termed nasoturbinal by various authors) attaches to the nasal bone; the ventral nasal concha (*concha nasalis ventralis*) (also called maxilloturbinal) attaches to the maxillary bone. The conchae curl inward to shape the scrolls, whose overhang forms the recesses of various lengths which ultimately communicate with the nasal cavity. In this species the conchae extend about 8 mm caudally into the lumen of the nasal cavity. The ventral concha, partially situated above the nasolacrimal duct (*ductus nasolacrimalis*) (Fig. 2–13) is shorter than the dorsal concha and bears no mucosal fold, unlike the Syrian golden hamster (Schwarze and Michel, 1959–60; Och, 1959).

More complicated than the conchal apparatus is a second group of projections in the ethmoid region, the ethmoturbinals (*ethmoturbinalia*) (Figs. 2–3, 2–4, 2–6). They are lined almost entirely by olfactory epithelium (Fig. 2–38) and are disposed in two rows, termed endoturbinals (*endoturbinalia*) and ectoturbinals (*ectoturbinalia*) (Figs. 2–16 to 2–20, 2–31 to 2–33). This hamster has four endoturbinals and three ectoturbinals (Reznik and Reznik-Schüller, 1974); similar counts are reported for rats (Kelemen and Sargent, 1946; Vidič and Greditzer, 1971; Giddens, *et al.*, 1971), mice (Kele-

men, 1953), guinea pigs (Kelemen, 1950) and rabbits (Kelemen, 1955). The ectoturbinals are situated ventral and caudal to the folds of the endoturbinals. Both groups represent true independent turbinals, as each arises separately from the wall of the ethmoid bone with an individual base.

The architecture of the turbinals is best seen in serial section. The basal lamella of the first endoturbinal (Fig. 2–16) is divided into two parts distally, each forming a spiral. Caudally (Fig. 2–17), only the dorsal spiral is present. The second endoturbinal (Figs. 2–16 to 2–19) is separated from the first and the third by separate meatuses. Rostrally (Figs. 2–16, 2–17) the second endoturbinal consists of only a tuberosity which broadens near the nasal septum. Caudally (Fig. 2–18) it bifurcates into two broad terminal parts. The third endoturbinal (Figs. 2–16 to 2–19) is longer and broader than the first and second ones. While the fourth endoturbinal bends only slightly dorsally and laterally, the third endoturbinal bends strongly dorsolaterally (especially prominent in Figs. 2–17 and 2–18); in this way, a semicircle is formed which is distinctly isolated from the nasal cavity.

The three ectoturbinals (Figs. 2–16, 2–17) are smaller than the endoturbinals; they are enclosed by the first and second endoturbinals, the cribriform plate (*lamina cribrosa*) of the ethmoid bone and the medial wall of the maxillary sinus. The first ectoturbinal (Figs. 2–16, 2–17) extends ventrally from the roof of the nasal cavity, recurving mediodorsally. Cranially the second ectoturbinal projects mediodorsally without curling (Figs. 2–16, 2–17); caudally however, it rolls ventrolaterally forming a small recess (Fig. 2–18). The third ectoturbinal (Figs. 2–16, 2–17), the smallest of all the turbinals, projects vertically from the medial wall of the maxillary sinus, nearly touching the second ectoturbinal.

The nasal conchae define three nasal passages or meatuses (Figs. 2–3, 2–4, 2–11 to 2–14, 2–38). The dorsal nasal meatus (*meatus nasi dorsalis*) (Fig. 2–13) lies between the dorsal wall of the nasal cavity and the dorsal nasal concha. The limits of the dorsal meatus include the dorsal concha, the nasal septum and the dorsal wall of the nasal cavity. Caudally, it narrows and ends at the cribriform plate of the ethmoid bone. The middle nasal meatus (*meatus nasi medius*) (Fig. 2–13) is located between the dorsal nasal concha and the ventral nasal concha and is a narrow fissure which joins the dorsal meatus along the rostral edge of the endoturbinals and ends shortly thereafter. The ventral nasal meatus (*meatus nasi ventralis*) (Fig. 2–13), which is the continuation of the nostril, lies between the ventral nasal concha and the base of the nasal cavity. The middle and ventral conchae and meatuses comprise the respiratory portion of the nasal cavity, since they converge at the caudal end of the conchae and continue as a single median passage, the ventral meatus (formerly the nasopharyngeal duct) ventral to the endoturbinals, (Figs. 2–3 to 2–5, 2–16 to 2–26, 2–31 to 2–37, 2–38). The endoturbinals are thus supplied with air via all three nasal meatuses (Fig. 2–39). In passing the endoturbinals, the ventral meatus gradually turns ventrally, not continuing in the straight caudal direction typical of the Syrian golden hamster (Schwarze and Michel, 1959–60).

2.4 NASOPHARYNX

The nasal cavity passes caudally into the nasopharynx (*pharynx, pars nasalis*) at the level of the soft palate, by means of the internal nostril or *choana* (Fig. 2–3). The choana is bordered laterally and ventrally by the palatine, and dorsally by the *vomer* and presphenoid (*os praesphenoidale*) bones (Fig. 2–8). The nasopharynx stretches 1.5 to 1.8 cm from the choana to the epiglottis, and varies in width from 1.5 to 3.0 mm (Figs. 2–16 to 2–26, 2–31 to 2–37) (Jensen, 1977).

It is lined for most of its length by respiratory epithelium, but caudally the ventral portion is protected with multilayered unkeratinized squamous epithelium, which becomes keratinized lateral to the epiglottis.

Lateral to the epiglottis, the tiny Eustachian tube (*tuba auditiva*) establishes communication between the nasopharynx and the auditory bulla (*bulla tympanica*). The tube measures 2 mm in length and 0.25 mm in diameter (Jensen, 1977).

It is lined with respiratory epithelium, and is supported by hyaline cartilage.

2.5 VOMERONASAL ORGANS

Paired vomeronasal organs (*organum vomeronasale*) are situated at the ventral margin of the

anterior nasal septum, as far caudally as the palatine fissure (Figs. 2–10 to 2–15, 2–29, 2–30). They are involved in the sense of smell, since they are supplied by twigs of the olfactory nerve (Nickel, *et. al.,* 1960). Each measures 5 mm in length, while the width ranges between 0.4 to 1.0 mm (Jensen, 1977). Rostrally it has a laterally compressed, eliptical cross-section, which caudally assumes a half-moon shape, convex medially. The organ is invested by a bony covering of the vomer, and communicates with the incisive duct (Fig. 2–14), ending blindly slightly caudal to that structure.

The vomeronasal organs are lined by two types of epithelium. The ventral margins of the glands are covered by epithelium similar to the olfactory region of the nose, including olfactory sensory cells interspersed throughout the supporting columar epithelium, which is nonciliated, pseudostratified and free of goblet cells. The dorsal edges are continuous with the respiratory epithelium of the nasal cavity, which is pseudostratified, ciliated, columar and interspersed with goblet cells (Fig. 2–40).

The initial part of the nasal cavity, the nasal vestibule (*vestibulum nasi*) approximately 4 mm in length, is lined with stratified squamous epithelial mucosa. The nasal cavity proper, the nasopharynx and the nasal septum are lined with a respiratory mucosa consisting of ciliated pseudostratified columnar epithelium with goblet cells (Figs. 2–40, 2–41, 2–42). The ethmoturbinals are invested with olfactory epithelium (Fig. 2–38).

2.6 PARANASAL CAVITY

The European hamster has only one true paranasal cavity (*sinus paranasalis*), the maxillary sinus (*sinus maxillaris*) (Figs. 2–16 to 2–18, 2–31, 2–32). It is surrounded by the outer and inner surfaces of the maxillary bone and extends 4.5 mm from the level of the union of the ventral nasal meatuses to an imaginary line drawn perpendicular from the orbits to the lower jaw. Two portions can be distinguished, a smaller rostrodorsal portion 2.5 mm high and 1 mm wide, and a larger caudoventral portion, 5 mm high and 1 mm wide (Jensen, 1977). The maxillary sinus communicates with the nasal cavity via the nasomaxillary opening (*apertura nasomaxillaris*) into the middle nasal meatus.

The paranasal sinus is lined with pseudostratified ciliated columnar epithelium containing goblet cells (Figs. 2–43, 2–44). Directly beneath this epithelium are situated glandular bundles (100 μm in diameter) composed of serous and mucous parts. In the oral region these glands demonstrate a more mucous character, whereas caudally they contain more serous parts.

2.7 ORAL CAVITY

The oral cavity (*cavum oris*) extends from the lips (*labia oris*) to the oropharynx. Its bony structure consists dorsally of paired incisive and maxillary (Figs. 2–2, 2–8) and single palatine bones, and ventrally of the paired dentary bones constituting the mandibles (*mandibulae*) (Fig. 2–45). The oral cavity is bordered rostrally by the lips and laterally by the cheeks (*buccae*). The roof of the oral cavity consists of the hard palate (*palatum durum*) and the soft palate (*palatum molle*) (Figs. 2–3, 2–46). The oral cavity is floored by the tongue and by the reflections of mucous membrane extending from the tongue to the gum (*gingiva*) on the medial surface of the mandible (Fig. 2–46).

The oral vestibule (*vestibulum oris*), between the teeth and lips, is separate from the oral cavity proper (*cavum oris proprium*); however, the separation is incomplete due to the long diastema in the tooth row. Associated with the presence of cheek pouches is a longitudinal separation of the vestibule into buccal and labial parts (*vestibulum buccale, vestibulum labiale*). The separation, better developed in the mandibular than the maxillary vestibule, results from a fold of oral mucosa (*tunica mucosa oris*). Median labial frenula (*frenulum labii maxillaris, frenulum labii mandibularis*) separate maxillary and mandibular labial vestibules into left and right halves and serve to bind the lips tightly to the gums.

2.8 LIPS

The entrance of the oral cavity (*rima oris*) is enclosed by the upper lip (*labium maxillare*) and the lower lip (*labium mandibulare*). The relatively short lips cannot be completely closed, so the incisors always remain visible. The upper and lower lips join at the labial commissure (*angulus oris*), 20 to 25 mm caudal to the mandibular incisors. The commissure is actually a compound structure, with maxillary and mandibular portions, separated by a mucosal fold. The resulting valve-like structure controls entrance into the cheek pouches, as in the Syrian golden hamster (Schwarze and Michel, 1959–60). The lips are not confined to the rima oris, but project prominent flaps of hair-covered skin, the buccal pads (*pulvini buccales*) into the

oral cavity, approaching to within a millimeter of the midline from each side. The buccal pads line the hard palate, and the corresponding surface of the lower jaw, between the molars and the incisors.

2.9 CHEEKS

The cheeks (*buccae*) of the European hamster are occupied by remarkable structures, the cheek pouches (*bursae buccales*), which are situated between the skin and masticatory muscles (Fig. 2–48). The pouches begin at the labial commissure and run caudodorsally along the base of the ear musculature, covering the ventral part of the parotid gland, and are applied to the dorsolateral surface of the neck, extending to the scapulae (Fig. 2–49). Their length varies with the size of the animal, the adult pouches ranging between 60 and 70 mm. The empty pouches, the mucosa of which is relaxed and marked by deep folds, are 12 to 15 mm wide. When filled, the cheek pouches become thin-walled and evaginate the buccal mucosa which lies immediately under the external skin. The diameter of the fully filled cheek pouches expands up to 30 mm. The cheek pouches are longest when empty because the carrying capacity, between 20 and 30 g, is not dependent upon elongation of the pouches but rather upon their widening.

The pale pink, simple squamous epithelium, marked with delicate longitudinal folds, is covered with multiple, small papillary elevations visible only with the aid of magnification.

Hamsters empty their cheek pouches by pushing the food mass with their forepaws out of the cheek pouch and into the oral cavity for mastication, thereby employing the underlying and supporting musculature (*retractor bursae buccalis et retractor buccinator*), which originates in the lumbodorsal fascia (*fascia lumbodorsalis*) at the level of the first two lumbar vertebrae (slightly caudal to the origin of these muscles in the Chinese hamster (Geyer, 1973) and inserts on the cheek pouch in the vicinity of the scapula (Fig. 2–50).

2.10 PALATE

The palate is approximately 20 mm long and is divided into the rostral hard palate (*palatum durum*), which extends 20 to 25 mm from the incisors to a line posterior to the third molar, and the caudal soft palate (*palatum molle*) 7 to 9 mm long, which is attached to the caudal margin of the hard palate (Fig. 2–3). The mucous membrane of the hard palate lines the ventral surface of the bony palate and forms eight symmetrical pairs of palatine rugae (*rugae palatinae*) (Fig. 2–46); they are compact, smooth and pinkish-red in color. These rugae are divided into four large rostral pairs and four smaller caudal pairs located between the molars. The smaller rugae adjacent to the molars decrease rostrally, while the four large rostral pairs decrease caudally. With the exception of the fourth and also usually the third, or widest (9 mm), the rugae decline obliquely toward the median plane. The first four pairs unite in the median plane but the last three pairs do not completely join. In contrast to the Syrian golden hamster (Schwarze and Michel, 1959–60), the European hamster has an additional eighth rugal pair which completely coalesces in the adult and is positioned at a right angle to the median plane. The first rugal pair forms a V-shape in the median plane with its apex directed rostrally. At the rostral surface of the first pair, 0.5 to 1 mm from the lateral margin of the apex, lie the oral orifices (*papillae incisivae*) of the two incisive ducts. By applying pressure to the first rugal pair, the orifices can be made to appear. The rugae between the molars are flatter laterally than medially. At the termination of the hard palate, 7–9 mm of caudally oriented soft palate is attached.

The mucosa of the soft and hard palates is pinkish-red in color, completely smooth and lined with keratinized stratified squamous epithelium (Fig. 2–51). Beneath the epithelium of the hard palate, mucous glands are located on either side of the median plane. These glands are especially prominent at the level of the orbit.

The tonsils, which lie between the caudal ends of the palatine rugae in other rodents, are neither histologically nor grossly demonstrable in the hamster (Roscher, 1909; Kittel, 1953, 1955).

2.11 GUMS AND TONGUE

The smooth mucosal surface of the floor of the mouth meets the molars laterally as the gums (*gingivae*) and is continuous with the mucosal surface of the tongue (*lingua*).

At the median plane from the floor of the mouth extending to the tip of the tongue, the keratinized stratified squamous cell mucosa forms a rather indistinct lingual frenulum (*frenulum linguae*).

At the base of the frenulum are located small,

paired, flattened, pyramidal toruli, the tips of which are oriented towards the lips; these are the sublingual carunculae (*carunculae sublinguales*) through which the ducts of the mandibular and the sublingual glands discharge.

C. cricetus has an especially well-developed spoon-shaped tongue (*lingua*) (30–55 mm long and 10–12 mm wide); since the tip is not attached at the sides, it is freely mobile (Fig. 2–47). The rostral portion of the tongue is so broad that its surface accounts for about two-thirds of the total area. The tip of the tongue (*apex linguae*) is approximately twice as wide as the body (*corpus linguae*) which is situated between the molars. The median sulcus (*sulcus medianus linguae*) is restricted to the dorsal surface of the tip of the tongue. The root of the tongue (*radix linguae*) coalesces ventrolaterally with the surrounding tissue.

Located on the keratinized stratified squamous epithelium of the tongue are numerous papillae (*papillae linguales*).

Multiple small, filiform papillae, scarcely visible to the naked eye, are distributed over the lateral and ventral surfaces of the tongue (Fig. 2–52), conferring a velvety texture to the surface.

-At the root of the tongue, seromucous glandular bundles can be identified.

2.12 TEETH

The dentition (*dentes*) of the European hamster is composed only of incisors (*dentes incisivi*) and molars (*dentes molares*); canines (*dentes canini*) and premolars (*dentes premolares*) are lacking (Figs. 2–53, 2–54). In total there are 4 incisors and 12 molars arranged in the following manner:

$$I\frac{1}{1} \quad C\frac{0}{0} \quad P\frac{0}{0} \quad M\frac{3}{3}$$

Only a single generation of permanent teeth (*dentes permanentes*) is present.

The incisors are very long rooted and evergrowing. The roots of the lower incisors pass nearly through the entire length of the mandible, terminating caudal to the roots of the last molar (Fig. 2–53). About one-third of the lower incisor is erupted, while two-thirds is seated in the alveolus (*alveolus dentalis*). The crowns (*corona dentis*) of the upper incisors are much shorter (4 mm) than those of the lower incisors (10–12 mm) (Fig. 2–53); correspondingly, their roots (*radices dentes*) penetrate the premaxilla only to the level of the first molars. The labial surface of the incisors is coated with whitish-yellow enamel. The cross section of the upper incisor within the alveolus changes rostrocaudally from oval (Fig. 2–11), to triangular (Fig. 2–12), and finally becomes round at the base (Fig. 2–13). The pulp cavity is long and narrow. The configuration of the temporomandibular joint (*articulatio temporomandibularis*) and of the corresponding articular process (*processus condylaris*) of the jaw is such as to permit fore and aft movement of the jaw. Consequently, the positions of the upper and lower incisors can vary greatly relative to one another, while the molars are in occlusion, the lower incisors are retracted out of contact with the upper incisors (Fig. 2–53), but during gnawing the lower incisors work against the labial side of the upper incisors. In addition, the mandibular symphysis (*symphisis intermandibularis*) does not fuse completely even in adults, and therefore independent movement of each jaw is possible (Habermehl, 1970a, b on the Chinese hamster); this is more prominent, however, in juveniles.

The molar tooth rows are not parallel, but converge slightly towards the midline caudally, so that the first molars are more widely separated than are the third molars (especially for the upper dentition) (Fig. 2–54). The molar crowns are rectangular and flat, with three small cusps on the first, two cusps on the other two (Figs. 2–46, 2–47, 2–55, 2–56). The crown of the first lower molar is 3 mm long, 2 mm wide and 1.2 mm high. The roots are long and narrow (Fig. 2–57). The first upper molar has four roots, the second and third but three roots.

The first teeth to appear are the incisors, which erupt on the 4th and 5th day postpartum. Thereafter, the first mandibular and maxillary molars follow on about the 10th or 11th day; the second molar appears in both the upper and lower jaws around the 20th day; and the third molar erupts on the 33rd day, completing the dentition.

2.13 SALIVARY GLANDS

The secretion of the salivary glands (*gll. oris*), the saliva, wets the food as well as the wall of the oral and pharyngeal cavities and begins the digestive process.

In general, there are two kinds of salivary glands, those of serous type which produce a watery secretion and those of mucous type, the secretion of which is viscous.

The salivary system consists of the following glands: the parotid (*parotis*), the mandibular (*glandula mandibularis*), the sublingual (*glandula sublingualis*) and the zygomatic (*glandula zygomatica*), and various other glands which are only detectable histologically.

2.14 MANDIBULAR GLAND

The triangular mandibular gland (*gl. mandibularis*) lies superficially in the ventral cervical region caudal to the larynx and covering the cranial part of the sternohyoid muscle (Figs. 2–58, 2–59, 2–60). The two glands contact each other in the median plane. The length of the gland ranges between 14 and 16 mm, the width between 8 and 10 mm and the thickness between 4 and 5 mm; each mandibular gland weighs between 350 and 400 mg (Figs. 2–60, 2–61). Macroscopically, these glands present a distinct lobular structure, after removal of the connective tissue; the lobes are larger than those of the parotid gland (Tables 20, 20a).

The mandibular glands show a compact tubuloalveolar structure with both serous and mucous alveoli, the majority of which are of mucous type (Fig. 2–62).

The gross and histological appearance of this gland is similar to that described for the Syrian golden hamster (Schwarze and Michel, 1959–60) and Chinese hamster (Horber, *et al.,* 1974).

2.15 SUBLINGUAL GLAND

Cranial to the mandibular gland lies the sublingual gland (*gl. sublingualis*) which is in close relation to the former and can be distinguished only by its lighter color (Figs. 2–58, 2–59, 2–60, 2–61, 2–62). The sublingual gland, similar in both sexes, is 4 to 5 mm long and 3 to 4 mm wide and weighs between 40 and 60 mg (Tables 21, 21a). The sublingual gland is a mucous gland, with a compact surface like the mandibular but with a more delicate lobular structure.

The sublingual glands are tubuloalveolar, consisting of both mucous and serous parts, with the mucous type predominating (Fig. 2–63).

The secretory ducts of both glands coalesce intraglandularly to form either the mandibular duct (*ductus mandibularis*) or the sublingual duct (*ductus sublingualis*). Both ducts discharge at the sublingual caruncles which are located at the root of the frenulum of the tongue. The mandibular and sublingual glands press cranially against the parotid gland (Fig. 2–59). Both glands are connected by dense connective tissue. The mandibular and sublingual glands obscure the caudal part of the laryngeal musculature, the ventral pharyngeal musculature and the cranial portion of the thoracic musculature. These glands are not firmly attached to the musculature, especially caudally, since brownish fatty tissue separates the glands and the musculature at this position.

2.16 PAROTID GLAND

The parotid gland (*parotis*) (Fig. 2–58) lies at the base of the ear, embedded within a pocket of fatty tissue (*panniculus adiposus*), the amount of which varies during different seasons of the year. Especially in late summer and fall when the hamster stores up fat for hibernation, this gland is surrounded by a very thick deposit of fat. The parotid has a width of 8 to 10 mm at the base of the ear and a width of 3 to 4 mm in the area of the larynx (Figs. 2–59, 2–60; Tables 19, 19a). Caudally, it borders the sublingual gland for a distance of several millimeters. The weight of the parotid gland ranges from 400 to 500 mg and the color of a fresh specimen is light pinkish-red (Fig. 2–62). Macroscopically, the parotid demonstrates a lobular structure with a honeycombed appearance. This lobular structure is made quite prominent by the presence of well developed interstitial connective tissue. The secretions of the parotid are transported through the parotid duct (*ductus parotideus*) which courses superficially along the lateral surface of *m. masseter* before it discharges in the buccal vestibule in the form of a salivary papilla (*papilla parotidea*) located about 4 mm rostral to the first upper molar.

The parotid gland is of tubuloalveolar type and its cells predominately serous (Fig. 2–64).

In the immediate vicinity of the parotid gland, between the external auditory meatus (*meatus acusticus externus*) and the ascending condylar process of the mandible, a sebaceous gland is present.

These glands can be classified as typically holocrine; histologically they resemble the Zymbal glands of the rat (Zymbal, 1933) (Fig. 2–65).

2.17 ZYGOMATIC GLAND

The zygomatic gland (*gl. zygomatica*) (sometimes called the external orbital gland), (Fig. 2–58) is an oval-shaped gland which lies rostral to the parotid gland on the lateral surface of the masseter and temporalis muscles, completely outside the orbital cavity. It is yellowish-brown to brown in color (Figs. 2–61, 2–62) and measures 8–10 mm in length, 6.3–7.5 mm in breadth and 2.5–2.8 mm in thickness, depending on sex and season (Tables 22, 22a). The dorsal portion is located immediately under the epidermis while the ventral portion is covered by the cheek pouch. It is applied to the lateral aspect of the masseter muscle and the ventral aspect of the temporal muscle. It overlaps the parotid duct as well as the buccal nerve and, macroscopically, presents an indistinct lobular structure. The secretory ducts of the zygomatic gland join intraglandularly and form the main duct, which leaves the dorsorostral fourth of the gland.

The zygomatic gland has a tubuloalveolar structure and is of the serous type. The columnar cells which line the glandular acini do not contain fat droplets. The cytoplasm of the cells is finely granulated and the nuclei spherical and basally situated.

In contrast to the parotid gland, which is continuous with the surrounding tissues, the zygomatic gland is easily ablated. It is firmly attached only at the excretory ducts rostrally and afferent blood vessels caudally.

2.18 NEUROCRANIUM AND BRAIN

The brain (*encephalon*) is overlaid dorsally by paired frontals (*os frontale*) in part, and parietals (*os parietale*) and a median interparietal bone (*os interparietale*) (Fig. 2–7). Lateral support is provided by petrous and tympanic portions of the temporal bone (*os temporalis, pars petrosa et tympanica*) and the wing of the sphenoid bone (*ala sphenoidalis*) (Fig. 2–2). The base of the braincase is formed by the sphenoid (*os sphenoidale*) and the occipital (*os occipitale*), which also forms the caudal limit of the neurocranium (Figs. 2–6, 2–8). The cribriform plate of the median ethmoid bone (*lamina cribrosa, os ethmoidale*) demarcates the rostral border of the neurocranium (Fig. 2–6).

The brain (*encephalon*) of the European hamster has an average weight of 2.85 g in animals with a body weight of 450 g (Brauer and Schober, 1970). The following measurements were obtained from brains fixed in formalin:

Brain length:	29 mm
Brain width:	18.5 mm
Brain depth:	11.9 mm
Telencephalon length:	23 mm
Hemispheric length:	16.7 mm
Hypothalamus length:	5.7 mm
Rhombencephalon length:	11.4 mm
Cerebellum width with Pons:	18.2 mm
Cerebellum width without Pons:	15.3 mm

The European hamster has well-developed cerebral hemispheres (*hemispheria cerebri*) which are without sulci (lissencephalous) (Fig. 2–66). The olfactory bulbs (*bulbi olfactorii*) are relatively large and are overlapped caudally by the hemispheres to a depth of 5 to 8 mm. The *cerebellum* is about half as large as the cerebral hemispheres. The *vermis cerebelli,* the *lobi paramediani* and the lateral *paraflocculi* (Figs. 2–67, 2–68, 2–69, 2–70) are distinctly developed. The large rami of the trigeminal nerve (*n. trigeminus*) and the optic chiasma (*chiasma opticum*) are prominent on the ventral aspect (Fig. 2–69).

2.19 HYPOPHYSIS

The pituitary gland (*hypophysis*) (Fig. 2–70) lies in the *sella turcica* of the sphenoid bone, flat against the base of the brain between the trigeminal nerves. Caudally, it presses against the *pons* whose ventral surface it partly covers. The hypophysis also overlaps the cerebral crurae (*pedunculi cerebri*) with the oculomotor nerve (*n. oculomotorius*) and the trochlear nerve (*n. trochlearis*), as well as the mamillary body (*corpus mamillare*). At the ventrolateral edge of the hypophysis the abducens nerves (*nn. abducentes*) emerge. Also noteworthy is the large space between the hypophysis and the optic chiasma which is bridged by the *tuber cinereum*. The hypophysis is positioned dorsal, and somewhat rostral, to the *synchondrosis sphenooccipitalis* (Fig. 2–71). At this position, trepanation is performed for hypophysectomy. The origins of the cranial nerves are similar to those reported for other rodents (Brauer and Schober, 1970; Horber, *et al.*, 1974).

The schematic longitudinal view of the hypo-

physis (Fig. 2–72) demonstrates its structure in the European hamster. The largest part is the *adenohypophysis* or anterior lobe, with its ventrally disposed distal part (*pars distalis*). The middle lobe (*pars intermedia*) is small and surrounds the *neurohypophysis,* or posterior lobe, ventrally and laterally. Between the distal and intermediate parts of the adenohypophysis is the prominent interhypophyseal cleft (*cavum hypophysis*) which extends to the caudal third of the hypophysis. The neurohypophysis is relatively small and lies dorsomedially. The short, narrow, cone-shaped infundibular cavity (*pars cava infundibuli*) penetrates into the neurohypophysis. The details of the hypophysis of the European hamster are similar to those of the Syrian golden hamster (Schwarze and Michel, 1959–60) and the Chinese hamster (Horber, *et al.*, 1974).

The adenohypophysis contains acidophilic, basophilic and chromophobic cells in hematoxylin-eosin stains. Each type is either loosely dispersed or arranged in cords surrounding sinusoids and sparse interstitial connective tissue elements. The acidophils include somatotropes, producing growth hormone (STH) and mammotropes, producing mammotropic hormone (LTH). The basophils include the gonadotrophs, thyrotrophs and corticotrophs; the gonadotrophs are the source of the follicle-stimulating hormone (FSH), luteinizing hormone (LH) and male interstitial cell-stimulating hormone (ICSH). The thyrotrophs produce thyroid stimulating hormone (TSH) and the corticotrophs produce adrenocorticotrophic hormone (ACTH). Chromophobe cell function is still unclarified. The chromophobe cell is thought to be either a precursor acidophil or basophil or else a mature cell without staining potential due to cytoplasmic degranulation (Herlant, 1975).

Histometrical studies in the European hamster show variations in cell frequency, distribution and size of the nucleus during hibernation (Schlotter, 1976). Nuclear size is construed as a measure of the cell's functional state (Muschke, 1953) and frequency of cell type as a shift in total amount of hormones secreted. In females the basophils were most active in May and in non-hibernating animals in January. In males the highest activity was also in May but, in contrast to the female, the January values in nonhibernating animals were significantly lower. Lowest activity in both sexes was recorded during hibernation. Only the males showed a significant decrease in acidophilic cells during hibernation. There was significant change during October, May and in the nonhibernating animals, in January (see Table 9). From examination of the testes (Reznik-Schüller and Reznik, 1973, 1974), ovaries (Züchner, 1975) and the thyroids (Schlotter, 1976), variation in basophil function can be attributed to variation in number and function of the gonadotropic component.

2.20 ORBITAL ADIPOSE TISSUE

The orbital adipose tissue (*corpus adiposum orbitae*) occupies much of the orbit, especially the ventral portion (Figs. 2–18 to 2–21, 2–32, 2–33).

At low magnification, it resembles glandular tissue, but higher magnification demonstrates that it consists of multivacuolated fat cells (Fig. 2–73).

2.21 LACRIMAL APPARATUS

The lacrimal apparatus (*apparatus lacrimalis*) consists of the lacrimal gland (*gl. lacrimalis*), the accessory lacrimal gland (*gl. lacrimalis accessoria*) (Fig. 2–58) and associated ducts. The lacrimal or tear glands have the function of lubricating the cornea and preventing the drying of the epithelium. In addition to their secretory function, the accessory lacrimal gland, along with the opthalmic plexus and orbital adipose tissue, has the function of protecting the very large eye balls (*bulbi oculi*).

2.22 LACRIMAL GLAND

The lacrimal gland is the smallest of the tear glands, lying in a triangle formed by the zygomatic arch, the temporal muscles and the eye ball (Fig. 2–58). Its medial surface presses against the ophthalmic plexus, and it is partially covered on the lateral side by the *periorbita.*

The glandular structure is of the tubuloalveolar type and the secretion is serous.

2.23 ACCESSORY LACRIMAL GLAND

The accessory lacrimal gland is situated ventrolaterally, completely within the orbit (Fig. 2–58). It forms a triangular mass between the zygomatic arch and the temporal muscle, surrounding the eyeball and the optic nerve, investing them rostromedially as it does in the Chinese hamster (Horber *et al.,* 1974). The gland extends caudally 3–4 mm from the zygomatic arch to the area of the optic foramen (*foramen opticum*). Numerous excretory ducts (*ductuli excretorii*) discharge into the conjunctival sac (*saccus conjunctivae*). The fluid is

conveyed through the tear canals (*canaliculi lacrimales*) in the upper and lower eyelids (*palpebrae superior et inferior*) to the lacrimal sac (*saccus lacrimalis*) located at the medial canthus (*angulus oculi medialis*). The lacrimal sac represents the enlarged proximal portion of the nasolacrimal duct (*ductus nasolacrimalis*). Macroscopically, the accessory lacrimal glands are grayish-white to yellow in color.

Histologically, they are compound and tubuloalveolar in structure. The glandular acini are lined by a simple layer of columnar cells. The cells of the glandular epithelium are large, with relatively small, round nuclei basally located. The cytoplasm is very finely granulated.

2.24 NASOLACRIMAL DUCT

Lacrimal secretions drain from the orbit to the nasal vestibule through the nasolacrimal duct (*ductus nasolacrimalis*). As there is no lacrimal bone in the European hamster, the duct exits the orbit through the infraorbital canal (*canalis infraorbitalis*) of the maxillary bone, accompanied by vessels and nerves. Emerging from the infraorbital canal, the duct runs along the lateral wall of the maxilla covered only by muscle. It penetrates the nasal cavity through a small oval foramen located between the maxilla and incisive bone, at about the level of the rostral end of endoturbinal I (Jensen, 1977). It then runs along the internal surface of the incisive bone, ventromedial to the root of the incisor (Figs. 2–12, 2–13), terminating in the nasal vestibule at the level of the incisive duct.

The terminal portion of the nasolacrimal duct is lined with multilayered unkeratinized squamous epithelium, but for most of its length, it is of double-layered prismatic transitional epithelium (Jensen, 1977). In certain places, this epithelium resembles ciliated epithelium.

2.25 CRANIAL AND FACIAL VASCULARIZATION

2.25.1 Arteries

Arterial blood is carried to the head by branches of the common carotid (*a. carotis communis*) and the vertebral (*a. vertebralis*) arteries. The common carotid divides at the level of the thyroid gland into the internal (*a. carotis interna*) and external carotid (*a. carotis externa*) arteries. The external carotid first gives off the occipital artery (*a. occipitalis*) to the neck and then the lingual artery (*a. lingualis*) to the tongue. The continuation of the external carotid is called the maxillary artery (*a. maxillaris*). It gives off the common vascular stem from which the arteries to the masseter (*a. masseterica*) and the cheek pouch (*a. bursa buccalis*) originate. Also coming off this common vascular stem are the transverse facial artery (*a. transversa faciei*) to the zygomatic arch, the auricular arteries (*aa. auricularis caudalis et rostralis*) to the ear, and the superficial temporalis artery (*a. temporalis superficialis*) to the temporal region, respectively. The maxillary artery runs to the *incisura vasorum facialium* and supplies the face as the facial artery (*a. facialis*).

The internal carotid artery (Fig. 2–70) extends to the caudal edge of the mastoid process of the temporal bone (*os temporale, pars mastoidea*). Here it separates into a dorsal and a ventral branch. The ventral branch (*a. intercarotica rostralis*) enters the cranial cavity through the jugular foramen (*foramen jugulare*), at the level of the hypophysis, between the basisphenoid and the mastoid process, and supplies the base of the brain rostral to the hypophysis. The caudal portions of the brain are served by the basilar artery (*a. basilaris*) and its branches, the rostral and caudal cerebellar arteries (*aa. cerebelli rostralis et caudalis*). The dorsal branch extends dorsally along the bulla. Rostral to the *bulla tympanica,* it divides into a ventral branch (*a. maxillaris interna*) which runs through the pterygoid to the orbit, nose and palate, and into a dorsal branch which enters the cranium, runs lateral to the brain and finally becomes the internal ophthalmic artery (*a. ophthalmica interna*) which accompanies the optic nerve. The internal carotid artery does not wind through the base of the cranium nor within the cranial cavity, a pattern also characteristic of the rabbit (Mone, *et al.*, 1973) and the rat (Wells, 1968; Horber, *et al.*, 1974). The nomenclature and distribution of some important arteries of the brain can be seen in Figure 2–70.

2.25.2 Venous Drainage of the Skull and the Ophthalmic Plexus

The external jugular vein (*v. jugularis externa*), the principal vessel draining the head, is formed from the junction of the linguofacial vein (*v. linguofacialis*) and the maxillary vein caudal to the lower jaw (Figs. 2–58, 2–74). At the level of the *incisura*

vasorum facialium the linguofacial vein receives the lingual vein (*v. lingualis*) and facial vein (*v. facialis*). The lingual vein drains the mandibular glands and the tongue. The facial vein drains the lips (*v. labialis mandibularis* and *v. labialis maxillaris*), the dorsal part of the nose (*v. lateralis nasi*) and the medial corner of the eye (*v. angularis oculi*). The latter anastomoses with the superficial temporal vein (*v. temporalis superficialis*), and thereby also with the ophthalmic plexus (*plexus ophthalmicus*).

From caudal to rostral, the maxillary vein (*v. maxillaris*) receives the caudal auricular vein (*v. auricularis caudalis*) and the superficial temporal vein. Thereafter, it runs medially from the jaw joint and takes up a large branch draining the ventral sinus system of the brain. The rostral auricular vein (*v. auricularis rostralis*), the transverse facial vein (*v. transversa faciei*) and the masseteric vein (*v. masseterica*) discharge into the superficial temporal vein which itself ultimately communicates with the caudal edge of the ophthalmic plexus.

The ophthalmic plexus is a large complex of venous blood vessels in the orbit. Blood may be easily drawn from this vascular plexus in the European hamster, just as in the rat (Wells, 1968), mouse (Cohrs, *et al.*, 1958) and Syrian golden hamster (Stewart, *et al.*, 1944; House, *et al.*, 1961; Hoffman, *et al.*, 1968). It fills the caudal half of the orbit completely and invests much of the medial surface of the eyeball and optic nerve. Its largest mass is positioned caudolaterally. The venous plexus also gives off a medial vessel which accompanies the maxillary artery and connects with the basal sinus system of the brain above the *foramen orbitorotundum*. The nomenclature and distribution of the most important veins of the brain can be seen in Figs. 2–58 and 2–74.

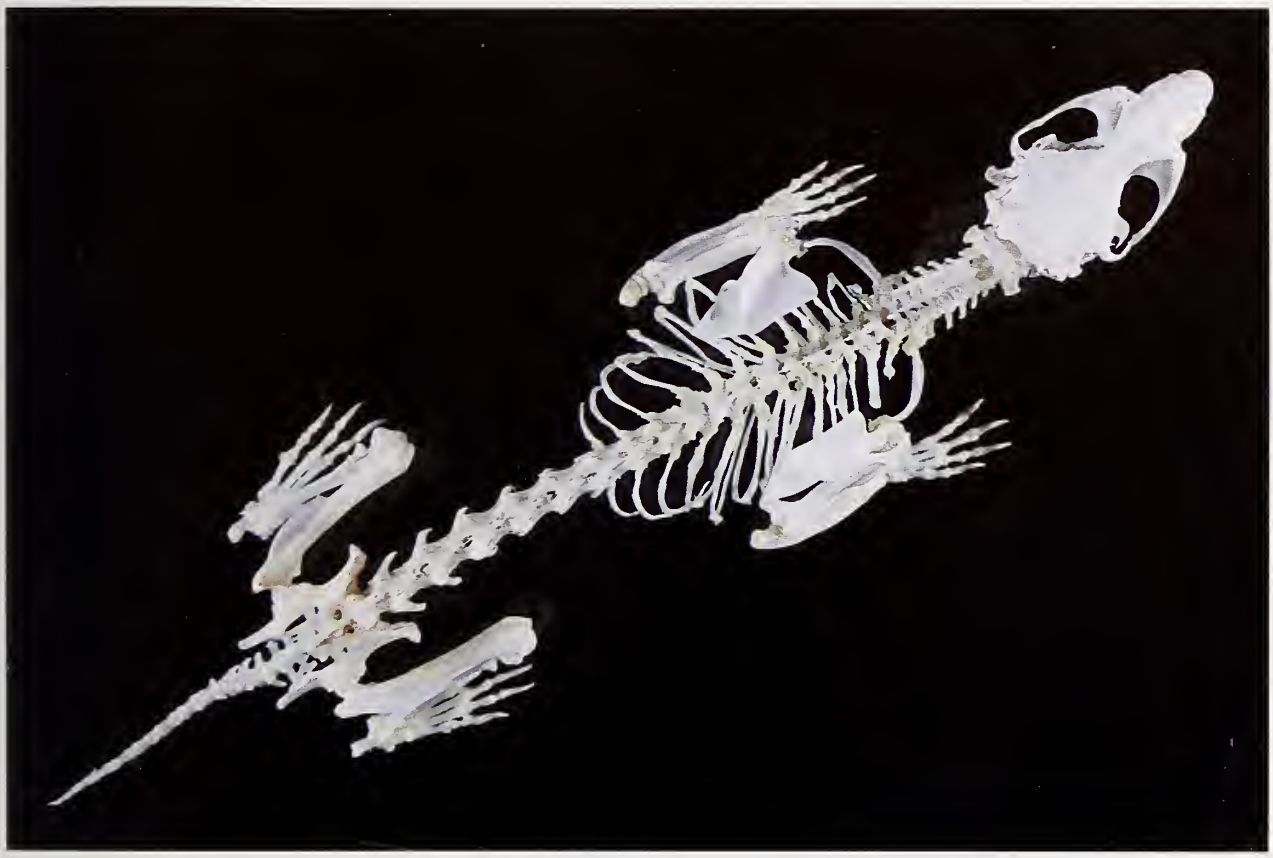

Figure 2-1: Bony skeleton of adult male European hamster; dorsal view.

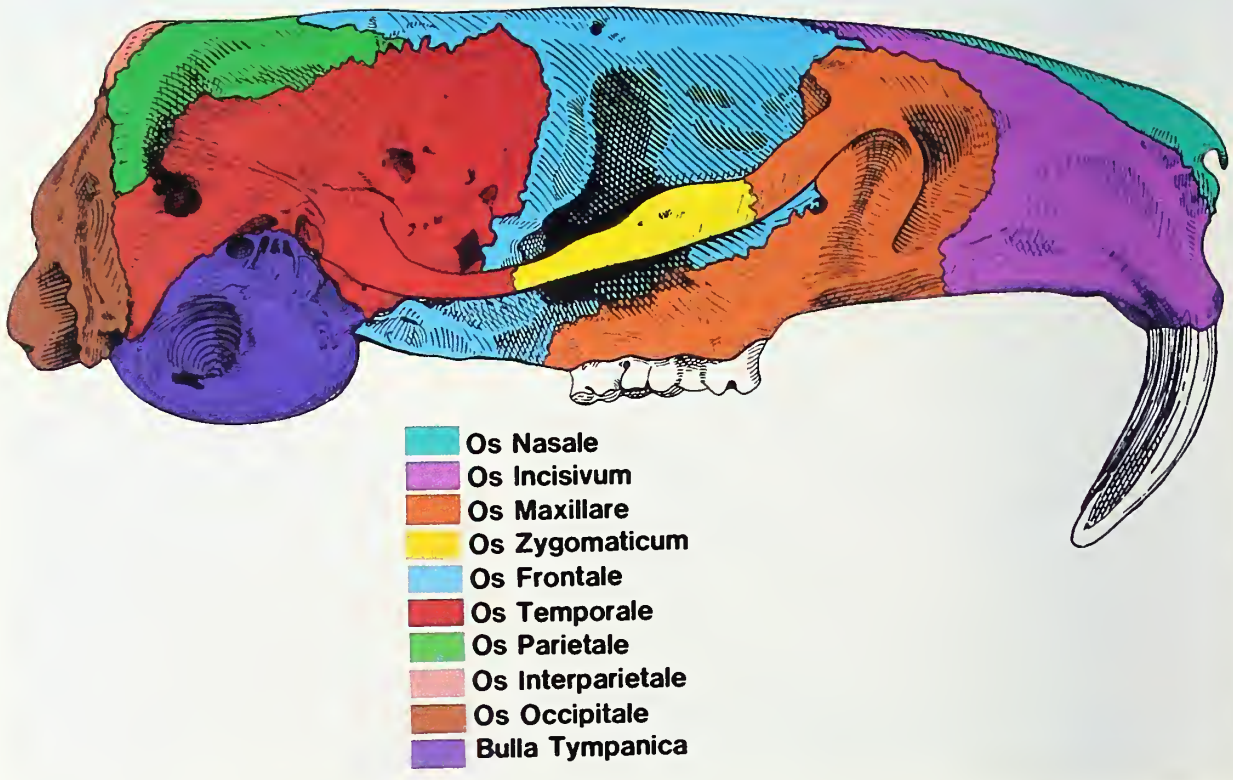

Figure 2-2: Skull of adult hamster with mandibles removed; lateral view.

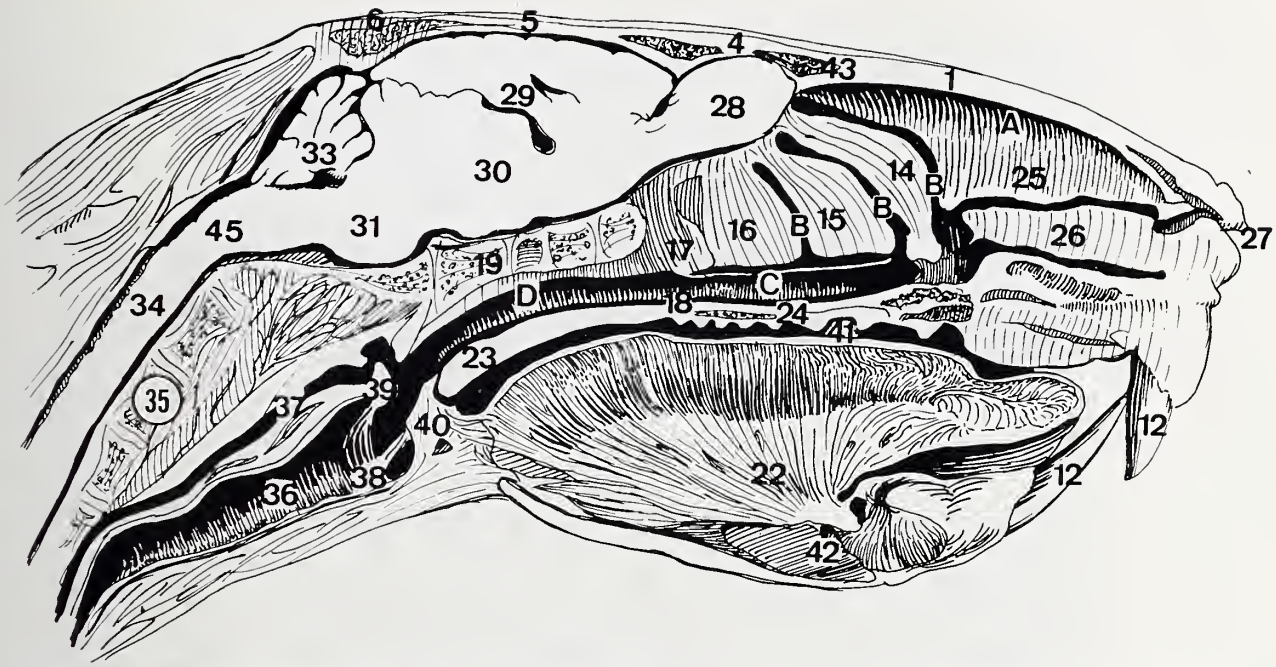

Figure 2-3: Sagittal section sketch of skull and adjacent parts of neck of adult hamster at level of nasal septum (nasal septum lacking). 1=os nasale; 4=os frontale; 5=os parietale; 6=os interparietale; 12=dens incisivum; 14=endoturbinale I; 15=endoturbinale II; 16=endoturbinale III; 17=endoturbinale IV; 18=choanae; 19=os sphenoidale; 22=lingua; 23=palatum molle; 24=palatum durum; 25=concha nasalis dorsalis; 26=concha nasalis ventralis; 27=naris; 28=bulbus olfactorius; 29=cerebrum; 30=adhesio interthalamica; 31=pons; 33=cerebellum; 34=medulla spinalis; 35=vertebrae cervicales; 36=trachea; 37=esophagus; 38=larynx; 39=cartilago arytaenoidea; 40=epiglottis; 41=cavum oris; 42=mandibula; 45=medulla oblongata: A=meatus nasi dorsalis; B=meatus nasi medius; C=meatus nasi ventralis; D=nasopharynx.

Figure 2-4: Sagittal section of skull after fixation in 4% formalin; nasal septum removed except at rostral end of ventral meatus. Note well-developed turbinal apparatus.

Figure 2-5: Sagittal section of formalin fixed skull at level of nasal septum. Note clearly visible nasopharynx which curves only slightly downwards at entrance into larynx.

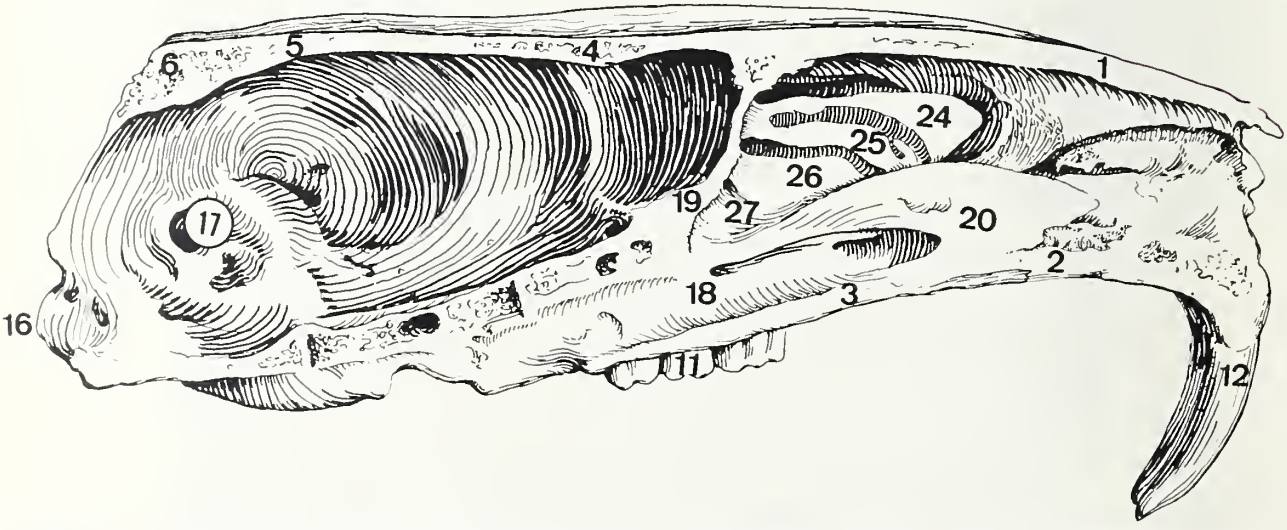

Figure 2-6: Drawing of skull with mandibles removed; sagittal section taken at level of nasal septum. 1=os nasale; 2=os incisivum; 3=maxilla; 4=os frontale; 5=os parietale; 6=os interparietale; 11=dentes molares; 12=dentes incisivi; 16=condylus occipitalis; 17=meatus acusticus internus; 18=choanae; 19=os ethmoides; 20=lamina perpendicularis; 24=endoturbinale I; 25=endoturbinale II; 26=endoturbinale III; 27=endoturbinale IV.

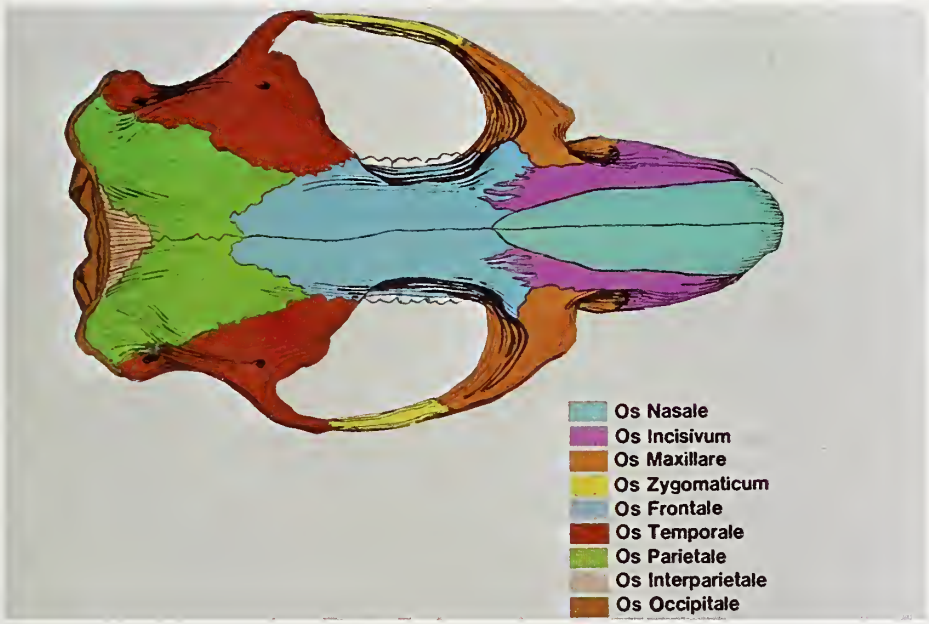

Figure 2-7: Drawing of the skull with the mandibles removed, dorsal view. 1=Os nasale; 2=Os incisivum; 3=Maxilla, processus zygomaticus; 4=Os frontale; 5=Os parietale; 6=Os occipitale; 7=Os interparietale; 9=Os temporale, processus zygomaticus; 10=Os zygomaticum; 11=Dentes molares; 12=Meatus acusticus externus; 13=Orbita.

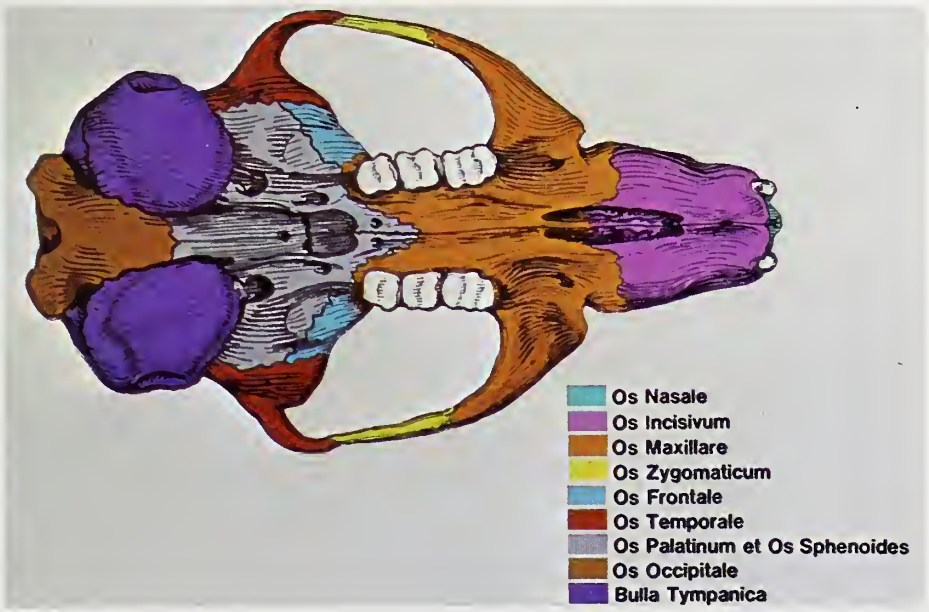

Figure 2-8: Drawing of the skull with the mandibles removed, ventral view. 2=Os incisivum; 3=Maxilla; 7=Os occipitale; 8=Bulla tympanica; 9=Os temporale; 10=Os zygomaticum; 11=Dentes molares; 12=Dentes incisivi; 14=Vomer; 15=Foramen incisivum; 16=Foramen magnum; 17=Meatus acusticus externus; 18=Foramen lacerum; 19=Processus pterygoideus; 20=Foramen jugulare; 21=Synchondrosis sphenooccipitalis; 22=Os sphenoidale; 23=Foramen ovale; 24=Processus pterygoideus; 25=Os palatinum; g=Condylus occipitalis.

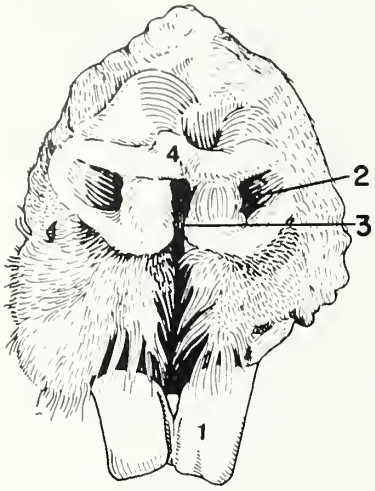

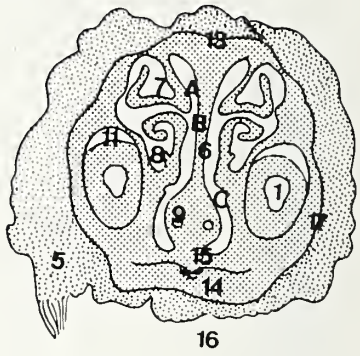

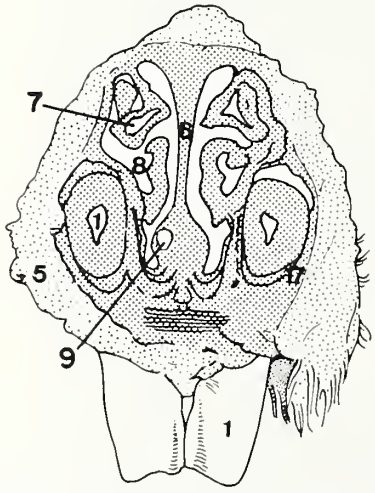

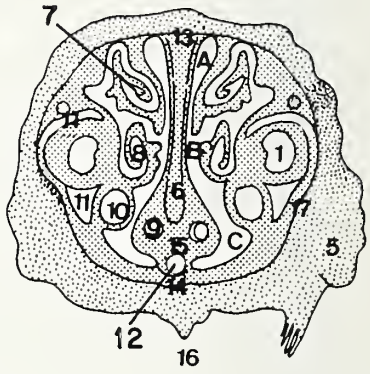

Figure 2-9 (upper left): External appearance of nasal apex in adult hamster. 1=dens incisivus; 2=naris; 3=philtrum; 4=planum nasale.

Figure 2-10 (lower left): Section caudal to lingual aspect of incisors. 1=dens incisivus; 5=cutis; 6=septum nasale; 7=concha nasalis dorsalis; 8=concha nasalis ventralis; 9=organum vomeronasale; 17=maxilla.

Figure 2-11 (upper right): Rostral view of 2 mm thick transverse section immediately caudal to that of Fig. 2-10. Note slightly curled parts of dorsal and ventral conchae. 1=dens incisivus; 5=cutis; 6=septum nasale; 7=concha nasalis dorsalis; 8=concha nasalis ventralis; 9=organum vomeronasale; 11=processus alveolaris; 13=os nasale; 14=palatum durum; 15=vomer; 16=cavum oris; 17=maxilla; A=meatus nasi dorsalis (meatus olfactorius); B=meatus nasi medius; C=meatus nasi ventralis (meatus respiratorius).

Figure 2-12 (lower right): Caudal view of above section (Fig. 2-11) demonstrating highly developed curling of conchal parts. Note nasolacrimal duct (10) and vomeronasal organ (9). 1=dens incisivus; 5=cutis; 6=septum nasale; 7=concha nasalis dorsalis; 8=concha nasalis dorsalis; 9=organum vomeronasale; 10=ductus nasolacrimalis; 11=processus alveolaris; 12=ductus incisivus; 13=os nasale; 14=palatum durum; 15=vomer; 16=cavum oris; 17=maxilla; A=meatus nasi dorsalis; B=meatus nasi medius; C=meatus nasi ventralis.

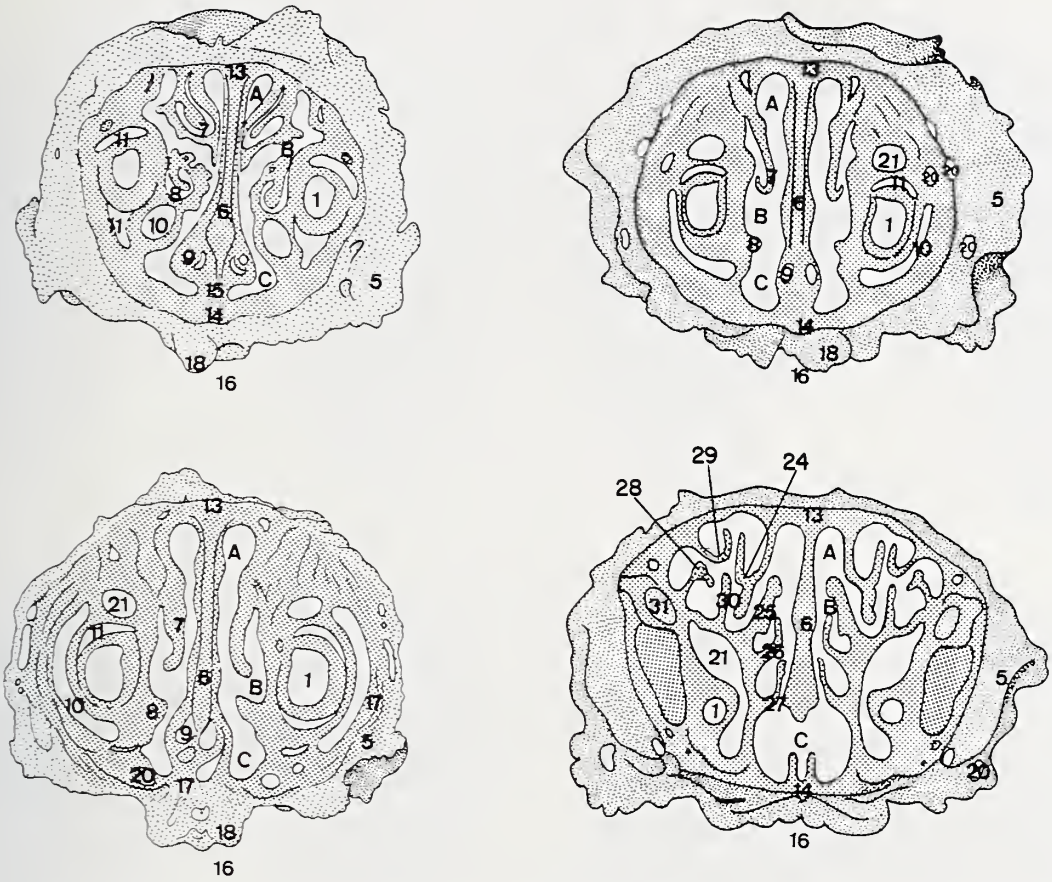

Figure 2-13 (upper left): Rostral view of succeeding section demonstrating distribution of dorsal and ventral conchae and three meatuses in nasal cavity. 1=dens incisivus; 5=cutis; 6=septum nasale; 7=concha nasalis dorsalis; 8=concha nasalis ventralis; 9=organum vomeronasale; 10=ductus nasolacrimalis; 11=processus alveolaris; 13=os nasale; 14=palatum durum; 15=vomer; 16=cavum oris; 18=ruga palatina; A=meatus nasi dorsalis; B=meatus nasi medius; C=meatus nasi ventralis.

Figure 2-14 (lower left): Caudal view of above section. 1=dens incisivus; 5=cutis; 6=septum nasale; 7=concha nasalis dorsalis; 8=concha nasalis ventralis; 9=organum vomeronasale; 10=ductus nasolacrimalis; 11=processus alveolaris; 13=os nasale; 16=cavum oris; 17=maxilla; 18=ruga palatina; 20=blood vessel; 21=sinus maxillaris; A=meatus nasi dorsalis; B=meatus nasi medius; C=meatus nasi ventralis.

Figure 2-15 (upper right): Rostral view of succeeding section: 1=dens incisivus; 5=cutis; 6=septum nasale; 7=concha nasalis dorsalis; 8=concha nasalis ventralis; 9=organum vomeronasale; 11=processus alveolaris; 13=os nasale; 14=palatum durum; 16=cavum oris; 18=ruga palatina; 19—recessus cavi nasi; 20=blood vessel; 21=sinus maxillaris; A=meatus nasi dorsalis; B=meatus nasi medius; C=meatus nasi ventralis.

Figure 2-16 (lower right): Caudal view of above section. Note endoturbinals (24-27), ectoturbinals (28-30), and maxillary sinus (21), the only paranasal cavity of European hamster. 1=dens incisivus; 5=cutis; 6=septum nasale; 13=os nasale; 14=palatum durum; 16=cavum oris; 20=blood vessel; 21=sinus maxillaris; 24=endoturbinale I; 25=endoturbinale II; 26=endoturbinale III; 27=endoturbinale IV; 28=ectoturbinale I; 29=ectoturbinale II; 30=ectoturbinale III; 31=glandula lacrimalis; A=meatus nasi dorsalis; B=meatus nasi medius; C=meatus nasi ventralis.

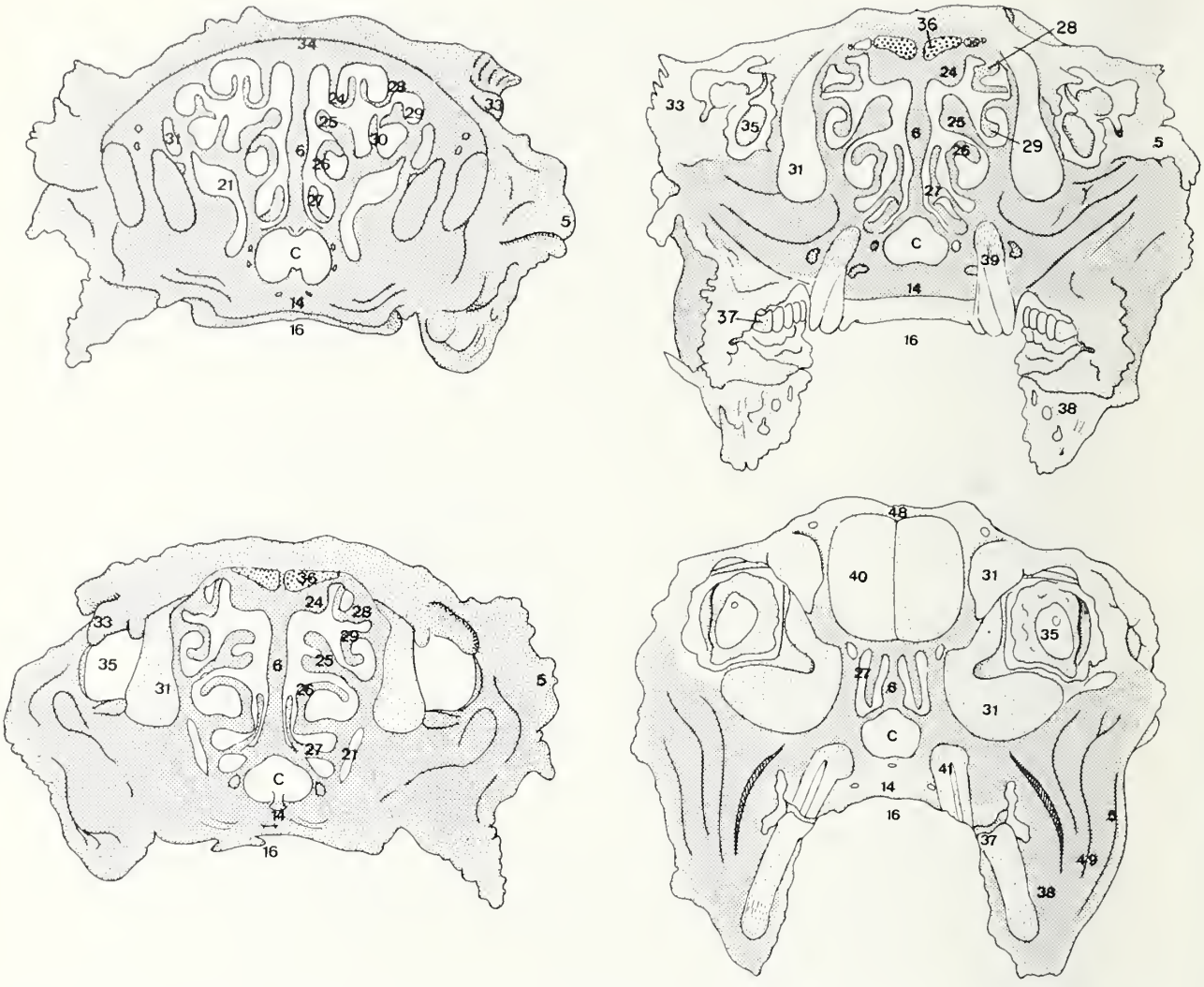

Figure 2-17 (upper left): Rostral view of succeeding section: 5=cutis; 6=septum nasale; 14=palatum durum; 16=cavum oris; 21=sinus maxillaris; 24=endoturbinale I; 25=endoturbinale II; 26=endoturbinale III; 27=endoturbinale IV; 28=ectoturbinale I; 29=ectoturbinale II; 30=ectoturbinale III; 31=glandula lacrimalis; 33=palpebra; 34=os frontale; C=meatus nasi ventralis.

Figure 2-18 (bottom left): Caudal view of above section; note eyes (35) and orbital adipose tissue with lacrimal gland (31). 5=cutis; 6=septum nasale; 14=palatum durum; 16=cavum oris; 21=sinus maxillaris; 24=endoturbinale I; 25=endoturbinale II; 26=endoturbinale III; 27=endoturbinale IV; 28=ectoturbinale I; 29=ectoturbinale II; 31=corpus adiposum orbitae et glandula lacrimalis; 33=palpebra; 35=bulbus oculi; 36=diploë; C=meatus nasi ventralis.

Figure 2-19 (upper right): Rostral view of succeeding section. 5=cutis; 6=septum; 14=palatum durum; 16=cavum oris; 24=endoturbinale I; 25=endoturbinale II; 26=endoturbinale III; 27=endoturbinale IV; 28=ectoturbinale I; 29=ectoturbinale II; 31=corpus adiposum orbitae et glandular lacrimalis; 33=palpebra; 35=bulbus oculi; 36=diploë; 37=dens molaris; 38=mandibula; 39=radix molaris; C=meatus nasi ventralis.

Figure 2-20 (lower right): Caudal view of above section. 5=cutis; 6=septum; 14=palatum durum; 16=cavum oris; 27=endoturbinale IV; 31=corpus adiposum orbitae et glandula lacrimalis; 35=bulbus oculi; 37=dens molaris; 38=mandibula; 40=bulbus olfactorius; 41=pulpa dentis; C=meatus nasi ventralis.

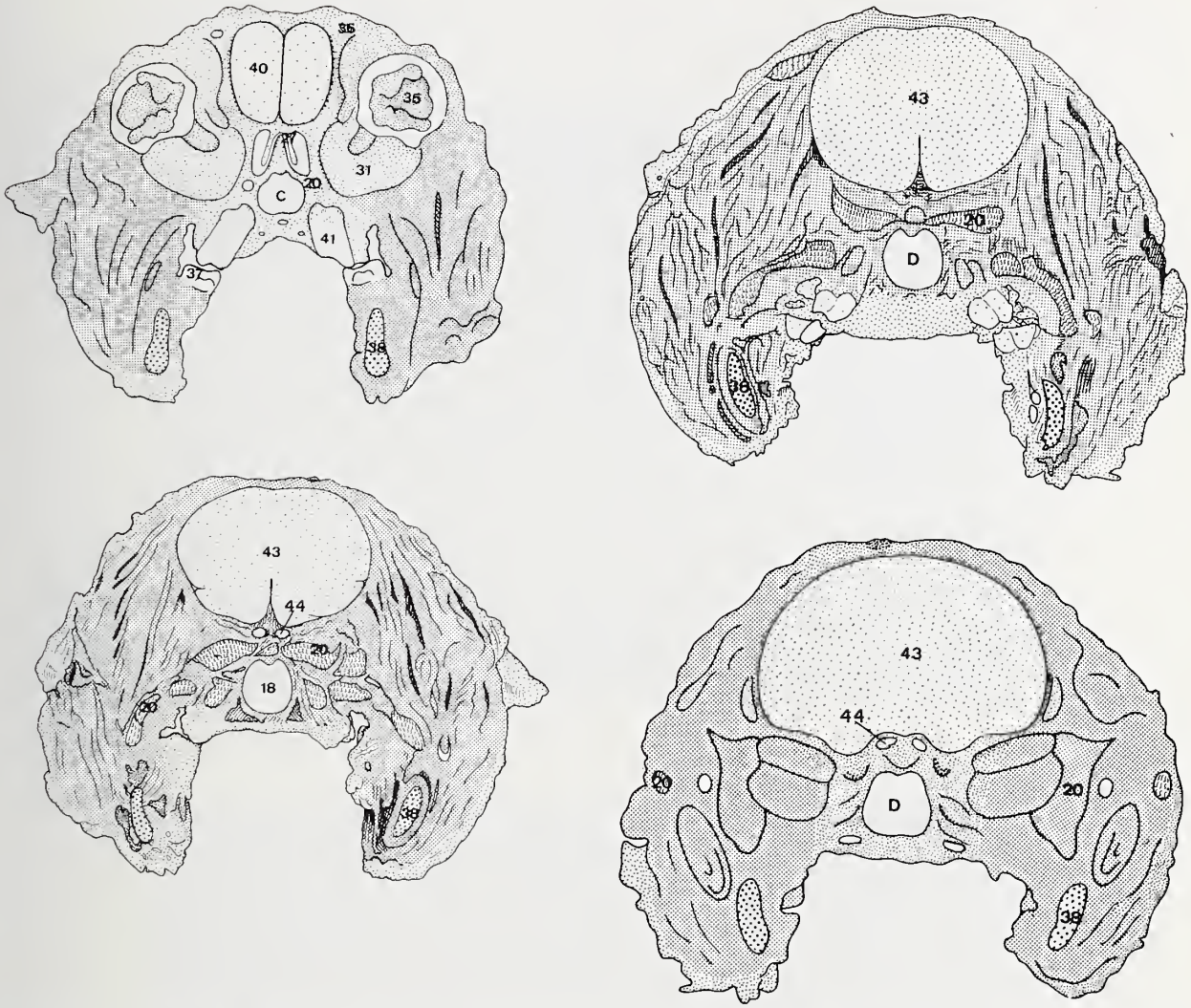

Figure 2-21 (upper left): Rostral view of succeeding section. 20=blood vessel; 27=endoturbinale IV; 31=corpus adiposum orbitae et glandula lacrimalis; 35=bulbus oculi; 36=diploë; 37=dens molaris; 38=mandibula; 40=bulbus olfactorius; 41=pulpa dentis; C=meatus nasi ventralis.

Figure 2-22 (lower left): Caudal view of above section; 18=choanae; 20=blood vessel; 38=mandibula; 43=cerebrum; 44=nerve.

Figure 2-23 (upper right): Rostral aspect of succeeding section. 20=blood vessel; 38=mandibula; 43=cerebrum; 44=nerve; D=nasopharynx.

Figure 2-24 (lower right): Caudal view of above section. 20=blood vessel; 38=mandibula; 43=cerebrum; 44=nerve; D=nasopharynx.

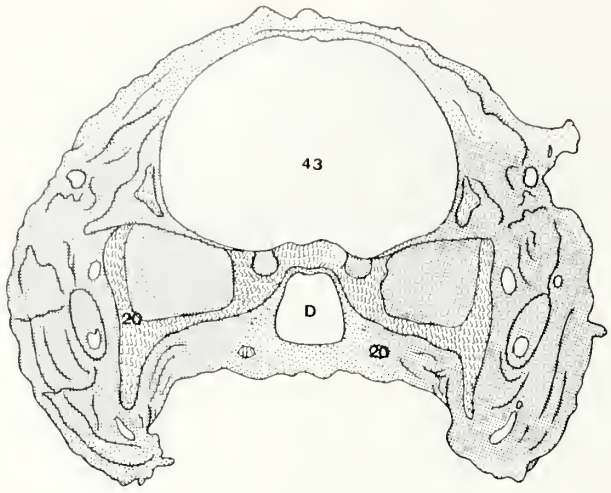

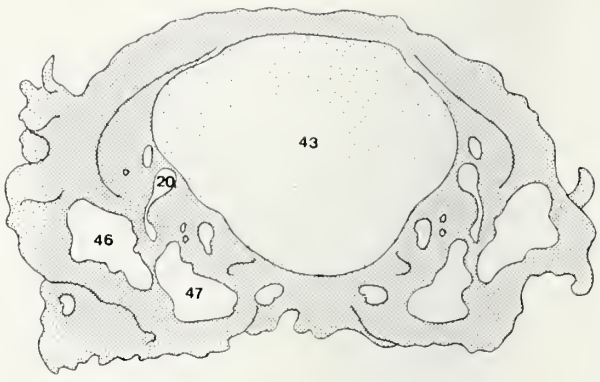

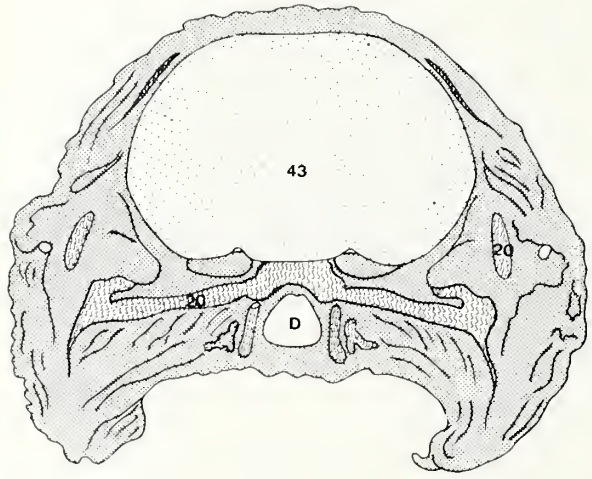

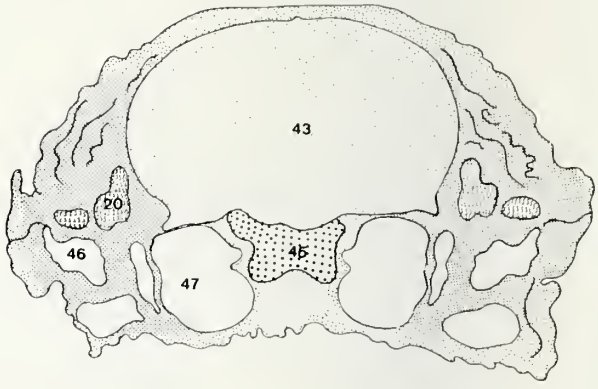

Figure 2-25 (upper left): Rostral view of succeeding section. 20 = blood vessel; 43 = cerebrum; D = nasopharynx.

Figure 2-26 (lower left): Caudal view of above section. 20 = blood vessel; 43 = cerebrum; D = nasopharynx.

Figure 2-27 (upper right): Rostral view of succeeding section. 20 = blood vessel; 43 = cerebrum; 46 = meatus acusticus externus; 47 = auris media.

Figure 2-28 (lower right): Caudal view of above section. 20 = blood vessel; 43 = cerebrum; 45 = os basisphenoidale; 46 = meatus acusticus externus; 47 = auris media.

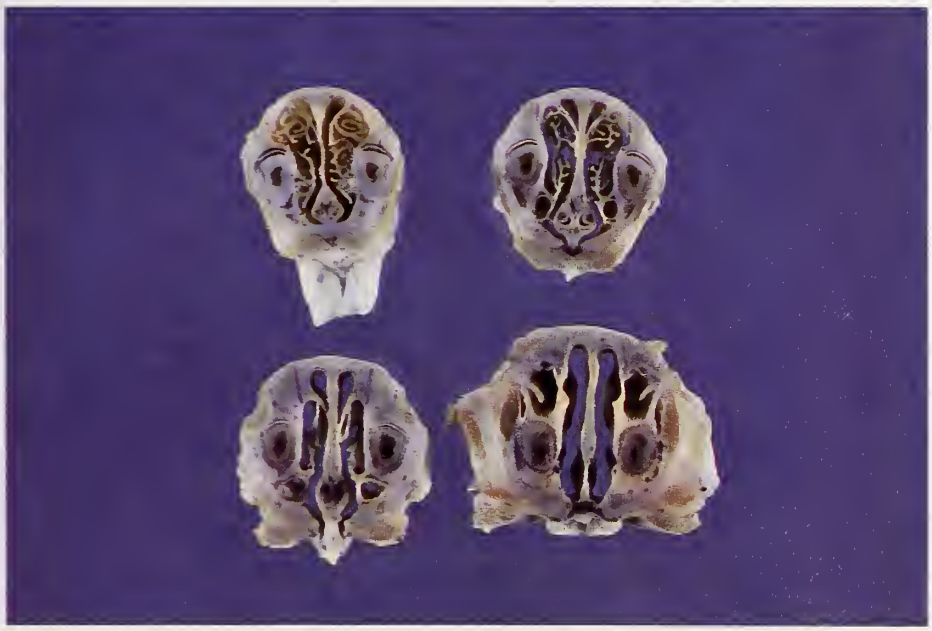

Figure 2-29: Rostral view of first four sections demonstrating beginning of dorsal and ventral nasal conchae.

Figure 2-30: Caudal view of above sections.

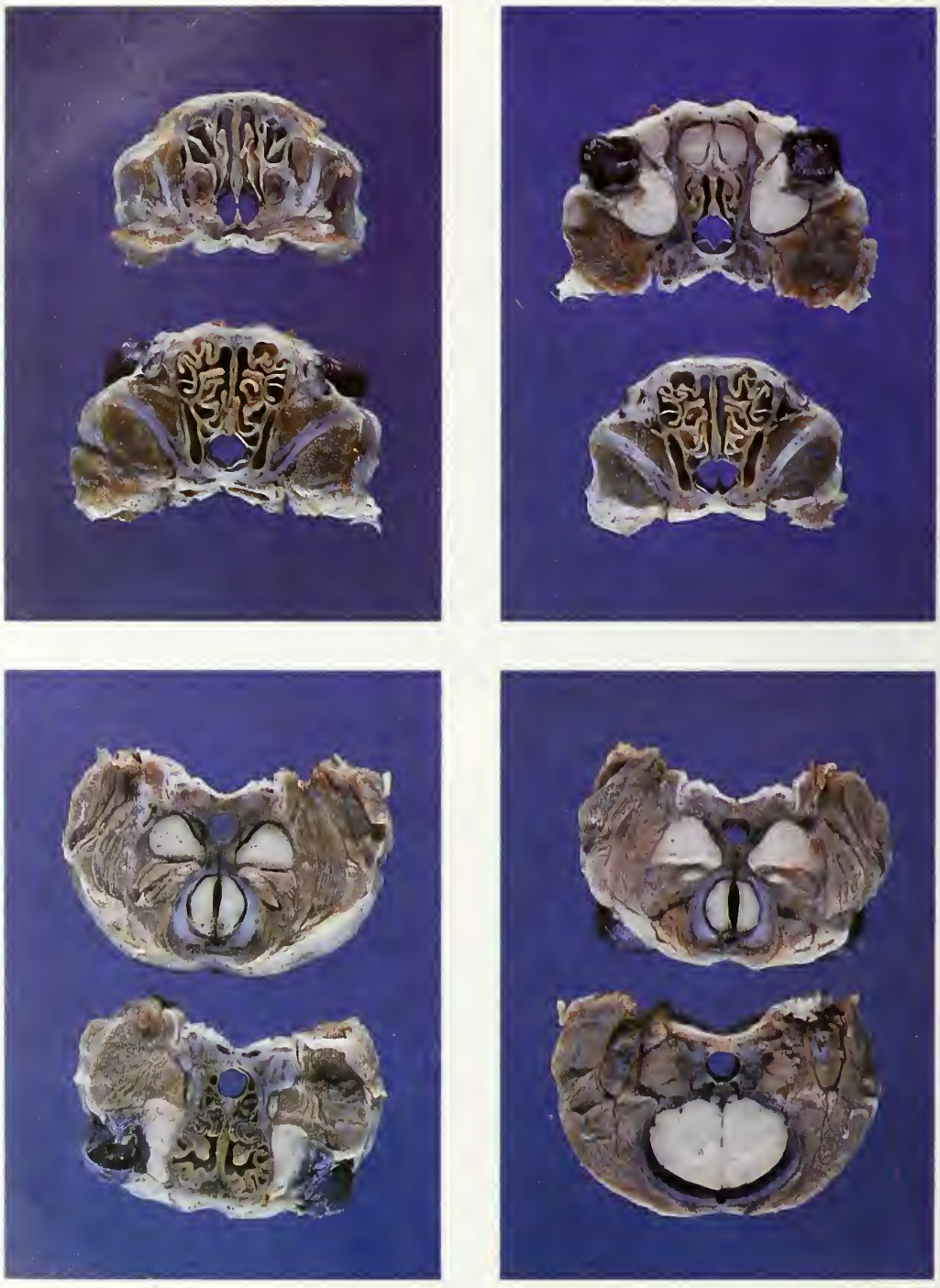

Figure 2-31 (upper left): Rostral view of succeeding two serial sections. Note maxillary sinus on lower section.

Figure 2-32 (upper right): Caudal view of above sections. Note large mass of orbital adipose tissue in upper section.

Figure 2-33 (lower left): Rostral side of following two sections; note endo- and ectoturbinals in upper section.

Figure 2-34 (lower right): Caudal view of above two sections; note olfactory bulb in lower section.

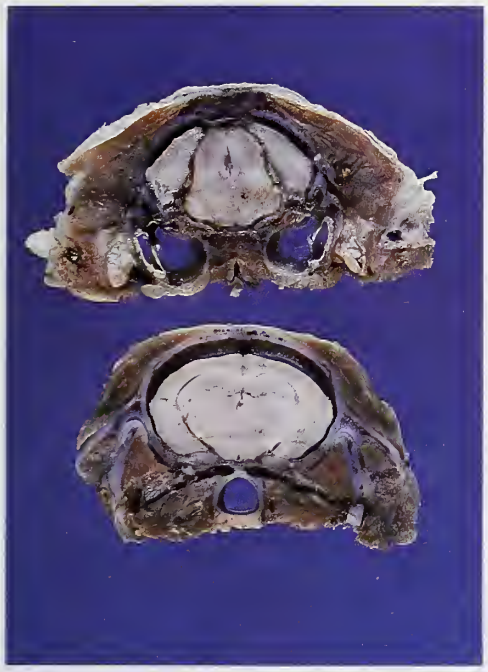

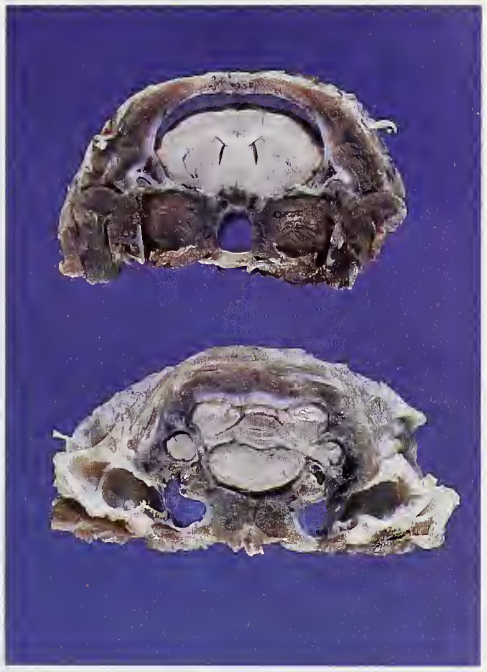

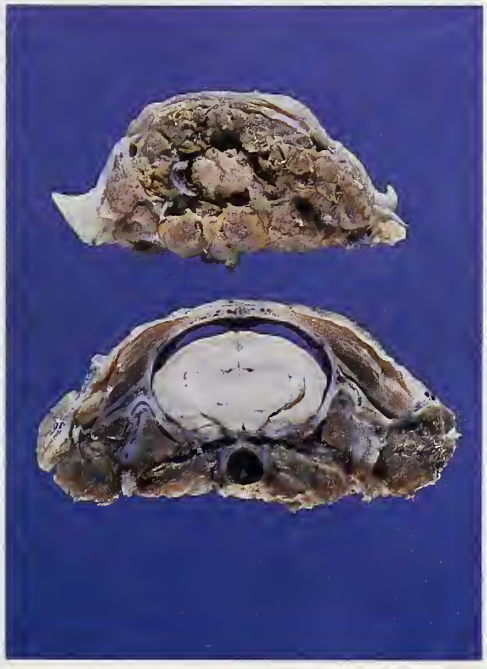

Figure 2-35 (upper left): Rostral view of next two serial sections; upper shows middle ear.

Figure 2-36 (upper right): Caudal view of above two sections.

Figure 2-37 (lower): Caudal view of last two sections: top, cervical region; bottom, last section of skull.

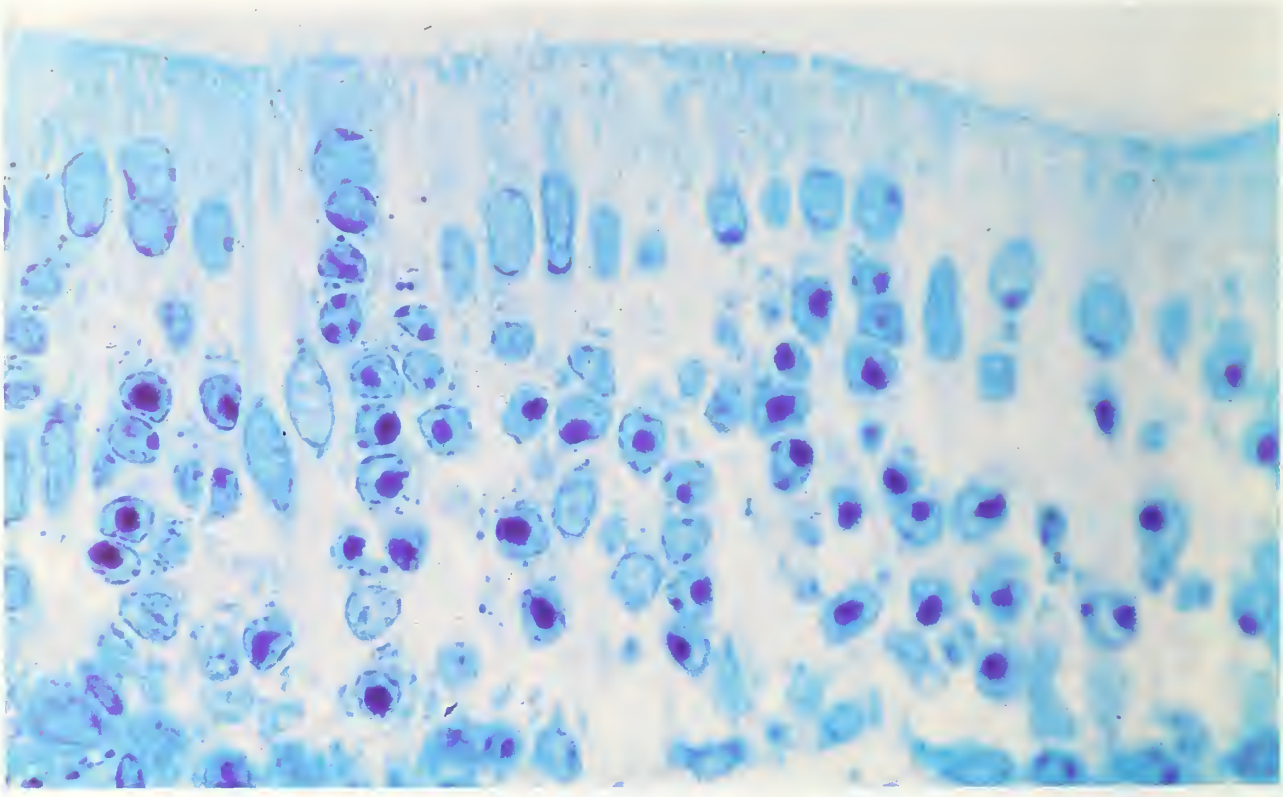

Figure 2-38 (above): Histology of epithelial layer of endoturbinals: olfactory epithelium. (Toluidine blue, X1043).

Figure 2-39 (below): Lateral sketch of skull demonstrating major air-conducting pathways.

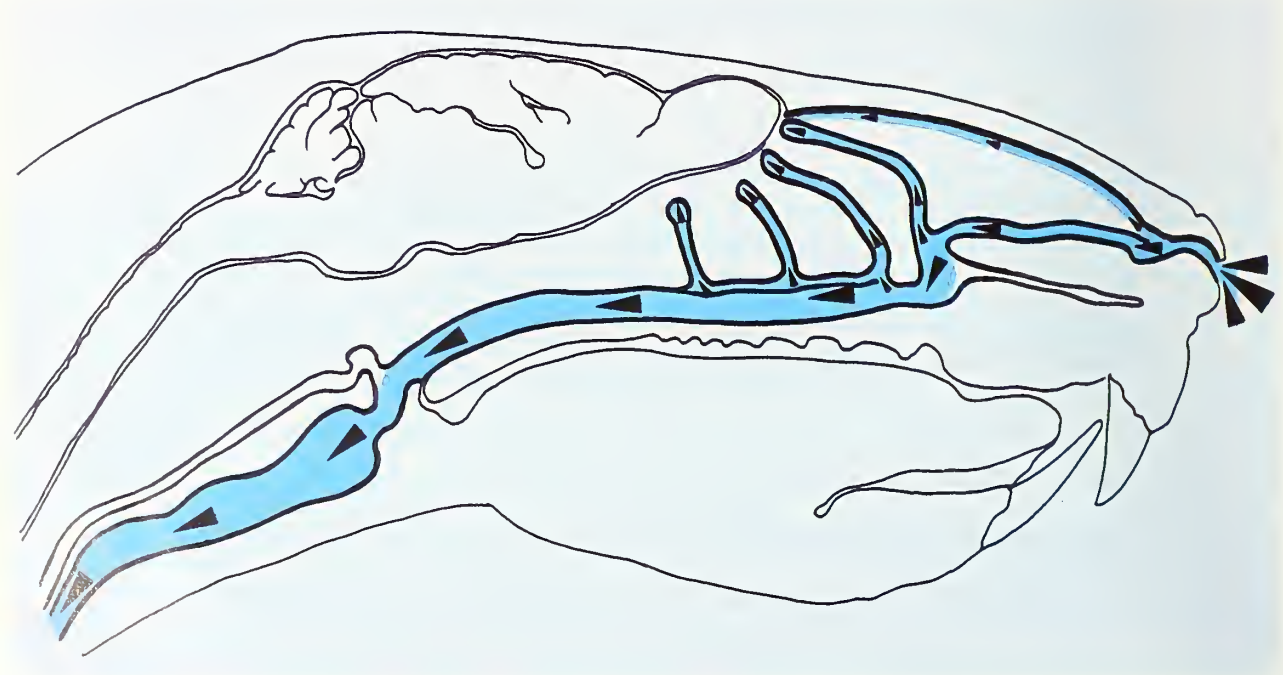

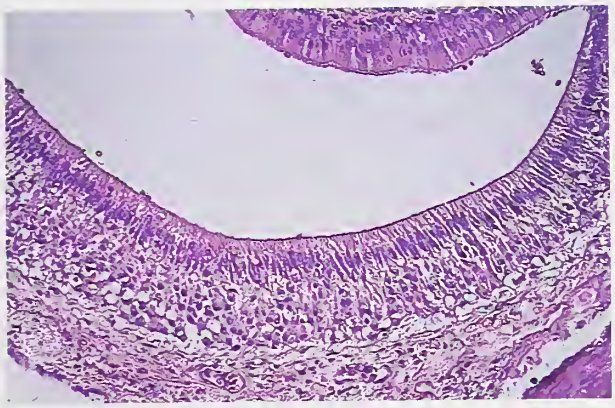

Figure 2-40: Histology of vomeronasal organ, one side of which (above) is covered with olfactory epithelium and the other (below) with pseudostratified ciliated columnar epithelium. (H & E, X37).

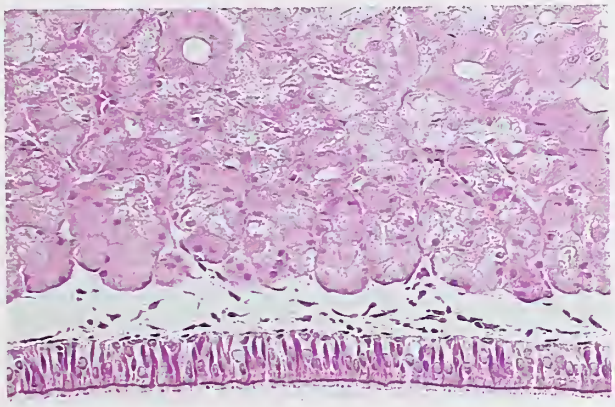

Figure 2-41: Histology of dorsal nasal concha, covered by pseudostratified ciliated columnar epithelium. (H & E, X145).

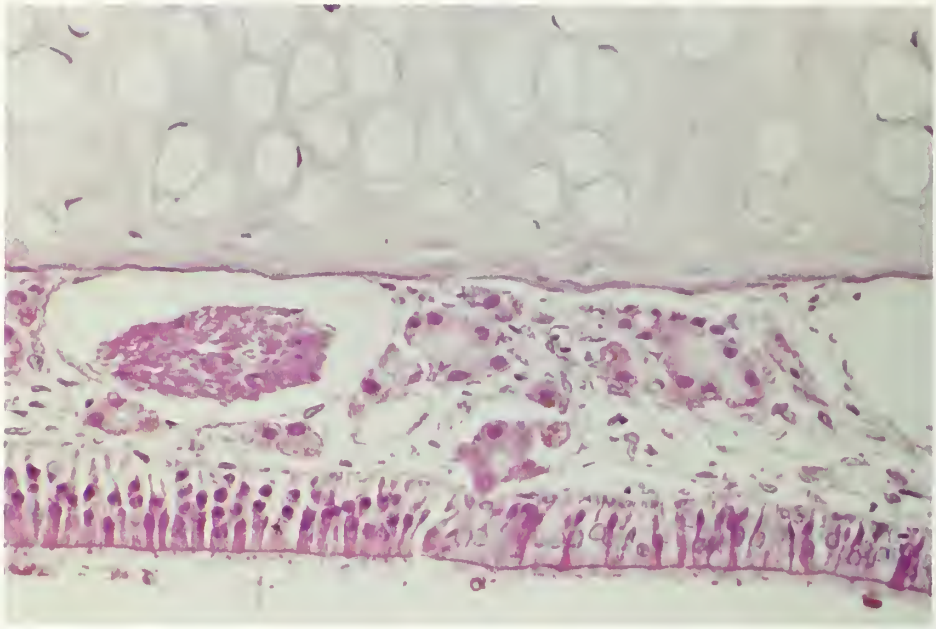

Figure 2-42 (lower): Nasal septum coated with pseudostratified columnar ciliated epithelium on left and with olfactory epithelium on right. Between epithelium and cartilage is well developed submocosal layer. (H & E, X60).

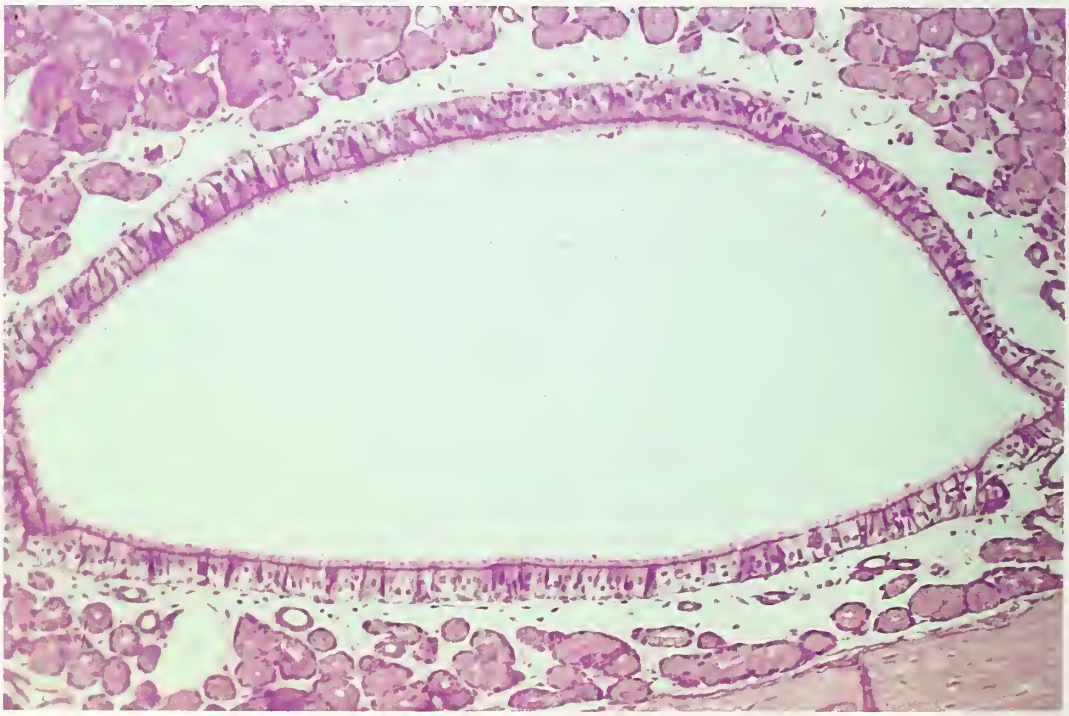

Figure 2-43: Wall of maxillary sinus at low magnification, consisting of three layers: epithelium, subepithelial (lateral nasal) glands, and maxillary bone. (H & E, X64).

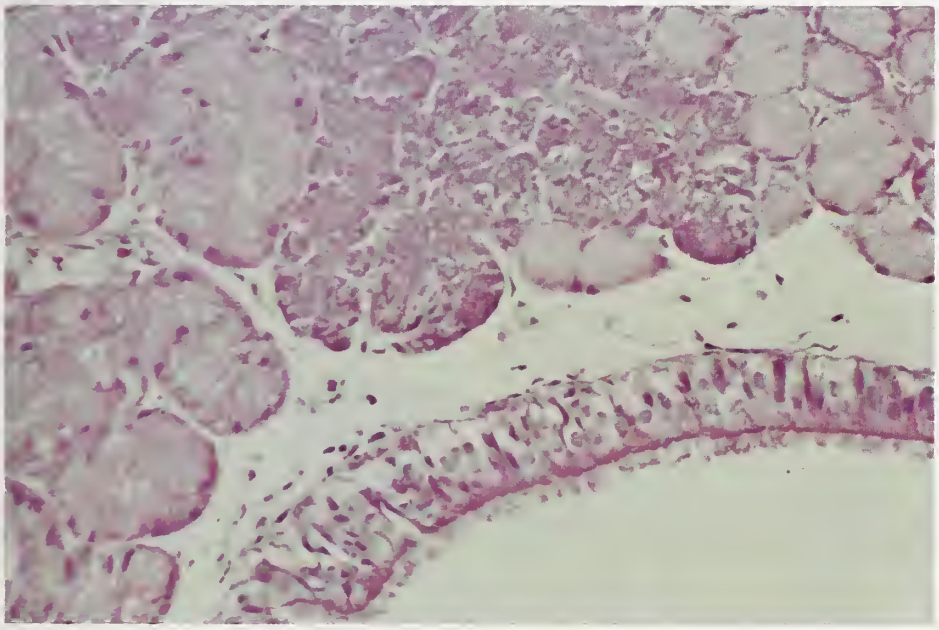

Figure 2-44: Histology of maxillary sinus at higher magnification, demonstrating that pseudostratified columnar epithelium is of ciliated type, and that subepithelial layer consists of mucous glands. (H & E, X160).

Figure 2-45: Mandible. a, lateral view; b, medial view; A = corpus mandibulae; 1 = dens incisivus; 2 = dentes molares; 3 = processus condylaris; 4 = processus angularis; 5 = processus coronoideus; 6 = incisura vasorum facialium; 7 = foramen mentale; 8 = foramen mandibulae; 9 = fossa masseterica; 10 = fossa pterygoidea; 11 = articulatio intermandibularis.

Figure 2-46: Dorsal aspect of oral cavity, showing hard palate and soft palate. Note four well-developed rostral palatine rugae, and four smaller caudal pairs, which do not fuse completely in midline.

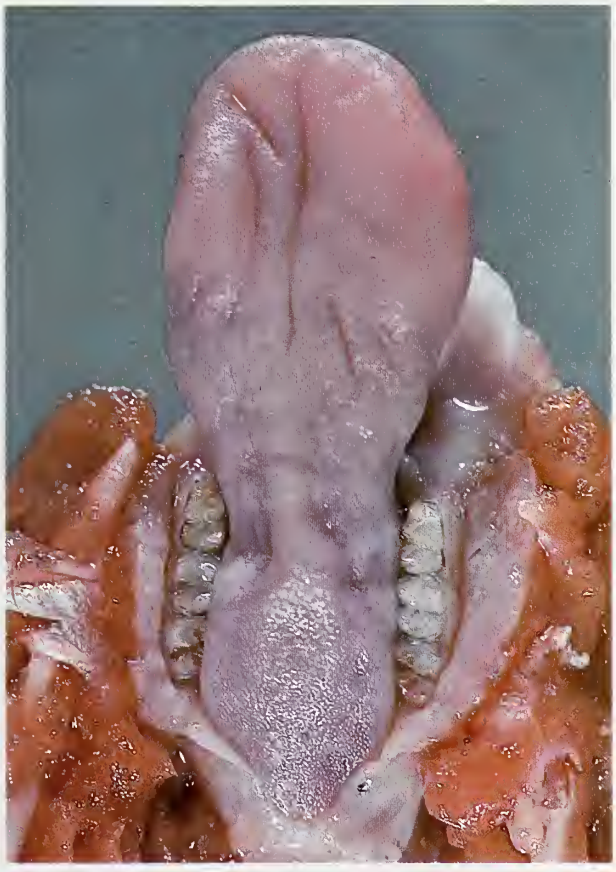

Figure 2-47: Floor of the oral cavity; main part formed by spoon-shaped tongue.

Figure 2-48: Cheek pouch *in situ,* demonstrating superficial position of this structure. Note mucous membrane, which forms delicate longitudinal folds.

Figure 2-49: Radiogram of adult European hamster, demonstrating size and shape of cheek pouches in distended state. Cheek pouches filled with 10 ml mikropaque (Nicolas).

Figure 2-50: *In situ,* preparation of m. retractor bursae buccalis et retractor buccinator. The muscle originates in m. longissimus dorsi at the level of first and second lumbar vertebrae and inserts on the caudal aspect of cheek pouch.

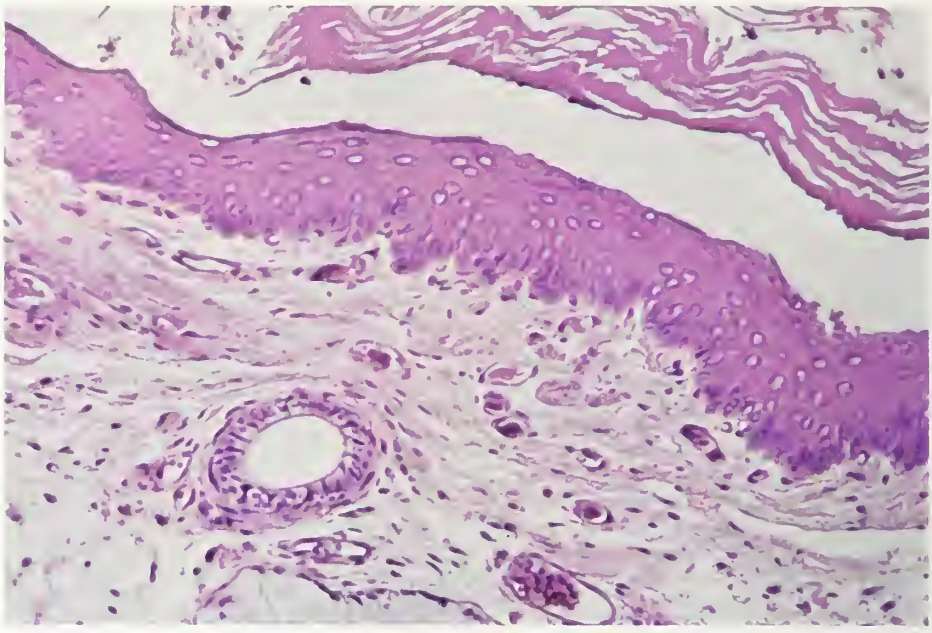

Figure 2-51: Histology of hard palate. Mucous membrane consists of stratified squamous epithelium with keratinization. Note presence of submucous gland. (H & E, X57).

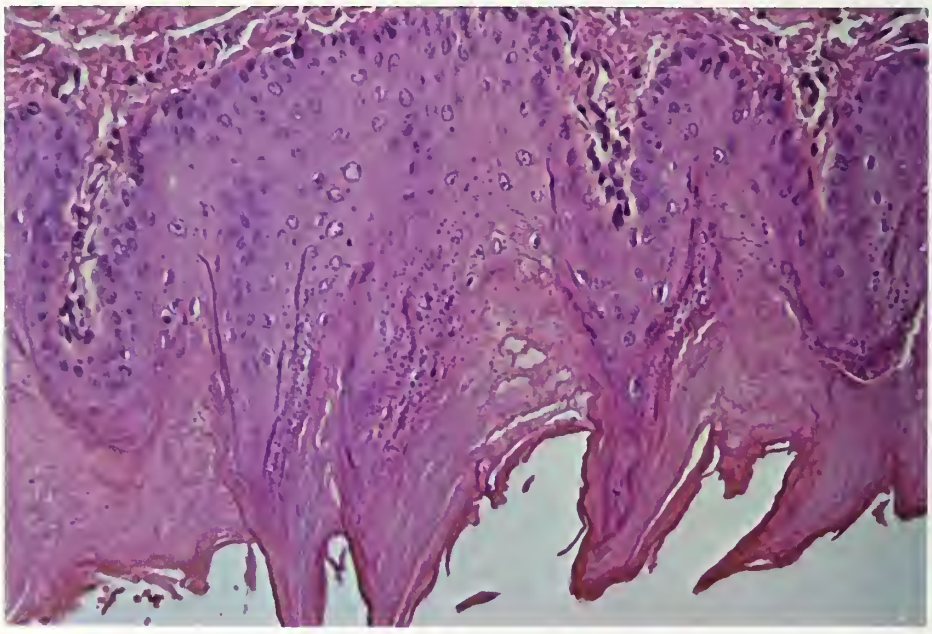

Figure 2-52: Histology of tongue. Stratified squamous epithelium forms prominent papillae which show thick superficial layer of cornified cells. (H & E, X141).

Figure 2-53: Radiogram of skull of adult hamster demonstrating long roots of incisors and molars. Note also bony skeleton of endo- and ectoturbinals. (X2.5).

Figure 2-54: Radiogram of dorsal view of skull from 1-year-old male. (X2.5).

Figure 2-55: Occlusal views of upper and lower jaws. Note: rows of molars do not parallel each other.

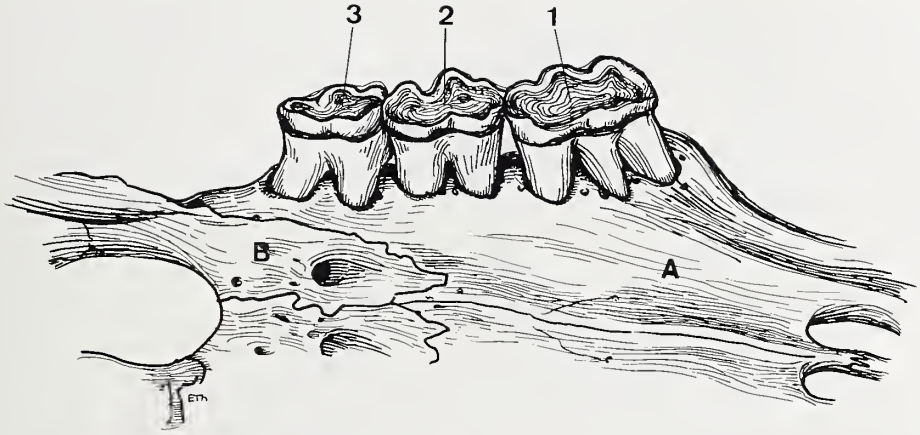

Figure 2-56: Right palatine, ventral view. A=maxilla; b=palatine; 1=first molar; 2=second molar; 3=third molar.

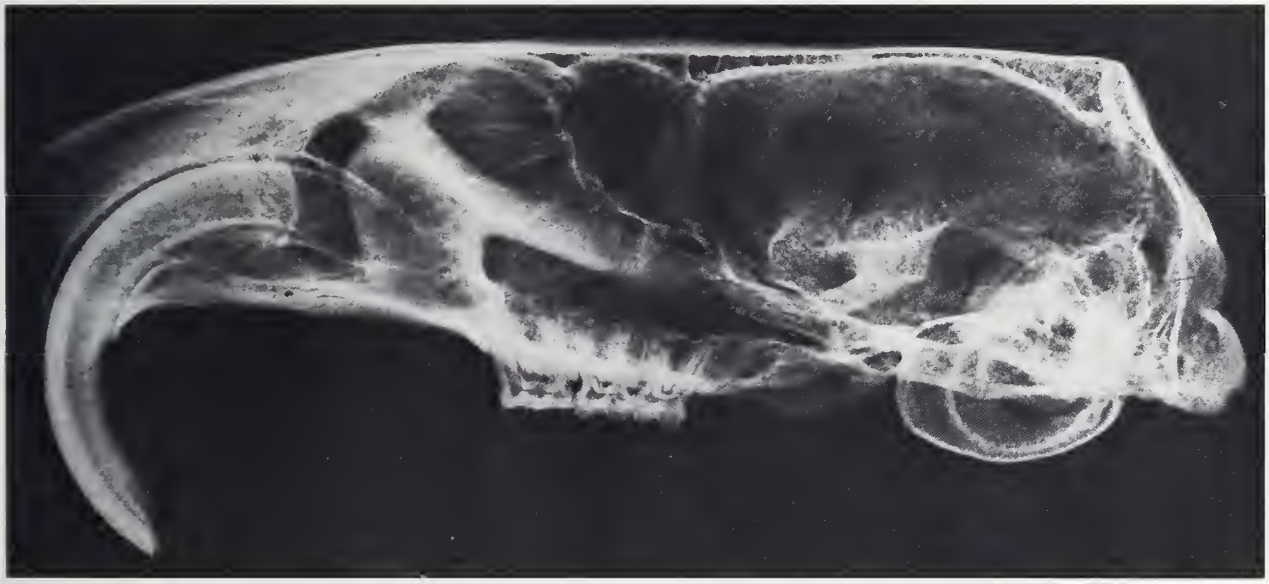

Figure 2-57: Radiogram of lateral aspect of adult hamster skull. Note long root of incisor, which originates far caudally in incisive bone and bony base of turbinal apparatus. (Mandibles are removed, X2.5) (See also Figure 2-53).

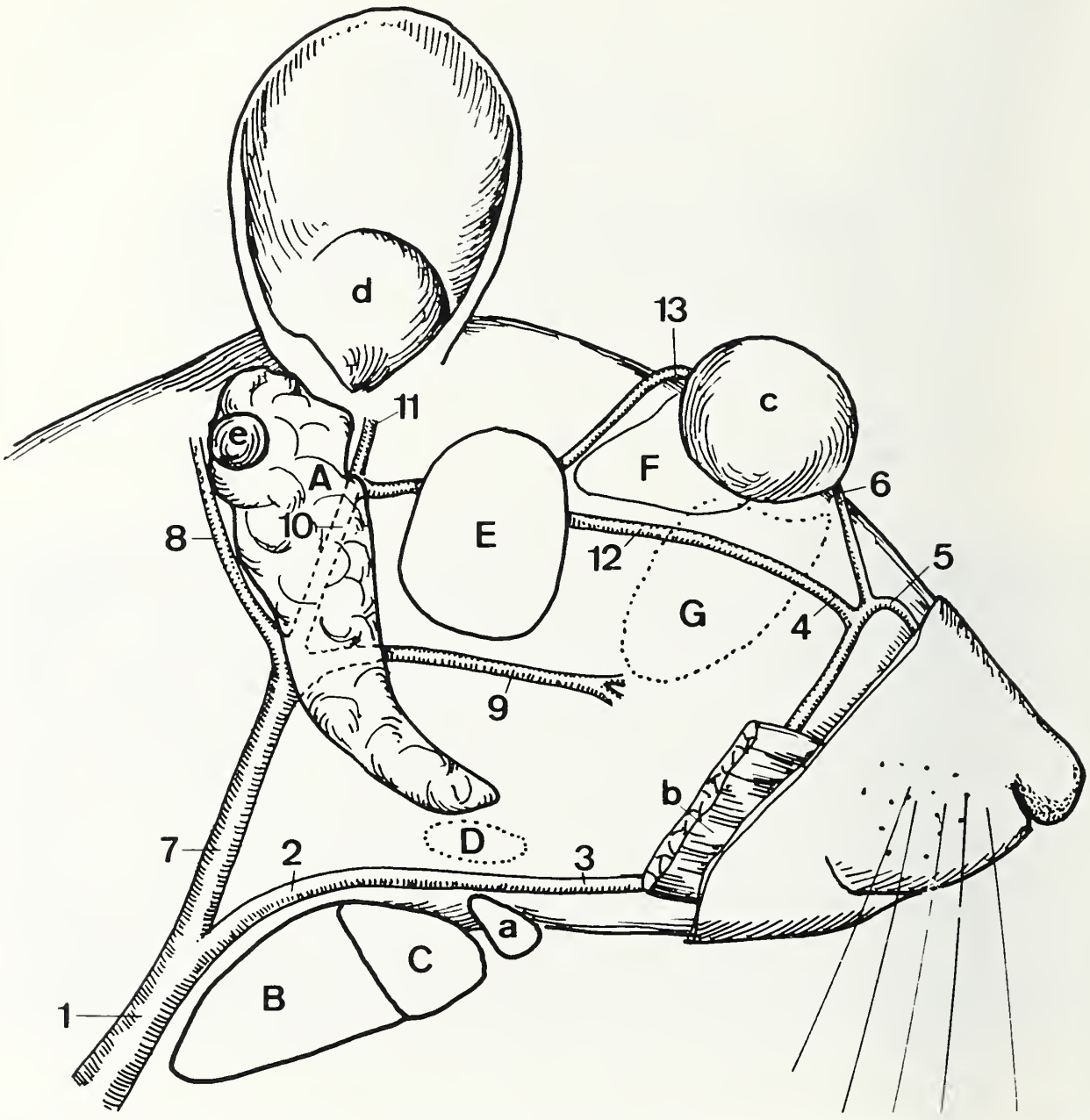

Figure 2-58: Schematic drawing of head of one-year-old male European hamster, lateral view. A–D=salivary glands; A=parotis; B=gl. mandibularis; C=gl. sublingualis major; D=gl. sublingualis minor; E=gl. zygomatica; F–G=lacrimal glands; F=gl. lacrimalis; G=gl. lacrimalis accessoria; a=lymphocentrum mandibulare; b=bursa buccalis; c=bulbus oculi; d=ear; e=ln. parotideus; 1=v. jugularis externa; 2=v. linguofacialis; 3=v. facialis; 4=anastomosis to v. transversa faciei; 5=v. lateralis nasi; 6=v. angularis oculi; 7=v. maxillaris; 8=v. auricularis caudalis; 9=v. masseterica; 10=v. temporalis superficialis; 11=v. auicularis rostralis; 12=v. transversa faciei; 13=connecting branch of v. temporalis superficialis to ophthalmic plexus.

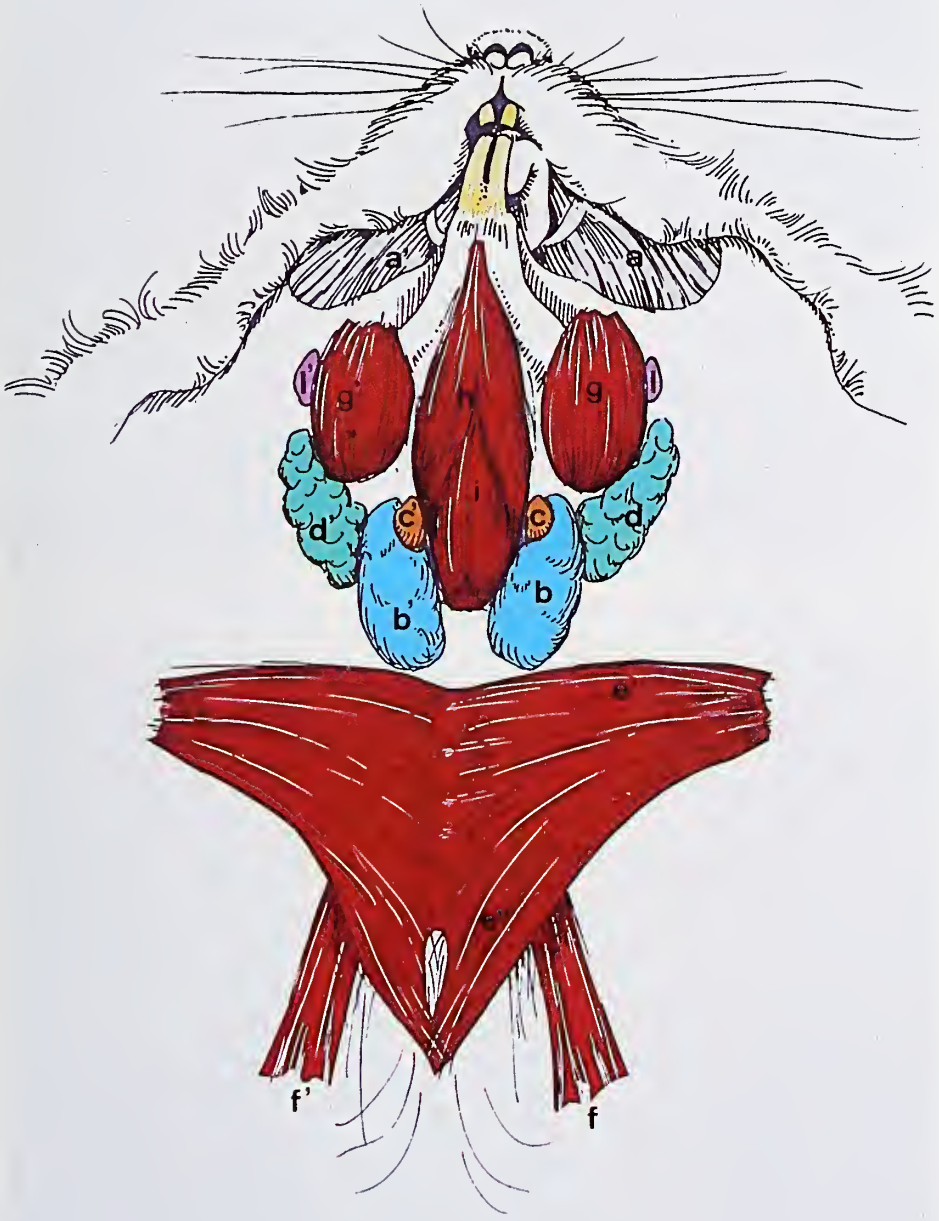

Figure 2-59: Schematic drawing of ventral cervical region demonstrating positions of salivary glands in relation to surrounding tissues: a–a′=bursa buccalis; b–b′=glandula mandibularis; c–c′=glandula sublingualis; d–d′=parotis; e′–e″=m. pectoralis superficialis; e′=pars clavicularis; e″=pars sternocostalis; f–f′=m. obliquus abdominis externus; g–g′=m. masseter; h=m. digastricus; i=m. sternohyoideus; l–l′=glandula zygomatica.

Figure 2-60: Paired salivary glands *in situ*. Larger mandibular glands show lobular structure. At cranial poles are smaller sublingual glands.

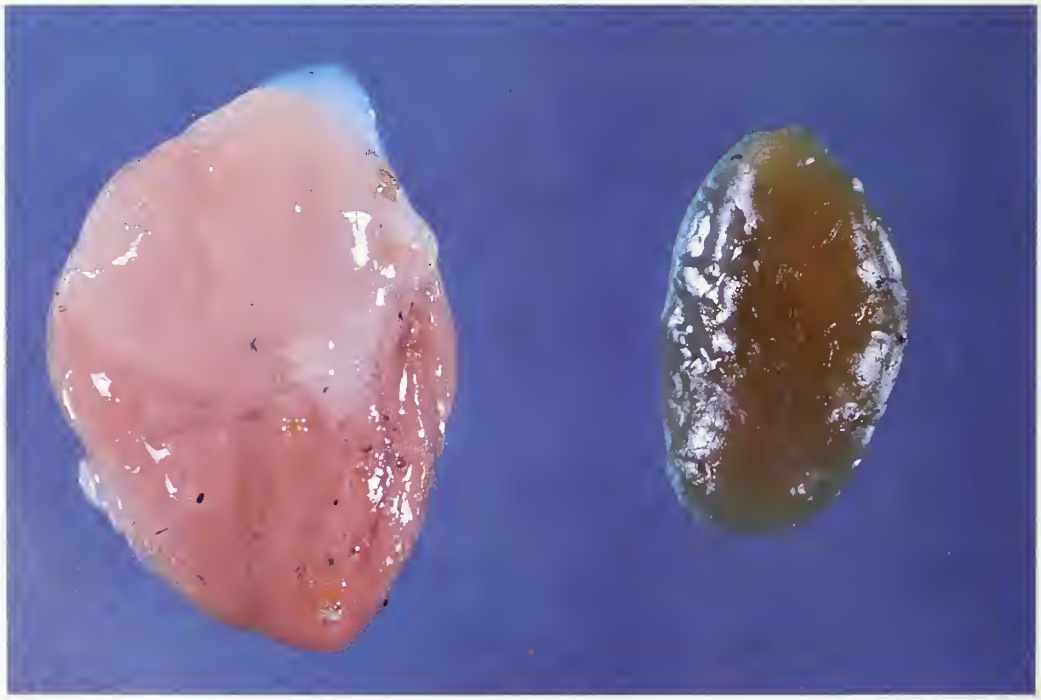

Figure 2-61: Some isolated digestive glands of adult European hamster: on left is pinkish-white mandibular gland, at cranial pole of which lies a whitish, smaller sublingual gland.

Figure 2-62: Isolated glands of head. From left to right are parotid gland, submandibular gland, sublingual gland, and zygomatic gland. Note excavation at cranial pole of mandibular gland from which sublingual gland was removed.

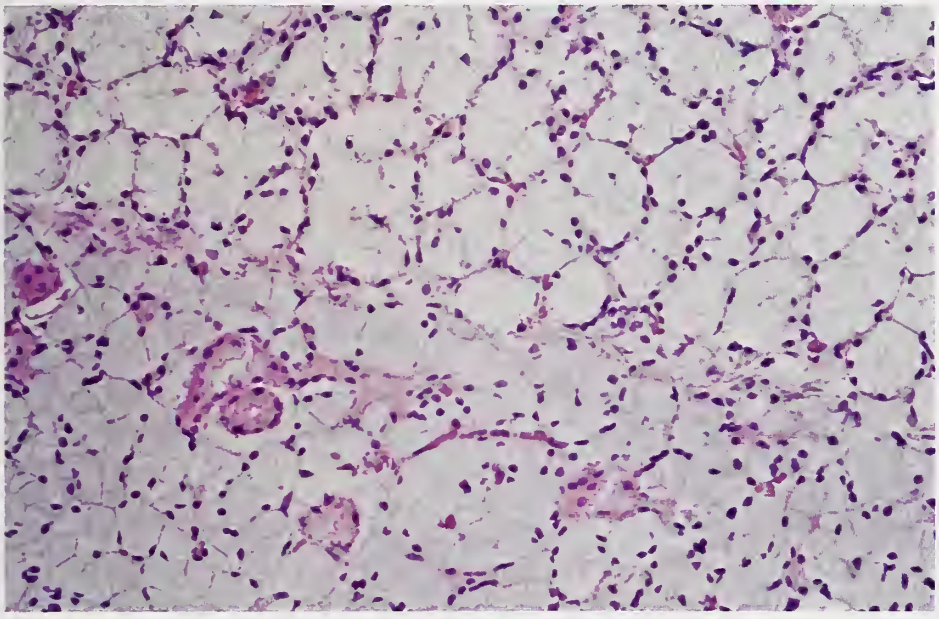

Figure 2-63: Histology of mandibular and sublingual glands. Both glands consist of mucous and serous parts and can be distinguished by their different colors; lighter one in upper half of plate is sublingual gland; while darker staining submandibular gland is located in lower half. (H & E, X37).

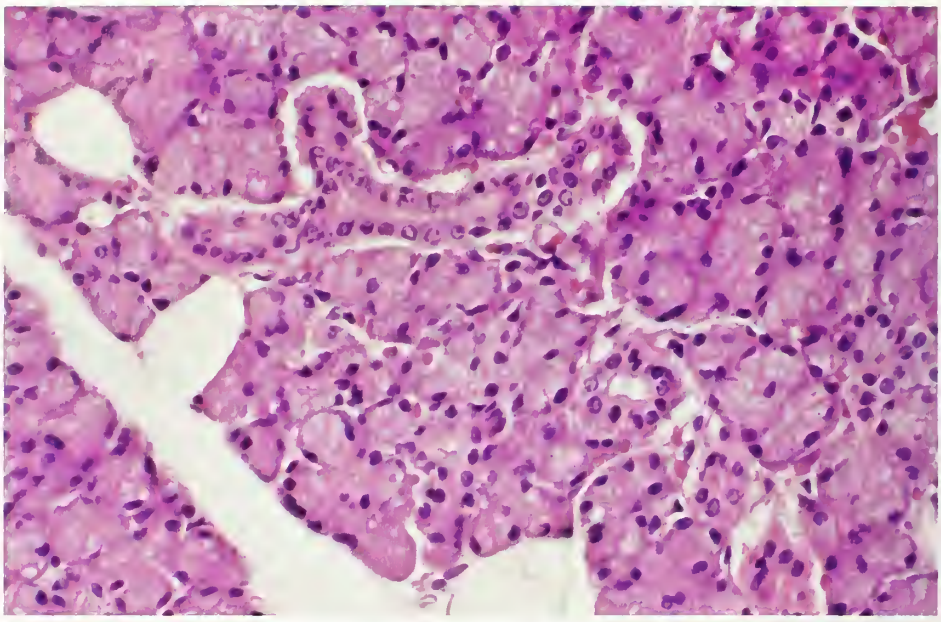

Figure 2-64: Histology of parotid gland, showing serous acini. (H & E, X58).

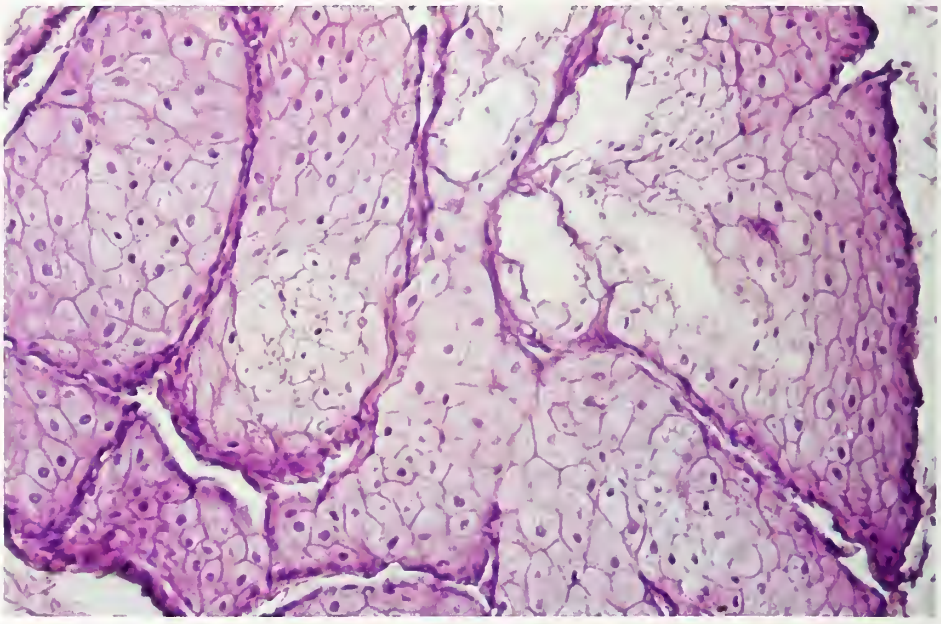

Figure 2-65: Histology of sebaceous gland situated behind ear. This gland resembles Zymbal gland in other rodents. (H & E, X93).

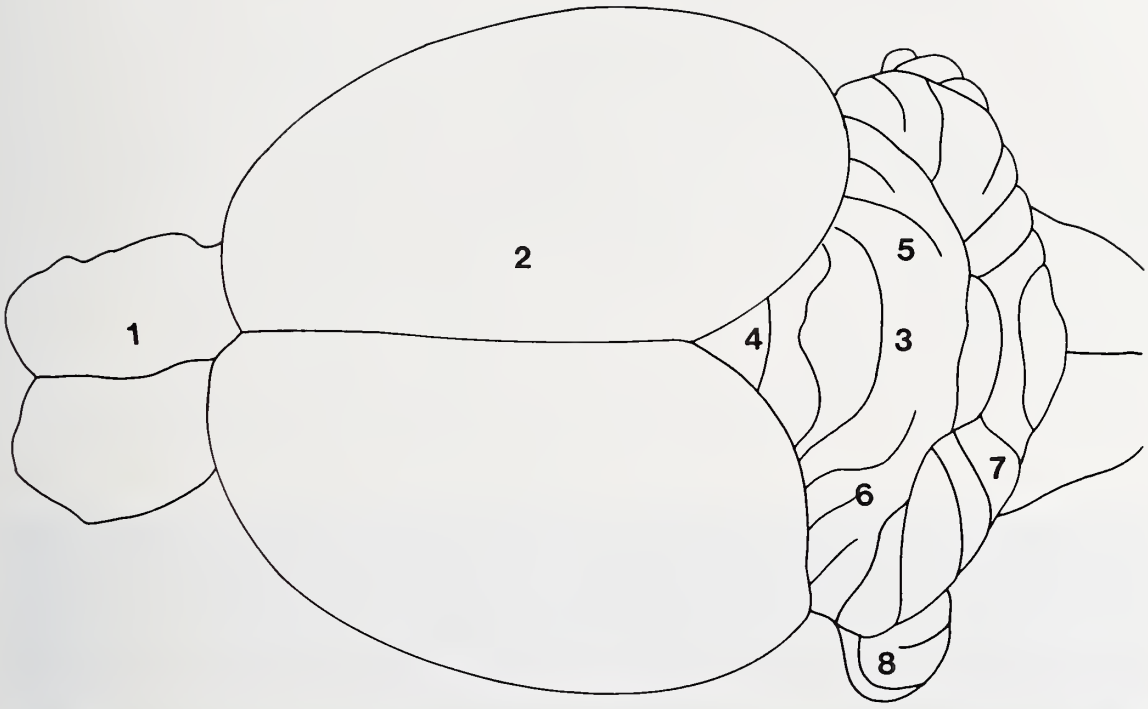

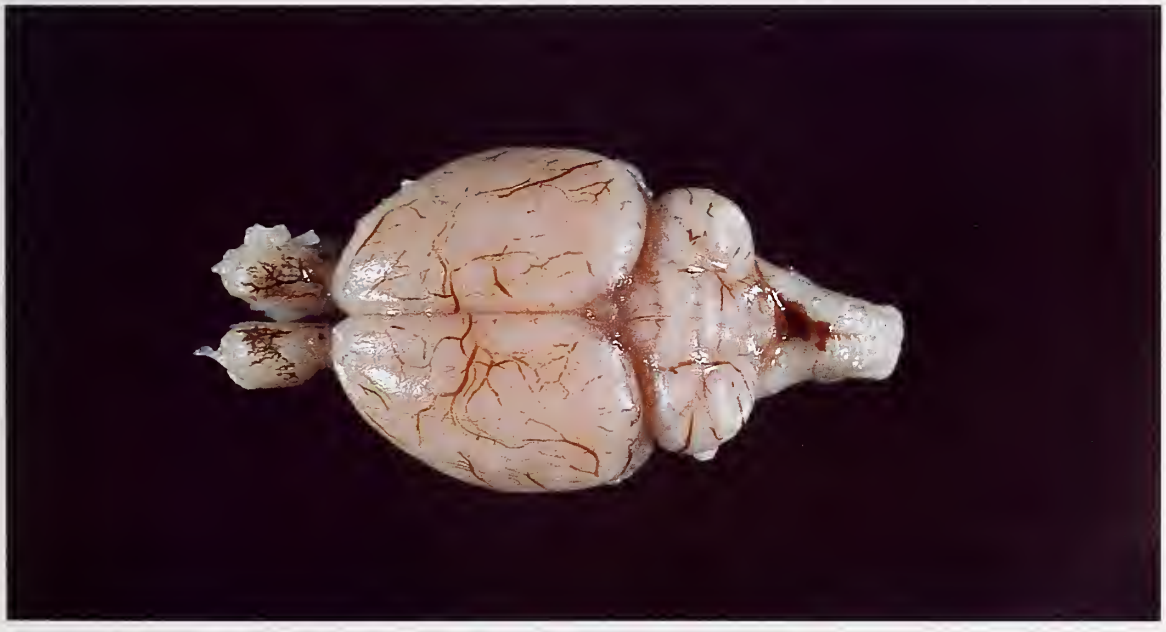

Figure 2-66: Above. Drawing of brain in male European hamster, 1 year old, formalin fixed, dorsal view. 1 = bulbus olfactorius; 2 = neopallium; 3 = fissura V cerebelli (f. prima); 4 = lamina tecti; 5 = lobulus simplex; 6 = crus I lobuli ansiformis; 7 = crus II lobuli ansiformis; 8 = paraflocculus. Below. Formalin fixed brain of male European hamster, 1 year old, dorsal view.

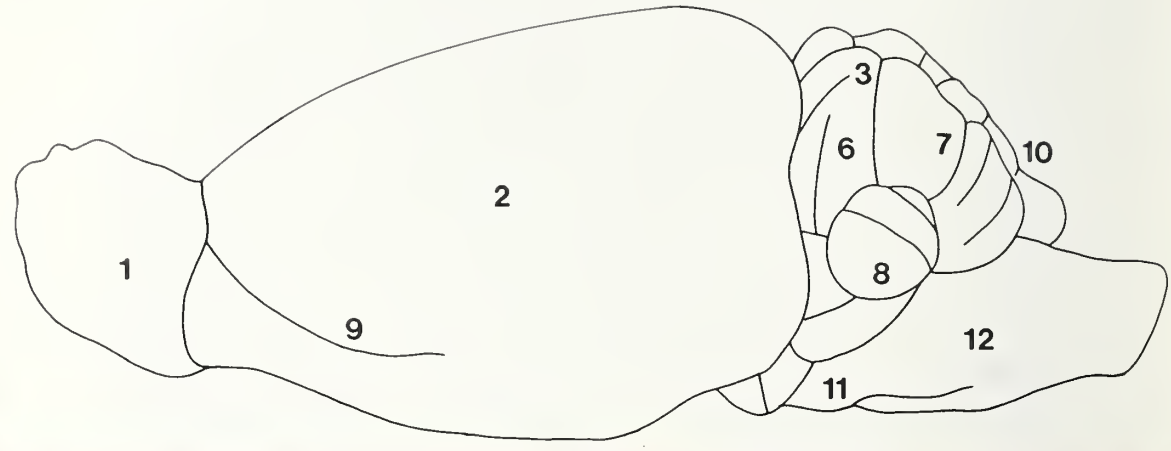

Figure 2-67: Above. Schematic drawing of brain in 1-year old male European hamster, lateral view. 1 = bulbus olfactorius; 2 = neopallium; 3 = fissura V cerebelli (f. prima); 6 = crus I lobuli ansiformis; 7 = crus II lobuli ansiformis; 8 = paraflocculus; 9 = sulcus rhinalis lateralis (fissura palaeo-neocorticalis); 10 = fissura VIII cerebelli; 11 = pons; 12 = medulla oblongata. Below. Formalin fixed brain of male European hamster, 1 year old, lateral view.

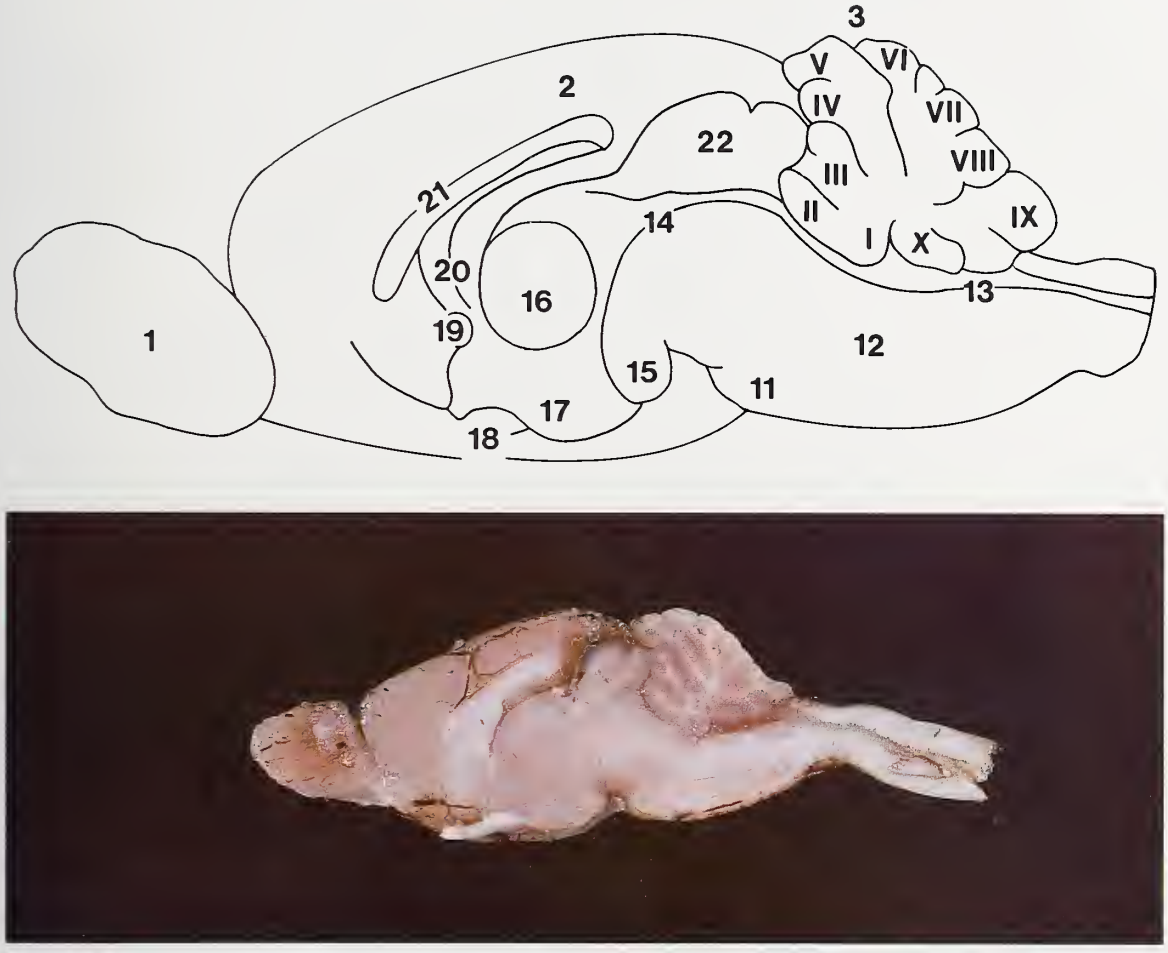

Figure 2-68: Above. Schematic drawing of brain of male European hamster, 1 year old; sagittal section. 1=bulbus olfactorius; 2=neopallium; 3=fissura V cerebelli (f. prima); 11=pons; 12=medulla oblongata; I=lobuli I cerebelli; II=lobuli II cerebelli; III=lobuli III cerebelli; IV=lobuli IV cerebelli; V=lobuli V cerebelli; VI=lobuli VI cerebelli; VII=lobuli VII cerebelli; VIII=lobuli VIII cerebelli; IX=lobuli IX cerebelli; X=lobuli X cerebelli; 13=ventriculus quartus; 14=aquaeductus mesencephali; 15=corpus mamillare; 16=massa intermedia; 17=ventriculus tertius; 18=chiasma opticum; 19=commissura rostralis; 20=fornix; 21=corpus callosum; 22=colliculus rostralis. Below. Sagittal section through formalin fixed brain of male European hamster, 1 year old.

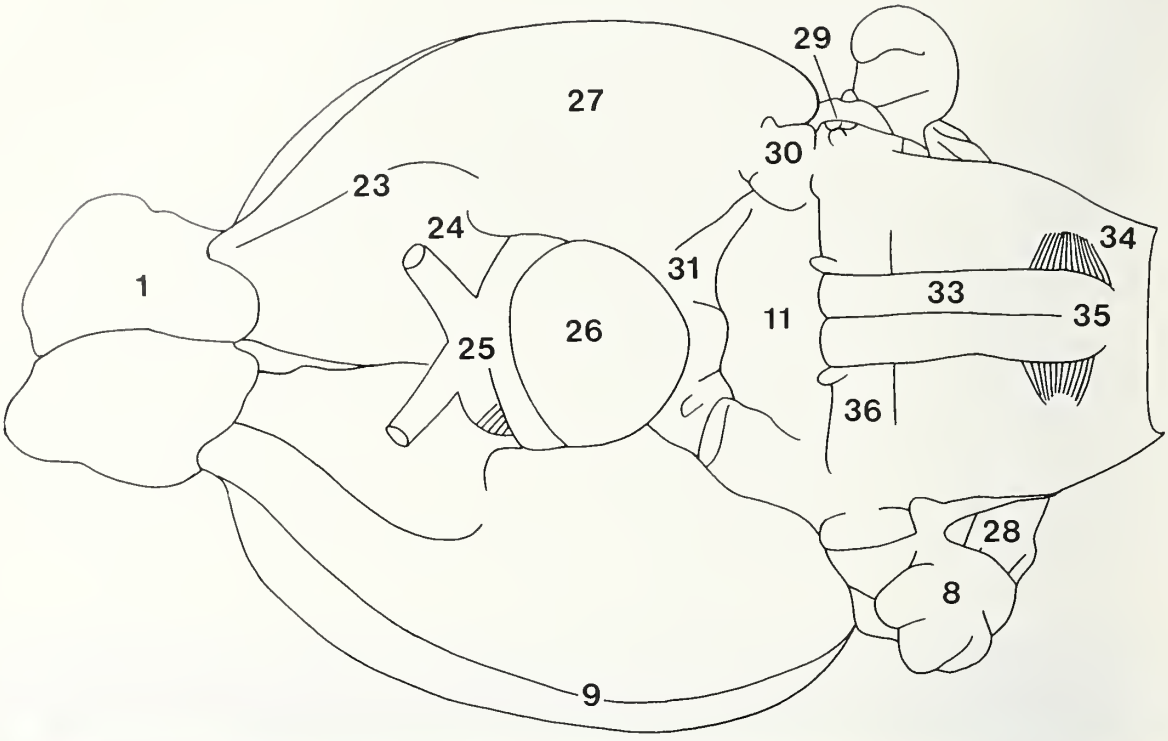

Figure 2-69: Above. Schematic drawing of brain of male European hamster, 1 year old; ventral view. 1 = bulbus olfactorius; 8 = paraflocculus; 9 = sulcus rhinalis lateralis (fissura palaeo-neocorticalis); 11 = pons; 23 = tractus olfactorius lateralis; 24 = tuberculum olfactorium; 25 = chiasma opticum; 26 = infundibulum; 27 = palaeopallium; 28 = lobulus paramedianus; 29 = n. facialis; 30 = n. trigeminus; 31 = n. oculomotorius; 33 = pyramis; 34 = n. hypoglossus; 35 = decussatio pyramidum; 36 = corpus trapezoides. Below. Formalin fixed brain of male European hamster, 1 year old, ventral view.

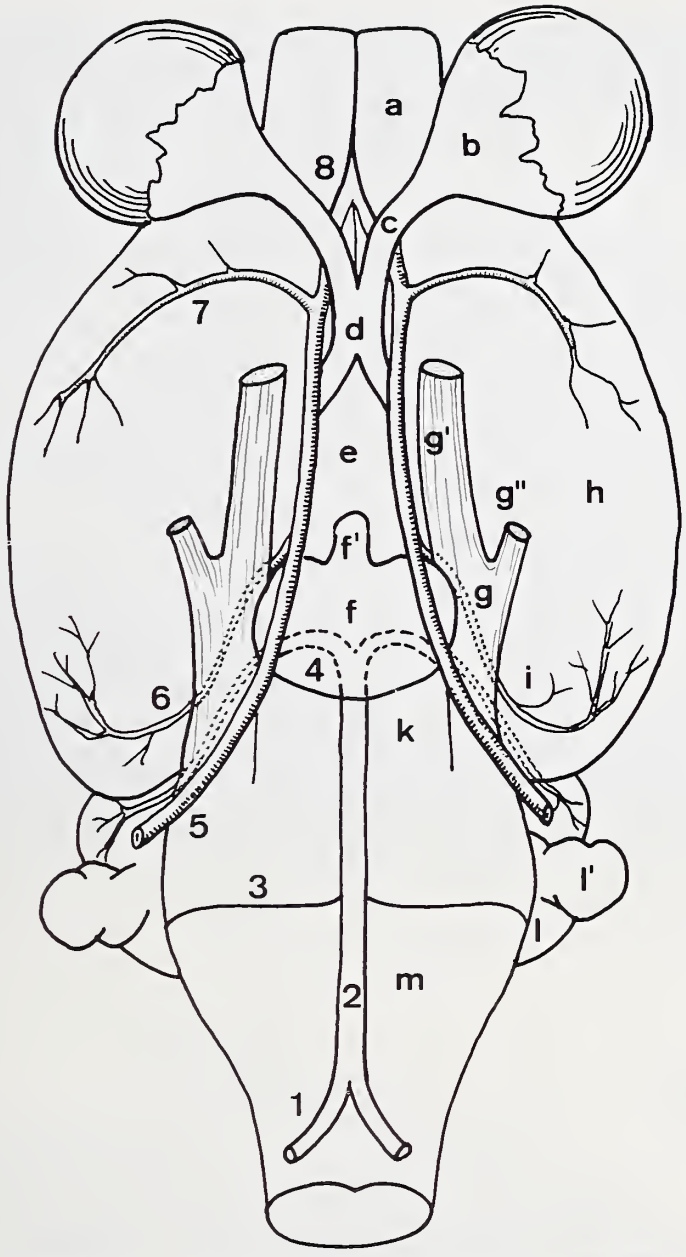

Figure 2-70: Ventral view of brain of male European hamster representing basal arteries of the brain. a=bulbus olfactorius; b=bulbus oculi; c=n. opticus; d=chiasma opticum; e=tuber cinereum; f=hypophysis; f'=infundibulum hypophysis; g=n. trigeminus; g'=n. maxillaris; g''=n. mandibularis; h=hemispherium cerebri; i=lobus piriformis; k=pons; l=hemispherium cerebelli; l'=paraflocculus; m=medulla oblongata; 1=a. vertebralis; 2=a. basilaris; 3=a. cerebelli caudalis; 4=a. cerebelli rostralis; 5=a. carotis interna; 6=a. cerebri caudalis; 7=a. cerebri media; 8=a. cerebri rostralis.

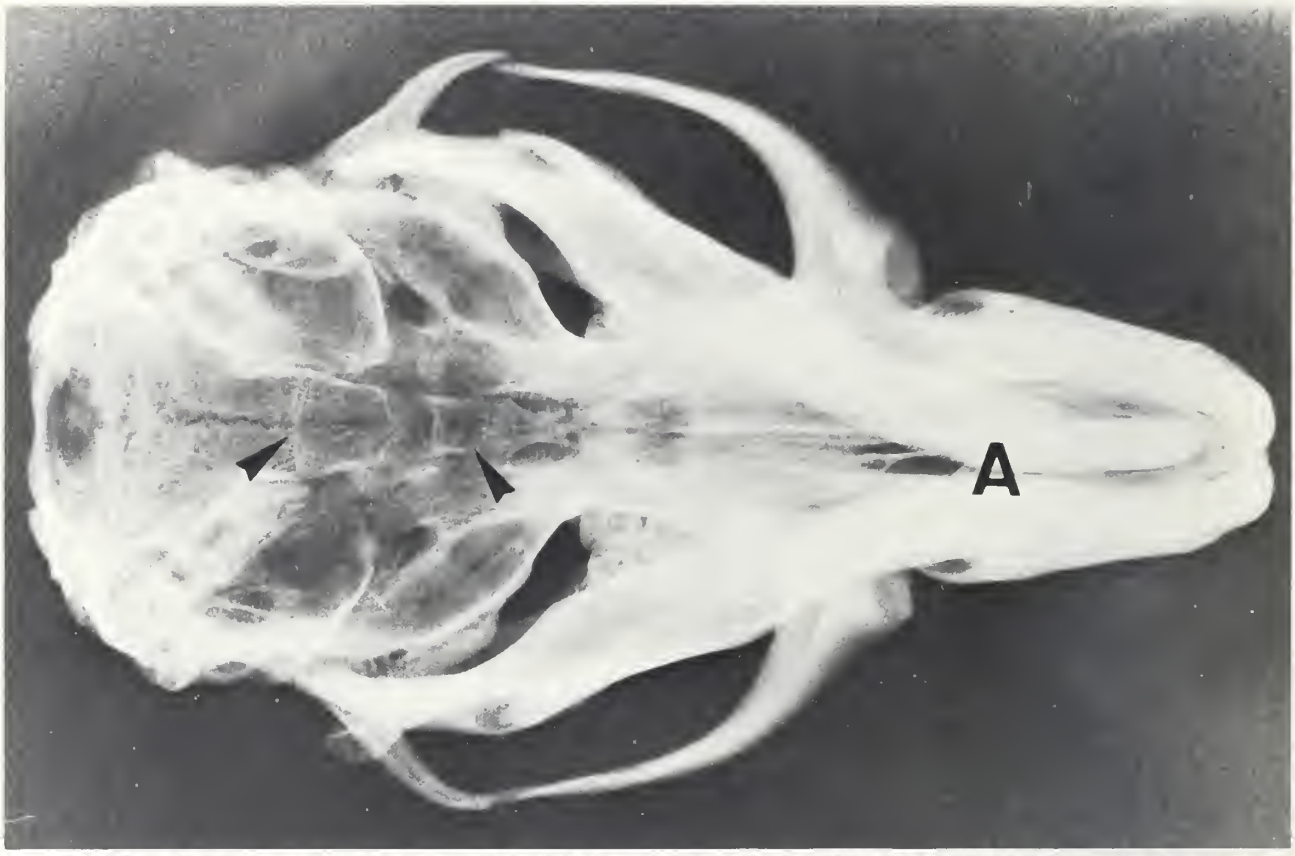

Figure 2-71: Radiogram of ventral aspect of adult hamster skull. Note sphenoid bone which consists of two parts: basisphenoid and presphenoid (arrows). Two mandibles are connected by intermandibular symphysis (A).

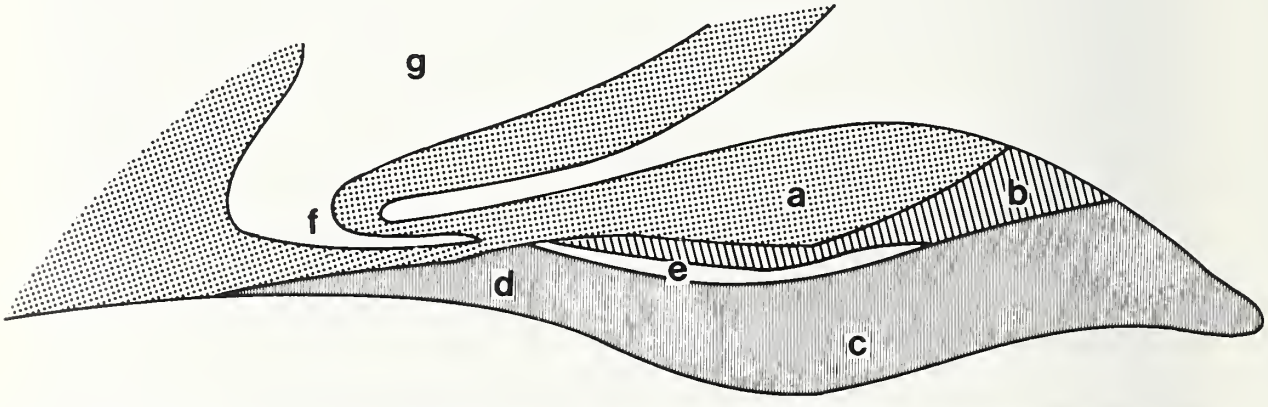

Figure 2-72: Schematic drawing of longitudinal section through hypophysis of European hamster, 1-year-old female. a=neurohypophysis; b–d=adenohypophysis; b=pars intermedia; c=pars distalis; d=pars infundibularis; e=cleft or cavum hypophysis; f=pars cava infundibuli; g=ventriculus tertius.

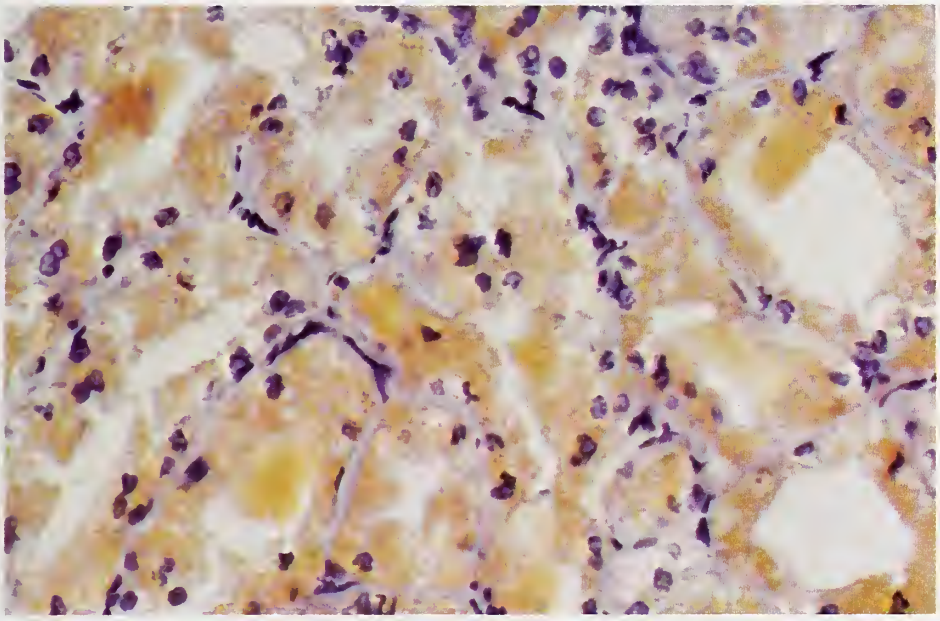

Figure 2-73: Histologic features of orbital adipose tissue, demonstrating glandular appearance but actually consisting of multivacuolated fat cells. (Sudan III, X58).

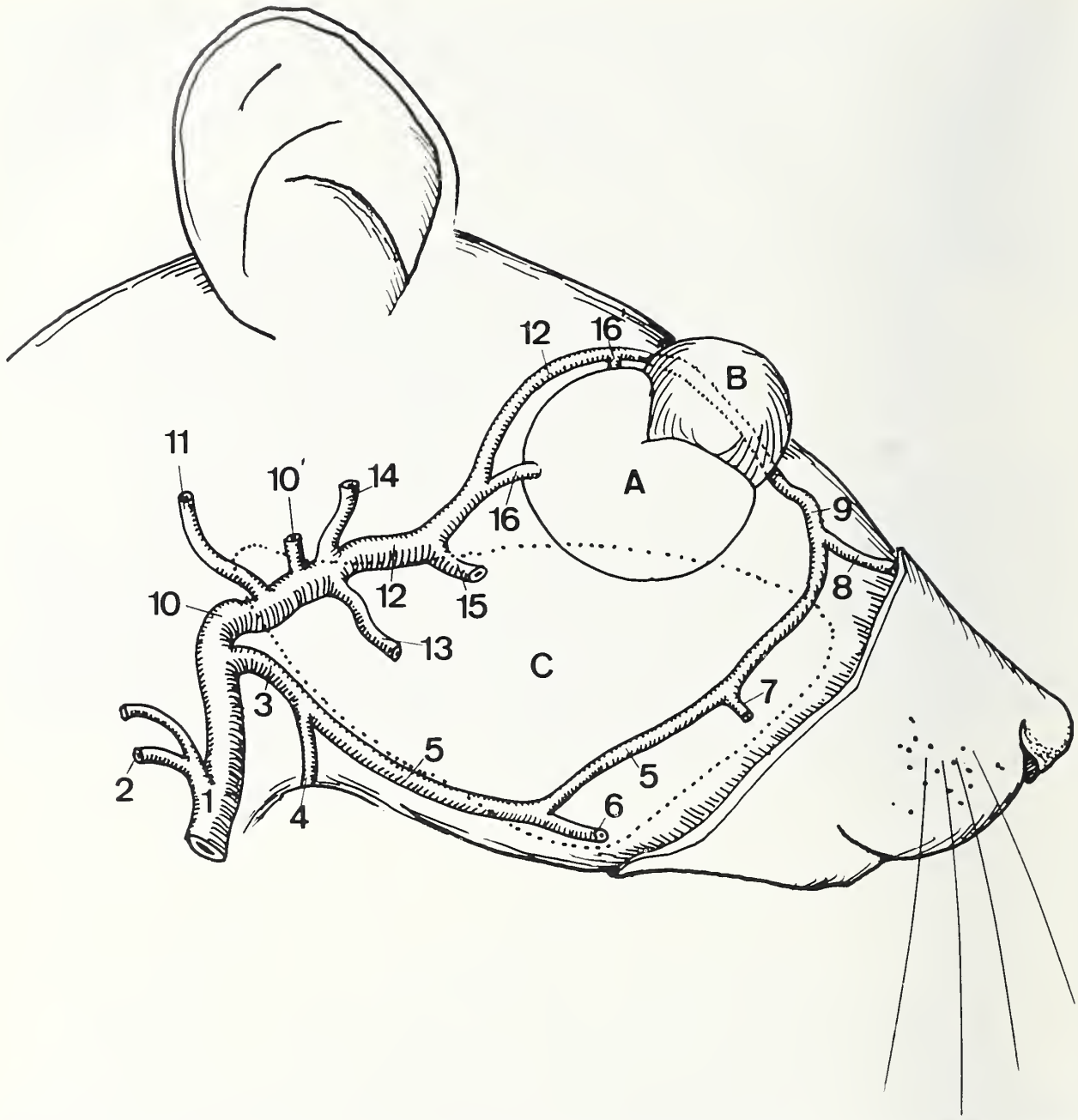

Figure 2-74: Ophthalmic plexus and the cranial veins of a male European hamster, 1 year old. 1=vena jugularis externa; 2=vena cervicalis superficialis; 3=vena linguofacialis; 4=vena lingualis; 5=vena facialis; 6=vena labialis mandibularis; 7=vena labialis maxillaris; 8=vena lateralis nasi; 9=vena angularis oculi; 10/10'=vena maxillaris; 11=vena auricularis caudalis; 12=vena temporalis superficialis; 13=vena masseterica; 14=vena auricularis rostralis; 15=vena transversa faciei; 16/16=flow of blood to ophthalmic plexus; A=plexus venosus; B=bulbus oculi; C=cheek pouch (dotted lines).

CHAPTER THREE
CERVICAL REGION

3.1 CERVICAL SKELETON

The cervical vertebrae form a lordosis between the sixth cervical and second thoracic vertebrae (Fig. 3–1). There are seven cervical vertebrae (*vertebrae cervicales*) with a total length of 26.6 mm (Figs. 3–1, 3–2). The first vertebra, or *atlas,* has a ring shape (Fig. 3–3). Its outer and inner diameters are 14.1 and 10.3 mm, respectively. Dorsoventrally flattened, its external height is 8.2 mm and its internal height is 6.2 mm. The ventral side is thin and frail. The caudoventrally directed transverse processes are perforated by the vertebral artery and vein, which pass through the transverse foramen (*foramen transversarium*). The second cervical vertebra, the *axis* or epistropheus, has a spinous process 9.5 mm long (Fig. 3–4). Its length is 6.3 mm. The axis includes a body (*corpus*), odontoid process (*dens*), vertebral arch (*arcus vertebrae*), spinous process (*processus spinosus*), transverse processes (*processus transversi*) and articular processes (*processus articulares*). The dens, which is a cranial extension of the vertebral body supporting the atlas, is 9 mm long and 4.7 mm high. The vertebral arch is angled somewhat caudal to the vertebral body. It begins with a thin root above the base of the transverse process and broadens into a small, caudal articular process. From the dorsal posterior edge of the vertebral arch, a hatchet-shaped spinous process arises and elongates caudally, projecting over the third cervical vertebra (Fig. 3–1). A cranial projection touches the posterior tubercle of the atlas.

The third to seventh cervical vertebrae are practically identical. Their bodies are dorsoventrally flattened and shorter than those of the second vertebra. The dorsoventral obliquity of the articular ends of the vertebral bodies is partly responsible for the definite cervical lordosis. The thin spike-shaped transverse processes are perforated at their bases by transverse foramina.

3.2 TOPOGRAPHY OF THE VENTRAL CERVICAL REGION

The paired mandibular glands (Fig. 2–59) are prominent superficial structures of the ventral cervical region. The two glandular bodies press against each other in the median plane, and lateral to these glands is adipose tissue. This fat accumulation, along with the mandibular glands, covers the ventral cervical surface and the cranial portion of the thoracic musculature. The sternohyoid muscle (*m. sternohyoideus*) parallels the trachea on its ventral surface. Caudally, the sternohyoid muscle is covered at its origin on the manubrium by the sternocephalic muscle (*m. sternocephalicus*). The omotransversarius muscle (*m. omotransversarius*) originates on the acromion process of the *scapula* (Fig. 3–5), extends dorsal to the omohyoid muscle (*m. omohyoideus*), and continues to the cervical vertebrae. The digastric muscle (*m. digastricus*) lies cranial to the sternohyoid and omohyoid muscles (Figs. 3–6, 3–7).

The clavicle (*clavicula*)(Figs. 3–2, 3–9) separates the brachiocephalic muscle (*m. brachiocephalicus*) into a cleidobrachial muscle (*m. cleidobrachialis*) and a cleidocephalic muscle (*m. cleidocephalicus*). The cleidobrachial muscle extends from the distal humerus to the lateral half of the clavicle in a fan-shaped array. The cleidocephalic muscle originates further medially on the clavicle, lies against the sternocephalic muscle laterally and extends with the latter to the skull. The sternocephalicus extends from its origin on the manubrium in a laterodorsal direction to the head and inserts on the occiput. The dorsal scalene muscle (*m. scalenus dorsalis*) connects the second, third, and fourth ribs with the transverse processes of the second, third, fourth and fifth cervical vertebrae. The middle scalene muscle (*m. scalenus medius*) extends ventral to the dorsal scalene muscle as a thin cervical muscle from the first rib to the third through fifth cervical vertebrae. The *longus colli* muscle lies between the trachea and the cervical vertebrae and extends caudally within the thoracic cavity to the fourth thoracic vertebra. The pectoralis muscles connect the sternal area with the humerus and form a triangular surface between the clavicle, the xiphoid process of the sternum and the humerus.

In the European hamster, the pectoralis musculature consists of the superficial pectoralis (*m. pectoralis superficialis*) and the pectoralis profundus (*m. pectoralis profundus*) muscles. A cranial descending (*pars descendens*) part and a caudal transverse (*pars transversus*) part of the former can be distinguished. The deep pectoral is covered by the superficial pectoral. Since the caudal part of the latter muscle is very thin, it is very difficult to separate the two muscles at this point (Figs. 3–7, 3–8).

At the thoracic aperture (*apertura thoracis cranialis*), each cranial vena cava divides into a subclavian vein (*v. subclavia*), an external jugular vein (*v. jugularis externa*) and internal jugular vein (*v. jugularis interna*). The external jugular vein emerges into the cervical region between the clavicle and the pectoral and sternocephalic muscles; it then extends lateral to the sternocephalic and cleidocephalic muscles until it reaches the head. The internal jugular vein turns medially and runs with the common carotid artery along the trachea towards the head. The right subclavian artery, which originated from the brachiocephalic trunk in the ventral part of the cranial mediastinum, passes dorsal to the right external jugular vein at the level of the thoracic aperture. The right common carotid artery, also originating from the brachiocephalic trunk, and the left common carotid artery, arising directly from the aortic arch (Figs. 3–10, 3–11, 4–18) in the cranioventral mediastinum, both divide at the level of the larynx, giving rise to the external and internal carotid arteries of either side.

The cranial cervical ganglion (*ganglion cervicale craniale*) of the sympathetic trunk (*truncus sympathicus*) is dorsolateral to the thyroid gland. The vagus and sympathetic nerves run together in the neck as the vagosympathetic trunk (*truncus vagosympathicus*) (Fig. 3–11) ventrolateral to the common carotid artery, but separate before entering the thoracic cavity. Adjacent to the cranial thoracic aperture and ventrolateral to the edge of the longus colli muscle, the stellate ganglion (*ganglion stellatum*) and the middle cervical ganglion (*ganglion cervicale medium*) of the sympathetic trunk are located. The sympathetic trunk runs ventrolateral to the longus colli to the caudal end of that muscle; then it is dorsolateral to the vertebral column. The sympathetic trunk and the cervical ganglia are only visible histologically. However, the vagosympathetic trunk in the cervical area and the vagus nerve in the thoracic cavity are visible under low power magnification.

3.3 PHARYNX

Caudal to the oral cavity is the *pharynx,* the chamber common to the respiratory and digestive systems. The pharynx is divided into three parts, the nasal part (*pars nasalis*) rostrodorsally, the oral portion (*pars oralis*) rostroventrally, and the laryngeal portion (*pars laryngea*) caudally. The oropharynx extends 6 mm from the entrance to the pharynx (*aditus pharyngis*) to the epiglottis (*vallecula epiglottica*) and is floored by the tongue (Figs. 2–3, 2–4). The soft palate separates the oropharynx from the nasopharynx, which lies between the choana and the epiglottis. The laryngeal portion is continuous posteriorly with the esophagus.

The epiglottis projects into the dorsal pharyngeal space and lies with its cranioventral surface on the free caudal edge of the soft palate (*velum palatinum*). Ventral to the free edge, the pharyngeal cavity is closed by the epiglottis. The epiglottis guides the swallowed food down the pharyngeal furrow which lies lateral to the aryepiglottic fold (*plica aryepiglottica*). The free crest of the soft palate continues bilaterally along the pharyngeal walls, forming the palatopharyngeal arch (*arcus palatopharyngeus*) which attaches the pharynx to the esophagus.

3.4 LYMPHATIC SYSTEM OF NECK AND ADJACENT THORACIC REGION

Tonsils are neither macroscopically recognizable nor histologically demonstrable. The mandibular lymph center (*lymphocentrum mandibulare*) is a cluster of four lymph nodes in the laryngeal region. It lies rostral, dorsal and lateral to the large complex consisting of the mandibular and sublingual glands (Fig. 3–12). Usually, two of the lymph nodes (*lnn. mandibulares rostrales*) are embedded in adipose tissue in front of the salivary glands. In general, the lymph nodes can be seen only with a magnifying glass, but in some animals the nodes are

visible without magnification, contrasting with the surrounding tissue by their red color and discrete boundaries. Additional nodes lie between the two salivary glands and the laryngeal surface of the parotid gland (*lnn. mandibulares caudales*). They are medial to the facial vein.

The retropharyngeal lymph complex (*lymphocentrum retropharyngeum*) consists of two lymph nodes (*lnn. retropharyngei*). They lie deep to the sternocephalic and cleidocephalic muscles, dorsolateral to the carotid artery and extend from the pharynx to the thyroid gland. Usually the parotid node (*ln. parotideus*) can be found under the parotid gland caudal to the ear.

Superficial cervical lymph nodes are not found in this species. The deep cranial cervical node (*ln. cervicalis profundus cranialis*) is located between the trachea and the lateral margin of the omohyoid muscle. Via the rostral mandibular nodes, it drains the tongue, floor of the mouth, face, and cheek pouches, and itself drains the neck musculature and pharynx and empties into the jugular system. The deep caudal cervical lymph node (*ln. cervicalis profundus caudalis*) is located between the trachea and the insertion of the sternocephalic muscle. It drains the neck musculature and the pharynx and empties into the jugular system.

The axillary lymph node (*ln. axillaris*) (usually one large node, occasionally two small nodes) is situated between lateral thoracic wall and *teres major* muscle, near the insertion of the *latissimus dorsi* muscle (Fig. 3–12). It drains the pectoral limb, thoracic and dorsal skin, lateral abdominal wall, the accessory axillary lymph node and overflows to the subclavian vein.

The accessory axillary lymph node (*ln. axillaris accessorius*) is situated between the long head of the *triceps brachii* and the latissimus dorsi muscles. It drains the pectoral limb and skin of the thorax, and flows to the axillary lymph node.

3.5 LARYNX

The *larynx* is situated behind the root of the tongue and ventral to the pharynx. It is a sphincter valve at the entrance to the windpipe, preventing food from entering the trachea, and controlling the air flow. The larynx may be up to 9 mm long and has an outer diameter of about 6 mm (Figs. 3–13, 3–14, 3–15, 3–16). In one year old males, it weighs 222±36 mg and in females, 185±36 mg (Table 5), when freed of all superficial muscles. The larynx is positioned between the caudal ends of the mandibles and is adjoined to the proximal part of the overlying esophagus (Fig. 2–3). Laterally, the larynx is flanked by the thyroid and parathyroid glands (*glandula thyreoidea et glandula parathyreoidea*) which extends to the level of the cricoid cartilage (Figs. 3–13, 3–14). Cranially, the interior of the larynx empties through the laryngeal opening (*aditus laryngis*) into the dorsal part of the pharynx, while caudally the larynx merges into the trachea.

The larynx of the European hamster contains three single median cartilages: thyroid (*cartilago thyreoidea*), cricoid (*cartilago cricoidea*) and epiglottis (*cartilago epiglottica*); and three paired cartilages: arytenoid (*cartilago arytenoidea*), corniculate (*cartilago corniculata*) and cuneiform (*cartilago cuneiformis*), the latter two of which are identifiable only under magnification (Figs. 3–17, 3–18).

The thyroid cartilage (Fig. 3–18), which defines the body of the larynx, has a concave shape, open dorsally. It is formed by two sagittal cartilaginous plates (*laminae thyreoideae*) that bend ventrally towards the median plane where they fuse to form a ventral median crest. The dorsal edge of each lamina extends cranially as a short horn (*cornu rostrale*) and caudally as a longer horn (*cornu caudale*) with another short horn (*cornu dorsale*) projecting from the dorsal edge of the lamina. The lamina has an oblique ridge, running caudally on the dorsolateral surface, which serves as the insertion of *m. cricothyreoideus*.

The smaller cricoid cartilage, which is overlapped craniolaterally by the caudal thyroid horns, is shaped like a signet ring. It is composed of elastic cartilage and consists of the arch (*arcus cricoideus*) and lamina (*lamina cricoidea*) (Fig. 3–18). A connective tissue membrane, the crico-thyroid ligament, (*lig. cricothyreoideum*) is stretched over a cartilaginous free space between the thyroid cartilage and the cricoid arch. A dorsal median ridge (*crista mediana*) projects caudally over the first one to two tracheal rings.

The arytenoid cartilages are paired sagittal

elastic cartilages that are almost triangular in shape (Fig. 3–18). They lie between the thyroid laminae, and their caudal ends articulate with the craniodorsal cricoid laminae. A muscular process (*processus muscularis*) is bent laterally, while a vocal process (*processus vocalis*) points ventrally and possesses a small hook at its cranial edge.

The *epiglottis* is a leaf like structure that protects the entrance to the glottis (Fig. 3–18). The craniodorsal surface of the epiglottis lies adjacent to the free, caudal edge of the soft palate, and the tip (*apex*) projects dorsally into the pharynx. Ventral to this free edge, the epiglottis closes the pharynx caudally. The craniodorsal edge of the epiglottis forms an arch which bends laterally and continues medially, narrowing to form the base (*basis*). The epiglottis is composed of elastic cartilage.

At the dorsal part of its inner surface, the epiglottis is covered by stratified squamous epithelium, while the remaining inner surface is of a pseudostratified ciliated columnar epithelium. At the cranial base of the epiglottis, the uniform structure of this epithelium is interrupted by excretory ducts of some subepithelial glands so that the epithelium sometimes takes on a mixed appearance (Fig. 3–18).

The dorsal part of the lateral walls of the vestibule of the larynx is covered with stratified squamous epithelium, whereas its ventral surface is coated with pseudostratified ciliated columnar epithelium. At the vestibular fold (*plica vestibularis*) this stratified columnar epithelium is also found, while the vocal folds (*plicae vocales*) are coated with stratified squamous epithelium. Between these two folds is situated the ventricle of the larynx, which is lined by a pseudostratified ciliated cylindrical epithelium with areas of stratified squamous epithelium. Caudally from the vocal folds begins a ciliated columnar epithelium, two-cell-layers thick, which extends to the trachea (Fig. 3–19).

3.5.1 Ligaments of the Larynx

The various cartilages of the larynx are connected with each other by ligaments. For example, the cricothyroid ligament (*lig. cricothyreoideum*) and the thyroepiglottic ligament (*lig. thyreopiglotticum*) are distinctly visible microscopically. A cricotracheal ligament (*lig. cricotracheale*) is likewise recognizable. In horizontal section through the larynx, the vocal ligament (*lig. vocale*) is especially prominent histologically.

3.5.2 Muscles of the Larynx

Except for *m. arytaenoideus transversus* and the *m. hyoepiglotticus,* all muscles of the larynx are paired. *M. thyreohyoideus* joins the hyoid bone to the thyroid cartilage. *M. sternothyreoideus* is prominent, originating with *m. sternohyoideus* on the manubrium and extending craniodorsally to insert on the lateral surface of the thyroid lamina.

M. cricothyreoideus originates on the cricoid arch and runs craniodorsally to the caudal thyroid lamina. *M. cricoarytaenoideus dorsalis* originates dorsally on the cricoid lamina and inserts laterally on the muscular process of the arytenoid cartilage. *M. arytaenoideus transversus* forms a muscular connection between the dorsal edges of the two arytenoid cartilages. *M. cricotrachealis* runs from the cricoid arch to the first and second tracheal rings dorsally. The minute *m. cricoarytaenoideus lateralis* extends craniodorsally from the cricoid to the vocal process of the arytenoid cartilage. *M. thyreoarytaenoideus* runs ventrally from the vocal process of the arytenoid cartilage. The prominent *m. vocalis* parallels *m. thyreoarytaenoideus.*

The interior of the larynx is divided into the vestibule (*vestibulum laryngis*), the *glottis* and the infraglottis (*cavum infraglotticum*). The vestibule extends from the laryngeal opening (*aditus laryngis*) to the vestibular folds (*plicae vestibulares*). The laryngeal opening is bordered ventrally by the epiglottis, laterally by the aryepiglottic folds (*plicae aryepiglotticae*) and dorsally by the arytenoid cartilages. A *plica lateralis* is not found. A median ventricle (*ventriculus laryngis medianus*) is formed at the base of the epiglottis; this is more pronounced in older animals. The vestibular fold at the caudal end of the vestibule is formed by *m. ventricularis* and its mucosa. It extends obliquely ventrally from the vocal process of the arytenoid cartilage to the base of the epiglottis.

Between the vestibular fold and the vocal fold (*plica vocalis*), a perpendicular fissure is located, the lateral ventricle (*ventriculus laryngis lateralis*), which begins cranial to the vocal process of the arytenoid cartilage and extends ventrally to lie between the *m. vocalis* and the *m. ventricularis.* The glottis is a laterally compressed space between the vocal folds cranially and the infraglottis caudally. The vocal folds are folded into the *rima glottidis,* especially by the vocal ligament (*lig. vocale*), a connective tissue extension of the vocal process of the arytenoid cartilage, which extends ventrally, lying lateral to *m. vocalis.* Caudally, the interior of the larynx broadens to form the infraglottis, which assumes the inner diameter of the first tracheal ring, with which it is continuous caudally.

3.6 TRACHEA

The cervical and thoracic *trachea* is a nearly

cylindrical tube extending from the larynx at the level of the cervical vertebra to the sixth rib where it divides into a smaller left and larger right main *bronchus*. The trachea *in situ* (Fig. 3–20) is 33.7± 2.9 mm long in the adult hamster. Isolated, the organ has an average length of 23.0±4.3 mm and weighs about 86 mg in adult males and 68 mg in adult females (Tables 1, 5).

The ventral surface of the cervical trachea is covered by the sternohyoid muscle, which also overlaps the thymus, thyroid and parathyroid glands; the caudal thyroid veins; cervical fascia and, superficially, the anastomosing branches of the jugular veins. The lateral surface is related to the common carotid arteries, the right and left lobes of the thyroid gland, the caudal thyroid arteries and the recurrent laryngeal nerves. The cervical trachea lies ventral to the esophagus in the dorsal part of the neck (Fig. 3–16). It is accompanied on both sides by the common carotid arteries.

The skeleton of the trachea consists of 14 or 15 hyaline cartilaginous rings (Figs. 3–12, 3–15, 3–16) (Reznik, *et al.,* 1973). The first tracheal ring, 3.9 mm in luminal diameter, is the largest while the last tracheal ring, with a lumen diameter of 2.7 mm, is the smallest (Table 1). All of the rings are approximately 0.5 mm thick, even though their luminal diameters vary (Figs. 3–15, 3–17, Table 1). The tracheal cartilages (*cartilagines tracheales*) are slightly compressed; the c-shaped rings are incomplete dorsally (Fig. 3–16). The first tracheal ring is joined to the cricoid cartilage by the cricotracheal ligament, while annular ligaments (*ligg. annularia*) connect all tracheal rings in series. Very thin transverse muscle fibers (*mm. tracheales*) connect the two open ends of each ring on the dorsal aspect of the tube.

The tracheal lumen is lined by pseudostratified ciliated columnar epithelium, with only a few submucosal glands interspersed, especially cranially; some isolated seromucous glands are found in the adventitia (Fig. 3–21).

3.7 THYROID AND PARATHYROID GLAND

The thyroid (*gl. thyreoidea*) and parathyroid glands (*gl. parathyreoidea*) belong to the endocrine hormonal system and supply the body with thyroxin and parathormone. In contrast to the findings of other workers (Kittel, 1952–53), the gland lies lateral and dorsal to the trachea between the caudal plate of the thyroid cartilage and the first three tracheal rings (Fig. 3–14). This highly vascular gland is larger in hibernating than in non-hibernating animals. In hibernating animals it weighs around 10 mg (Kittel, 1952-53) and consists of two longitudinally oval glandular bodies which can be up to 7 mm long and 3 mm thick (Tables 10, 10a). An isthmus is not present in this species and only small strips of each ventral wall are visible ventrally.

The gland, whose surface is smooth and without conspicuous lobulation, is of the alveolar type.

The follicles composing the gland are lined by simple cuboidal epithelium and vary in size up to 100 μm. The epithelial cells secrete the colloid which is subsequently stored in the follicular lacunae and contains the thyroid hormones, tri- and tetra-iodothyronin (Fig. 3–22).

Production and release of the thyroid hormones are controlled by the thyrotropic pituitary hormone (TSH). Histometrically, small follicles indicate a high secretory activity, while large follicles a low activity (Neumann, 1963; Eickhoff, 1965; Warner, 1971; Matthiesen and Messow, 1972; Messow, *et al.,* 1973). A change in cylindrical epithelial cells from large to small nuclei indicates reduced activity (Warner, 1971; Matthiesen and Messow, 1972; Messow, *et al.,* 1973). Based on follicle size and nuclear volume, both males and females showed maximum glandular activity in October before the onset of hibernation. The male thyroid activity was lowest during hibernation, while female activity was lowest in May following hibernation.

The parathyroid is a paired gland consisting of two oval glandular bodies located dorsolaterally within the thyroid gland.

The glandular structure is compact with interstitial capillaries and sparse connective tissue elements surrounding epithelial cells in cord or cluster patterns. Two cell types can be differentiated with hematoxylin-eosin staining: the water-clear cells are regarded as the site of parathyroid hormone production; the chief cells are thought to be inactive, depot phases of the water-clear cell (Leonhardt, 1971).

In both males and females the peak number of cells and nuclear volume in the water-clear component occurred during hibernation, with the fewest in May after reanimation.

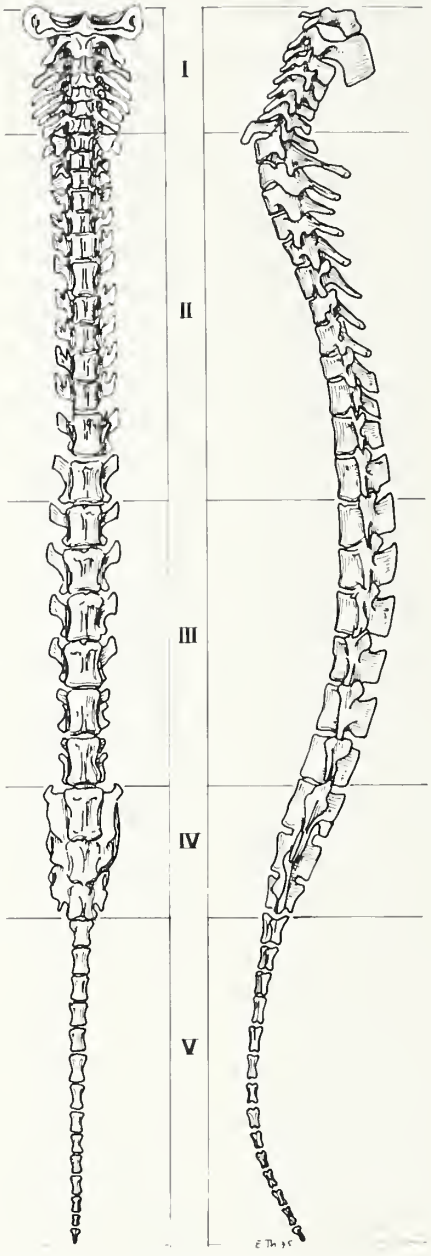

Figure 3-1: Vertebral column. Left, dorsal view. Right, lateral view. Regions: I=cervical; II=thoracic; III=lumbar; IV=lumbar; V=caudal.

Figure 3-2: Radiogram of skull, neck, and pectoral region. Note well-developed clavicles consolidating pectoral girdle (scapula and clavicle), and connecting forelegs (which have both grasping and climbing functions in hamster) with trunk.

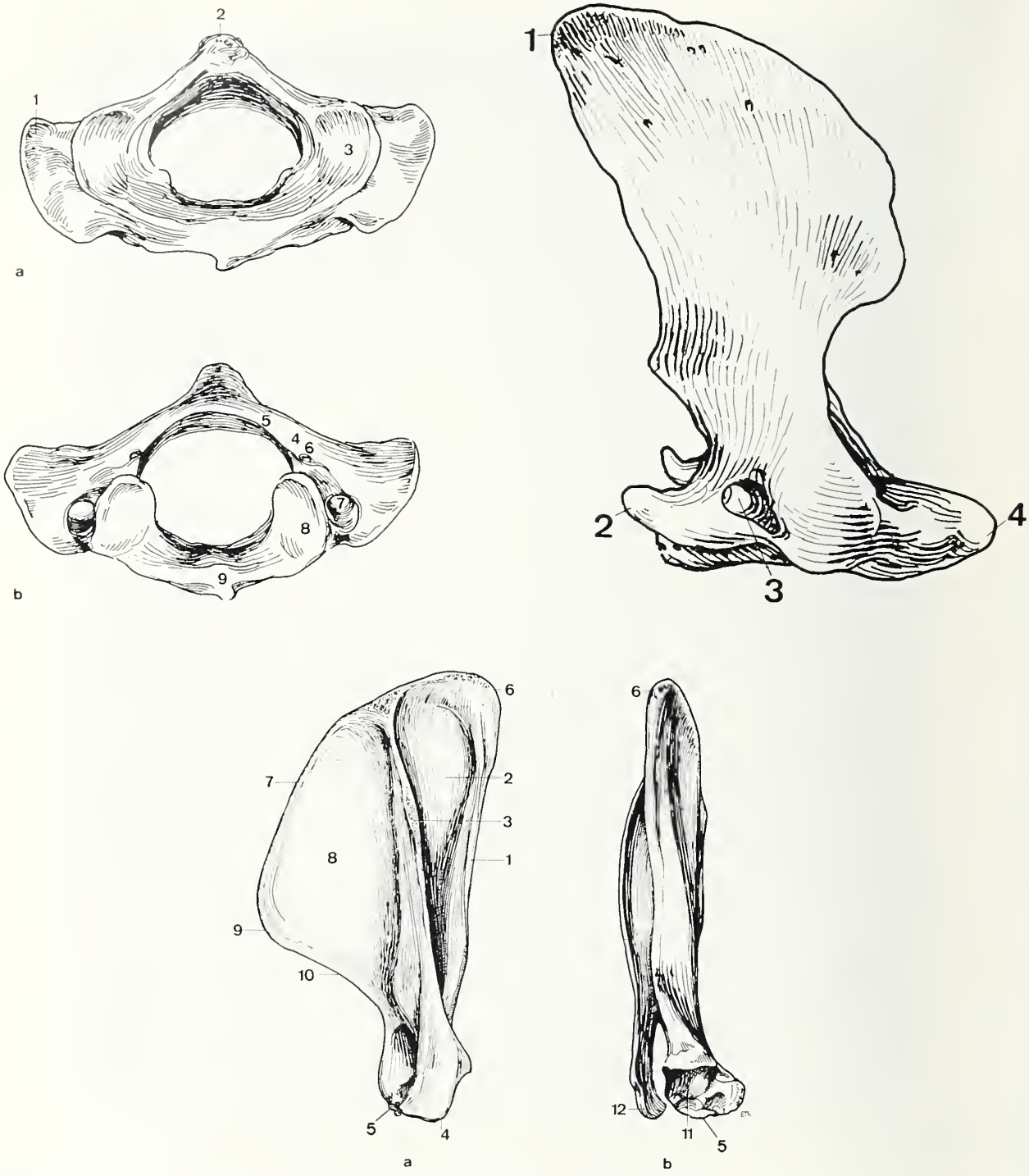

Figure 3-3 (above, left): Schematic drawing of first cervical vertebra (atlas). a, cranial aspect; b, caudal aspect. 1 = processus transversus; 2 = tuberculum dorsale; 3 = fovea articularis cranialis; 4 = massa lateralis; 5 = arcus caudalis; 6 = foramen alare; 7 = foramen transversarium; 8 = fovea articularis caudalis; 9 = tuberculum ventrale.

Figure 3-4 (above, right): Axis, right lateral view. 1 = processus spinosus; 2 = processus transversus; 3 = foramen transversarium; 4 = dens.

Figure 3-5 (below): Left scapula. a, lateral view; b, caudal view. 1 = margo caudalis; 2 = fossa infraspinata; 3 = spina scapulae; 4 = processus suprahamatus; 5 = processus coracoideus; 6 = angulus caudalis; 7 = margo dorsalis; 8 = fossa supraspinata; 9 = angulus cranialis; 10 = margo cranialis; 11 = facies articularis; 12 = acromion.

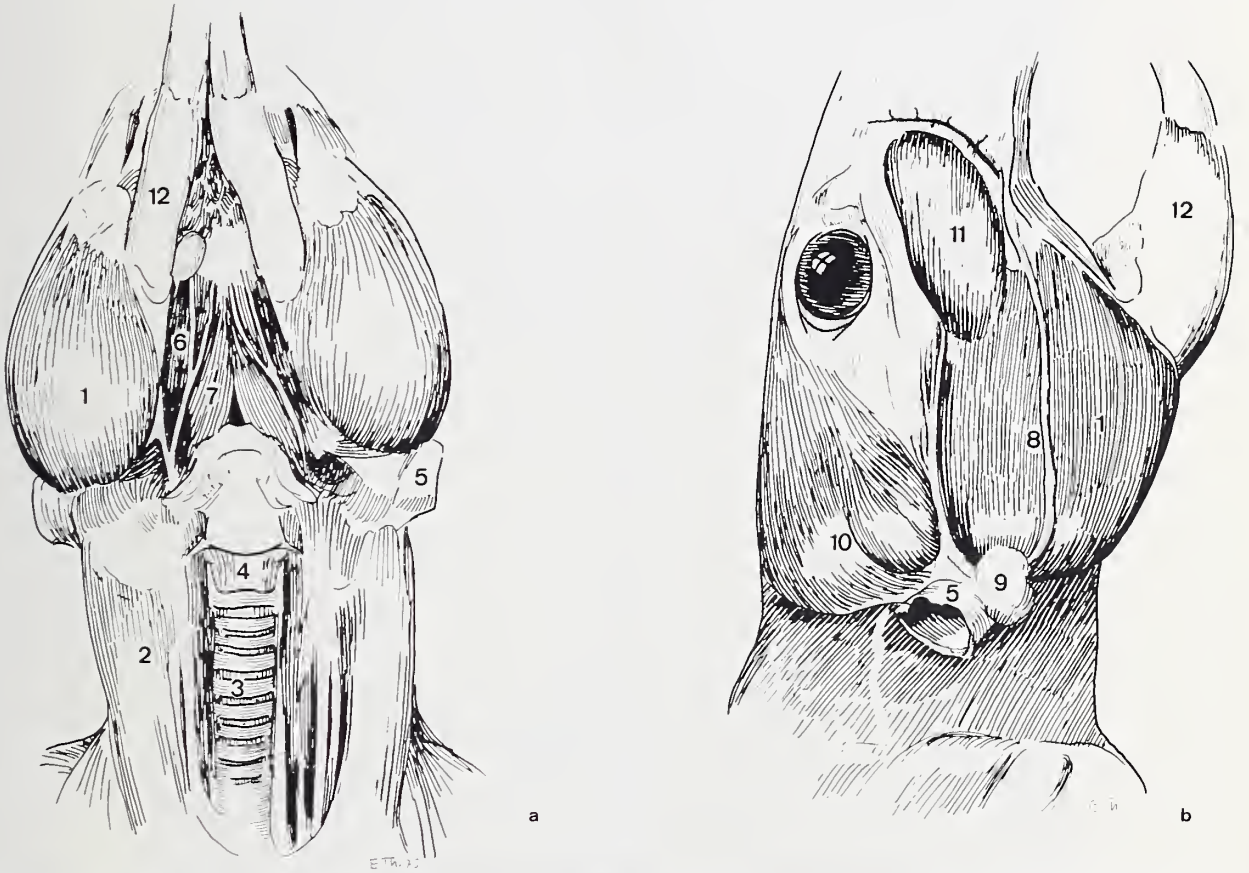

Figure 3-6: Prominent features of head and neck regions; a, left ventral aspect; b, right lateral aspect. 1=m. masseter, pars superficialis; 2=m. cleidocephalicus; 3=trachea; 4=larynx; 5=meatus acusticus externus; 6=m. digastricus; 7=m. thyrohyoideus; 8=ductus parotideus; 9=parotis; 10=m. temporalis; 11=m. masseter medialis, pars rostralis; 12=mandibula.

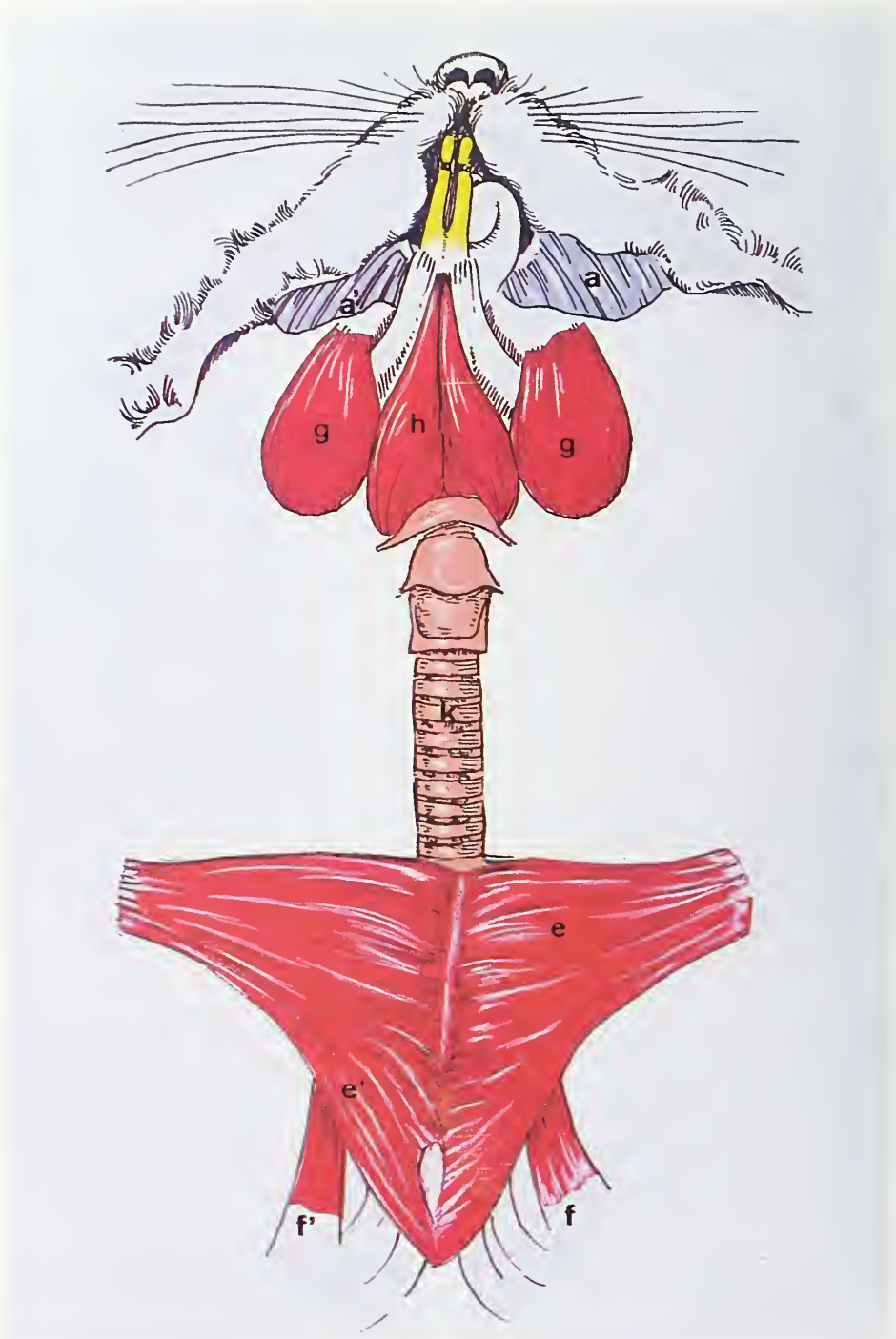

Figure 3-7: Sketch of larynx and first tracheal rings demonstrating position of these organs in respect to surrounding musculature. a–a′ = bursa buccalis; e′–e″ = m. pectoralis superficialis; e′ = pars clavicularis; e″ = pars sternocostalis; f–f′ = m. obliquus abdominis externus; g–g′ = m. masseter; h = m. digastricus; i = m. thyrohyoideus; k = trachea.

Figure 3-8: Larynx and first tracheal rings *in situ,* demonstrating position of these structures in relation to surrounding musculature.

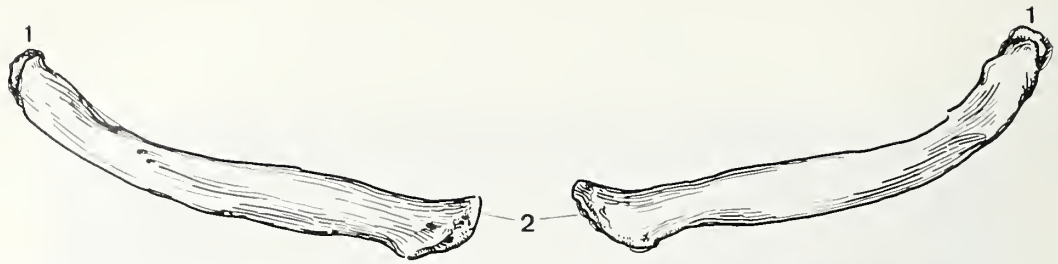

Figure 3-9: Clavicles; cranial view. 1 = extremitas acromialis; 2 = extremitas sternalis.

Figure 3-10: Venogram of head, neck, and chest regions. Internal, external jugular, and pulmonary veins prominently displayed by X-ray contrast method.

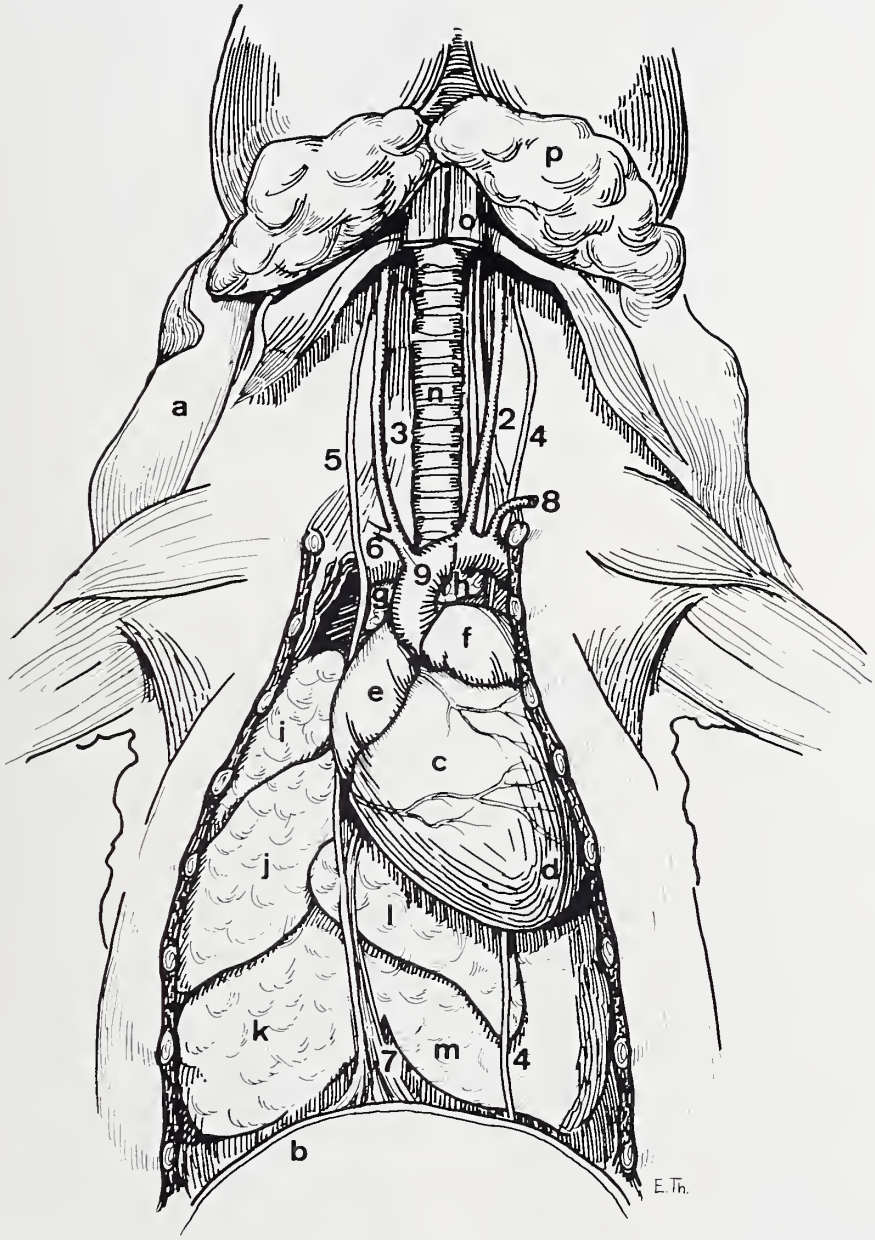

Figure 3-11: Cervical and thoracic organs of 1-year-old male European hamster. Sternum, clavicle, and parts of ribs and cervical muscles removed; mandibular gland folded back. a=bursa buccalis; b=diaphragma; c=ventriculus dexter; d=ventriculus sinister; e=auricula dextra; f=auricula sinistra; g=thymus dexter; h=thymus sinister; i–l=pulmo dexter; i=lobus cranialis; j=lobus medius; k=lobus caudalis; l=lobus accessorius; m=pulmo sinister; n=trachea; o=mm. sternohyoid et sternothyroid; p=gl. mandibularis; 1=arcus aortae; 2=a. carotis communis sinistra; 3=a. carotis communis dextra; 4=n. vagus sinister; 5=n. vagus dexter; 6=a. subclavia dextra; 7=v. cava caudalis; 8=a. subclavia sinistra; 9=a. brachiocephalica.

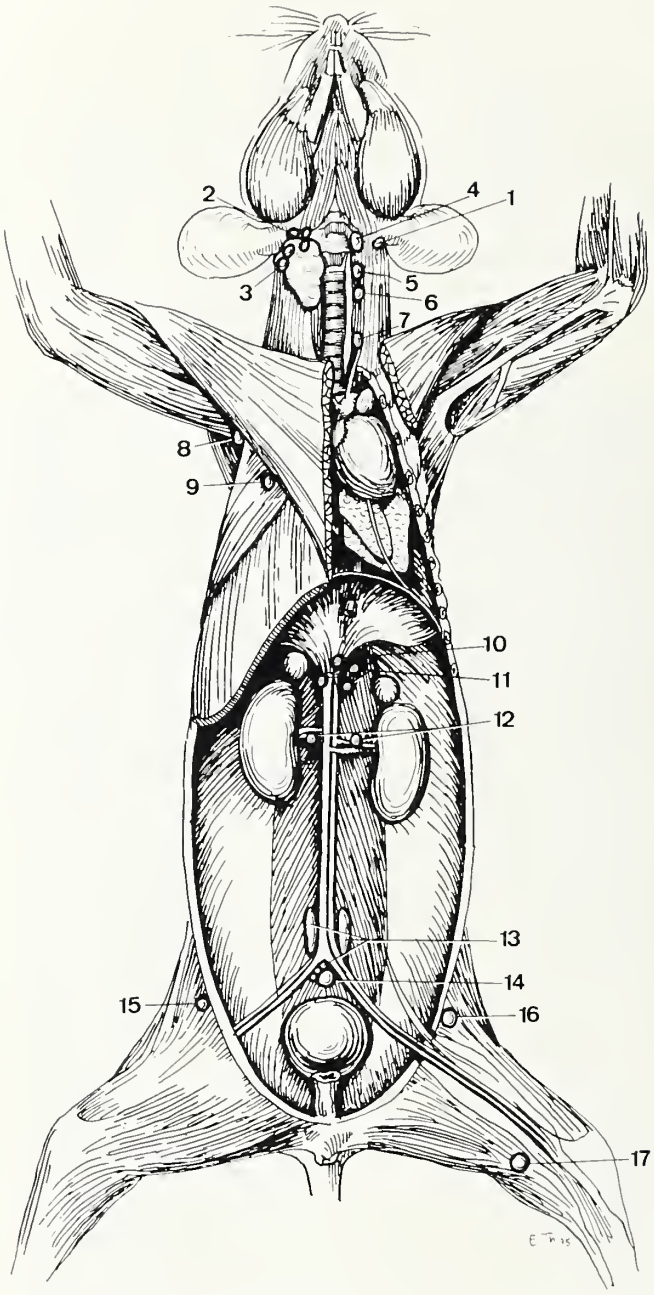

Figure 3-12: Superficial (left side of animal) and deep (right side of animal) lymph nodes of European hamster. Lymph nodes of thorax and gastrointestinal tract omitted. 1=In. parotideus; 2=Inn. mandibulares rostrales; 3=Inn. mandibulares caudales; 4=In. retropharyngeus lateralis; 5=In. retropharyngeus medialis; 6=In. cervicalis profundus cranialis; 7=In. cervicalis profundus caudalis; 8=In. axillaris; 9=In. axillaris accessorius; 10=In. hepaticus; 11=Inn. hepatici accessorii; 12=Inn. renales; 13=Inn. iliaci; 14=In. sacralis; 15=In. inguinalis superficialis; 16=In. inguinalis profundus; 17=In. popliteus.

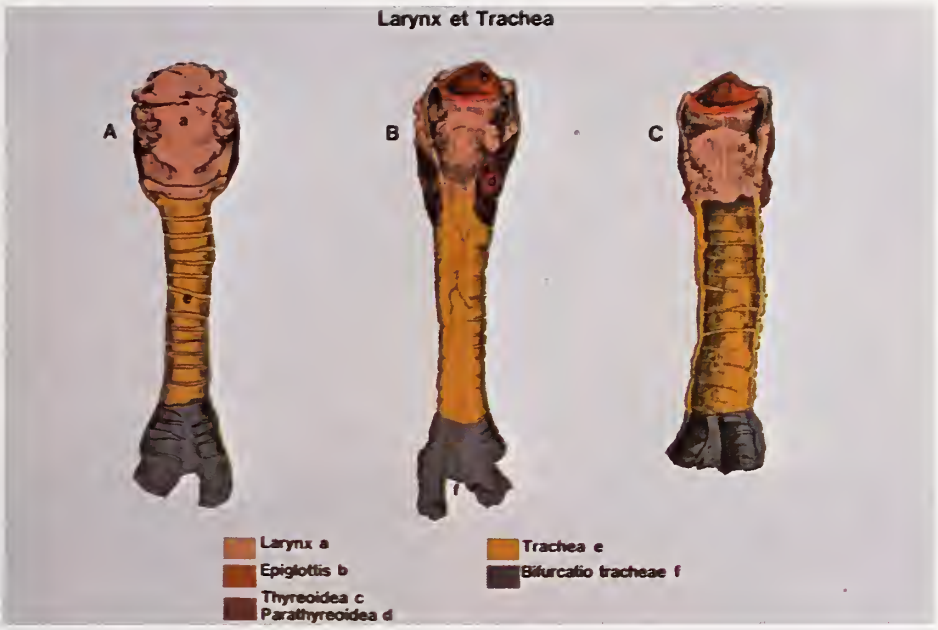

Figure 3-13: Diagram of trachea and larynx, including thyroid and parathyroid glands. A, ventral view; B, dorsal view; C, internal view.

Figure 3-14: Isolated trachea with larynx and bifurcation, dorsal view. Open ends of C-shaped tracheal rings connected by thin, transverse muscle fibers. At caudal end of larynx, dark red thyroid glands are visible, with small white parathyroid glands on surface.

Figure 3-15: Isolated trachea with larynx and bifurcation, ventral view, demonstrating 14 well-defined cartilaginous rings.

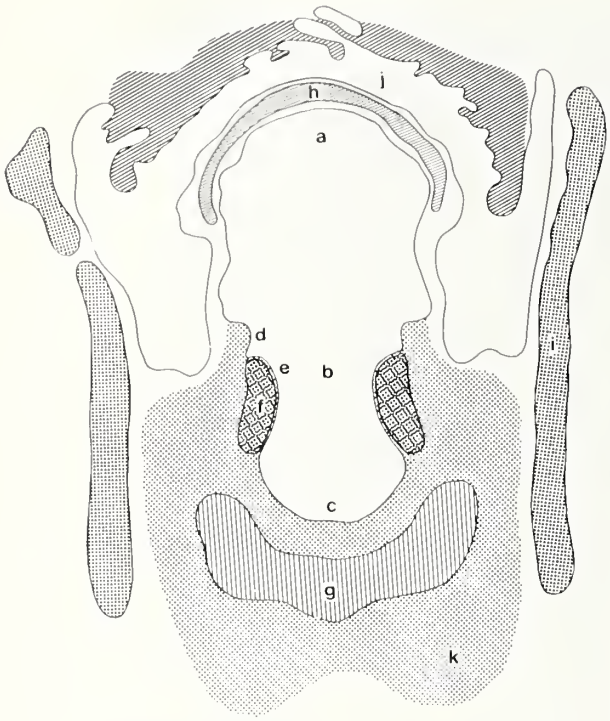

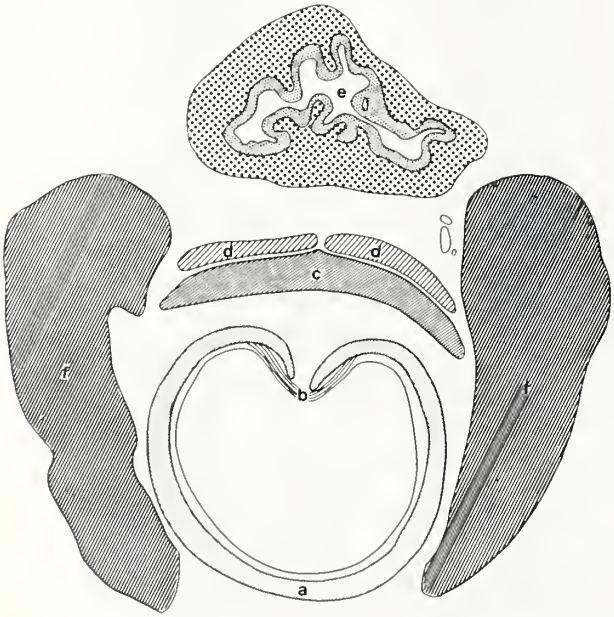

Figure 3-16 (above, left): Drawing of transverse section through larynx of female European hamster, 5 months old. a=vestibulum laryngis; b=cavum laryngis intermedium; c=cavum laryngis caudale; d=ventriculus laryngis lateralis; e=plica vocalis; f=cartilago arytaenoidea; g=cartilago cricoidea; h=cartilago epiglottica; i=cartilago thyroidea; j=pharynx; k=m. cricoarytaenoideus.

(below, left): Schematic drawing of section through trachea at level of second tracheal ring in a female European hamster, 5 months old. a=cartilage of tracheal ring; b=m. transversus tracheae; c=lamina cricoidea; d=m. cricoarytaenoideus dorsalis; e=esophagus; f=glandula thyreoidea.

Figure 3-17 (right): Isolated trachea with larynx and bifurcation, trachea longitudinally resected. Right, ventral aspect; left, internal surface. Cartilaginous rings clearly discernable through shiny epithelial layer of internal surface of trachea.

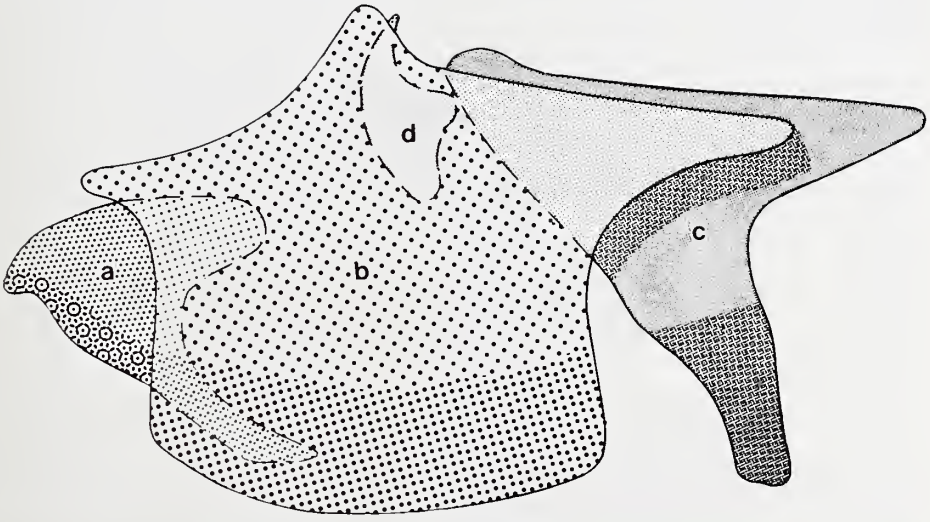

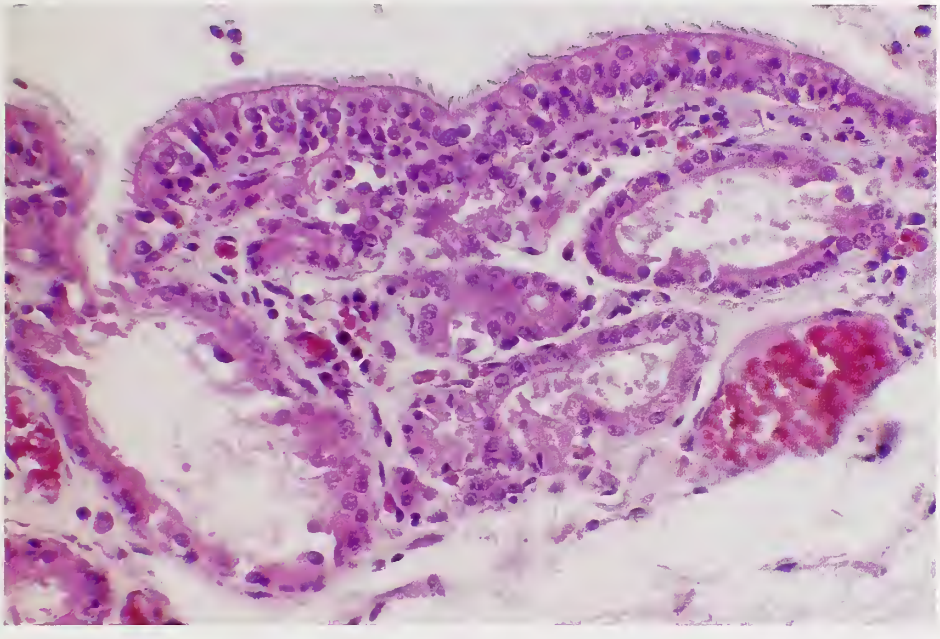

Figure 3-18 (above): Cartilaginous parts of larynx in male European hamster, 8 months old. Lateral view. a=cartil. epiglottica; b=cartil. thyreoidea; c=cartil. cricoidea; d=cartil. arytaenoidea.

Figure 3-19 (below): Histology of larynx. This part covered by pseudostratified ciliated columnar epithelium. Note subepithelial glands, which on left interrupt epithelial layer with an excretory duct. (H & E, X116).

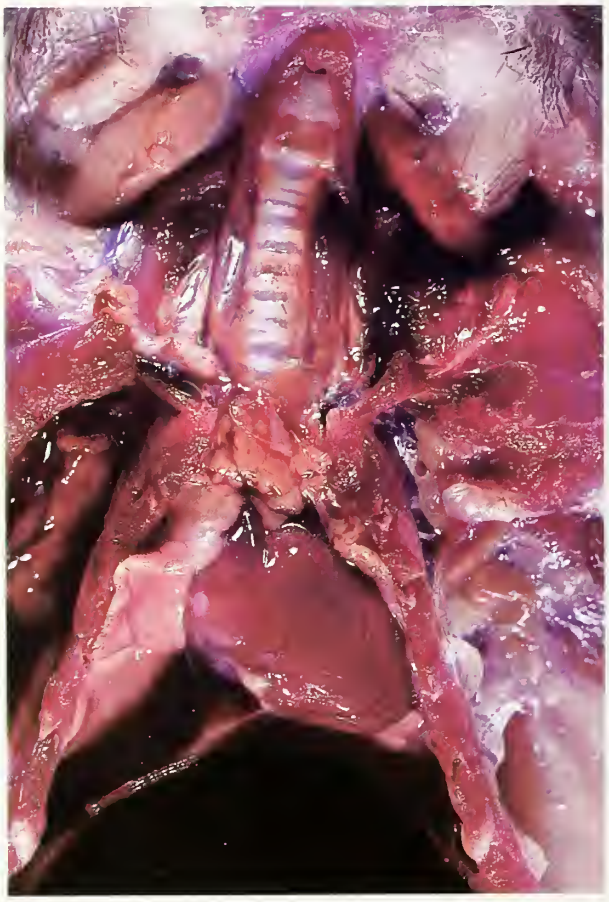

Figure 3-20: Ventral aspect of cervical and thoracic regions demonstrating position of trachea, larynx, and heart.

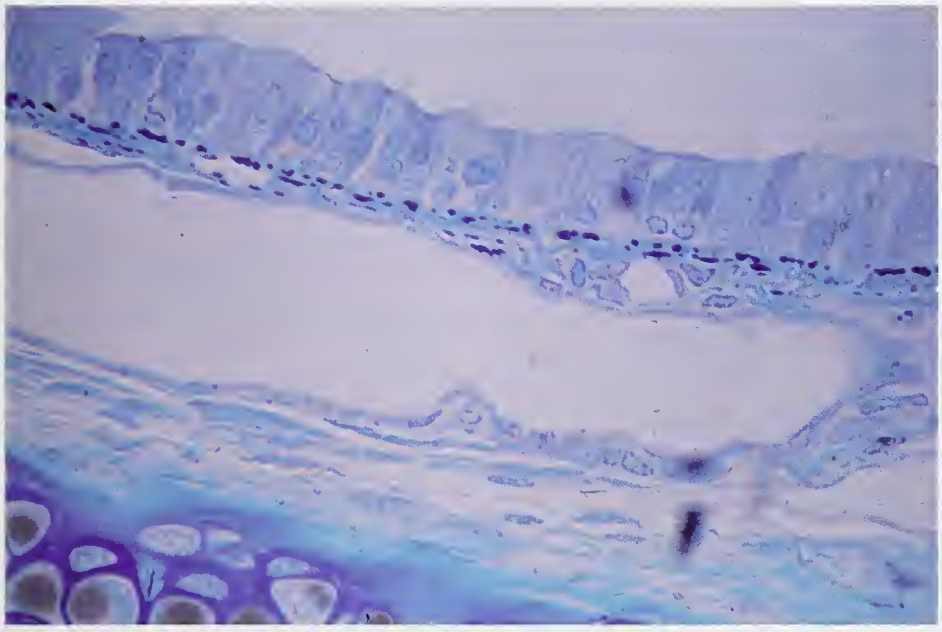

Figure 3-21: Histology of tracheal epithelium, composed of pseudostratified ciliated columnar type with goblet cells and a few basal cells. (1-μm-thick section; toluidine blue, X223).

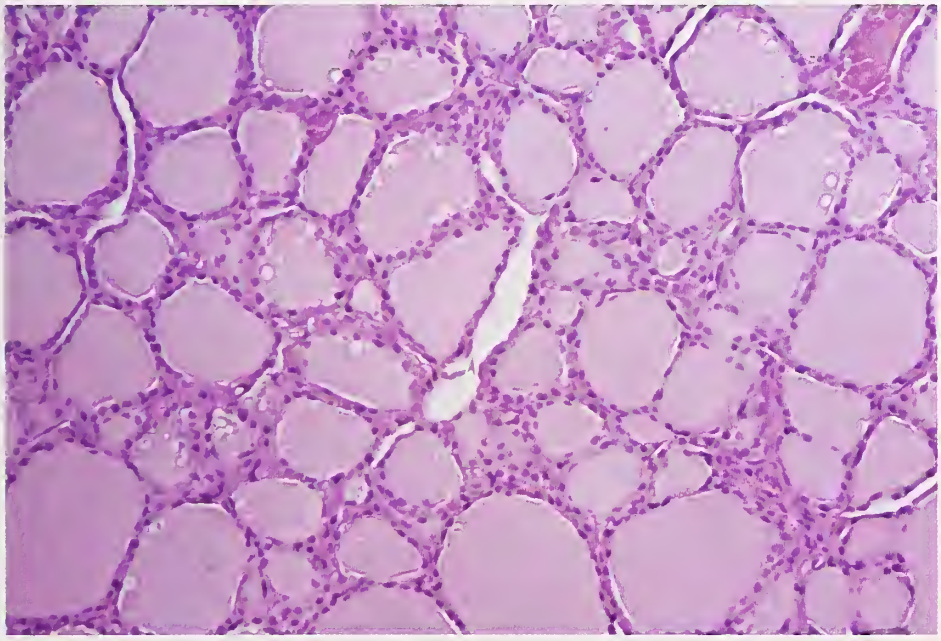

Figure 3-22: Histology of thyroid gland, demonstrating follicles filled with serous secretion and surrounded by flattened epithelial cells (H & E, X57).

CHAPTER FOUR
THORAX

The shape of the thorax resembles that of a truncated cone (Figs. 3–1, 4–1, 4–2). Its cranial apex at the level of the thoracic inlet (*apertura thoracis cranialis*) is a concave surface circumscribed dorsally by the seventh cervical vertebra, laterally by the first rib pair and ventrally by the sternum at the level of the clavicular notch (*incisura clavicularis*). The diaphragm serves as its much larger caudal base, curving upward from the eleventh and twelfth thoracic vertebrae. The ribs, with prominent curvature, are the lateral limits.

The capacity of the thoracic cavity, which varies with the phase of respiration, is less than that of the bony thorax, because the lower part of the region enclosed by the ribs is encroached upon by the diaphragm.

4.1 BONY THORAX

The bony thoracic cage (*ossa cavi thoracis*) includes the sternum, ribs and vertebrae (Figs. 2–1, 4–1, 4–2), reinforced ventrally and laterally by a thin layer of soft tissue. The cavity is separated from the cervical region cranially by the first rib. The boundaries are formed by the ribs (*costae*), the spinal column (*columna vertebralis*) and the *sternum* (Figs. 2–1, 4–1, 4–2, 4–3, 4–4). The eleventh rib, the xiphoid process (*processus xiphoideus*) and a dorsal line connecting the last rib and the intervertebral disc (*discus intervertebralis*) of the twelfth and thirteenth thoracic vertebrae are regarded as the caudal borders of the thoracic cavity, which is finally enclosed by the diaphragm (Figs. 4–2, 4–3). The length of the thorax from the midpoint of the cranial aperture to the midpoint of the caudal aperture (*apertura thoracis caudalis*) is 61 mm. The external depth of the thoracic space measured from the fifth thoracic vertebra to the sternum is 40 to 43 mm in males and 35 to 40 mm in females (Figs. 4–1, 4–4); the internal depth is 37 mm. The thoracic inlet has an external depth of 18 to 20 mm and an internal depth of 8.5 to 9.5 mm in males and females.

The sternum consists of the manubrium (*manubrium sterni*), the body (*corpus sterni*) and the xiphoid process (Fig. 4–6). The sternum is subcutaneous and readily palpable. A chondral plate (*episternum*) lies cranial to the manubrium while a thin, longitudinally oval xiphoid cartilage (*cartilago xiphoidea*), with an approximate dimension of 8 × 10 mm, lies caudal to the xiphoid process. The xiphoid cartilage lies in the epigastric region, projects into the ventral abdominal wall and, under extreme distension markedly protrudes, especially in young animals, outwards. Four bony sternebrae compose the body of the sternum (Figs. 4–2, 4–5, 4–6), the length of each decreasing caudally. From the cartilaginous plate of the manubrium (*cartilago manubrii*) to the caudal end of the cartilaginous plate of the xiphoid process, the sternum has a length of between 45 and 50 mm in adult males and between 40 and 45 in adult females.

The manubrium articulates with the clavicle and the first rib pair. The junction of the manubrium and the sternal body is opposite the second rib. At this point the cranial edge of the body is displaced ventrally, lying above the caudal edge of the manubrium, to form a projection, or sternal angle (*angulus sternae*). The angle marks the level of the conventional separation of cranial and caudal mediastina. The sternal body represents a craniocaudal line below which the pulmonary pleurae nearly contact. The cranial margin of the manubrium is opposite the lower edge of the first thoracic vertebra, the caudal edge of the sternal body is opposite the fifth and the tip of the xiphoid cartilage is opposite the seventh. The line of junction between the sternal body and the xiphoid cartilage makes a palpable depression, to each side of which the cartilage of the seventh rib is felt. The tracheal bifurcation is at the level of the third to fourth sternebrae (Fig. 4–7).

There are thirteen rib pairs, of which nine are sternal (*costae verae*) and four are asternal (*costae spuriae*). The ribs are not perpendicular but present a dorsoventral obliquity which is most pronounced in the first two rib pairs (Figs. 2–1, 4–1, 4–2, 4–3, 4–4, 4–5). Accordingly, with a caudodorsal to cranioventral curvature, the first rib ventrally corre-

sponds to the fourth rib dorsally. The second rib curves somewhat caudally in its dorsal aspect and somewhat cranioventrally in its ventral aspect. Therefore, the ventral part is markedly wider than the dorsal part of the first intercostal space (*spatium intercostale*), which is the broadest of the 12 spaces. The remaining ribs run caudoventrally from their dorsal origin to the manubrium and bend somewhat cranial in the cartilaginous parts ventrally (Figs. 4–3, 4–4). The second to sixth ribs end at the cartilaginous discs between the sternebrae. The seventh rib pair does not reach the sternum but fuses with the cartilaginous ends of the sixth rib pair (Fig. 4–1). The twelfth and thirteenth ribs are floating (Figs. 4–1, 4–3).

The thoracic vertebrae form a kyphosis, whose vertex lies between the thirteenth thoracic and first lumbar vertebrae and which is continued into the lumbar and sacral parts of the vertebral column (Figs. 3–1, 4–1). The length of the thoracic column is 63.3 mm, nearly three times that of the cervical column (Fig. 3–1). The axial thoracic skeleton consists of thirteen vertebrae (*vertebrae thoracicae*) whose length and breadth increase caudally (Figs. 4–1, 4–2). The second thoracic vertebra has the tallest spine (*processus spinosus*), 9.5 mm high (Fig. 4–8). The spinal processes of the first nine thoracic vertebrae are caudally oriented, each overhanging the body of the next vertebra, while the remaining four lie in a cranial or perpendicular direction and do not overhang adjacent vertebrae (Fig. 3–1). The first vertebral bodies are dorsoventrally compressed (Fig. 3–1). With increasing vertebral number, the transverse section becomes more semi-circular.

Up to the ninth or tenth vertebra, the surface of each articular process (*processus articularis*) lie almost horizontally permitting lateral as well as dorsoventral movement.

4.2 THORACIC MUSCULATURE

The pectoralis muscle (*m. pectoralis*), which connects the sternal region with the humerus and forms a triangular surface between the clavicles, xiphoid process and humerus (Fig. 3–7), is divided into a superficial pectoral (*m. pectoralis superficialis*) and a deep pectoral (*m. pectoralis profundus*). There is a cranial descending part (*pars descendens*) and a caudal transverse part (*pars transversus*) of the superficial pectoral (Figs. 3–12), The deep pectoral is overlapped by the superficial pectoral. Since the caudal part of the latter is very thin, it is difficult to separate the two muscles at this point. The intercostal muscles, which span the intercostal spaces, are subdivided into internal and external divisions. The external intercostals (*mm. intercostales externi*), which regulate inspiration, originate on the caudal margin of the cranial rib of each intercostal space and run caudoventrally to the cranial margin of the caudal rib. The internal intercostals (*mm. intercostales interni*), which regulate expiration, originate on the cranial edge of the caudal rib of the intercostal space and run cranioventrally to the caudal margin of the cranial rib. The *mm. levatores costarum* represent a vertebral reinforcement of the external intercostals, from which they can not be completely separated. The levators originate on the transverse processes of the first to twelfth thoracic vertebrae and run caudoventrally to the angle (*angulus costae*) of each succeeding caudal rib, where they insert on the cranial margins.

4.3 THE DIAPHRAGM

The diaphragm (Figs. 4–9, 4–10, 4–11), which curves from the twelfth rib to the xiphoid process (Fig. 4–3), has a horseshoe-shaped central tendon (*centrum tendineum*) and a periphery consisting of strong muscle fibers (*pars muscularis*), grouped into three parts: sternal, costal and lumbar. The muscle fibers of sternal origin are affixed to the ventral side of the second lumbar vertebra cranial to the curvature of the last costal pair and ventral to the dorsal surface of the xiphoid process. The lumbar muscle fibers are composed of the left and right lumbocostal arches (*arcua lumbocostales*), which originate at the third lumbar vertebra (*vertebra lumbalis*). The crura are not sharply differentiated, as in larger mammals. The esophageal aperture (*hiatus oesophageus*), which lies at the level of the eighth or ninth rib, is located in the muscular part of the diaphragm dorsal to the crural bifurcation of the central tendon. Dorsal to the esophageal hiatus and close to the vertebral column is the aponeurotic opening for the descending aorta (*hiatus aorticus*), found in the muscular part between the left and

right fibers of the central tendon at the level of the last thoracic vertebra. The aperture of the vena cava (*foramen venae cavae*) is ventrolateral to the esophageal hiatus and rests on the right side of the central tendon (Figs. 4–10, 4–11). During expiration the diaphragmatic dome projects forward to the fourth or fifth rib.

4.4 THORACIC CAVITY

4.4.1 Pleura and Pleural Sinuses

Unlike the abdomen, which contains a single sac, the chest cavity (*cavum thoracis*) presents three completely separate serous sacs, the two pleurae (*cavum pleurae sinistrum, cavum pleurae dextrum*) and the pericardium (*cavum pericardiacum*). The pleurae are two serous membranes forming independently closed cavities and into each of which the respective lung is invaginated. Appended to, and patent with, the right pleural cavity is the intermediate pleural sac (*cavum pleurae intermedium*) which invests the accessory and intermediate accessory lobes of the right lung. The right cavity is thus larger than the left. There are two layers of pleura: the parietal (*pleura parietalis*), adherent to the thoracic wall and diaphragm and reflected over the structures in the middle of the thorax, and the visceral layer (*pleura pulmonalis*) applied over the surface of the invaginating lung. The layers, which are normally continuous with each other around the root of the lung, allow excursion of the lungs over the thoracic wall with a minimum of friction. Between the two layers is the pleural cavity, normally a potential space with a minute amount of serous fluid and constituting a true cavity only in pathology. The very thin visceral pleura is bound to the lung surface and dips into the interlobar fissures (*fissurae interlobares*). Continuous with the pleura over the mediastinum, or space between the two pleural sacs, at the root of the lung, the visceral pleura cannot be detached without laceration of lung tissue. The disposition of the pleurae resembles that of domesticated mammals (Nickel, *et al.*, 1960).

The four divisions of the parietal pleura are named according to their position in the thorax and the structures invested by each are named after their division.

The costal pleura (*pleura costalis*) contacts the ribs, costal cartilages, intercostal musculature and endothoracic fascia. It separates easily from the chest wall due to its loose attachment to the endothoracic fascia. It normally continues ventrally into the mediastinal pleura and forms with it a vertical sinus, or recess, along the costomediastinal line of pleural reflection.

The diaphragmatic pleura (*pleura diaphragmatica*) contacts the superior, or convex, surface of the diaphragm and invests the caudal margin of the two pleural sacs. The phrenic nerves follow the pleural extensions over the diaphragm. Adhering tightly to diaphragmatic muscle, the pleura covers the area not touched by the diaphragmatic pericardium. It does not extend to the line of attachment of the diaphragm to the chest wall, but is separated from it by fatty areolar connective tissue.

The mediastinal pleura (*pleura mediastinalis*) covers the lateral wall of the mediastinum and is only in loose contact with the structures against which it rests. It consists of a double fold that separates to pass around each side of the pericardial space, joining again dorsally to enclose the pericardium. In the cranial part of the mediastinum it extends without interruption from the sternum to spine; in the caudal part it reflects from the pericardium over the root of the lung and becomes continuous with the costal pleura.

The cervical pleura (*pleura cervicalis*), or *cupula pleurae*, is bounded medially by the trachea and attaches dorsally to the ventral border of the transverse process of the seventh cervical vertebra. It is covered by the scalene muscles and its surface topography is indicated by a cranially convex curve drawn from the center of the sternoclavicular joint to the junction of the sternal and middle thirds of the clavicle. The apices of the lung fill the domes completely during normal inspiration. The dorsal and middle scalene fibers lie on the lateral surface of the pleura before attaching to the upper surface of the first rib. The subclavian artery (*arteria subclavia*) lies in a groove on the medial and dorsal aspect of the pleural dome. The internal thoracic vessels, the beginning of vertebral and intercostal arterialization, the inferior ganglion of the cervical chain and the lower trunk of the brachial plexus also rest on the cervical pleura.

The intermediate pleural cavity, which freely opens with the right pleural cavity, is bordered cranially by the wall of the pericardium, lateroventrally and on the right by the plica venae cavae, on the left by the dorsal mediastinum, ventrally by the sternum and caudally by the diaphragm. The accessory lobe of the right lung, which the intermediate pleural sac invests, lies in a recess (*recessus mediastini sive cavum pleurae intermedium*) between the dorsal mediastinum and the pleural fold (*plica venae cavae*) surrounding the vena cava at this site. Because of the large size of the accessory lobe, the ventral part of the dorsal mediastinum is displaced to the left and the capacity of the left pleural sac is correspondingly reduced.

The pericardial sac lies between the two pulmonary pleurae and is fixed to the sternum by two sternopericardial ligaments (*ligamenta sternopericardiaca*). The pericardium extends between the second and seventh thoracic vertebrae.

The pleura are completely in contact with the lungs only when the lungs are fully distended. In ordinary diaphragmatic breathing, when the lungs are not fully inflated, the ventral and caudal margins of the lung do not extend as far as the medial and caudal limits, respectively, of the pleural reflection. Since the costal pleura is also loosely attached to the endothoracic fascia and separates easily from the chest wall, it collapses on the mediastinal pleura forming a thin bursa-like slit, or costomediastinal sinus (*recessus costomediastinalis*). Further, the costal pleura, which is not approximated caudally by the inferior border of the lung, dips into the groove between the costal wall and diaphragm forming another slit-like narrowing, the costodiaphragmatic sinus (*recessus costodiaphragmaticus*). These two recesses are called reserve sinuses.

The collapse of the edges of the two pleural folds along the lines of reflection prevents the formation of a cavity under physiological conditions. Just as the pleural space becomes a true cavity only in pathology, so the reserve sinuses become visible only under abnormal conditions. The reserve sinuses are sensitive to effusions or adhesions, and conversion of the slits to true cavities can serve as useful indices for regional tumors. For example, the presence of noninflammatory transudates in hydrothorax, which will dilate the reserve sinuses, is often symptomatic of fluid accumulation from pulmonary compression. Moreover, the reserve sinuses are also useful in exploratory intervention. The costomediastinal sinus will allow transthoracic exploration of the mediastinal contents without opening the pleura. Further, the fatty areolar interval between the costal attachments to the diaphragm and the pleural reflection permits an extra-pleural approach to the diaphragm and subdiaphragmatic space.

4.4.2 THE MEDIASTINUM

The mediastinum, or central part of the thoracic cavity, is the space between the lungs bounded by the dorsal aspect of the sternum, the ventral surface of the vertebral column, the two pulmonary spaces and the diaphragm. Its dorsoventral depth at the level of the fifth thoracic vertebra is approximately 40 mm (Fig. 4–1). It includes all of the thoracic viscera, except the lungs and pleurae, embedded in a thickened extension of the thoracic subserous fascia. The mediastinum can be artificially divided into a ventral and dorsal part by a frontal plane passing ventral to the trachea and its bifurcation and the dorsal surface of the heart. It is effectively insulated from the abdominal cavity except at the three following points: the aortic opening dorsally, the esophageal hiatus, and ventrally the narrow space between the sternal and costal attachments of the diaphragm filled with loose connective tissue.

4.4.2.1 The Ventral Mediastinum

The cranial part of the ventral mediastinum is bounded by the craniothoracic inlet, the cranial edge of the pericardium, the manubrium, the frontal plane passing ventral to the tracheal bifurcation and, laterally, the mediastinal pleura of the two lungs. It contains the aortic arch (at the level of the first rib pair), the brachiocephalic trunk with its right common carotid and right subclavian branches, the thoracic parts of the left common carotid and left subclavian arteries, the cranial half of the two cranial venae cavae (all of which are extrapericardial), the thymus gland, scattered lymph nodes and, between the venous and arterial layers, the vagus and phrenic nerves.

The caudal part of the ventral mediastinum in-

cludes the heart, pericardium, ascending aorta, caudal half of the cranial vena cava (with the azygos vein opening), the pulmonary arteries (all of which are intrapericardial), the right and left pulmonary veins and the phrenic nerves.

4.4.2.1.1 Heart

The heart (*cor*) (Figs. 3–11, 4–7, 4–12 to 4–19) is a hollow muscular organ with the form of a truncated cone and lies in the caudal part of the ventral mediastinum between the second and fifth rib pairs (Fig. 3–10). It is enclosed within a fibroserous sac, the *pericardium,* which consists of a visceral and parietal portion (*lamina visceralis et parietalis*). The pericardium is formed from collagenous fibrous tissue.

The base of the heart (*basis cordis*) is situated predominately in the right half of the thorax, while the apex (*apex cordis*) is oriented caudally and to the left (Figs. 3–10, 3–11). The horizontal position of the heart is maintained by the phrenicopericardial ligament (*ligamentum phrenicopericardiacum*), which is composed of two small sagittal ligaments (Kittel, 1953) drawn from the apex of the pericardium to the diaphragm. During expiration of the lungs, the heart is covered dorsolaterally only by the pulmonary lobes. It does not contact the diaphragm. The tracheal bifurcation is craniodorsal to the heart and the vertebral column; caudodorsal to the heart are the esophagus, aorta (*aorta thoracica*) and vagus nerves (*nn. vagi*). The pericardial surface also is applied to the visceral pleura of the right accessory lobe. Cranially, the pericardium reaches to the height of the second intercostal space where it curves and lies adjacent to the thoracic artery. The surfaces of the heart are named according to their relation to adjacent organs. The sternocostal surface (*facies sternocostalis*) is formed by a large part of the cranial wall of the right ventricle and by the medial part of the right atrium. The vertebral side of the heart is primarily formed by the dorsal wall of the left atrium and the smaller cranial portion of the wall of the left ventricle. The greatest portion of the cardiac surface is made by the right and left pulmonary surfaces (*facies pulmonales dextra et sinistra*). The former is represented by the dorsal wall of the right ventricle and the largest part of the right atrium with its auricle; the latter is formed by the main part of the left ventricular wall and the dorsal wall of the left atrium with its auricle. The sternocostal surface is flattened while the rest of the cardiac surface is rounded; in this way, a dull edge is formed on the dorsal side of the heart.

The right atrium (*atrium dextrum*) lies in the second intercostal space and is bordered laterally by the right lung. It is bent ventrally before the origin of the ascending aorta. The dorsal wall of the right atrium extends caudally to the level of the fourth thoracic vertebra. The right ventricle (*ventriculus dexter*) lies in the second and third intercostal space and borders the right medial and right diaphragmatic lobes (Figs. 3–10, 3–11) of the lung. The left atrium (*atrium sinistrum*), lying at the level of the fourth thoracic vertebra, assumes the space dorsal to the fourth costal cartilage and lies adjacent to the left pulmonary lobe. The left ventricle (*ventriculus sinister*) is in the fourth intercostal space and projects cranially and caudally (Fig. 4–7, 4–18). It is bordered by the left and right accessory lobes. The heart measures approximately 19 mm from base to apex. Its width is about 11 mm and 10 mm and its weight approximately 1.46 g and 1.30 g for males and females, respectively (Tables 2, 5).

The heart is divided into four major chambers, the left and right atria and left and right ventricles. Externally, the atria are separated from one another by a very indefinite, vertical, interatrial sulcus; and the coronary sulcus (*sulcus coronarius*) separating the atria from the ventricles is also quite obscure (Fig. 4–15). Within these grooves lie the trunks of the coronary vessels. The shallow longitudinal grooves do not coincide with the ventricular boundaries (Fig. 4–15). Even though a right descending longitudinal groove (*sulcus interventricularis*) of the right ventricular wall is present in most cases, a left descending longitudinal sulcus is rarely recognizable; rather, in the area of the latter longitudinal groove, an oblique vascular sulcus is usually formed which runs caudodorsally (Fig. 4–15). In the area of the interatrial, interventricular and coronary grooves, very little or no adipose tissue is visible. The paths of the coronary vessels vary greatly from animal to animal.

Externally, the atria are recognizable only by the triangular auricles (*auriculae*) (Fig. 4–14), of which

the right is usually larger than the left. The thin-walled right ventricle (Fig. 4–14), in contrast to the thick-walled left ventricle, does not extend to the apex of the heart. Internally, the left atrium is separated from the left ventricle by a bicuspid valve (*valva bicuspidalis*), of which the papillary muscles (*mm. papillares*) are a very prominent part (Fig. 4–16). The right atrioventricular valve is a tricuspid valve (*valva tricuspidalis*), the cusps of which are named angular (*cuspis angularis*), parietal (*cuspis parietalis*) and septal (*cuspis septalis*). The angular and parietal cusps normally fuse in adults to form one large cusp. The third cusp is smaller and assumes a caudodorsal attachment to a fibrous ring (*annulus fibrosus*). All three papillary muscles originate from the ventricular septum. The aortic (*valva aortae*) and pulmonary (*valva truncae pulmonis*) valves exist in the form of three crescentic semilunar valves (*valvulae semilunares*) (Fig. 4–16).

The heart consists of 3 layers: epicardium, myocardium and endocardium. The epicardium is the outer covering of the heart and the great vessels of the heart; it is the serous visceral layer of pericardium intimately applied to the heart. The myocardium constitutes the muscular body of the heart, with fibers which are transversely and longitudinally situated and are intricately interlaced. They can be subdivided into atrial fibers, ventricular fibers and fibers of the conduction system. The endocardium is a thin smooth glistening membrane which is composed of endothelial cells placed upon a stratum of connective tissue and elastic fibers.

4.4.2.1.2 The Great Vessels

The ascending aorta (*aorta ascendens*) has its origin from the left ventricle on the dorsal side of the heart at the level of the second thoracic vertebra. It is oriented slightly to the left, ascending cranially and dorsally along the cranial vena cava—to which it is not fully applied, since parts of thymus tissue intervene between the two vessels—and finally crosses over the pulmonary artery at the level of the third thoracic vertebra.

At the sternal end of the second costochondral joint the brachiocephalic trunk (*truncus brachiocephalicus*) arises at the initial curvature of the aortic arch (*arcus aortae*), or 7 mm distal to the origin of the aorta (Figs. 3–11, 4–17, 4–18). Thereafter the aorta continues cranially along the cranial part of the ventral mediastinum where it changes direction caudally at the level of the first rib pair to complete the arch, which curves from a right ventral to a left dorsal direction. The left pulmonary hilus is caudal to the site where the aortic arch disappears dorsal to the left lobe of the lung.

The length of the brachiocephalic trunk in the cranial part of the ventral mediastinum is about 4 mm; it represents the largest branch from the arch (Figs. 3–11, 4–18). Initially it runs cranially along the right side of the trachea and then dorsally and to the right of the right internal jugular vein before dividing into the right subclavian and right common carotid arteries. The right common carotid (*a. carotis communis dextra*) runs cranially while the right subclavian (*a. subclavia dextra*) diverges to the right brachium. The left common carotid, the second and smallest branch from the arch, originates at the level of the second thoracic vertebra ventral to the left wall of the trachea and runs cranially in close proximity to the tracheal wall (Figs. 3–11, 4–17, 4–18, 4–19). A third branch, the left subclavian artery, arises 2 mm distal to the left common carotid and continues from the aortic arch in a cranial direction dorsal to the left internal jugular vein until it turns into the upper brachium dorsal to the clavicle (Fig. 4–19). The left internal thoracic artery (*a. thoracica interna*) is given off from the subclavian artery 1 mm distal to its origin; it runs caudoventrally close to the lateral borders of the sternum and just dorsal to the costal cartilages, between the intercostal spaces.

After the caudal turn at the level of the third thoracic vertebra, the aortic arch continues as the descending aorta (*aorta descendens*) down the dorsal mediastinum ventrally and laterally along the thoracic column to the aortic hiatus of the diaphragm.

The pulmonary artery (*a. pulmonalis*) (Fig. 4–17) is the most dorsal of the great vessels leaving the heart in the caudal ventral mediastinum. It originates from the right ventricle ventral to the proximal aorta and dorsal to the right auricle, whose medial edge covers it, then extends to the left between the ascending aorta and the left auricle in alignment with the hilus of the lungs where it meets and partially winds around the bronchus, continuing along the medial wall of the aorta before doubling back dorsally. About 7 mm from its origin, at the level of the fourth thoracic vertebra and ventral to the tracheal bifurcation, it divides into a right and

left branch. The left branch enters the root of the left lung close to the tracheal bifurcation, where it runs between and cranial to the left main bronchus and the bronchial artery. It continues on the dorsal surface of the bronchus, finally ramifying into three parts within the left lobe of the lung. The right branch of the pulmonary artery extends between the trachea and the right main bronchus, where it gives off one branch to the right cranial lobe. Distally the right pulmonary artery gives off a second branch to the right middle lobe and then a third branch to the right caudal lobe. Accordingly, a fourth and fifth is given off to the right accessory and intermediate accessory lobes, respectively.

The pulmonary veins (*vv. pulmonales*), two from each lung, arise from pulmonary capillaries that coalesce into increasingly larger branches running through the parenchyma of the lung, finally forming a single venous trunk (*vena pulmonalis*). Their network is generally independent of the pulmonary bronchi and arteries. The pulmonary veins are the only veins which carry oxygenated blood. The left pulmonary vein accompanying the left bronchus, which lies dorsal to the left auricle, runs transversely and cuts ventral to the esophagus, collecting the branches originating from the right accessory and intermediate accessory lobes; it takes up a right branch from the right accessory lobe during the terminal fourth of its length, continuing obliquely and cranially to the left and lying ventral to the entry of the bronchus into the lung. The course of the right venous branches conforms roughly to that described for the right pulmonary arteries, both vessel layers lying in the caudal part of the ventral mediastinum. The left and right pulmonary veins join before emptying into the left auricle of the heart immediately after crossing the cranial vena cava (Fig. 4–17).

The European hamster has two cranial venae cavae (*venae cavae craniales*), one caudal vena cava (*vena cava caudalis*) and one azygos vein (*vena azygos sinistra*).

At the level of the eleventh thoracic vertebra the caudal vena cava is admitted to the thorax from the abdominal cavity via the aperature of the vena cava in the diaphragm. At the level of the third thoracic vertebra, the caudal vena cava bends ventromedially and is applied to the side of the esophagus, emptying into the right auricle along with the cranial vena cava.

The right cranial vena cava arises from the internal jugular vein and a venous trunk composed of the right subclavian vein, which runs along the superficial pectoral muscle, and the external jugular veins, which run caudally just below the cervical superficial fascia before crossing the clavicle ventrally. It enters the thoracic cavity at the caudal border of the clavicle, dorsal to the insertion of the sternomastoid muscle (*m. sternomastoideus*) on the manubrium, and runs a short distance along the right side of the trachea in the dorsal mediastinum, crossing the right subclavian artery (immediately distal to the origin of the brachiocephalic trunk) into the cranial part of the ventral mediastinum and finally emptying into the dorsal wall of the right auricle. The left cranial vena cava is similarly positioned on the left side, originating from the left subclavian junction ventral to the clavicle and the left internal jugular vein. The left external jugular—left subclavian trunk anastomoses distally with branches of the right internal jugular vein, which crosses the left subclavian artery 2 mm before emptying into the left cranial vena cava. The left cranial vena cava then crosses the left subclavian artery, passes ventral to the left branch of the pulmonary artery and the left bronchus and empties into the dorsal wall of the right atrium near the left side of the caudal vena cava. At the level of the third rib, the left cranial vena cava takes up the azygos vein (*v. azygos*) which runs cranially along the vertebral column, taking up the intercostal veins.

4.4.2.1.3 Thymus and Lymphatic Tissue

The thymus, part of the lymphatic system, lies intrathoracically at the ventrolateral surface of the auricles of the heart (Fig. 4–20). This two-lobed organ is about 8 mm long and each lobe has a width of about 2 mm. The thymus is proportionally much larger in young than in adult animals. The entire organ is invested by a fibrous capsule from which originate several septae which subdivide the two lobes into various, irregular lobules.

Histologically, epithelial reticular cells, lymphocytes and corpuscles of Hassall can be distinguished.

To date, only benign tumors have been induced, with some spontaneous tumors observed in this organ.

The tracheobronchial lymph nodes (*lnn. tracheobronchiales*) consist of eight to ten nodes, of which the smaller are found in the ventral mediastinum. There are three right ventral bronchial lymph nodes located lateral to the thymus gland on the right side of the trachea. They drain the heart, esophagus and trachea and empty into the right lymphatic duct (*ductus lymphaticus dexter*), which empties into the right jugular vein. There are also three left ventral bronchial lymph nodes lateral to the trachea and directly ventral to the bifurcation. They drain the left lungs and empty into the thoracic trunk (*truncus thoracicus*) which opens into the left brachiocephalic vein (Fig. 4–24).

4.4.2.1.4 Nerves

The right vagus nerve (*n. vagus dexter*) (Figs. 3–11, 4–17) enters the thoracic cavity to the right of the right common carotid artery. There it veers dorsally and extends along the right side of the esophagus throughout the thoracic cavity. The left vagus nerve (*n. vagus sinister*) (Figs. 3–11, 4–17) runs dorsally along the left common carotid, dorsal to the left external jugular vein and left cranial vena cava, and crosses between the left common carotid and the left subclavian arteries, ventral to the aortic arch, running in the serosa ventral to the root of the left lung. Here it gives rise to a branch, the left recurrent laryngeal nerve (*n. laryngeus recurrens sinister*), which wraps around the aortic arch and runs cranially up the left side of the trachea to the laryngeal muscles. The right recurrent nerve (*n. laryngeus recurrens dexter*) originates from the right vagus nerve at the level of the base of the heart. It wraps around the truncus costocervicalis and runs cranially up the right side of the trachea to the laryngeal muscles. Caudal to the aortic arch, the left vagus turns toward the surface of the left cranial vena cava, where it is found just dorsal to the thoracic aorta. It then runs along the left side of the esophagus, which it accompanies into the abdominal cavity. In addition to the vagus nerves, the thoracic cavity also houses the paired phrenic nerves (*nn. phrenici*) originating from the brachial plexus. The right phrenic nerve enters the thoracic cavity dorsal to the right subclavian vein and proceeds dorsally along the right cranial vena cava to the right auricle of the heart, continuing left of the caudal vena cava to the central diaphragmatic tendon. The left phrenic nerve runs along the left side of the cranial vena cava and lies dorsal to the left ventricle of the heart and ventral to the esophagus. It runs with the esophagus to the diaphragm where it divides into several smaller branches. The brachial plexus (*plexus brachialis*) is composed of the large ventral branches of the fifth to eighth cervical and first thoracic nerves. Only by very careful preparation can two additional fine ventral branches be recognized under magnification. These come from either the fourth cervical or second thoracic nerves. The nerves from the brachial plexus wrap around the first rib and approach the shoulder ventral to the middle scalene muscle.

4.4.2.2 The Dorsal Mediastinum

The dorsal mediastinum lies behind the frontal plane passing in front of the tracheal bifurcation and the dorsal surface of the pericardium, running parallel with the vertebral column. It is an irregularly shaped space extending caudally beyond the pericardium, due to the slope of the diaphragm. The pericardium is its ventral border and the vertebral column from the second to the eleventh thoracic vertebrae is the dorsal boundary. The mediastinal pleurae are the lateral limits and the diaphragm is the caudal boundary. Meshed in abundant alveolar tissue, its structures include the thoracic part of the descending aorta, the azygos vein, the vagus and phrenic nerves, the tracheal bifurcation with the two main bronchi and lung roots, the esophagus, thoracic duct and clusters of large lymph nodes.

4.4.2.2.1 Lymphatic Tissue

The dorsal mediastinum includes the largest of the tracheobronchial lymph nodes. The two right dorsal bronchial nodes are found adjacent to the laterocranial wall of the right main bronchus at the level of the tracheal bifurcation. These nodes drain the right lung and heart and empty into the right lymphatic duct. The left dorsal bronchial lymph node is located at the level of the tracheal bifurcation and adjacent to the aortic arch. It drains the left

thoracic wall and empties into the thoracic trunk (Fig. 4–24).

4.4.2.2.2 The Esophagus

The *esophagus* is a tube-like organ connecting the pharynx with the forestomach (Fig. 4–21). The cranial thoracic esophagus lies in the medial line. Dorsal to the left ventricle it is displaced to the left of the trachea and accompanies the aorta. It then turns somewhat ventrally and runs in relation to the venous branch from the intermediate accessory lobe, continuing in the dorsal mediastinum toward the esophageal hiatus (*hiatus oesophageus*) of the diaphragm. The thoracic esophagus is approximately 25 to 30 mm long (Figs. 4–21, 4–22).

Lined with a keratinized stratified squamous epithelium, the entire musculature of the esophagus is striated (Fig. 4–23).

The right and left vagus nerves descend through the dorsal mediastinum on the right and left sides, respectively, of the esophagus. The left phrenic nerve runs caudally on the ventral surface of the esophagus where it branches at the diaphragm. Paired sympathetic nerves (*trunci sympathici*) descend through the mediastinum to the right and left of the vertebral column.

4.5 RESPIRATORY SYSTEM

4.5.1 Trachea and Extrapulmonary Bronchi

The trachea, occupying the median sagittal plane of the chest ventral to the esophagus in the cranial part of the dorsal mediastinum, runs for about 10 mm (Tables 1, 5) from the cranial margin of the sternum to the level of the fourth or fifth rib where it divides into a smaller left and larger right main bronchus (*bronchi principales*) (Figs. 3–13, 3–14, 3–15, 4–7, 4–17, 4–21). It is covered by the manubrium, parts of the thymus, the brachiocephalic vein, the aortic arch, and the left subclavian and common carotid arteries. Dorsally, the trachea is in contact with, and remains ventral to, the esophagus, which runs above the trachea cranially but which now bends slightly to the left in the thorax. The right common carotid artery and brachiocephalic trunk lie to the right, and the left common carotid to the left, of the trachea, which crosses dorsal to the aortic arch. Parts of the thymus gland separate the vessels layer from the trachea.

The caliber and structure of the thoracic trachea resemble those of the cervical part. The bifurcation of the trachea (*bifurcatio tracheae*) is at the level of the fourth thoracic vertebra where it divides into the two main bronchi (*bronchi principales*) (Fig. 4–7). The main bronchi are strengthened by C-shaped cartilages which run obliquely downward. At the margins of the main bronchi, a sagittal spur (*carina*), 3–4 mm in length, runs upward into the lumen. The right bronchus continues closely in the original tracheal direction, but the left diverges more laterally. The bifurcation is displaced to the right by the aorta, and the left lung root is displaced to the left by the heart. The right main bronchus, about 9 mm in length, is about 1 mm longer than the left and has 6 or 7 cartilaginous rings while the left main bronchus consists of 5 or 6 cartilaginous rings. The left and right branches of the pulmonary artery run alongside their respective dorsal bronchial surfaces.

The left main bronchus, which does not divide into lobar bronchi (Eckel, *et al.,* 1974a), runs caudolaterally from the trachea at an angle of 15° from the right main bronchus and then continues to the base of the left lobe (*lobus sinister*). Within the left lobe parenchyma the main bronchus gives rise to eight or ten segmental bronchi, from which several subsegmental bronchi and the terminal (lobular) bronchioles (*bronchi terminales*) originate (Fig. 4–7).

Before entering the right lung, the right main bronchus gives rise to four branches, the lobar bronchi, supplying five lobes of the right lung (Eckel, *et al.*, 1974a). The first lobar bronchus runs dorsally to the right and ventilates the cranial lobe (*lobus cranialis*). Extending to the right, the second ventilates the middle lobe (*lobus medius*). Only the third lobar bronchus, which supplies the accessory lobe (*lobus accessorius*) and the intermediate accessory lobe (*lobus intermedius accessorius*), branches to the left side of the lung. The fourth lobar bronchus extends caudally, supplies the diaphragmatic lobe (*lobus caudalis*) and is the immediate continuation of the main bronchus (Fig. 4–24).

Although a single cartilaginous ring is occasionally found on a lobar bronchus in the lung paren-

chyma, the rings lose their cartilaginous support when the main bronchi divide into the lobar bronchi (*bronchi lobares*) (Fig. 4–25) before entering the right lung.

The interior of the bronchi is lined with pseudostratified ciliated columnar epithelium (Figs. 4–26, 4–27, 4–28, 4–29, 4–30).

4.5.2 The Intrapulmonary System

The lung is structurally the sum of all bronchial branchings. All of the lobar bronchi divide into several smaller intrapulmonary segmental bronchi (*bronchi segmentales*) which ultimately aerate a circumscribed conical region, the "bronchopulmonary segment," of the lungs (Fig. 4–25). A bronchopulmonary segment is theoretically a subsection of the lung to which any particular segmental bronchus is distributed, including even the secondary lobule and the terminal (lobular) bronchiole which aerates it. Practically, however, the bronchopulmonary segment is defined as that part of the lung supplied by direct branches of the lobar bronchi, or segmental bronchi in the case of the left hamster lung. These bronchopulmonary segments are as discrete as the lobes and can be teased apart by following the connective tissue planes. The fact that most of the extra fissures in the lung follow planes of separation between segments tends to confirm their morphogenetic and morphometric reality.

The intrapulmonary bronchi become increasingly smaller by continuous division and subdivision of the bronchial tubes in the lung parenchyma, from the segmental level down to the terminal, or lobular, bronchioles. This transition is mainly characterized by diminishing luminal diameter rather than qualitative change in structure.

Throughout this interval of division each bronchiole presents a mucous layer lined by cuboidal epithelium with a few ciliated and many non-ciliated (Clara) cells, on a basement membrane surrounded by a smooth layer invested by fibrous tissue, with more or less regular mucous acini.

The middle layer of smooth muscle remains more or less continuous with the segmental bronchi and subsegmental bronchioles.

Each terminal, or lobular, bronchiole ventilates a secondary lobule, which is an aggregate of primary lobules and is separated from neighboring secondary lobules by varying amounts of areolar and fibrous tissue. Secondary lobules are the basic structural units of the lung parenchyma. Terminal bronchioles divide within the secondary lobule into respiratory bronchioles, each of which aerates a primary lobule or basic functional unit of the lung. The respiratory bronchiole divides into several alveolar ducts, each of which contains increasingly large numbers of alveoli, or clusters of alveolar (air) cells, as the duct approaches its terminus in an evaginated blind cavity of alveolar cells, or atria. From each atrium arises a variable number of expanded alveolar sacs, whose walls are lined by alveolar cells. The ramification of the bronchial tree coincides with the findings of Ehard (1973) in the Syrian golden hamster.

The alveoli, or luminal evaginations of the respiratory bronchiole, alveolar duct and atrium are lined by a continuous layer of epithelial cells; the nuclei of these cells extend into the air space and the cytoplasm is extended into thin sheets along a basement membrane. The alveolar wall also includes capillary endothelium, with its basement membrane, but the alveolar and capillary layers are not adherent and can be distinguished by varying depths of connective tissue elements. The blood-air barrier, therefore, is at least two cell layers thick. The alveolar epithelium is of the two following types: Type I is a littoral cell with thin cytoplasmic extensions along the alveolar lumina lying back-to-back with cytoplasmic extensions of capillary endothelium; the Type II ("niche" or "septal") cell has a larger, rounder cell body, larger nucleus, more cytoplasmic inclusions and is usually found in the interstices of the capillary networks, often at the termini of Type I extensions.

The right and left pulmonary arteries arising from the pulmonary trunk divide into branches which accompany the bronchi, relating especially to their dorsal surface. The main intrasegmental branches, which are usually single, follow the segmental bronchi. Unlike segment aeration, however, segment vascularization is likely to overlap, with each artery to one segment supplying branches to another. The arterial network is continuous with the capillary plexus forming part of the epithelial barrier in the alveolar system. The capillary plexus is also continuous with the venule anastomosis carrying aerated blood from the lung, but subsequent venous arborization is independent of the arterial layer.

The bronchial arteries, which arise from the aorta (or intercostal arteries) and which vascularize the lung parenchyma, often form capillary plexuses which link with those from the pulmonary artery, forming small venous trunks that are one source of the pulmonary vein. Most of the blood supplied by the bronchial arteries is believed to return via the pulmonary, and not by the bronchial veins, which arise in, and drain, the hilar area only before empty-

ing in the azygos or intercostal system.

The nonparenchymatous part of the lung is composed of an external serous membrane, the visceral pleura, under which there is an areolar layer of mainly elastic fibers investing the whole lung surface and extending into the parenchyma to invest the secondary lobules.

4.5.3 Lungs and Pulmonary Topography

Each lung (*pulmo*) is roughly a half-cone with its base resting on the diaphragm and its apex occupying the cervical dome of the pleura and reaching the level of the first rib (Figs. 3–11, 4–17). The medial or concave surface lies against the mediastinum and the outer convex wall against the rib cage. The lungs are separated by a complete interpulmonary septum, the mediastinum, extending from sternum to spine. The soft, sponge-like tissue is molded against the walls of the chest cavity and bears the impression of the structures to which it is related.

In adult male hamsters the lungs have an average weight of 2.1±0.7 g and in adult females 1.8±0.4 g. Measured by water displacement, the volume of the organ is 2.6±0.6 ml in adult males and 2.0±0.5 ml in adult females (Tables 2, 5) (Reznik, *et al.*, 1973). In an exsanguinated hamster, the lungs are pinkish white in color and have an elastic consistency. When perfused, the lungs become nearly white (Fig. 4–31, 4–32). After *in situ* fixation, the lung turns dark brown and on the surface, especially at the margins, small and very delicate lobulations are visible (Fig. 4–33). The lungs float in water and crepitate when handled, due to the presence of air in the alveoli. As the left thoracic cavity houses not only the heart but also a large part of the accessory lobe of the right lung (Figs. 3–11, 4–17, 4–25, 4–34), the left lung is relatively small and is not divided into lobes (Figs. 4–25, 4–34, 4–35).

The right lung is divided into five lobes (*lobi*) by deep interlobar fissures that extend from the margins to the main bronchi; these lobes are completely isolated from one another, and there exists no parenchymatous communication between them excepting only some consolidation between accessory lobes. The apex of the right lung ends at the cranial margin of the first rib. The sharp edges (*margo acutus*) of the left lung extend from the diaphragm only to the midpoint of the first rib. The right middle lobe lies caudolaterally between heart and sternum. The diaphragmatic, or most caudal, lobe is the largest lobe and has the form of a right-angle triangle; it is related to the diaphragm, extending from the fifth or sixth intercostal space to the twelfth intercostal space. The accessory lobe and the intermediate accessory lobe begin cranial to the diaphragmatic lobe and immediately dorsal to the caudal vena cava, the mesentery of which separates the accessory lobes from the diaphragmatic lobe. The accessory lobes are connected by a broad parenchymatous fusion and are separated only by a short fissure. The intermediate accessory lobe lies partially dorsal to the heart and is displaced to the left lateroventrally and caudally. Most of the lateral surface of the accessory lobe is overlapped by the left lung (Fig. 4–36).

The pulmonary root (*radix pulmonis*) contains several pulmonary veins, the pulmonary artery, bronchi, bronchial arteries of small size, nerves in the form of the pulmonary plexus and bronchial lymph nodes (*lnn. bronchiales*) and lymphatics, bronchial glands and the origin of the pulmonary ligament—all bound in a cuff of pleura and connective tissue.

The costal, or lateral, surface of the lungs is smooth and convex, adapting accurately to the chest wall. The mediastinal surface is irregular and concave; its most important part corresponds to the pulmonary hilum and its primary relation is with the heart and pericardium. After reflecting off the sides of the vertebral bodies, where it is separated by the narrow dorsal mediastinum from the pleura on the opposite side, the mediastinal pleura passes to the side of the pericardium, where it is closely applied for a short distance before investing the dorsal part of the root of the lung.

From the caudal margin of the lung root, a dorsal and ventral layer of pleura come into opposition and are prolonged caudally to the diaphragm as one distinct fold, the pulmonary ligament (*lig. pulmonale*). From the ligament the ventral layer is reflected on the pericardium and dorsal surface of the sternum. From the dorsal margin of the lung root the pleura can be traced over the costal surface of the lung, apex and base, sides of the interlobar fissures, onto the mediastinal surface and ventral margin of the root.

The impression of the right heart (*impressio cardiaca dextra*) appears on the medial surface (*facies medialis*) of the right cranial and middle lobes. The right atrium of the heart is embedded within this impression. Cranial to the cardiac impression, there is a flat, sagittal groove (*sulcus venae cavae*) in which the cranial vena cava runs. The root of the lung lies upon the medial surface, dorsal to the right atrium and the end of the caudal vena cava. Out of the right pulmonary lobe, a branch of the pulmonary vein comes directly adjacent to the right stem bronchus. The right branch of the pulmonary artery branches dorsal to the bronchus and extends to the individual pulmonary lobes.

The hilus of the right lung conveys the following efferent and afferent vessels: cranially, the bronchial opening and the right branch of the pulmonary vein lie juxtaposed. Caudodorsal to these is the point of entry of the right branch of the pulmonary artery. The diaphragmatic surface (*facies diaphragmatica*) is formed by the medial edge of the right middle and right diaphragmatic lobes. The diaphragmatic surface of the right accessory lobe covers the largest part of the diaphragm and, therefore, conforms to the shape of the diaphragmatic arch (Figs. 4–17, 4–19). At the dorsal side of the right accessory lobe, a flat, sagittal groove-shaped depression extends in which the caudal vena cava is found. The intermediate accessory lobe is indented dorsally by the esophagus and ventrally by the caudal vena cava. The edges of the lungs are variously shaped, depending on their positions in relation to other organs. Whereas the sternal margin and the diaphragmatic margin are more sharply edged, the dorsal margin covered by the vertebral column is dull and in part even flattened as a result of the pressure applied by the esophagus.

In the cranial half of the medial surface of the left and intermediate lobes, the cardiac impression is found (Figs. 4–17, 4–19). The left impression is definitely larger than the right in that the greater part of the left ventricle and the cardiac apex is applied on the left. The cardiac apex is invested ventrally by the right accessory lobe. By forming the left cardiac impression, a sharp edge is produced on the right accessory lobe between the medial surface and the diaphragmatic surface. Similarly, a sharp edge is formed between the medial surface and the costal surface of the left lobe. The surface of the right accessory lobe, which lies adjacent to the left lobe, forms another sharp edge along its diaphragmatic surface.

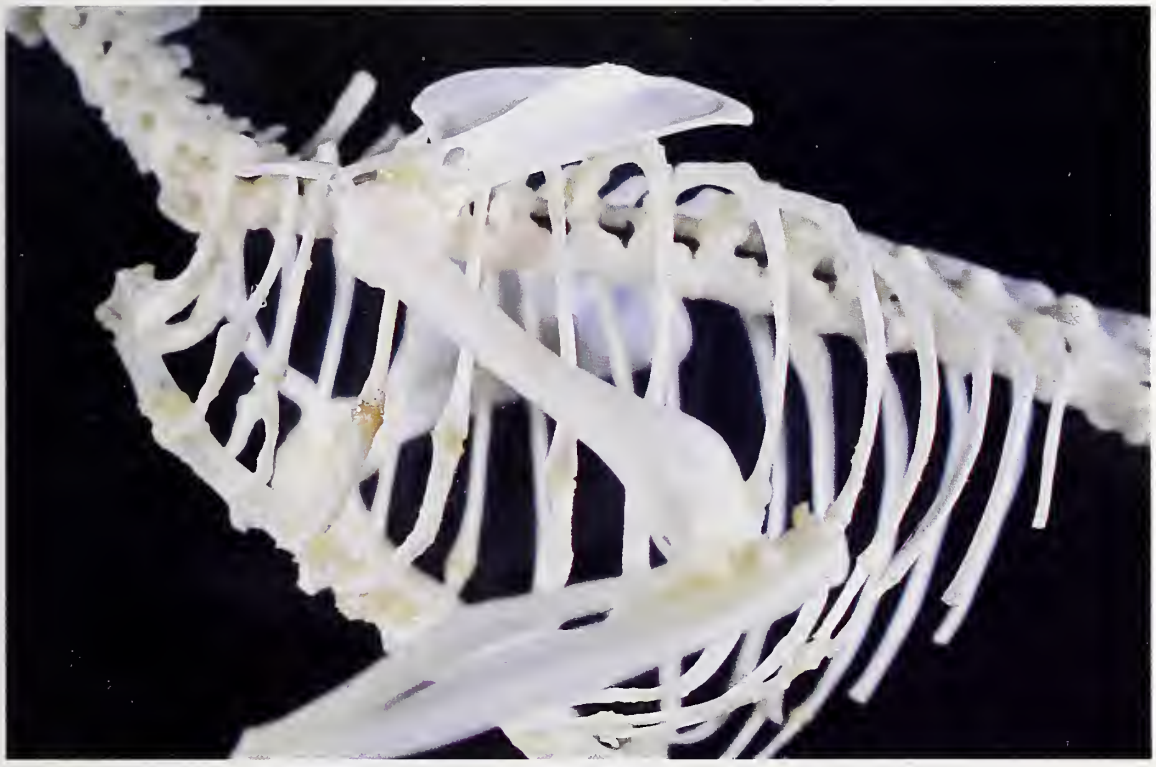

Figure 4-1: Bony thorax with parts of forelegs and neck.

Figure 4-2: Radiogram of bony thorax. Note four sternebrae of sternum.

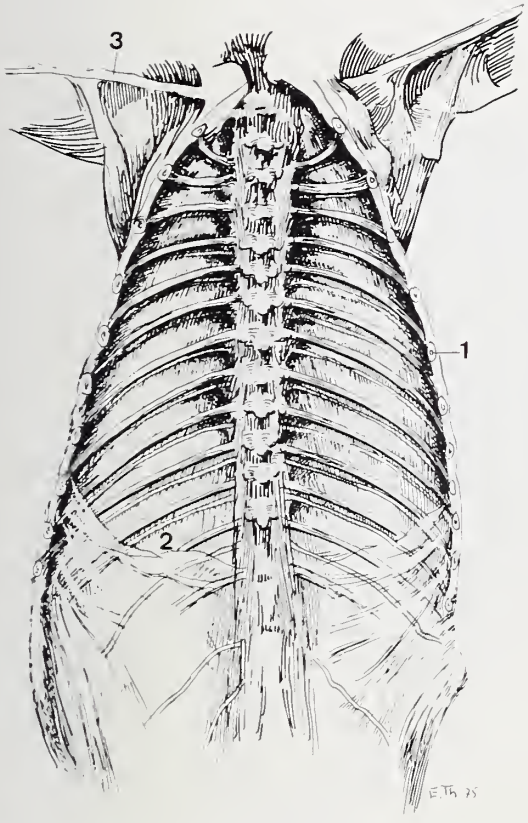

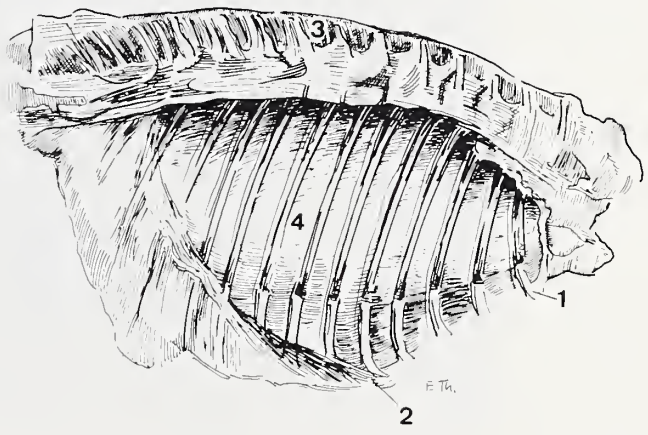

Figure 4-3 (left): Schematic drawing of dorsal aspect of thorax, internal view (ventral parts of ribs and sternum removed). Ribs demonstrate pronounced obliquity; first two rib pairs bend cranially, whereas remaining ribs bend caudally. 1 = costae; 2 = diaphragma; 3 = plexus brachialis.

Figure 4-4 (right): Schematic drawing of lateral aspect of thorax, internal view (animal cut longitudinally in midline). Ribs demonstrate marked dorsoventral obliquity most pronounced in first two ribs. First rib curves from caudodorsal to cranioventral, whereas second rib, in dorsal part, bends caudally and forms cranioventral curve with its ventral portion. Ventral part of intercostal space between first two ribs is thus markedly wider than dorsal part. 1 = costae; 2 = diaphragma; 3 = vertebrae thoracicae; 4 = pleura costalis.

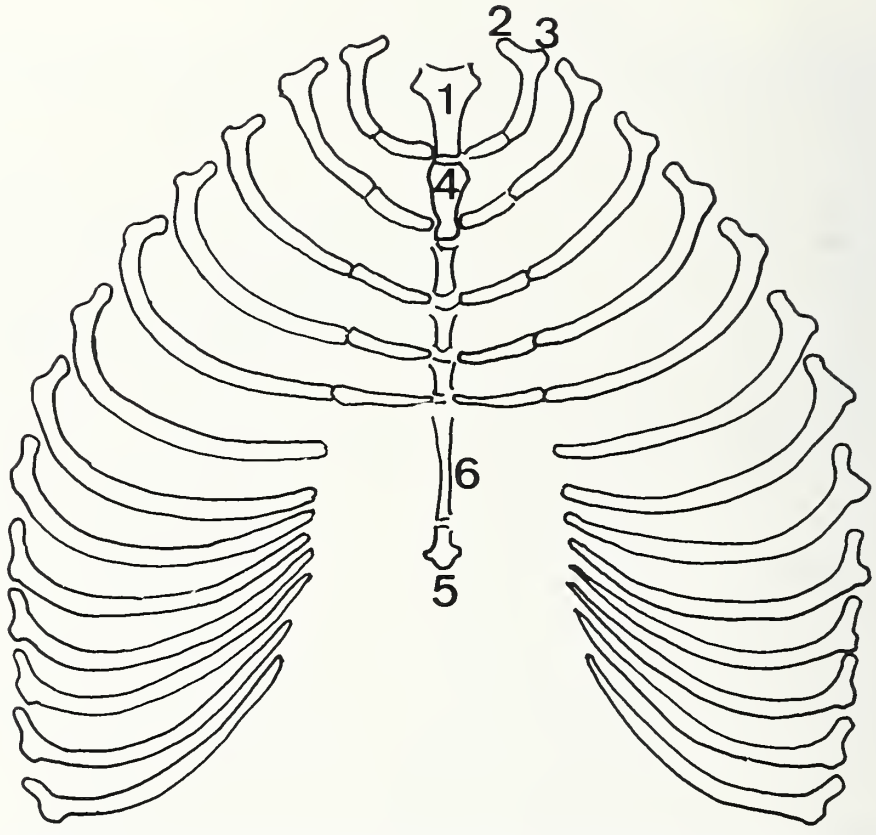

Figure 4-5: Ribs and sternum, ventral view. 1=manibrium sterni; 2=caput costae; 3=tuberculum costae; 4=sternebra; 5=cartilago xiphoidea; 6=processus xiphoideus.

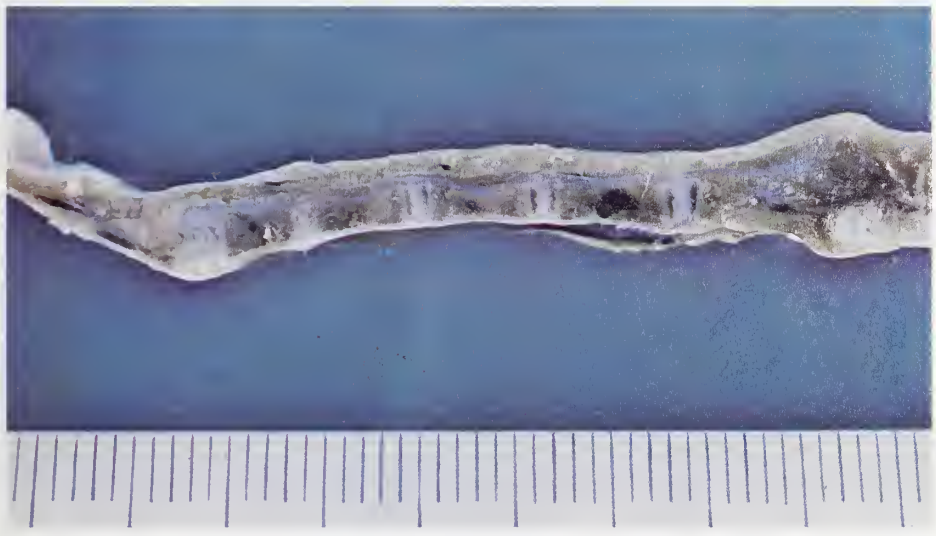

Figure 4-6: Isolated sternum. Note four sternebrae which constitute body of sternum.

Figure 4-7: Bronchogram of adult European hamster after intratracheal instillation of Hytrast R (Byk Gulden), demonstrating position of tracheal bifurcation at level of 6th rib and ramifications of bronchial tree. Note left main bronchus (L), smaller of two main bronchi: it branches into small segmental bronchi without first dividing into larger lobar bronchi, as does right main bronchus.

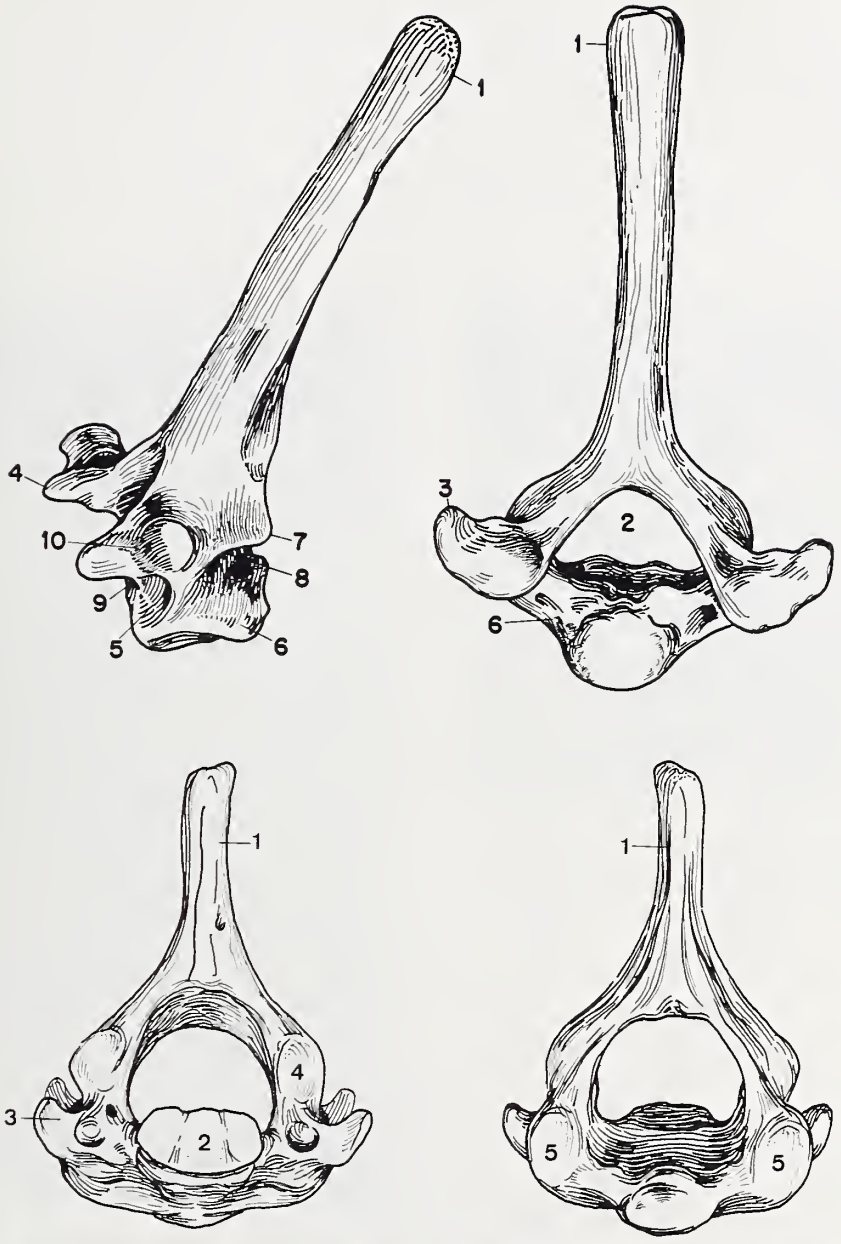

Figure 4-8: Above: Schematic drawing of second thoracic vertebra (left, lateral aspect; right, cranial aspect). 1=processus spinosus; 2=canalis vertebralis; 3=processus transversus; 4=processus articularis cranialis; 5=fovea costalis cranialis; 6=fovea costalis caudalis; 7=processus articularis caudalis; 8=incisura vertebralis caudalis; 9=incisura vertebralis cranialis; 10=fovea costalis transversalis.

Below: Schematic drawing of fourth thoracic vertebra (left, cranial aspect; right, caudal aspect). 1=processus spinosus; 2=corpus vertebrae; 3=processus transversus; 4=processus articularis cranialis; 5=processus articularis caudalis.

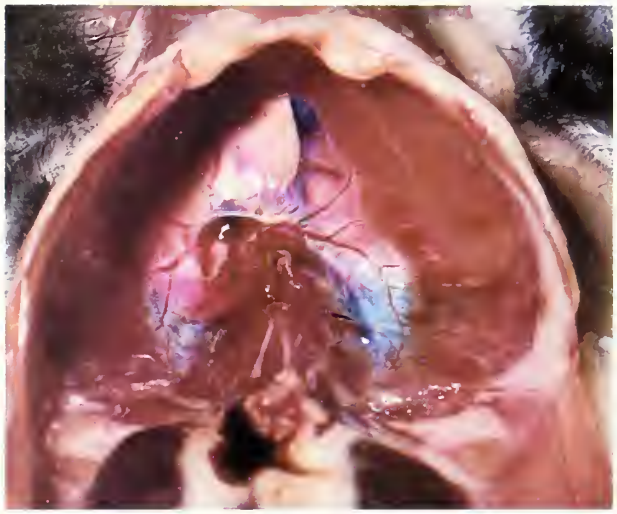

Figure 4-9: Diaphragm *in situ,* expiratory state. Portions of diaphragmatic surface of lungs are visible through central tendon.

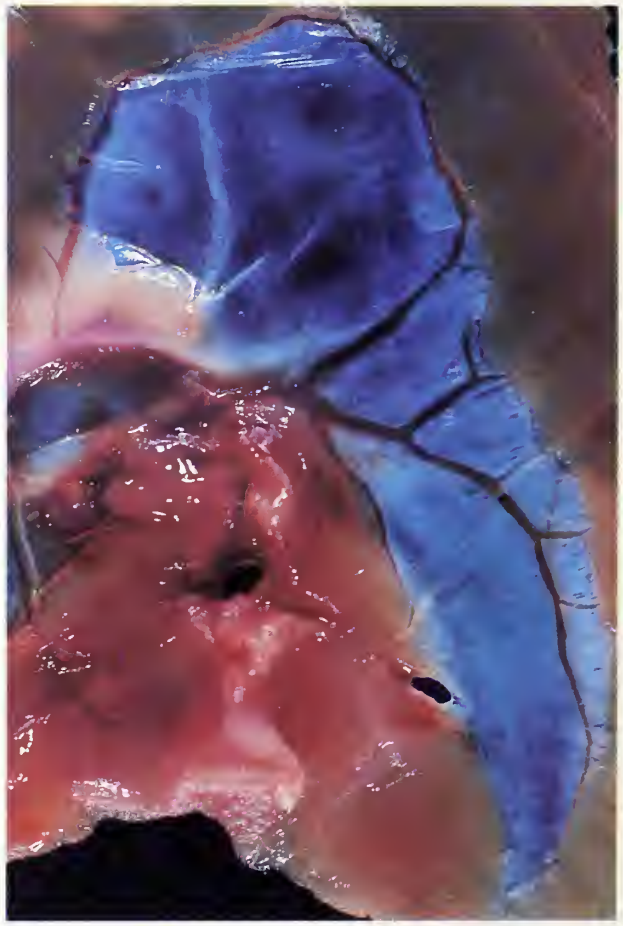

Figure 4-10: Isolated diaphragm demonstrating well-developed central tendon. Note esophageal hiatus in lower part.

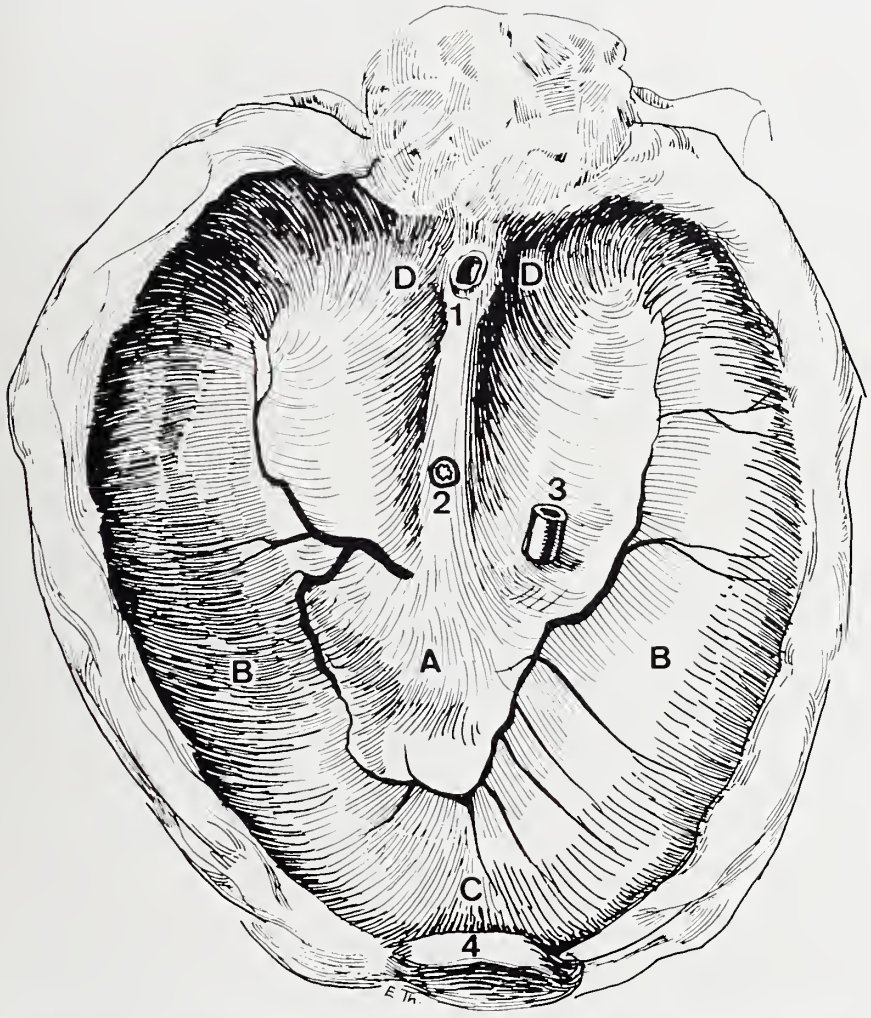

Figure 4-11: Drawing of diaphragm, cranial aspect. A=centrum tendineum; B=pars costalis; C=pars sternalis; D=pars lumbalis; 1=hiatus aorticus; 2=hiatus esophageus; 3=foramen venae cavae; 4=sternum.

Figure 4-12: Schematic drawing of heart, internal view. g=atrium dextrum; h=atrium sinistrum; c=ventriculus dexter; d=ventriculus sinister; i=trabecula septomarginalis; j=septum interventriculare; k=myocardium.

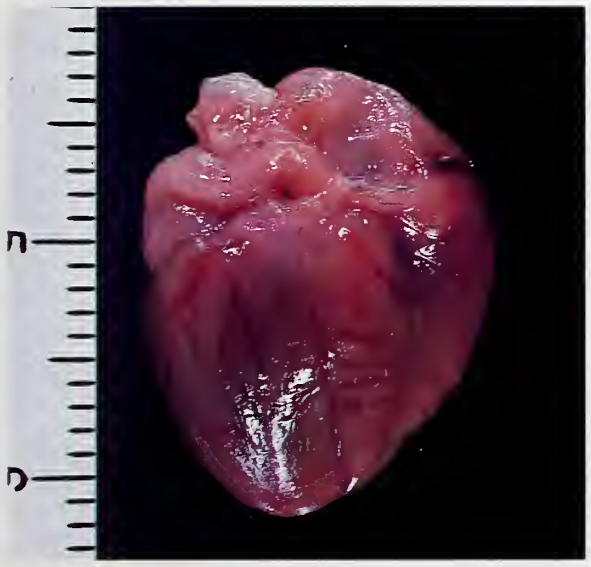

Figure 4-13: Isolated fresh heart, left side, demonstrating size of organ (scale in mm).

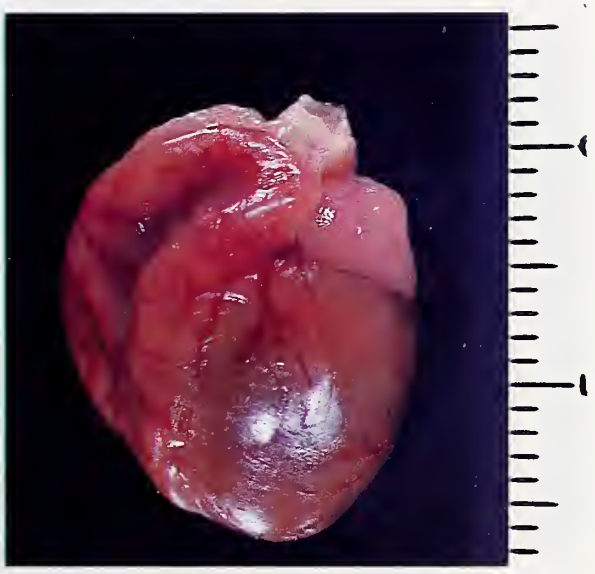

Figure 4-14: Isolated fresh heart, right side. Thin-walled musculature of right ventricle is collapsed (scale in mm).

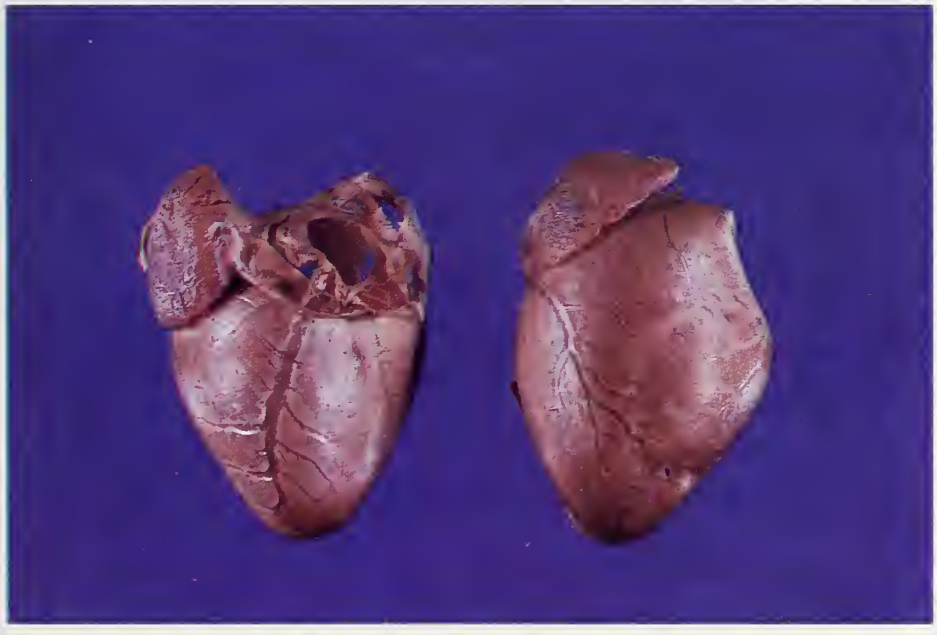

Figure 4-15: External surfaces of longitudinally bisected heart, fixed by perfusion with glutaraldehyde. Note distinct vascular sulcus of left half, which does not coincide with border between ventricles.

Figure 4-16: Internal view of longitudinally bisected heart, fixed by perfusion with glutaraldehyde. Note smaller, thin-walled right ventricle, which does not extend to apex of organ. In left half, well-developed trabecula septomarginalis runs obliquely through left ventricle.

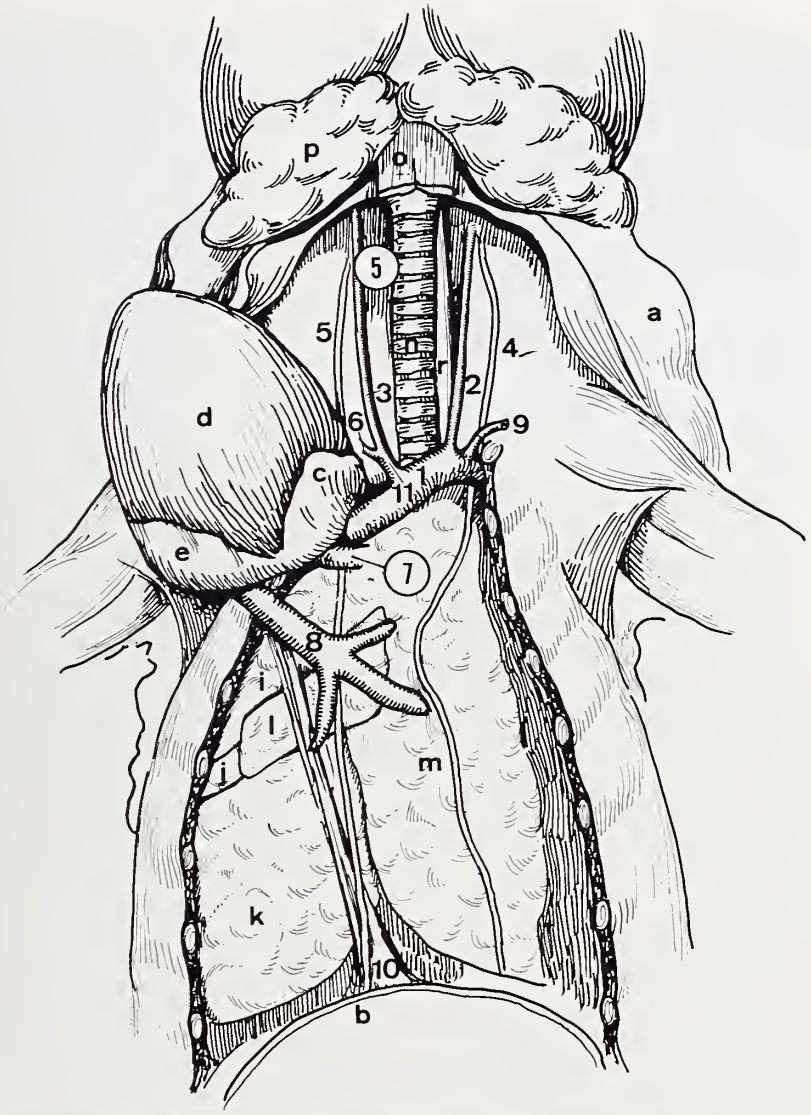

Figure 4-17: Cervical and thoracic organs of one-year-old male European hamster. Sternum, clavicle, and parts of ribs and cervical muscles removed. Gl. mandibulares folded back and heart displaced craniolaterally to right. a=bursa buccalis; b=diaphragma; c=auricula sinister; d=ventriculus sinister; e=auricula dexter; i–l=pulmo dexter; i=lobus cranialis; j=lobus medius; k=lobus caudalis; l=lobus accessorius; m=pulmo sinister; n=trachea; o=mm. sternohyoid et sternothyroid; p=gl. mandibularis; r=esophagus; s=thyroid; 1=arcus aortae; 2=a. carotis communis sinistra; 3=a. carotis communis dextra; 4=n. vagus sinister; 5=n. vagus dexter; 6=a. subclavia dextra; 7=v. pulmonalis; 8=a. pulmonalis; 9=a. subclavia sinistra; 10=v. cava caudalis; 11=truncus brachiocephalicus.

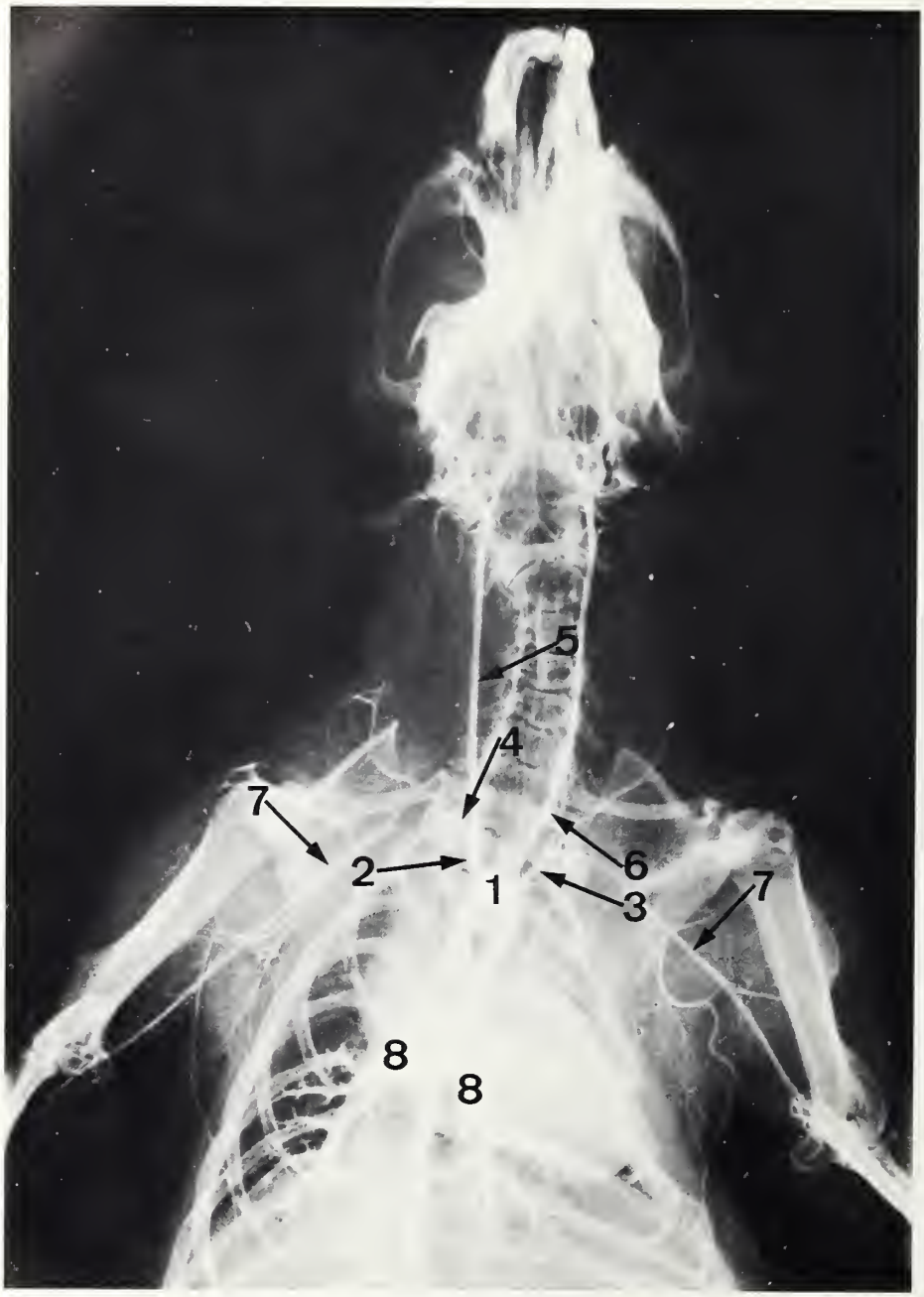

Figure 4-18: Arteriogram of thoracic and cervical region. 1=arcus aortae; 2=truncus brachiocephalicus; 3=a. subclavia sinistra; 4=a. subclavia dextra; 5=a. carotis communis dextra; 6=a. carotis communis sinistra; 7=aa. brachiales (dextra et sinistra); 8=vv. pulmonales.

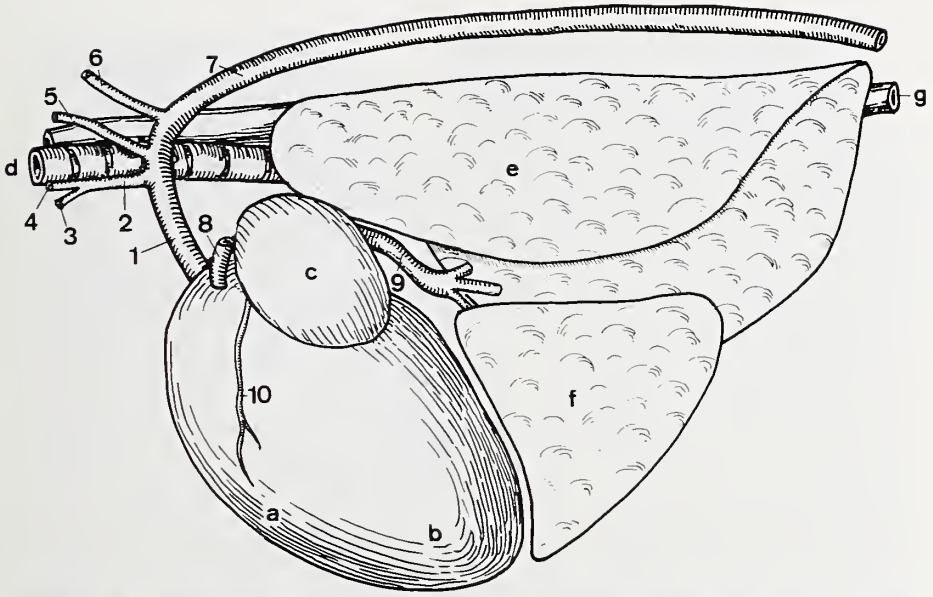

Figure 4-19: Schematic drawing of heart and lungs of 1-year-old male European hamster. Pulmonary artery cut through and left cranial vena cava removed. a=ventriculus dexter; b=ventriculus sinister; c=auricula sinistra; d=trachea; e=pulmo sinister; f=lobus accessorius (pulmo dexter); g=esophagus; 1=arcus aortae; 2=truncus brachiocephalicus; 3=a. subclavia dextra; 4=a. carotis communis dextra; 5=a. carotis communis sinistra; 6=a. subclavia sinistra; 7=aorta descendens; 8=a. pulmonalis; 9=v. pulmonalis; 10=v. cordis magna.

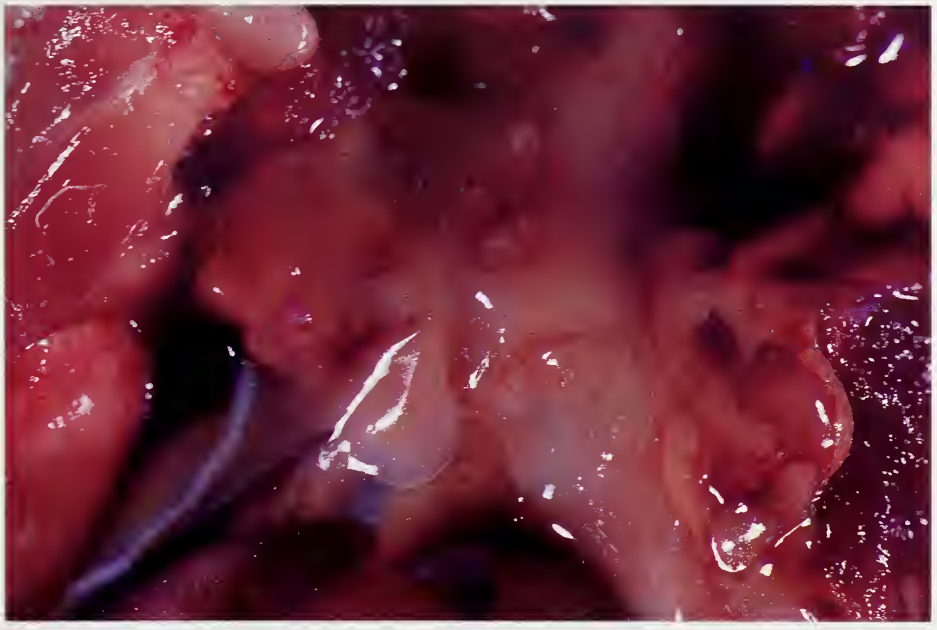

Figure 4-20: Thymus *in situ,* ventral aspect. Organ has fatty, pale appearance and is bordered caudally by heart, on left by lungs, and craniolaterally by clavicle.

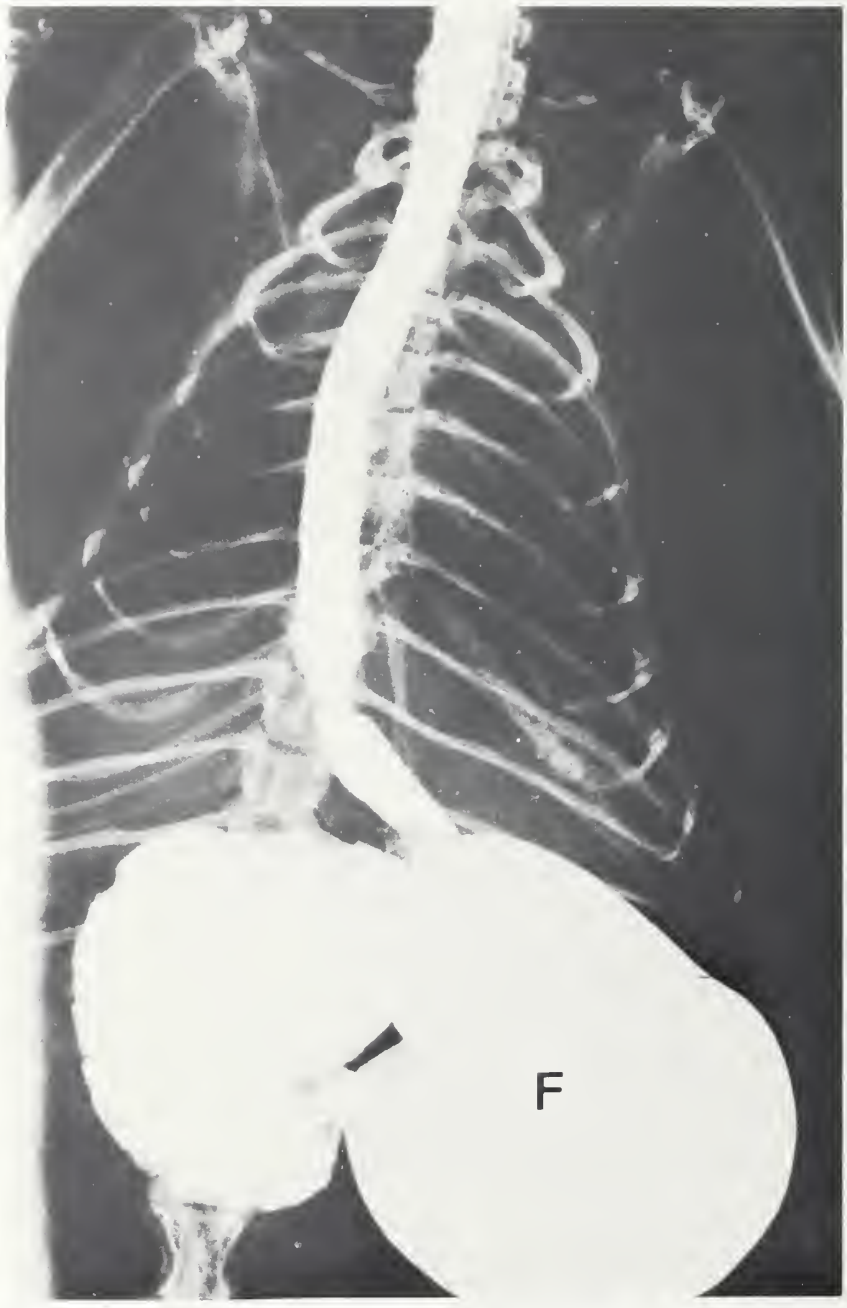

Figure 4-21: Radiogram of esophagus during instillation of contrast agent (gastrografin, Schering A. G. Berlin). At level of twelfth thoracic vertebra, esophagus bends to left and enters forestomach (F) at level of first lumbar vertebra.

Figure 4-22: Isolated esophagus, cut longitudinally. Mucosa thrown into distinct longitudinal folds.

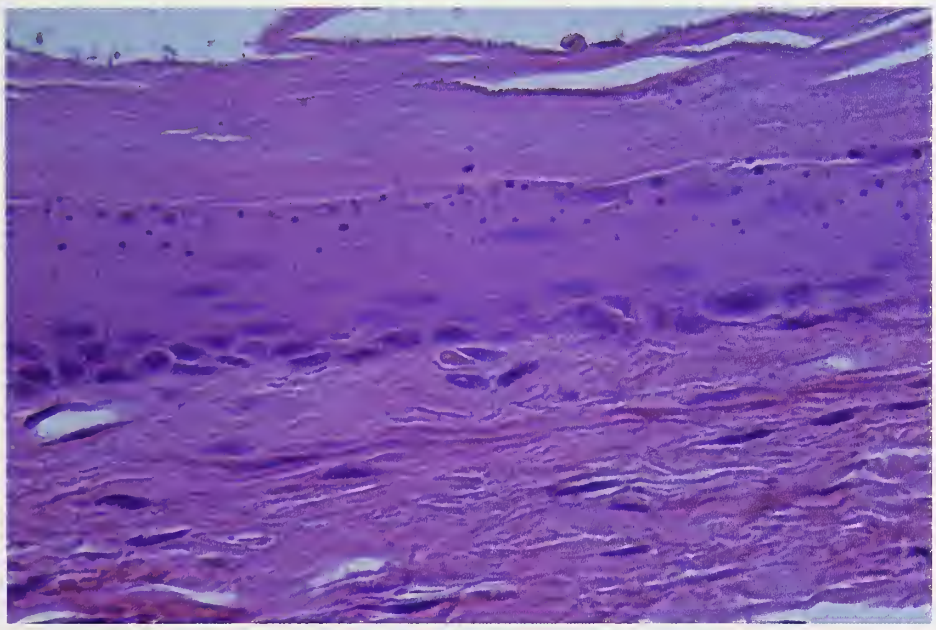

Figure 4-23: Histology of esophagus, longitudinal section. Stratified squamous epithelium covered with thick cornified layer at luminal surface (H & E, X141).

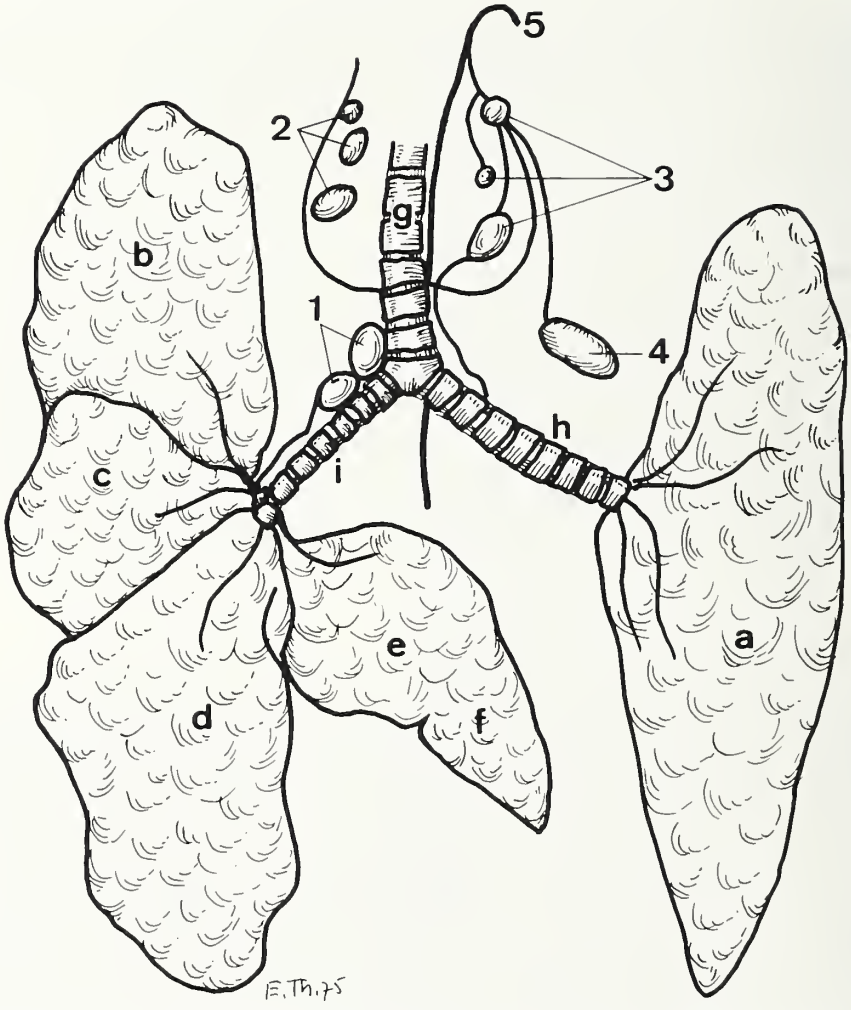

Figure 4-24: Schematic representation of lungs and thoracic lymph nodes. a=pulmo sinister; b=pulmo dexter: lobus cranialis; c=lobus medius; d=lobus caudalis; e=lobus accessorius; f=lobus intermedius accessorius; g=trachea; h=bronchus principalis sinister; i=bronchus principalis dexter; 1=lnn. tracheobronchales dextri dorsales; 2=lnn. tracheobronchales dextri ventrales; 3=lnn. tracheobronchales sinistri ventrales; 4=ln. tracheobronchalis sinister dorsalis; 5=ductus thoracicus.

Figure 4-25: Schematic drawing of lungs and bronchial tree. Right lung consists of five lobes; left remains undivided. Left main bronchus does not form lobar bronchi as does right.

Figure 4-26: Sagittal section of right cranial pulmonary lobe after formalin fixation. Hytrast R was instilled intratracheally (Byk Gulden) before death so that bronchi are prominent. In this section, larger lobar bronchus gives rise to three smaller segmental bronchi.

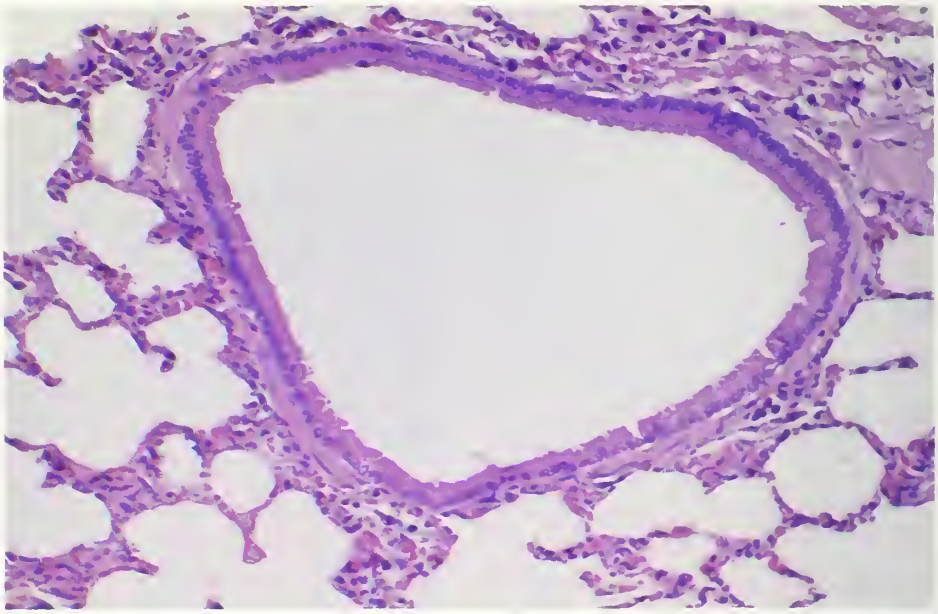

Figure 4-27: Histology of bronchial epithelium and surrounding lung tissue. (H & E, X58).

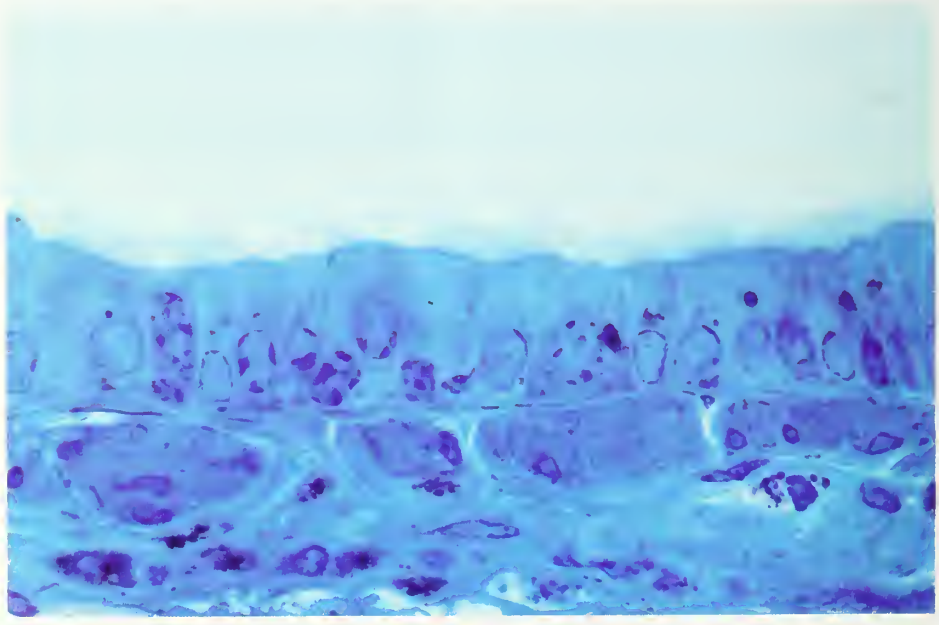

Figure 4-28: Detail of above, demonstrating characteristic pseudostratified ciliated columnar cells. (Toluidine blue, X500).

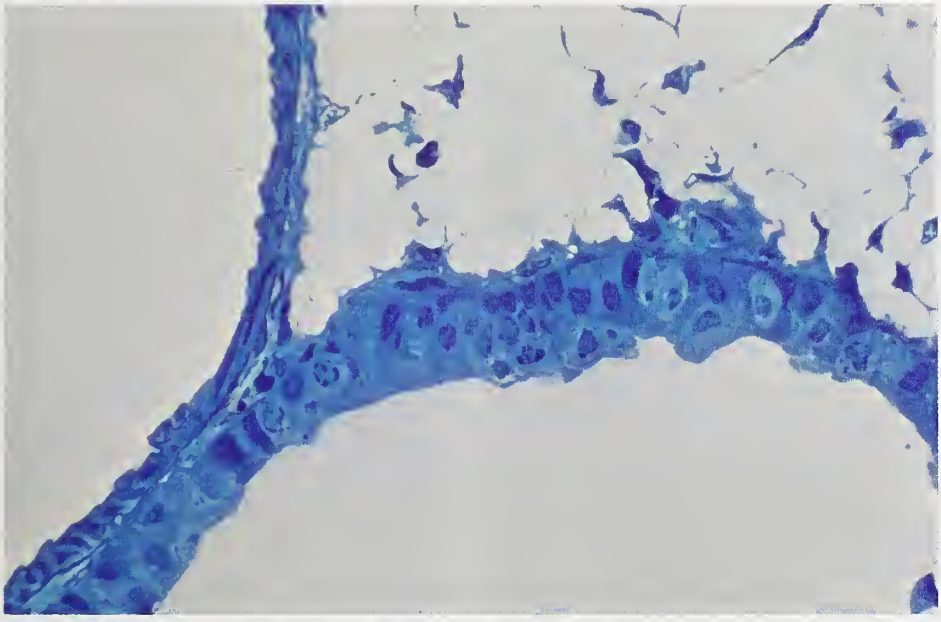

Figure 4-29: Histology of lung, demonstrating small bronchus on the right and a small blood vessel on the left. (Toluidine blue, X93).

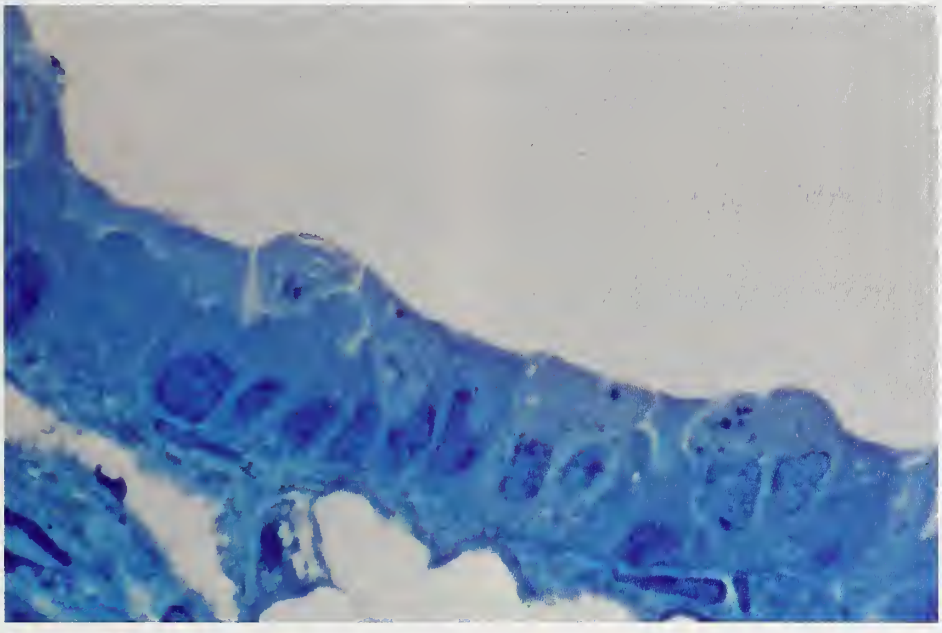

Figure 4-30: Histology of lung at higher magnification, demonstrating close resemblance of bronchiolar epithelium to tracheal epithelium. (Toluidine blue, X232).

Figure 4-31: Isolated lungs attached to trachea and heart, dorsal view. Organs have been fixed by perfusion with glutaraldehyde; thus lung tissue appears whitish.

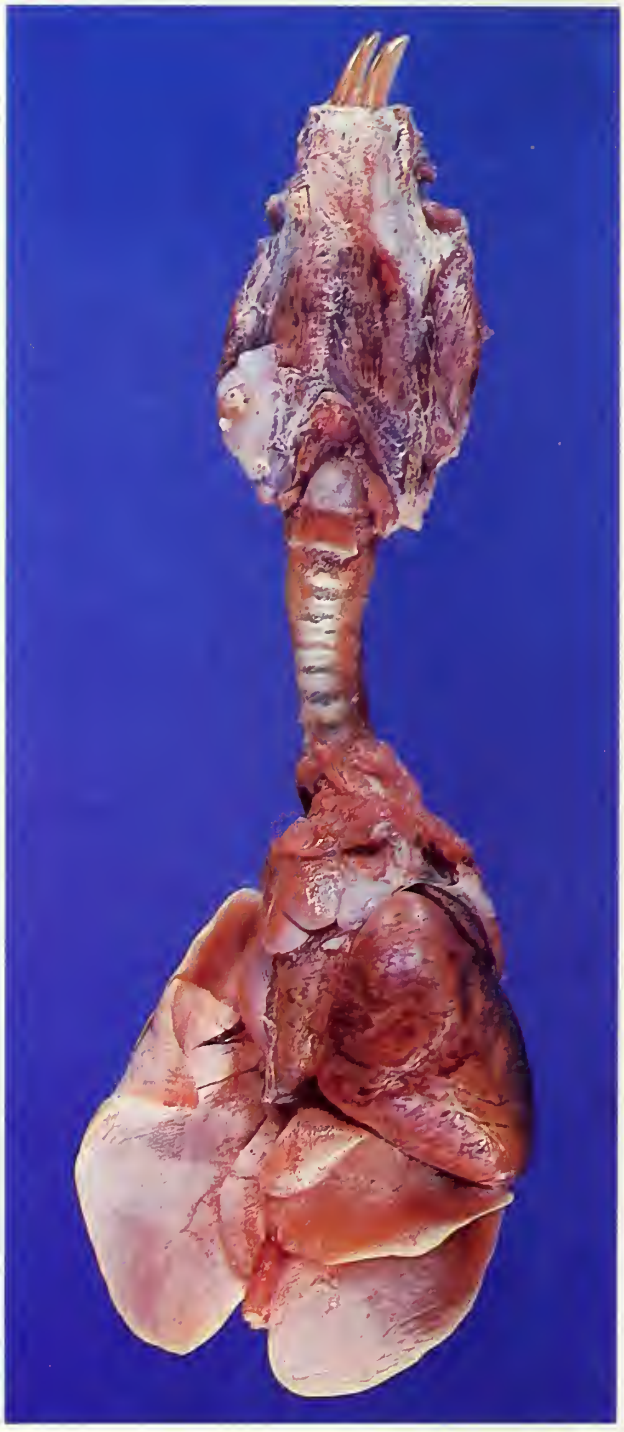

Figure 4-32: Ventral aspect of lungs with attached heart, trachea, larynx, and mandibles. Fixation by perfusion with glutaraldehyde.

Figure 4-33: Isolated lungs after formalin fixation, dorsal view. Note position of right middle lobe, almost entirely overlapped by right cranial lobe.

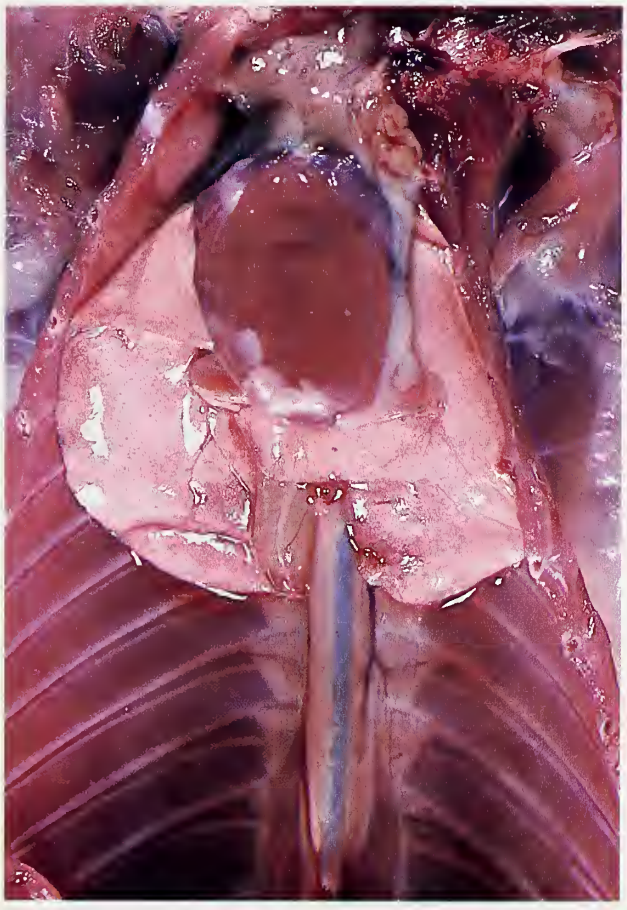

Figure 4-34: Lungs *in situ* (organ collapsed). Beneath right accessory lobe, part of esophagus and caudal vena cava are visible.

Figure 4-35: Isolated fresh lungs, dorsal aspect, demonstrating size and position of various lobes (scale in mm).

Figure 4-36: Ventral view of lungs and heart, demonstrating position of right intermediate accessory lobe, which projects far to left and thus lies close to heart. Organs fixed by glutaraldehyde perfusion.

CHAPTER 5
ABDOMEN AND PELVIS

5.1 LIMITS AND LANDMARKS

The abdominal cavity (*cavum abdominis*) is the largest serous sac in the body of the hamster, extending from the diaphragm to the pelvic inlet (*apertura pelvis cranialis*), or brim of the pelvis. Its greatest expansion is represented by a line from the diaphragmatic insertions on the sternum to the cranial margin of the pubic symphysis (*symphysis pubica*). The cranial boundary is formed by the diaphragm, describing a dome-like arch over the cavity, which protrudes high into the bony thorax up to the level of the seventh thoracic vertebra (Figs. 3–11, 5–1, 5–2).

The dorsal wall is supported by the lumbar vertebrae (*vertebrae lumbales*) (Figs. 2–1, 3–1). The dorsal wall includes the *psoas major*, *iliacus* and *quadratus lumborum* muscles. The lateral wall consists of the *obliquus internus*, and the ventral wall the *rectus abdominis* musculature. The lateral surface is supported cranially by the last rib and cartilages and caudally by the iliac crest (*crista iliaca*), and the ventral surface cranially by the end of the sternal body and the xiphoid process (Figs. 5–1, 5–2).

As in man, the abdominal cavity is separate from the pelvic cavity (*cavum pelvis*). The bony support of the pelvis dorsally is provided by the sacral vertebrae (*vertebrae sacrales*) and by the first caudal vertebrae (*vertebrae caudales*). The lateral boundary is formed by the ilium (*os ilium*) and the ischium (*os ischium*). The pubic bone (*os pubis*) and the ischium confer skeletal support ventrally. The pelvic inlet is obliquely situated and is described by a plane passing through the sacral prominence (*promontorium*) of the sacral base (*basis ossis sacri*) and the cranial rim of the symphysis. The cross-section of the pelvic inlet is heart-shaped, while that of the pelvic outlet (*apertura pelvis caudalis*) is oval.

5.2 BONY SKELETON OF THE ABDOMEN AND PELVIS

The lumbar-sacral column forms a spinal kyphosis (Figs. 3–1, 5–2). The six lumbar vertebrae roof the abdominal cavity, extending for a length of 52 mm. The vertebral bodies are relatively long, and kidney-shaped in transverse section (Fig. 5–3). The vertebral canal (*canalis vertebralis*) is dorsoventrally compressed. The spinous processes are long, rectangular, and of moderate height, with thickened dorsal borders. The last lumbar vertebra (Fig. 5–4) is the most prominent, with a spinous process 6.9 mm long and 5.1 high.

The sacrum (*os sacrum*) consists of usually three synostosed vertebrae measuring 21.3 mm in length (Fig. 5–5). The transverse processes of all three vertebrae form a continuous surface (*pars lateralis*), the cranial portion of which is expanded into an ear-shaped shallow concavity (*facies auricularis*) for articulation with the ilium (Figs. 3–1, 5–6). The sacral canal (*canalis sacralis*) is completely enclosed.

There are 17 caudal vertebrae (*vertebrae caudales*) disposed in a lordosis (Fig. 3–1). They decrease caudally in both length (from 5.8 mm to 1.3 mm) and complexity. The first four or five caudal vertebrae retain articular processes and transverse processes, but caudal to this, the vertebrae are simple pentagonal spools.

The pelvic bone (*os coxae*) ossifies from three separate centers: *os ilium*, *os ichii*, and *os pubis*. The sutures are obliterated by 12 months postpartum (Table 23), and a single adult structure 41 mm long and 16 mm wide remains (Fig. 5–7). The ilium is a long rod-like structure that diverges craniolaterally (Fig. 5–6). It constitutes a portion of the *acetabulum*. The craniomedial surface is roughened (*facies auricularis*) for articulation with the sacrum. The ischium constitutes the caudodorsal and caudal portions of the pelvis, while the pubis constitutes the ventral portion of the posterior pelvis. The pubes join across the ventral midline to form the pubic symphysis (*symphysis pubica*). The pubis and ischium surround the large triangular obturator opening (*foramen obturatum*). The acetabulum, the articular surface for the head of the femur (Fig. 5–6), is composed of all three pelvic bones, and measures 5.4 mm in diameter.

5.3 ABDOMEN AND PERITONEUM

Just as the thoracic cavity and its pleurae are not simply equivalent in the chest, so the abdominal and peritoneal cavities (*cavum peritonei*) are not coextensive. The peritoneal sac, but not the abdominal cavity, dips caudally into the pelvis. The abdominal space extends only to the pelvic inlet, while the peritoneum continues into the true pelvis, normally as far as the rectogenital and vesicogenital pouches (*excavationes rectogenitalis et vesicogenitalis*). Accordingly, there are two sections, intra-abdominal and intra-pelvic, of one continuous peritoneal surface.

Like the thoracic pleurae, the abdominal peritoneum consists of a parietal part (*peritoneum parietale*), applied to the abdominal wall, and a visceral part (*peritoneum viscerale*), reflected over the abdominal organs. Between the two surfaces is the peritoneal cavity, which—as with the pleural cavity—is only a potential space under normal conditions. It follows that no healthy tissue assembly is intraperitoneal.

It follows also that some surface of each invaginating abdominal and pelvic organ is not covered by peritoneum, usually between attachments. Accordingly, the extent of peritoneal reflection is a convenient criterion of intra-abdominal and intrapelvic organization. Those organs almost completely invested by peritoneum and only narrowly connected to the abdominal wall by peritoneum-covered connective tissue (carrying that organ's vascularization and innervation) are effectively suspended in the abdominal cavity by the parietal peritoneum. The suspensions represent the "ligaments," omenta, mesenteries (of the small intestine) or mesocolons (of the large intestine) nearly surrounding the post-diaphragmatic digestive tube and its supportive glands (liver and pancreas) and the spleen. The non-suspended organs more closely applied to the abdominal wall, projecting negligibly into the cavity and covered by peritoneum only on their visceral surfaces, such as the kidney, rectum and bladder, or situated caudal to the pelvic inlet, are said to be retroperitoneal.

Superficial to both visceral and parietal peritonea is a fibrous layer of connective tissue with more or less fatty tissue. Behind the parietal peritoneum the layer merges with the fascia transversalis. It is often impossible to differentiate the subperitoneal fat from the underlying fascia, especially in the mesentery, mesocolon, renal and inguinal regions; fatty herniation is not uncommon. The transverse fascial planes blend with, and invest, the visceral surface of the abdominal musculature surrounding the cavity. The marked variations in abdominal contour reflect principally the state of distention of the viscera and the subcutaneous fat accumulation. In this elasticity, the abdomen differs from the thorax and other body cavities.

The peritoneum is the abdominal expression of the pleural and pericardial layers.

Each is histologically identical fluid-secreting serous membrane of mesothelial cells derived embryologically from one continuous body cavity, the coelom.

The peritoneum is a lymph sac with great absorptive power (solids via the lymphatics, liquids via the capillaries) and high secretory potential (abundant exudate with actively phagocytic macrophages on inflammation).

The mesothelial pavement cells, each of which is cemented to its neighbors by an intercellular substance, can self-regenerate over small lesions. If the peritoneal tear is sufficiently large, repair is impossible, and the underlying connective tissue fibroblasts—which cannot form new serous cells—generate only fibrous adhesions.

5.4 SEGMENTAL TOPOGRAPHY OF THE ABDOMEN

. The topography of the abdominal space can be divided into cranio- and caudomesocolic regions. A plane drawn transversely at the level of the first lumbar vertebra will intersect the stomach, pylorus and proximal duodenum, spleen, kidneys, pancreas, transverse colon and the root of the transverse mesocolon (Figs. 5–8, 5–9). The tissues lying between the transverse plane and the diaphragmatic arch are craniomesocolic; those lying between the plane and the pelvic inlet are caudomesocolic. This topography reflects a functional difference: the craniomesocolic, unlike the caudomesocolic, systems are characterized by tractable fixation, connection to the secretory ducts of liver and pancreas and deep cavity position.

5.5 CRANIOMESOCOLIC REGION

5.5.1 Craniomesocolic Peritoneum

Viewed in a sagittal section and beginning at the

level of the transverse mesocolic root, the peritoneum sweeps cranially on the dorsal surface of the ventral abdominal wall relatively free of attachments until it passes across the visceral surface of the diaphragm, which it covers, to form the falciform ligament (*lig. falciforme hepatis*), enclosing the ligamentum teres (*lig. teres hepatis*) and spreading between the left medial and quadrate lobes of the liver. The falciform ligament runs just under the xiphoid process caudally into the umbilical region. Cranially, the peritoneal sheets separate laterally from the falciform fold to form the left coronary ligament (*lig. coronarium sinistrum hepatis*), between the diaphragm and the upper margin of the left lateral lobe, and the right coronary ligament, between the diaphragm and the dorsal wall of the right medial lobe. The peritoneum then reflects from the liver to the diaphragmatic part of the dorsal abdominal wall as the left and right triangular ligaments (*ligg. triangularia sinistrum et dextrum*). The right ligament reflects from the right lateral lobe and the left ligament from the left lateral lobe, and there is a bare area free of peritoneum between them.

After investing the liver, the peritoneal sheet leaves the transverse fissure and passes to the stomach, forming the ventral layer of the lesser omentum (*omentum minus*). The cranial end of the lesser omentum extends from the left side of the liver to the lesser curvature of the glandular stomach as the hepatogastric ligament (*lig. hepatogastricum*); the caudal end attaches the glandular stomach to the papillary process of the liver, to the right of which the hepatogastric ligament continues as the hepatoduodenal ligament (*lig. hepatoduodenale*).

The lesser omentum serves as part of the ventral wall of the lesser peritoneal cavity, or omental bursa (*bursa omentalis*), along with the caudate lobe of the liver in the cranial part and, in the dorsal part, the stomach and the greater omentum (*omentum majus*). Through the lesser omentum there is a perforation, the epiploic foramen (*foramen epiploicum*) which lies between the caudal vena cava and the portal vein and links the lesser with the greater peritoneal cavity. In effect, the edge of the lesser omentum, which spreads between the liver and the small intestine, borders the foramen on the right side. The caudal limit of the lesser peritoneum consists of the cranial section of the greater omentum and the transverse colon, while the transverse mesocolon, ventral surface of the pancreas, left adrenal gland and cranial pole of the left kidney form the caudodorsal boundary. Since the lesser omentum extends obliquely in a craniodorsal-caudoventral plane, the dorsal abdominal wall serves as its dorsal boundary until the parietal peritoneum on the dorsal wall is interrupted by the coronary ligament under the diaphragm, thus closing the sac. The visceral peritoneal layer is then reflected from the liver at the transverse fissure to the dorsal gastric surfaces, forming the dorsal layer of the hepatogastric ligament. From the greater curvature it passes caudally and then cranially to the transverse colon to form the dorsal layer of the greater omentum. From the dorsal margin of the transverse colon it runs as the cranial layer of the transverse mesocolon to the ventral surface of the pancreas.

After covering the ventral wall of the glandular stomach, by reflecting from one margin of the lesser curvature to the greater curvature on the other side, the peritoneum leaves the greater curvature of the glandular stomach, forestomach and duodenum to form the ventral layer of the greater omentum. It then passes dorsal to the transverse colon, which it invests, to the vertebral column at the lower edge of the pancreas, before passing caudally to cover the distal duodenum and caudomesocolic structures.

At its origin, the dorsal layer of the greater omentum forms adhesions with the transverse mesocolon in adult animals, settling between the stomach and ventral abdominal wall and extending only slightly caudally to cover the intestines.

Viewed in a transverse plane through the craniomesocolic viscera at the level of the epiploic foramen and beginning at the ventral midline, the parietal peritoneum moves to the right kidney without interruption, except for the falciform ligament ventrally, along the ventral and lateral abdominal walls. After covering the visceral surface of the right kidney and forming the dorsal wall of the epiploic foramen, it covers the caudal vena cava, aorta, vertebral column and pancreas on the left side of the animal. The peritoneum then passes

over the left kidney to the spleen, forming the ventral layer of the lienorenal ligament (*lig. lienorenale*), from which it reflects to the dorsal surface of the stomach to form the dorsal layer of the greater omentum. Passing over the dorsal stomach, past the pylorus to the cranial surface of the proximal duodenum, it winds around the hepatic artery, portal vein and common bile duct to reach the ventral surface of the stomach. This reflection forms the ventral layer of the greater omentum. The sheath then winds around both the costal and renal surface of the spleen before passing to the left kidney to form the dorsal layer of the lienorenal ligament. Moving dorsally to cover the lateral surface of the left kidney, it then reflects back on the abdominal wall, which it follows uninterruptedly on the left side back to the ventral midline.

5.5.2 Craniomesocolic Viscera and Relations

5.5.2.1 Esophagus

The abdominal portion of the *esophagus*, about 25 mm long, begins in the muscular part of the diaphragm at the level of the eighth or ninth thoracic vertebra, 6 mm ventral to the aortic hiatus, and just dorsal to the central tendon of the bifurcation into lateral leaflets (Fig. 4–11). From the esophageal foramen, the esophagus runs between the visceral surface of the left lateral lobe of the liver and the cranial margin of the forestomach, crossing the pylorus and the first duodenal flexure cranially. It enters the forestomach at the *margo plicatus*, the border between the glandular and forestomachs (Figs. 5–10, 5–11), slightly to the left of the midline.

As in the thoracic region, the abdominal esophagus is lined with keratinized stratified squamous epithelium surrounded by striated musculature (Fig. 4–23). The matte white mucosa is thrown into small longitudinal folds in its empty and contracted state (Fig. 4–22).

The gastrophrenic ligament (*lig. gastrophrenicum*), which becomes the point of origin for the greater omentum, extends dorsally from the lesser curvature of the forestomach to the diaphragm and there envelops the abdominal portion of the esophagus lying cranial to the liver.

5.5.2.2 Stomach

The European hamster receives its nourishment mainly from plants and utilizes a forestomach for predigestion. The compound stomach is thus divided by a distinct constriction into a larger blind forestomach (*proventriculus*) and a smaller true or glandular stomach (*ventriculus glandularis*) (Fig. 5–10). The European hamster differs from the rat (Wells, 1968) and the mouse (Theiler, 1972) in which no such constrictions are found. The compound stomach lies in the cranial abdominal region (*regio abdominis cranialis*) and completely occupies the left hypochondrium (*regio hypochondriaca sinistra*) (Figs. 5–8, 5–9). Depending upon the distention of the stomach, it protrudes to a greater or lesser extent into the corresponding right side of the abdominal cavity, where it presses against the lateral abdominal wall. In general, one-fourth of the glandular stomach lies to the right, and three-fourths to the left of the median sagittal plane of the body, the glandular stomach lying to the right of the forestomach (Figs. 5–8, 5–9). The most cranial part of the forestomach lies at the level of the 12th thoracic vertebra, while the greater curvature of the glandular stomach extends caudally to the level of the second or third lumbar vertebra. The weight of the fully distended stomach (forestomach and glandular stomach) is about 11 g and 10 g for male and female hamsters, respectively, while the empty stomach weighs approximately 3 g for both sexes (Tables 3, 6).

When markedly distended, the forestomach ranges from 45 to 50 mm long and from 15 to 25 mm wide (Figs. 5–11, 5–12). The grayish-white forestomach lies in the cranial portion of the peritoneal cavity near the left abdominal wall and extends obliquely in a caudoventral direction towards the umbilical region (Fig. 5–13). Its cranial surface usually impinges upon the left lateral lobe of the liver and, in formalin-fixed animals, leaves an impression of this lobe. From dorsal to ventral, the caudal surface is related to the spleen, the left part of the pancreas and the head of the caecum, respectively (Fig. 5–9). When very distended, the contents of the forestomach can be seen through the serous surface.

The epithelial lining of the forestomach is pale, almost white in color, and is thrown into delicate transverse and slightly curled folds (Fig. 5–14). At the blind end of the forestomach, these folds become distinctly more elevated, sometimes attaining a height of up to 7 mm (Fig. 5–14). Under magnification these folds easily can be misinterpreted as papillomas. The forestomach is lined with simple keratinized

squamous epithelium (Fig. 5–15), which is separated from the mucosal lining of the glandular stomach by a distinct margo plicatus.

At the level of the esophageal junction with the forestomach, a fissure bordered by two well-defined *labia* runs along the lesser curvature (*curvatura ventriculi minor*) to the transition of the two stomachs. The labia continue along the internal surface of the glandular stomach for about 3 or 4 mm, and their edges are considerably elaborated (Fig. 5–14). When fully distended, the glandular stomach is between 30 and 40 mm long and attains a diameter of 20 to 25 mm. When empty, the glandular stomach is bordered by the transverse colon, the duodenum and the head of the caecum; its greater curvature (*curvatura ventriculi major*) is oriented to the right (Fig. 5–14), and in an extremely distended state, it rests against the left lateral lobe of the liver. The parietal surface (*facies parietalis*) of the glandular stomach is affixed to the left lateral lobe of the liver by the hepatogastric ligament. The greater curvature is bordered sinistrodorsally by the ventral end of the spleen; when full, it is also bordered ventrally by the abdominal wall, to the right by the pancreas and, in some cases, by a portion of the S-shaped flexure of the ascending colon. Since the lesser curvature is markedly concave, the cardia (*pars cardiaca*) and pylorus are closely applied, with the opening to the forestomach lying caudal to the pylorus (Figs. 5–12, 5–14).

The largest part of the glandular stomach is lined with gastric glands consisting of tall columnar epithelium with many goblet cells (Fig. 5–16).

A circular constriction formed by the pyloric sphincter (*m. sphincter pylori*) separates the pylorus (*pars pylorica*) from the rest of the stomach. This segregated portion of the stomach tapers sharply towards the duodenum.

The serous surface of the glandular stomach is grayish-red in color, smooth, thick and surrounds an inner circular and an outer, faintly visible, longitudinal muscle layer. Extending up to 1.5 mm in height, the pyloric margin is white in color and possesses varying amounts of villi; however, macroscopically, one cannot distinguish color differences among the cardia, fundus (*fundus ventriculi*) and pylorus of the glandular stomach. The area with cardiac glands (*gll. cardiacae*) is found in varying striations along the pyloric margin, while the pyloric glandular zone (*gll. pyloricae*) circumscribes the pylorus.

5.5.2.3 Proximal Duodenum

The proximal, or cranial, duodenum (*pars cranialis*) arises from the pylorus, somewhat cranial and dorsal to the hilus of the liver (Fig. 5–17), where it doubles back caudoventrally to the right at the first flexure (*flexura duodeni cranialis*) before turning caudally at the right lateral hepatic lobe. The proximal duodenum is fixed to the liver by the hepatoduodenal ligament of the lesser omentum.

5.5.2.4 Liver

The functions of the liver (*hepar*) are manifold. During fetal life, it contains focal areas for the formation of blood, which function until birth. Even in the newborn animal, the liver occupies a large part of the abdominal cavity, but then it rapidly decreases in size. The liver is an important storage organ for glycogen produced from digested carbohydrates in the intestines and supplied via the portal blood. It can also store fat and protein in its cells. In addition to its storage function, the liver also has an excretory function. It synthesizes nitrogenous metabolites to urea and uric acid, which are then excreted by the kidneys. The liver extracts toxic substances from the blood and detoxifies them. Moreover, the liver secretes bile and removes the metabolic products of red blood cells that originate in the spleen.

The largest organ of the body is the liver. The size and weight of the liver can vary greatly; but, on an average, it weighs about 15 g in both males and females (Tables 2, 5). In an exsanguinated state, the liver is brown in color; however, this color is dependent upon the blood content, the age and especially the nutritional condition of the animals. In especially fat hamsters, usually in the fall, the liver is more yellow in color due to abundant fat deposits.

Due to the peritoneal lining, the surface of the liver is smooth and shiny. Its structure of many small lobules is macroscopically visible only if abundant interlobular connective tissue is present. Because of its elastic consistency, the liver accommodates the neighboring organs. Deep fissures (Figs. 5–18, 5–19) divide the liver into the following parts: a bipartite left portion with the left lateral lobe (*lobus hepatis sinister lateralis*) and the left medial lobe (*lobus hepatis sinister medialis*); an intermediate supraportal caudate lobe (*lobus cau-*

datus), including caudate (*processus caudatus*) and papillary processes (*processus papillaris*); the quadrate lobe (*lobus quadratus*); and a bipartite right portion with a right lateral lobe (*lobus hepatis dexter lateralis*) and a right medial lobe (*lobus hepatis dexter medialis*).

On its convex parietal surface (*facies diaphragmatica*) (Fig. 5–20) the liver is applied to the diaphragm, whose curvature encircles most of the organ right and left of the midline. To the right of the median sagittal plane, the liver lies between the diaphragm and duodenum, the jejunum and the right kidney. On the left, it lies between the diaphragm and the stomach. The visceral surface (*facies visceralis*) is only slightly concave (Fig. 5–21) and is characterized by deep impressions of the forestomach, convoluted intestine and kidneys; these impressions are particularly prominent in formalin-fixed animals. The edges of the liver are sharp and smooth except for a small area to the left of the dorsal midline, where the blunt edges show an esophageal impression (*impressio oesophagea*).

The left lateral lobe is the largest of the six separate hepatic lobes, and constitutes approximately ⅓ of the entire organ. Its diaphragmatic surface is bordered laterally by the lateral abdominal wall in the xiphoid region (*regio xiphoidea*). Cranially, the left medial lobe is inserted between the left lateral lobe and the diaphragm; it is overlapped extensively by the cranial surface of the former (Fig. 5–18). The visceral surface exhibits a rather pronounced impression of the forestomach and glandular stomach (*impressio gastrica*). The left medial lobe is smaller than the left lateral lobe and lies against the left ventral quadrant of the diaphragm. It is bordered medially by the parietal surface of the glandular stomach. The left medial lobe is separated from the quadrate lobe by a medial fissure (*fissura lig. teretis*) in which the ligamentum teres hepatis lies. A small portion of the left medial lobe may project ventrally into the xiphoid region. The right medial lobe extends ventrally to the xiphoid region, as does the left medial lobe; dorsally its cranial surface covers the caudal surface of the right lateral lobe. The right lateral lobe, almost as large as the right medial lobe, lies far dorsally in the intrathoracic part of the abdominal cavity and rests against the dorsal right quadrant of the diaphragm. Its dorsal edge is inserted between the dorsal abdominal wall and the cranial pole of the right kidney, which imposes a renal impression (*impressio renalis*). Its visceral surface is bordered dorsally by the right kidney and ventrally by the duodenum, which likewise makes an impression. The caudate lobe lies dorsal to the hepatic portal (*porta hepatis*), distinct from the right lateral lobe (contrary to Kittel [1953]), who denied the presence of a caudate lobe in the hamster). The papillary process is moderately developed, 6 to 9 mm long. It extends caudally and lies dextrodorsal to the forestomach, between the forestomach and the pancreas. The well-developed caudate process is about 9 mm long and extends to the right abdominal wall and sits as a cap at the cranial pole of the right kidney.

The triangular quadrate lobe lies ventral to the porta hepatis; it does not reach the ventral edge of the liver. On the left, it has a deep indentation in which the ligamentum teres lies and which separates it from the left medial lobe. The ligamentum teres runs from the interlobular fissure between the left medial lobe and the quadrate lobe in a cranial direction towards the diaphragm ventral to the xiphoid process and caudoventral to the umbilical region.

The liver is attached on the right and left to the diaphragm by two triangular ligaments (*ligg. triangularia*), the coronary ligament (*lig. coronarium*) and the falciform ligament (*lig. falciforme*). The left triangular ligament extends from the dorsal diaphragmatic edge of the left lateral lobe to the diaphragm. The right triangular ligament originates at the right lateral lobe and ends at the right dorsal quadrant of the diaphragm. The coronary ligament reaches from the left lateral and right medial lobes to the diaphragm, while the falciform ligament connects the right lateral lobe with the ventral abdominal wall in the umbilical region.

The European hamster possesses no gall bladder (*vesica fellea*). The common bile duct (*ductus choledochus*) originates from the porta hepatis and discharges into the duodenum 20 to 25 mm distal to the pylorus.

The liver is enclosed in peritoneum which covers the fibrous capsule (*capsula fibrosa*) of the organ.

From this capsule, several septa penetrate the liver tissue, thus subdividing the organ into hepatic lobules.

These lobules are polyhedral in shape and are composed of numerous liver cells which are radially arranged around the central vein (*v. centralis*), or venule of the hepatic vein (*v. hepatica*) (Fig. 5–22). Each lobule is surrounded at its edges by the portal triad, which is composed of a branch of the portal vein, a branch of the hepatic artery (*a. hepatica*) and an interlobular bile ductule (*ductulus biliferus*) (Fig. 5–23). Within the lobules, anastomosing sinusoids run from the portal to the central vein. Between these capillaries and the hepatic cells are found the spaces of Disse.

5.5.2.5 Pancreas

The pancreas produces enzymes which break down lipids, carbohydrates and proteins. Moreover, the pancreatic islets of Langerhans provide the body with insulin and glucagon, which play an important role in the metabolism of carbohydrates.

The pancreas is a rather large (up to 60 mm long) digestive gland of the "dendritic" type consisting of several elongated lobes (Fig. 5–24), which are inserted between various abdominal organs (Tables 11–11c). Unlike the human pancreas, no definite head, neck, body and tail can be distinguished in the hamster. The *in situ* pancreas is not visible in the superficial ventral aspect: it is covered by greater omentum and adipose tissue (Fig. 5–25). When the stomach is displaced caudoventrally, the right lobe of the pancreas (*lobus pancreatis dexter*) becomes visible (Fig. 5–26). This part extends along the greater curvature of the glandular stomach to the duodenum, occupying the entire space between the first duodenal flexure and the glandular stomach, lying dextrocaudal to the papillary process of the liver. From this part of the pancreas, a second portion extends within the duodenocolic ligament from the second duodenal flexure to the ascending colon (Fig. 5–27). The third part of the pancreas becomes visible by ventral displacement of the forestomach and spleen. This part occupies the space between the spleen and the descending colon (Fig. 5–28). The pancreatic duct (*ductus pancreaticus*) discharges into the duodenum 2 to 4 mm distal to the common bile duct.

Histologically, the pancreas consists of two different types of tissue, each of which represents an independent functional unit. The exocrine part consists of compound tubuloalveolar glands, while the endocrine part is represented by the islets of Langerhans, which are composed of aggregated alpha-cells, beta-cells and D-cells (Fig. 5–29).

5.5.2.6 Spleen

The spleen (*lien*) of the European hamster serves not only as a blood reservoir but also as a component of the lymphatic system. The color, consistency, size and weight of the spleen are dependent upon the age, nutritional status and sex of the hamster, and especially on the actual functional status of the organ. The spleen has an average weight of about 229 mg for males and 209 mg for females; it is approximately 34 mm long and 5 mm wide in both sexes (Tables 3, 6). The spleen is located in the left hypochondriac region and extends between the 11th and 12th intercostal spaces (Fig. 5–25). It is dorsoventrally disposed with its parietal surface (*facies parietalis*) adjacent to the dorsal and the left lateral abdominal walls; its dorsal end is slightly arched cranially, while the ventral end inclines slightly caudally. This organ lies against the greater curvature of the forestomach, and is attached at the hilus (*hilus lienis*) by the gastrosplenic ligament (*lig. gastrolienale*). The dorsal end (*extremitas dorsalis*) presses against the left kidney, while the ventral end (*extremitas ventralis*) is bordered by the junction of the transverse colon and the descending colon. The dorsal edge of the spleen is fixed to the left kidney by the lienorenal ligament.

The color of this organ is reddish-purple in fixed specimens, and dark red in fresh-killed animals. Macroscopically in cut section, the spleen is reddish-brown in color. It has a lanciform shape (Figs. 5–30, 5–31) and, as a result of its prominent hilus, a triangular cross-section.

In histological section, the serous coat and the fibroelastic capsule predominate. From this capsule originate the trabeculae, which pass into the spleen where they branch and form the framework for the parenchyma, or red and white pulp (Fig. 5–32). Numerous erythrocytes identify the red pulp (*pulpa lienis rubra*), whereas the white pulp (*pulpa lienis alba*) is composed of dense lymphatic tissue which surrounds the small splenic capillaries and forms the splenic lymphatic follicles, the Malpighian bodies.

5.5.3 Craniomesocolic Vascularization and Innervation

The aorta enters the abdominal cavity via the aortic hiatus of the diaphragm (Figs. 4–10, 4–11) and runs caudally along the left side of the spinal column and the medial edge of the left psoas major muscle (Fig. 5–33). Since the aorta lies dorsal to the abdominal space, running ventrally and applied to

the lumbar vertebrae, all of the intra-abdominal organs are ventral to it. The craniomesocolic part of the abdominal aorta relates to the left lateral lobe of the liver, the glandular stomach, the duodenum, the transverse colon and assorted small intestinal loops. At the level of the tenth thoracic vertebra, the aorta gives rise to the coeliac trunk (*a. coeliaca*); this, in turn, divides into the left gastric artery (*a. gastrica sinistra*), which runs to the cardia of the glandular stomach; the splenic artery (*a. lienalis*), which passes behind the stomach to the spleen; and the hepatic artery (*a. hepatica*). The latter gives off a gastroduodenal (*a. gastroduodenalis*) and a right gastric (*a. gastrica dextra*) branch to the greater and lesser curvatures of the compound stomach, respectively (Fig. 5–34). Somewhat distal to the coeliac trunk is the cranial mesenteric artery (*a. mesenterica cranialis*), which crosses the caudal vena cava (*v. cava caudalis*) ventrally before giving rise to the caudal pancreatoduodenal artery (*a. pancreatoduodenalis caudalis*), to the pancreas and proximal duodenal loop. It runs on the cranial root of the mesentery ventral to the stomach before turning caudally between the jejunal-ileal loops. More caudal branches join with the caudal mesenteric artery (*a. mesenterica caudalis*) to supply the caudomesocolic region.

Shortly after its point of origin, craniodorsal to the aortic bifurcation in the umbilical region (*regio umbilicalis*), the caudal vena cava runs cranially to the right of the aorta. At the level of the tenth and eleventh thoracic vertebrae, the vena cava turns dextroventrally and extends along the liver where it lies in close relation to the caudate lobe (Fig. 5–35). The caudal vena cava is subsequently invested completely by the right hepatic lobe before entering the thoracic cavity via the foramen venae cavae to the right of the falciform ligament. Shortly before the caudal vena cava passes through the diaphragm it receives the cranial phrenic veins (*vv. phrenicae craniales*).

5.5.4 Greater Nerves of the Abdominal Cavity

The vagus nerves enter the abdominal cavity on either side of the esophagus. The right vagus divides into two branches, of which the gastric branch (*ramus gastricus visceralis*) extends to the caudal margin of the stomach, while the coeliac branch (*ramus coeliacus*) innervates the liver, spleen, pancreas and kidneys. The left vagus nerve gives off branches to the ventral surfaces of the stomach and liver. From the lumbar plexus (*plexus lumbalis*), the iliohypogastric nerve (*n. iliohypogastricus*) can be followed between the kidney and the dorsal abdominal wall, where it enters *m. quadratus lumborum*. An additional branch of the lumbar plexus is the genitofemoral nerve (*n. genitofemoralis*), which passes obliquely over the psoas major; it crosses dorsal to the point of origin of the common iliac vein (*v. iliaca communis*) (Kittel, 1953) to enter the pelvic cavity. The sympathetic trunk (*truncus sympathicus*) runs along the vertebral column medial to the origin of the psoas major. The splanchnic nerves (*nn. splanchnici*), which arise from sympathetic ganglia (*ganglia trunci sympathici*) within the thoracic cavity, accompany the aorta as it enters the abdominal cavity. The splanchnic nerves (*nn. splanchnici major et minor*) run beside the abdominal aorta and ventral to the adrenal glands to the coeliac ganglia (*ganglia coeliaca*), which lie cranial to the origin of the cranial mesenteric artery.

5.6 CAUDOMESOCOLIC REGION

5.6.1 Caudomesocolic Peritoneum

After forming the ventral layer of the greater omentum and passing dorsal to the transverse colon and on to the vertebral column at the caudal limit of the pancreas, the peritoneum runs caudally to cover the distal duodenum and forms the ventral layer of the mesentery. It covers the small intestine, then moves dorsally back to the vertebral column to form the dorsal mesenteric layer. Passing caudally along the dorsal wall, it invests the cranial and ventral margins of the rectum, from which it is reflected ventrally onto the vagina and uterus, after covering the open interval between the rectum and female reproductive organs. This interval, the rectogenital pouch (*excavatio rectogenitalis*), is entirely patent. After reflecting over the uterine fundus and body, the peritoneum dips again caudally to cover the bladder at the level of the cervix, where it forms the vesicogenital pouch (*excavatio*

vesicogenitalis). In males, it covers a much less prominent vesicogenital pouch and reflects directly over the bladder. After investing the cranial surface of the bladder, the peritoneum moves cranially along the ventral abdominal wall.

5.6.2 Caudomesocolic Viscera and Relations

The convoluted intestines of the European hamster are subdivided into the duodenum, jejunum, ileum, caecum, colon and rectum (Figs. 5–36, 5–37). The total length of the gut averages 1425 mm in males (n=10, s.d.=250 mm) and 1100 mm in females (n=10, s.d.=250 mm). The total length of the gut is thus 4 to 5 times the length of the body. The weight of the distended intestines is 28.7 g ± 4.0 g in males and 22.9 g ± 4.0 g in females (Tables 3, 6).

5.6.2.1 Structure of the Small Intestine

The small intestine (*intestinum tenue*) extends from the pylorus to the iliocaecal junction (*ostium ileale*).

The intestinal wall is composed of serous, muscular, submucous and mucous layers (Fig. 5–38). The serous layer is formed of visceral peritoneum, which merges with the subserous stratum of areolar connective tissue. The muscular coat is thicker in the cranial than in the caudal part of the small intestine. It consists of a thin outer longitudinal and a thicker inner circular layer of nonstriated muscle fibres. The submucous layer consists of submucous glands and loose connective tissue with blood vessels, lymphatics and nerves. The mucous membrane is thick and highly vascular in the upper part of the small intestine but thinner and less vascular in the lower part. It is thrown into circularly or spirally arranged folds; the circular folds and the entire surface are composed of fingerlike, filiform projections, the intestinal *villi*. Extending into the mucosa from the surface between the intestinal villi are simple tubular intestinal glands (*gll. intestinales*). They reach almost to the muscular layer. In the duodenum are mucous tubuloalveolar duodenal glands (*gll. duodenales*), the ducts of which extend through the muscular layer to proliferate in the submucous coat.

5.6.2.2 Duodenum

The duodenum of the European hamster is segmented into cranial (*pars cranialis*), descending (*pars descendens*) and ascending (*pars ascendens*) parts. This portion of the intestine is about 140 mm long and 3.5 mm wide, and it is from light yellow to whitish-red in color. After the first flexure (*flexura duodeni cranialis*) the duodenum runs ventral to the caudal process of the liver and ventromedial to the right kidney and continues in a caudomedial direction as the descending part. The descending part forms an arch convex towards the midline, turns around at a second flexure (*flexura duodeni caudalis*) in the pelvic region and continues craniomedially as the ascending segment to the visceral surface of the stomach. The ascending part of the duodenum turns to the right and runs between the jejunal loops and the transverse colon, where it becomes the jejunum. The ascending duodenum is connected to the descending colon, and the descending duodenum is fixed to the ascending colon by the duodenocolic ligament (*plica duodenocolica*) ventral to the kidneys.

5.6.2.3 Jejunum

The transition of the duodenum into the jejunum is not visible superficially, nor is the transition of jejunum into the succeeding ileum. The sharply contorted loops of the jejunum are situated predominantly in the dorsal region of the mesogastrium, or mesentery attached to the greater curvature of the glandular stomach (Figs. 5–39, 5–40). Due to a long mesojejunum, the entire jejunum is easily tractable (Fig. 5–41). With a length of about 350 mm and a width of approximately 4 mm, it is the longest segment of the intestine; the serous surface is grayish-red in color. The jejunal loops rest dorsally against the duodenum and the ascending colon, ventrally against the abdominal wall in the umbilical region, and caudally against the urinary bladder as well as the epididymal fat in males. Cranial to the base of the caecum, the jejunum merges into the ileum.

In the jejunum the mucous membrane forms especially tall villi (Fig. 5–42).

5.6.2.4 Ileum

The length of the ileum is between 20 and 25 mm, while the width may be up to 3 mm. The serous surface of the ileum is generally grayish-yellow green in color. The ileocaecal ligament (*plica ileocaecalis*) extends as a broad band between the ileum and caecum. Originating at the border between the jejunum and ileum, the ligament gradually narrows as it approaches the dorsal surface of the caecum. At the point of attachment, the ileum

empties into the caecum through a cone-shaped process forming the so-called "ileocaecal valve" (*papilla ilealis*). This valve marks the transition from caecum to colon.

5.6.2.5 Structure of the Large Intestine

The large intestine (*intestinum crassum*) extends from the ileocaecal junction to the anus. The tissue layers in the wall of the large intestine are similar in structure to those of the small intestine. The mucous membrane of the caecum and colon is pale, smooth and free of villi; it is thrown into numerous crescentic folds which correspond with the intervals between sacculi. The mucous membrane of the rectum is thicker, of a darker hue, more vascular and more loosely connected with the muscular coat.

The epithelium of the caecum, colon and upper rectum consists of scattered mucous-secreting goblet cells and columnar absorptive cells with striated borders (Fig. 5–43). The solitary lymphatic follicles of the large intestine are most abundant in the submucous layer of the caecum.

5.6.2.6 Caecum

In European hamsters of good nutritional status, the *caecum* is a large structure (Figs. 5–36, 5–37, 5–39) with a distinct apex (*apex caeci*) body (*corpus caeci*) and base (*basis caeci*). The caecum measures up to 120 mm in length and 15 mm in width. The apex of the caecum lies in the left ventral part of the abdominal cavity and rests against the abdominal wall at an imaginary margin between the left lateral abdominal region (*regio abdominis lateralis sinister*) and the umbilical region. The caecum is bordered cranially by the visceral surface of the stomach, dorsolaterally by the descending colon and dorsomedially by the duodenum. The caecum proper, when distended, exhibits a helical shape (Fig. 5–36). The base of the caecum is freely mobile, consequently prohibiting exact establishment of its location. Neither *taeniae* nor *haustra* are recognizable in the caecum. The retaining capacity of the caecum exceeds that of the stomach.

5.6.2.7 Colon

The colon of *Cricetus cricetus* is divided into three parts: the ascending colon (*colon ascendens*), the transverse colon (*colon transversum*) and the descending colon (*colon descendens*) (Fig. 5–36).

The ascending colon has a grayish-green serous surface and, depending on the age of the hamster, a length of about 350 mm. It commences with a broad S-shaped loop which lies dorsal to the apex of the caecum. In this area, the colon has a diameter of 10 to 12 mm, depending upon its distention; it gradually constricts as it runs dorsomedially (to the left) toward the apex of the caecum. It extends along the apex of the caecum to the cranial border of the epididymal fat tissue in males, while in females it extends to the left inguinal region (*regio inguinalis sinister*) at the level of the third or fourth lumbar vertebra, where it forms a horseshoe-shaped loop (Fig. 5–44). Craniolateral to the urinary bladder, the ascending colon turns craniodorsally while continuing in an oblique direction to the level of the cranial pole of the right kidney, where it crosses the body of the caecum dorsally and the ileum and duodenum ventrally. At the cranial pole of the right kidney, it bends caudolaterally; in the right lateral abdominal region, it forms a large S-shaped loop about 30 mm in diameter. From the right kidney, it extends to the ventral abdominal wall and, alongside the right abdominal wall, executes another bend of about 180°. From this flexure, the ascending colon doubles back by means of an arch open caudally and proceeds caudodorsally nearly to the level of the right kidney, turning 180° a second time.

The distal part of the double loop is applied closely to the proximal part by means of a short, fatty, 5 mm long mesocolon which binds the two flexures together up to the level of the cranial pole of the right kidney. Between the kidney and the visceral surface of the right lateral lobe of the liver, the ascending colon becomes the transverse colon. Shortly before the U-shaped loop of the ascending colon, fecal formation begins (Fig. 5–44).

The transverse colon has a length of 60 to 70 mm and its diameter is about 3 mm. The serous surface of the transverse colon is grayish-green in color. This segment of the colon runs caudal to the stomach and liver and ventral to the cranial segment of the duodenum, remaining perpendicular to the median plane until it reaches the left abdominal wall. Here it turns caudally and at the end of the spleen

progresses as the descending colon.

The descending colon (Figs. 5–45, 5–46) is about 120 to 180 mm long and about 3 mm in diameter; it also has a grayish-green serous surface. It extends caudally along the left lateral abdominal wall; in male hamsters, it runs dorsal to the epididymal fatty tissue in a caudomedial direction and crosses the left ureter. In female hamsters, it crosses ventrally over the uterine horns. At about the level of the sacrum, the descending colon reaches the midline and, dorsal to the urinary bladder and the body of the uterus, runs between these organs and the sacrum where it continues into the rectum.

5.6.3 Retroperitoneal Viscera and Relations

5.6.3.1 Rectum

In European hamsters the rectum of the male is considerably longer (40 to 60 mm) than that of the female (35 to 45 mm). It extends from the descending colon through the pelvic cavity to the anus, which lies more caudally in males than in females. The grayish-green rectum lies dorsal to the urinary bladder, vagina and body of the uterus and ventral to the proximal caudal vertebrae and sacrum in females. It runs dorsal to the bladder, accessory glands and the origin of the penis, and ventral to the sacral and caudal vertebrae in males (Fig. 5–46).

5.6.3.2 Urinary Organs

The urinary organs (*organa uropoetica*) include the kidneys (*ren*), which secrete the urine; the ureters (*ureter*), which convey the urine to the bladder; the urinary bladder (*vesica urinaria*), which temporarily stores the urine and the urethra, through which the urine is discharged from the urinary bladder (Fig. 5–47).

5.6.3.2.1 Kidney

The kidneys constantly filter waste materials from the blood. They regulate body fluids and salts and maintain normal osmotic pressure of the blood and tissues. The bilaterally paired kidneys weigh about 930 mg each (Tables 2, 5) and lie retroperitoneally in the lumbar region (Fig. 5–48). The axes of the kidneys lie oblique to the midsagittal plane of the body; the distance between the caudal poles (*extremitates caudales*) of the kidneys being 18mm, while that between the cranial poles (*extremitates craniales*) is only 11 mm. The right kidney lies between the first and the third lumbar vertebrae and is covered cranioventrally by the caudate lobe of the liver (Fig. 5–33). The hilus (*hilus renalis*) of the right kidney lies at the level of the transverse process of the third lumbar vertebra, while the hilus of the left kidney is situated between the third and fourth lumbar vertebrae. One renal artery (*a. renalis*) and one renal vein (*v. renalis*) pass over the hilus of each kidney (Figs. 5–33, 5–47). At the cranial end of each kidney lies an adrenal gland (*gl. suprarenalis*), which is separated from the kidney proper by fatty and connective tissue.

The vessels to the right kidney originate more cranially than those supplying the left kidney (Fig. 5–33). Craniodorsal to the left renal vein, the left renal artery originates from the abdominal aorta between the second and third lumbar vertebrae. At this level, the right renal vein also runs towards the caudal vena cava.

The dorsal surfaces of both kidneys are flattened while the ventral surfaces are arched (Fig. 5–49). Both poles of the kidneys are rounded; the lateral edge is convex while the medial edge, on which the hilus is situated, is slightly concave. A longitudinal section through the kidney demonstrates a more triangular cut surface (Fig. 5–51). The right kidney is bean-shaped, and its lateral side is slightly bowed. The left kidney is more markedly curved so that the lateral wall forms a semicircle.

The color of the kidneys is red-brown (Fig. 5–49), the surface is smooth and, like the Chinese hamster (Geyer, 1972), Syrian Golden hamster Schwarze and Michel, 1959–60) and rat (Wells, 1968), each kidney contains one papilla (*papilla renalis*) (Figs. 5–50, 5–51). In sagittal section, the kidneys exhibit a white-gray to red-brown cortex about 3 mm wide, surrounded by a grayish-red medulla, which is from 3 to 4 times as wide as the cortex (Fig. 5–51). The cortical-medullary boundary is clearly defined; at this division are elevated interlobular vessels (*aa. et vv. interlobulares*) (Figs. 5–50, 5–51). Depending upon the nutritional

status of the animals the kidneys are embedded in perirenal fat (*capsula adiposa*) (Fig. 5–48). Especially in autumn, the hamsters accumulate much fat around the kidneys in preparation for hibernation.

The outer covering of the kidneys is a thin but dense connective tissue capsule (*capsula fibrosa*) from which thin filaments proceed into the kidney proper. The entire parenchyma consists of densely packed tubules which are embedded in loose connective tissue through which the renal vessels, lymphatics and nerves run. The renal cortex (*cortex renis*) is comprised of the renal corpuscles (*corpuscula renis*) (Figs. 5–52, 5–53), and the proximal convoluted tubules (*tubuli renales contorti*) the terminal parts of which become either straight (*tubuli renales recti*) or slightly spiralled (spiral tubules). These spiral tubules run toward the medulla (*medulla renis*) to become the descending limb of Henle's loop, connected by a U-turn to the ascending limb. The renal tubules are lined by a single layer of epithelial cells, outside of which is a basement membrane. The height of the epithelial cells varies in the different parts of the tubules. The renal medulla consists of radiating straight-running tubules which discharge at the papillary surfaces into the calyces (*calices renales*) (Fig. 5–54). The pelvis of the kidney (*pelvis renalis*) is lined with simple polygonal epithelium without glands (Fig. 5–55.)

5.6.3.2.2 Ureter

The ureter transfers the continually-produced urine from the renal pelvis to the urinary bladder (*vesica urinaria*), where the urine is stored. The ureters leave the renal pelves caudomedially and proceed in a caudal direction; they are protected by a rich retroperitoneal fatty tissue. They continue parallel to the aorta and caudal vena cava (Fig. 5–47) and discharge on each side into the dorsal wall of the urinary bladder. The course of the ureters differs somewhat between the sexes. In males the ureter runs dorsal to the vesicular gland (*gl. vesicularis*) and the ductus deferens, crossing the latter and emptying into the bladder. The female ureters run dorsal to the uterine horns (*cornua uteri*) and lateral to the cervix (*cervix uteri*).

The ureters have three layers: fibrous, muscular and mucous (*tunicae adventitia, muscularis, mucosa*). The fibrous layer is continuous at one end with the fibrous capsule of the kidney in the floor of the renal pelvis while, at the other end, it merges with the wall of the urinary bladder. The muscular coat consists of an outer circular part and an inner longitudinal part. The mucous layer is smooth with longitudinal folds. It contains many elastic fibers and is covered with a transitional epithelium, four or five cells thick.

5.6.3.2.3 Urinary Bladder

Depending upon the degree of distension, the urinary bladder (*vesica urinaria*) is about the size of a cherry and projects, even when only slightly distended, over the pubic crest into the ventral pubic region (*regio pubica*) (Fig. 5–48). The walls of the urinary bladder are so thin that one can view the contents of the bladder. In male hamsters, the bladder is bordered lateroventrally by the abdominal wall and cranially by the caecum or distended loops of the small intestine. Dorsal to the bladder lie the vesicular glands and the well-developed ampulla of the ductus deferens (Fig. 5–59). The male urethra (*urethra masculina*) extends along the ventral side of the penis. The external orifice of the urethra (*ostium urethrae externum*) is not at the end of the penis, which has two points at its tip, but rather on the ventral surface of the circular mucosal fold. In female hamsters, the urinary bladder pushes ventrally against the abdominal wall, cranially against the caecum and jejunal loops, and dorsally against the uterine horns and cervix. The middle ligament of the bladder (*lig. vesicae medianum*) is well defined, and two lateral true ligaments (*ligg. vesicae laterales*) are erected as small serous folds towards the lateral abdominal walls. The urethra of the female (*urethra feminina*) discharges separately from the vagina and the anus. Thus, while the female urethra is purely a urinary duct, the male urethra serves two functions, urinary and reproductive.

The bladder has a wall similar to that of the ureters. The abdominal surface is covered by peritoneum.

The muscular stratum (*m. pubovesicalis* and *m. rectourethralis*), consists of three layers of smooth muscle—an external and an internal layer of longitudinal fibers and a middle layer of circular fibers. The mucous membrane is whitish-pink in color. It is continuous above with the mucous membrane of the ureters and below with that of the urethra. The epithelium is of the transitional type, 3 or 4 cells thick (Fig. 5–56). The loose texture of the submucosa allows the mucosa to be thrown into folds or rugae when the bladder is in an empty state.

5.6.4 Adrenal Gland

The adrenal glands (*gll. suprarenales*) belong to the endocrine system. The cells of their cortex produce corticosteroids, whereas those of the medulla synthesize noradrenalin and adrenalin.

The adrenals are located at the level of the last thoracic vertebra or the first lumbar vertebra, craniomedial to the kidneys, 1 to 3 mm lateral to the abdominal aorta and caudal vena cava (Fig. 5–50). The right adrenal gland, like the right kidney, is

positioned about 1 to 2 mm more cranial than the left adrenal gland. The right lateral lobe of the liver overlaps the right adrenal ventrally. Both adrenal glands are almost completely embedded in areolar tissue containing much fat (Fig. 5–48).

The red brown to dark brown color of the smooth surfaces of the adrenal glands resembles that of the kidneys (Fig. 5–49). The glands are ovoid in shape, with a length of about 4 mm and width about 2 mm (Tables 3, 5, 12–12e).

Histologically, the adrenals show the typical structure of a darker cortical substance and a higher medullary substance (Fig. 5–57). The *cortex* of the adrenal glands exhibits an indistinct segmentation because the transition of the zona fasciculata, composed of small columnar cells, into the zona glomerulosa and the zona reticularis is indistinctly demarcated. The substance of the medulla is constructed from single cords that are separated by vessels and vascular capillaries.

The suprarenal arteries (*aa. suprarenales*), which arise from the renal arteries, supply the adrenal glands; the venous return is via the suprarenal veins (*vv. suprarenales*) , which join the renal veins.

5.6.5 Caudomesocolic and Retroperitoneal Vascularization

5.6.5.1 Arteries

The cranial mesenteric artery (Fig. 5–33) gives off a series of intestinal branches to the jejunum (*aa. jejunales*) and ileum (*aa. ilei*); an ileocolic branch (*a. ileocolica*) to the ileum, caecum and the proximal colon; a right colic branch (*a. colica dextra*) to the ascending colon; and a middle colic branch (*a. colica media*) to the transverse colon. The middle colic artery often anastomoses with branches from the caudal mesenteric artery (*a. mesenterica caudalis*), which arises from the ventral aorta near the level of its origin. The left colic branch of the caudal mesenteric artery supplies the descending colon, while the cranial rectal artery is the caudal continuation of the caudal mesenteric artery, and supplies the rectum (Fig. 5–58).

Close to the origin of the cranial mesenteric artery, the paired renal arteries arise to supply the kidneys, adrenals and other retroperitoneal tissue (Fig. 5–34). From the ventral side of the aorta at the level of the caudal pole of the left kidney, two relatively small vessels, the testicular arteries (*aa. testiculares*), originate in males, passing eventually through the inguinal canal (*canalis inguinalis*); the ovarian arteries (*aa. ovaricae*) are the female counterpart.

At the level of the cranial pole of the left kidney, the abdominal aorta approaches the left wall of the caudal vena cava and, after crossing the left renal vein dorsally, is applied ventrally to the vena cava until it bifurcates at the level of the sixth lumbar vertebra into its largest branches, the paired common iliac arteries (*aa. iliacae communes*), (Fig. 5–58) and the smaller median sacral artery (*a. sacralis mediana*) and median caudal artery (*a. caudalis mediana*), which continue the aorta into the tail. The common iliac arteries run initially along the medial borders of the psoas major muscles and then turn obliquely laterally. In males, they are covered by the vesicular glands (*gll. vesiculares*). In the female, they are crossed ventrally by the uterine horns, caudal to which they bifurcate into the internal and external iliac arteries (*aa. iliacae internae et externae*).

5.6.5.2 Veins

The caudal vena cava (*vena cava caudalis*) is formed from the junction of the right and left common iliac veins (*vv. iliacae communes*) at an acute angle craniodorsal to the bifurcation of the abdominal aorta at the level of the sixth lumbar vertebra. Each common iliac vein is formed by the junction of the external and internal iliac veins (*vv. iliacae externae et internae*) a short distance from the inguinal ligament (*lig. inguinale*) just medial to the origin of the respective arteries. Shortly after its point of origin, the vena cava crosses dorsal to the right common iliac artery and continues cranially along the right side of the abdominal aorta. At approximately the same level as the origin of the testicular arteries, the caudal vena cava takes up the right testicular vein (*v. testicularis*), while the left testicular vein empties into the caudal side of the left renal vein. In females, both ovarian veins (*vv. ovaricae*) empty symmetrically into the caudal vena cava. Cranial to the terminus of the right testicular vein, the caudal vena cava takes up the renal veins.

The main tributaries from the caudomesocolic viscera emptying into the vena cava (in cranial direction) include the testicular and ovarian, respectively, in males and females; the renal veins; and the portal shunt-hepatic vein system. Since the hepatic veins (*vv. hepaticae*) are so small and (Fig. 5–35) vary greatly from animal to animal, the exact number draining the different lobes of the liver cannot be exactly determined. For example, tributaries from the caudate lobe are not demonstrable and probably empty into the caudal vena cava during its transit through the liver. Other collecting branches enter the ventral side of the vena cava just caudal to the foramen venae cavae.

Because the walls of the larger vessels passing through the liver are embedded in liver connective tissue, they do not easily collapse, so that hemorrhage in the liver is often diagnostically critical.

5.6.5.3 Portal Circulation

The hepatic portal system includes those veins draining the gastrointestinal tract caudal to the diaphragm, whose blood is transported to the liver by the portal vein (*v. porta*) for circulation through the liver sinusoids before returning to the systemic circulation via the hepatic veins and caudal vena cava (Fig. 5–34). The portal vein is formed chiefly by the gastroduodenal vein (*v. gastroduodenalis*), splenic vein (*v. lienalis*) and cranial mesenteric vein (*v. mesenterica cranialis*). The cranial mesenteric vein is formed by branches from the jejunum (*vv. jejunales*) and ileum (*vv. ilei*), and by the ileocolic (*v. ileocolica*), right colic (*v. colica dextra*) and middle colic (*v. colica media*) veins, from the ascending and transverse colons. The caudal mesenteric vein (*v. mesenterica caudalis*), arising from the cranial rectal (*v. rectalis cranialis*) and left colic veins (*v. colica sinistra*), and draining the descending colon and rectum, also discharges into the cranial mesenteric vein. All of these vessels run through the mesentery and, at the level of the eleventh thoracic vertebra, join to form the portal vein, which runs to the liver, dorsal to the common bile duct and dextrodorsal to the hepatic artery within the hepatoduodenal ligament. At this level, the portal vein gives off two branches corresponding to the right and left lobes of the liver.

5.7 LYMPHATIC SYSTEM OF THE ABDOMEN AND PELVIS

5.7.1 Lymph Nodes of the Gastrointestinal Tract

The lymph nodes of the abdominal viscera are organized into two major lymph centers, the coeliac (*lymphocentrum coeliacum*) and the cranial mesenteric (*lymphocentrum mesentericum craniale*), which empty into the *cisterna chyli*. The cisterna chyli represents a dilated portion of lymphatic trunk situated between the crura of the diaphragm at the level of the last thoracic to the second lumbar vertebrae. It receives the coeliac (*truncus coeliacus*), lumbar (*truncus lumbalis*) and intestinal (*truncus intestinalis*) trunks, and continues intrathoracically as the thoracic duct.

5.7.1.1 Coeliac Lymph Center

The following nodes all drain through the coeliac trunk. The gastric lymph nodes (*lnn. gastrici*), 3 to 5 in number, are situated along the pylorus and the proximal duodenum, as well as within the gastrosplenic ligament. Occasionally one or two may also be found within the greater omentum. They drain the fore- and glandular stomachs, duodenum, spleen and greater omentum.

The hepatic lymph nodes (*lnn. hepatici*) lie dorsal to the right lobe of the pancreas, between the pancreas and the portal vein (Fig. 3–12). The accessory hepatic lymph nodes (*lnn. hepatici accessorii*) are situated within the hepatoduodenal ligament (Fig. 3–12). They too drain the liver.

The pancreaticoduodenal lymph nodes (*lnn. pancreaticoduodenales*), 4 to 7 in number, lie within the gastroduodenal ligament and the greater omentum immediately ventral to the right lobe of the pancreas. (They are sometimes difficult to distinguish from the pancreatic tissue.) They drain parts of stomach and liver, the pancreas and duodenum.

5.7.1.2 Cranial Mesenteric Lymph Center

The following nodes drain through the intestinal trunk: the cranial mesenteric lymph nodes (*lnn.*

mesenterici craniales) lie near the apex of the caecum, caudal to the pancreas at the root of the mesentery (*radix mesenterii*). All lymphatic vessels draining the intestines (except the descending colon) overflow to this lymph node.

The jejunal lymph nodes (*lnn. jejunales*) consist of an aggregation of up to 10 lymph nodes situated near the root of the mesentery of the small intestine, adjacent to the cranial mesenteric lymph nodes. They drain the jejunum and ileum and flow to the cranial mesenteric lymph nodes.

The ileocaecal lymph nodes (*lnn. ileocaecales*) form an aggregation of 3 to 5 lymph nodes in the region of the ileocaecal junction, within the mesentery between ileum and caecum. They drain the ileum and caecum and flow to the cranial mesenteric lymph node.

The colic lymph nodes (*lnn. colici*) vary in number from 3 to 6 and are situated within the mesocolon of the various segments of the colon. They drain the respective segments of the colon and flow to the cranial mesenteric lymph node.

5.7.2 Lumbar Lymph Center

The renal lymph nodes (*lnn. renales*) lie medial to the hilus of each kidney (Fig. 3–12) and drain the kidney into the lumbar trunk. The lumbar aortic lymph nodes (*lnn. lumbales aortici*), which are situated along the aorta and caudal vena cava, also are drained by the lumbar trunk.

5.7.3 Lymph Nodes of the Pelvis and Hind Limb

A number of separate lymph centers in this region are identified (*lymphocentra iliosacrale, iliofemorale, inguinofemorale, popliteum,* and others). However, all lymphatic flow from this region ultimately passes cranially through the lumbar trunk, via the iliac lymph nodes (*lnn. iliaci*).

The lateral iliac lymph nodes (*lnn. iliaci laterales*) consist of a pair of large ellipsoid nodes (Fig. 3–12) situated lateral to the aorta and vena cava immediately cranial to the origin of the common iliac arteries and veins. The medial iliac lymph nodes (*lnn. iliaci mediales*) consist of a group of two or more small nodes medial to the common iliac arteries just caudal to the bifurcation. The iliac lymph nodes drain the pelvis and pelvic organs, as well as parts of the hind limb directly, into the lumbar trunk. The sacral lymph nodes (*lnn. sacrales*) consist of one or two lymph nodes which lie immediately caudal to the bifurcation of the aorta (Fig. 3–12). They drain the sacral region, tail and reproductive organs into the iliac lymph nodes.

The superficial inguinal lymph nodes (*lnn. inguinales superficiales*) (Fig. 3–12) are very small and lie superficially on the proximal medial surface of the hind limb, covered only by the skin. They drain the skin of the abdominal wall and proximal parts of the hind limb and flow to the deep inguinal nodes (*lnn. inguinales profundi*) (Fig. 3–12). The latter are situated lateral to the femoral vein (*v. femoralis*) at the point where it courses through the abdominal wall. They drain the superficial inguinal and the popliteal lymph nodes and flow to the iliac lymph nodes.

The popliteal lymph node (*ln. popliteus*) (Fig. 3–12) lies at the bend of the knee medial to the biceps muscle of the thigh (*m. biceps femoris*), lateral to the semitendinous muscle (*m. semitendinosus*), and cranial to the gastrocnemius muscle (*m. gastrocnemius*). It drains the lateral and dorsal parts of the foot and overflows to the deep inguinal lymph node.

5.8 MALE GENITAL ORGANS

The *testes* are located within the *scrotum* when active, and are responsible for the formation of the sperm. The *ductus deferens* originates from the *epididymis* and empties into the urethra. In this way, a urogenital canal is formed, around which the following accessory genital glands (*gll. genitales accessoriae*) are grouped: vesicular glands (*gll. vesiculares*), prostate gland (*prostata*) and bulbourethral glands (*gll. bulbourethrales*). Also considered as accessory genital glands are the glandular portions of the vas deferens, the *ampullae*. All empty into the pelvic part (*pars pelvina*) of the urethra. The ejaculate is formed at the time of ejaculation, when the secretions of these glands mingle with the discharged sperm.

5.8.1 Testis

The *testes* are compound tubular glands, slightly flattened and oval in shape, with the function of sperm formation and production of androgen. They have a length of 20 to 25 mm and a breadth of 11 to 13 mm in adult animals during spring and summer (Tables 4, 6) (Reznik, *et al.*, 1973). During the sexually active period of the year, they each weigh about 2.6 g and are completely lodged within the vaginal tunic (*tunica vaginalis*). In autumn and winter, the testes weigh only about 0.55 g (Tables 4, 6, 7, 13, 13a). Only during the mating period are the testes located within the scrotum of wild European hamsters. Coiled testicular veins are detectable on the surface of the tunic that tightly invests the testis (*tunica albuginea*) (Fig. 5–61).

The parenchyma of the testicles is yellowish-white in color and is of such soft spongy consistency that the seminiferous tubules (*tubuli seminiferi*) protrude. During the months of August through October, the testes migrate back through the inguinal canal into the pelvic cavity. Within the pelvic cavity, both testes rest within a large fat pad which almost completely invests them (Fig. 5–62). While situated within the pelvic cavity, the right testis lies between the caudolateral abdominal wall and the urinary bladder. Its caudomedial surface is adjacent to the ascending portion of the ampulla of the ductus deferens. The left testis is similarly situated, except its dorsal surface rests against the descending colon.

During the sexually active period, various cell types are microscopically demonstrable within the seminiferous tubules of adult males. Spermatogonias A and B, Sertoli cells, resting spermatocytes, spermatocytes, spermatids in different stages of maturity (Leblond and Clermont, 1952a and b) and mature sperm (Fig. 5–63) are visible on the tubule walls.

The interstitial tissue of the testes consists of the cells of Leydig (Fig. 5–64) and various other cells, some of connective tissue type, together with the vessels and nerves. Only during hibernation is spermiogenesis reduced to the 15th stage (Fig. 5–65); however, all other cell types are represented (Reznik-Schüller and Reznik, 1973, 1974b) (Fig. 5–67).

5.8.2 Epididymis

The *epididymis* serves as storage site for the sperm, and is connected with the testis by the *rete testis*. Under the influence of the epididymal secretion, the maturation of the previously immobile sperm is completed. At the time of ejaculation, the sperm are transported into the ductus deferens by peristaltic contractions.

The cranial extremity of the head of the epididymis (*caput epididymidis*) (Figs. 5–59, 5–60) is firmly attached to the cranial pole of the testis in a hood-like manner and is surrounded by yellowish-white fat bodies. The head of the epididymis and a portion of the fat bodies lie intra-abdominally. The body of the epididymis (*corpus epididymidis*) is quite thin and extends dorsolaterally to the ductus deferens and dorsomedially to the testis (Figs. 5–59, 5–60). The caudal extremity, or tail (*cauda epididymidis*) (Fig. 5–59), has the form of a blunted cone and is located at the caudal pole of the testis (*extremitas caudata*). The convolutions of the epididymal duct (*ductus epididymidis*) are clearly recognizable. At the level of the pelvic inlet, the ductus deferens expands to form the prominent ampulla, doubles back medially to join the dorsally situated urethra through the ejaculatory duct (*ductus ejaculatorius*) (Fig. 5–59). The weights and sizes of the epididymal regions are given in Tables 14–14c.

The coiled efferent ductules lined with ciliated columnar epithelium contain circularly arranged muscle fibers in their walls; they form the small vascular cones (*coni vasculosi*) of the head of the epididymis (Fig. 5–66). Their union forms a coiled tube that constitutes the body and tail of the epididymis and becomes the ductus deferens (Fig. 5–59). Within this duct, the muscle layer becomes thicker, the epithelium is pseudostratified columnar and the superficial cells have long, regular microvilli.

5.8.3 Accessory Genital Glands

The accessory genital glands (*gll. genitales accessoriae*) are grouped around the pelvic part of the urethra. Their growth and function are controlled by the sex hormones. During hibernation, they are markedly atrophied (Tables 15, 16, 16a, 17). The secretion of the accessory genital glands provides the specific substrate for the completion of the maturation and mobilization of the sperm.

5.8.3.1 Vesicular Gland

The paired vesicular glands (*gll. vesiculares*) are flattened falciform or sickle-shaped coiled tubes which are concave medially, lying dorsal to the urinary bladder and ampulla of the ductus deferens, and ventral to the rectum. The small tubes stretch cranially to form two points which often press

against the bladder when the latter is distended. The vesicular gland discharges dorsally into the urethra through the *ductus excretorius,* situated near the ejaculatory duct. During summer, these glands weigh ten times more than they do in the winter months (Tables 4, 6, 16, 16a). They are grayish-white in color, up to 25 mm long, and their surfaces are nodular. Internally, each gland has a spacious, central main duct which gives rise to lateral ducts, ramifying as diverticula and ending blindly.

The vesicular glands have three layers: an external areolar sheath (*tunica adventitia*); a two-layered middle muscular sheath (*tunica muscularis*), thinner than that of the ductus deferens, which includes an outer longitudinal and inner circular layer; and an internal mucous coat (*tunica mucosa*) with a reticular structure. The epithelium is columnar or flat, depending upon its functional state (Fig. 5–68), and goblet cells, the secretion of which increases the volume of the seminal fluid, are present in the diverticula.

5.8.3.2 Prostate Gland

The prostate gland (*prostata*) appears as flattened bodies composed of many glandular lobules separated from one another by loose connective tissue. The two largest lobes lie dorsal and lateral to the base of the urinary bladder and ventral to the caudal segment of the ductus deferens. Three smaller lobes are situated ventral to the neck of the bladder and the end of the ampulla of the ductus deferens. From the glandular lobes of the prostate several efferent ducts (*ductuli prostatici*) enter the urethra dorsolaterally. During hibernation, these glands are barely recognizable macroscopically. Prostate weights and sizes are given in Table 15. Unlike the rat (Wells, 1968), no paraprostate is present.

The muscular tissue constitutes the stroma of the prostate, the connective tissue being very scanty and merely forming thin trabeculae between the muscle fibers where the vessels and nerves of the gland ramify. The glandular substance is composed of numerous follicles with frequent internal papillary elevations. The lining of the canals and follicles is of the simple columnar variety (Fig. 5–69).

5.8.3.3 Bulbourethral Gland

The bulbourethral glands (*gll. bulbourethrales*) are paired small, rounded, somewhat lobulated, lentil-sized, yellowish bodies, about 5 mm in diameter (Fig. 5–59; Table 17). They are positioned at the caudal border of the ischial tuberosity (*tuber ischiadicum*), almost in the middle of the penis and are surrounded by striated musculature. Each discharges its secretion through a separate thin duct (*ductus gl. bulbourethralis*) into the urethra at the root of the penis.

Each lobule consists of a number of acini lined with columnar epithelial cells.

5.8.4 Penis

The penis is the male organ of copulation and comprises a glans (*glans penis*), a body (*corpus penis*) and a root (*radix penis*), all of which lie subcutaneously, enclosed within the prepuce (*praeputium*). The fibrous penis of the European hamster originates in two crura arising from the ischial arch. When lying within the prepuce, it has the form of a cylinder kinked about 90° (Fig. 5–70) and is approximately 30 mm long when erected.

Its dorsal surface (*dorsum penis*) is flat while its ventral urethral surface (*sulcus urethralis*) forms a deep groove. The erectile mechanism is based on two parallel and anastomosing corpora cavernosa, both of which are invested by a compact connective tissue sheath (*tunica albuginea corporum cavernosorum*). The urethra is partially surrounded ventrally by m. ischiourethralis. Many microscopically visible mucosal papillae are found on the surface of the glans penis. At the apex of the glans, the mucosa forms a circular fold and the urethra discharges into its ventral surface (*ostium urethrae externum*). The os penis is located in the apex of the corpus cavernosum, covered by the glans, and is a small pyramid shaped bone (Kittel, 1953).

The prepuce is composed of external and internal laminae (*laminae externa et interna*), which exhibit many macroscopic rugae. The large praeputial glands (*gll. praeputiales*) form paired submucosal cylindrical structures.

The corpora cavernosa, which confer a spongy consistency to the fibroelastic penis, are lined with endothelium only in the area of the root. The trabeculae are composed of white fibrous tissue, elastic fibers and nonstriated muscle fibers; they are richly vascularized and innervated. The cavernous spaces are filled with blood during erection. In an erected state, the penis lies along the abdominal wall oriented cranially, as opposed to the caudal orientation when lying subcutaneously.

5.9 FEMALE GENITAL ORGANS

The reproductive organs of the female include the ovaries; oviducts; uterus with uterine horns and cervix, and the vagina (Fig. 5–71). Externally, the female hamster also has a quite prominent clitoris as well as a bulb of the vestibule.

5.9.1 OVARY

The ovaries (*ovaria*) have two functions: producing ova and synthesizing the hormones estradiol and progesterone. Each lies dorsolateral to the most caudal quarter of the corresponding kidney, between the kidney and the dorsal abdominal wall (Figs. 5–71, 5–72). Only rarely do the ovaries lie at the level of the caudal pole of the respective kidneys. Depending on the nutritional condition of the hamster and the season of the year, the ovaries are embedded in varying amounts of adipose tissue. In many cases, only the ventral side of the ovaries are free from fat; in especially well-nourished hamsters, the ovaries are totally surrounded by fat (Fig. 5–72). Each ovary weighs about 26 mg (Tables 4, 6, 8, 18, 18a). In general, the variance in weight of the ovaries is greater during the seasonal cycle than during the estrus cycle (Fig. 5–73). The maximum diameter is about 5 mm (Züchner, 1975).

On the ventral side of the ovaries, the knobbed, grayish-red surface shines through a pale, glossy bursa (*bursa ovarica*), which has the shape of a longitudinal oval and surrounds the entire ovary. The bursa is compressed laterally so that the tubal extremity of the ovary (*extremitas tubaria*) is oriented cranially and the uterine extremity (*extremitas uterina*) caudally, while each surface—lateral or medial—is oriented ventrolaterally or dorsomedially. The ovaries are invested by the mesovarium which originates from the broad ligament (*lig. latum uteri*). At the ovarian hilus (*hilus ovarici*), the ovarian bursa and ligament of the ovary (*lig. ovarii proprium*) are inserted; the latter is relatively well developed and runs to the lateral angle of the uterus at a point just dorsal to the uterine horns.

The ovary consists of a peripheral cortex (*zona parenchymatosa*) and a central medulla (*zona vasculosa*). The cortex is surrounded by connective tissue (*tunica albuginea*), the outer surface of which is covered by a simple cuboidal epithelium. The cortex contains follicles (*folliculi ovarici*) at various stages of maturation (Fig. 5–74), which are surrounded by the stroma. In the cortex, intact or involuting corpora lutea, corpora albicantia, atretic follicles and corpora atretica are found. The central medulla is composed of reticular fibers, elastic fibers and connective tissue cells and contains numerous vessels. The medulla also contains numerous interstitial cells which appear epitheloid. During hibernation a pronounced decrease in the number of mature follicles occurs, and corpora lutea are almost completely lacking (Fig. 5–75) (Züchner, 1975). This effect is not observed in nonhibernating animals during winter (Züchner, 1975). Females kept under standard laboratory conditions (i.e., nonhibernating) demonstrate the highest ovarian activity (most numerous mature follicles and corpora lutea) from February to the end of May. Females that hibernate during winter develop the same degree of functional activity at the beginning of May (Züchner, 1975).

5.9.2 Oviducts

The oviducts (*tuba uterina*) are present as winding, narrow tubes which run caudally from the ovary to the pointed uterine horns, with which they merge at the ostium uterinum tubae. The ovarian end of the oviduct is funnel-shaped and broadens into the infundibulum (*infundibulum tubae uterinae*) which surrounds the caudolateral ovarian pole and opens freely into the abdominal cavity. The infundibular funnel includes finger-like projections (*fimbriae tubae*), some of which are oriented along the lateral ovarian wall.

The oviduct is lined by a simple columnar epithelium which is also in distinct papilliform folds (Fig. 5–77).

5.9.3 Uterus

All ova are transmitted to the uterine horns where they adhere to the wall of the tube before passing to the uterus; if unfertilized, they degenerate with extrusion of the debris through the uterus and vagina. The uterus is bipartite, composed of an undivided body (*corpus uteri*), and the uterine horns (*cornua uteri*) (Fig. 5–76). Caudodorsal to the urinary bladder, the uterine horns separate, diverging

craniolaterally. The uterine horns rest upon the dorsal abdominal wall and extend to the region of the caudal pole of the kidneys. The diameter of the cylindrical uterine horns is about 2 to 3 mm and their length about 59 mm (Tables 4, 6).

The two uterine horns continue as two distinct channels within the body of the uterus, separated by a septum (*velum uteri*), and they coalesce near the cervix. Thus, cranially there are two internal orifices (*ostia uteri interna*) within the uterus, while caudally only a single external orifice (*ostium uteri externum*) exists. On palpation, the cervix, or neck of the uterus, a tube 10 mm long, presents a firm consistency which distinguishes it from the vagina and uterus.

From the cervix to the vagina, the mucosal lining of the uterus is composed of simple cylindrical epithelium (Fig. 5–78) which is thrown into high longitudinal folds.

In the propria, which is also folded, there are transient tubular uterine glands lined with ciliated columnar epithelium (Fig. 5–78). The stratified squamous epithelium of the cervix is thrown into shallow folds.

5.9.4 Vagina

The vagina, the female organ of copulation, is a fibromuscular tube whose orifice (*ostium vaginae*) lies at the base of the clitoris. It is dorsoventrally compressed, investing the urethra ventral to it and enclosing the rectum to almost half the latter's height.

Caudally, the vagina is lined with a keratinized stratified squamous epithelium; cranially, where the major alterations occur during the sexual cycle, the mucosa is a nonkeratinized stratified squamous epithelium.

Since the European hamster has only a short sexual cycle (4 to 6 days) (Reznik-Schüller, *et al.*, 1974), the epithelium of the vaginal mucosa is constantly in a state of restoration, transformation and disintegration. Young female hamsters reach sexual maturity when they weigh about 200 g; at this time the epithelium closing the vagina disappears. Throughout hibernation, the vaginal orifice is tightly closed by an epithelial layer which disappears in the spring at the end of hibernation. The orifice is almost completely round and, depending on the age of the animals, about 3 mm in diameter. The urethra is separated from the vagina and discharges at the dorsal surface of the clitoris, which stands in distinct relief from the surrounding tissues and overlaps the vaginal orifice caudoventrally. Caudodorsal to the vaginal orifice lies the anus (Figs. 1–1, 1–8).

Figure 5-1: Radiogram of thorax and abdomen of hamster, illustrating bony landmarks of these regions.

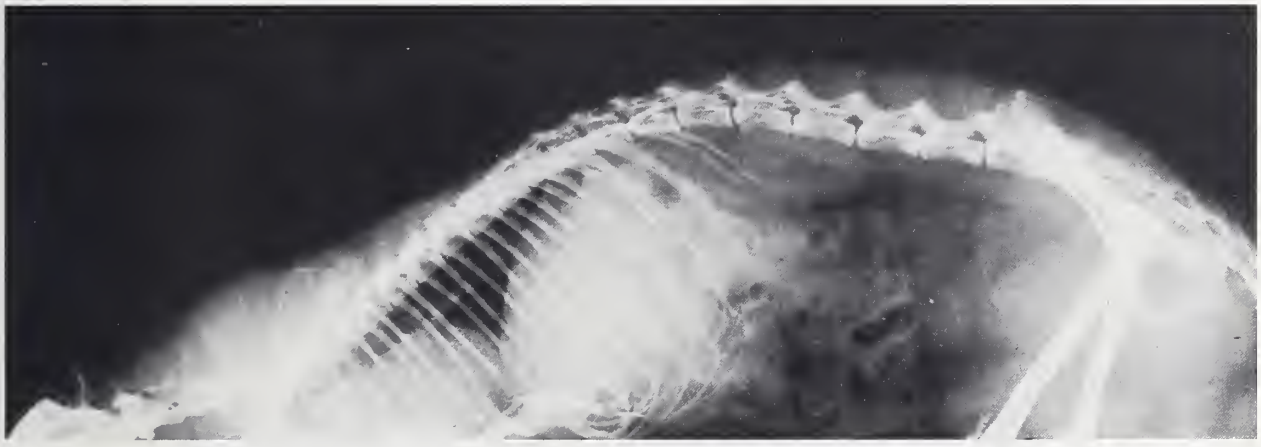

Figure 5-2: Lateral radiogram of thorax and abdomen. Note spinal curves (kyphosis, lordosis) and dorsoventral obliquity of ribs.

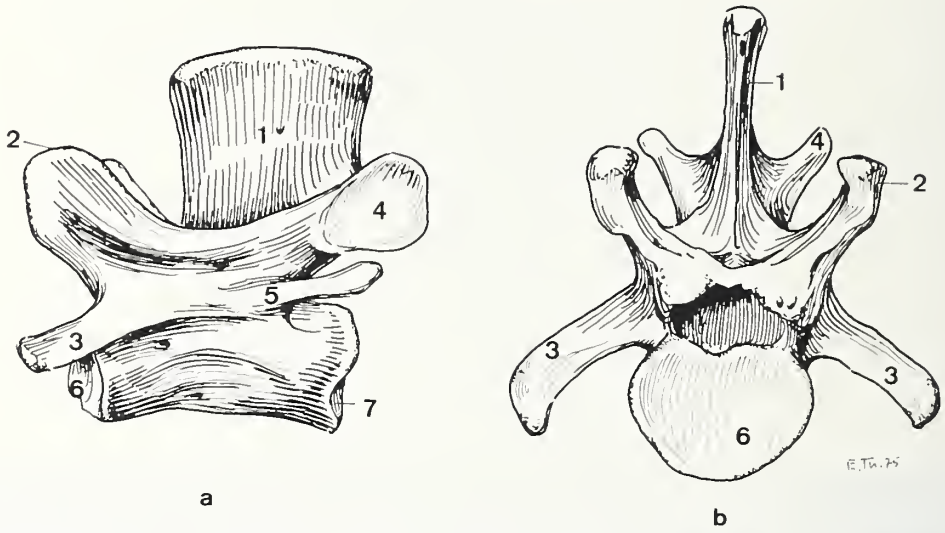

Figure 5-3: Third lumbar vertebra. a, lateral view; b, cranial view. 1=processus spinosus; 2=processus articularis cranialis; 3=processus mamillaris; 4=processus articularis caudalis; 5=processus accessorius; 6=centrum, cranial articular surface; 7=centrum, caudal articular surface.

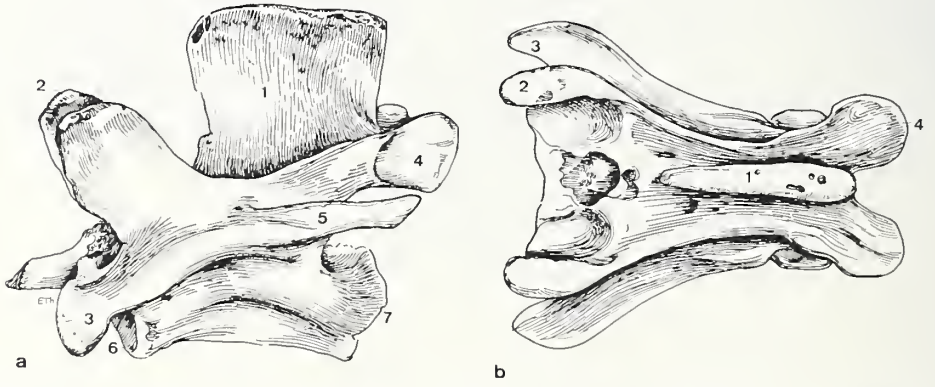

Figure 5-4: Sixth lumbar vertebra. a, lateral view; b, dorsal view. 1=processus spinosus; 2=processus articularis cranialis; 3=processus mamillaris; 4=processus articularis caudalis; 5=processus accessorius; 6=centrum, cranial articular surface; 7=centrum, caudal articular surface.

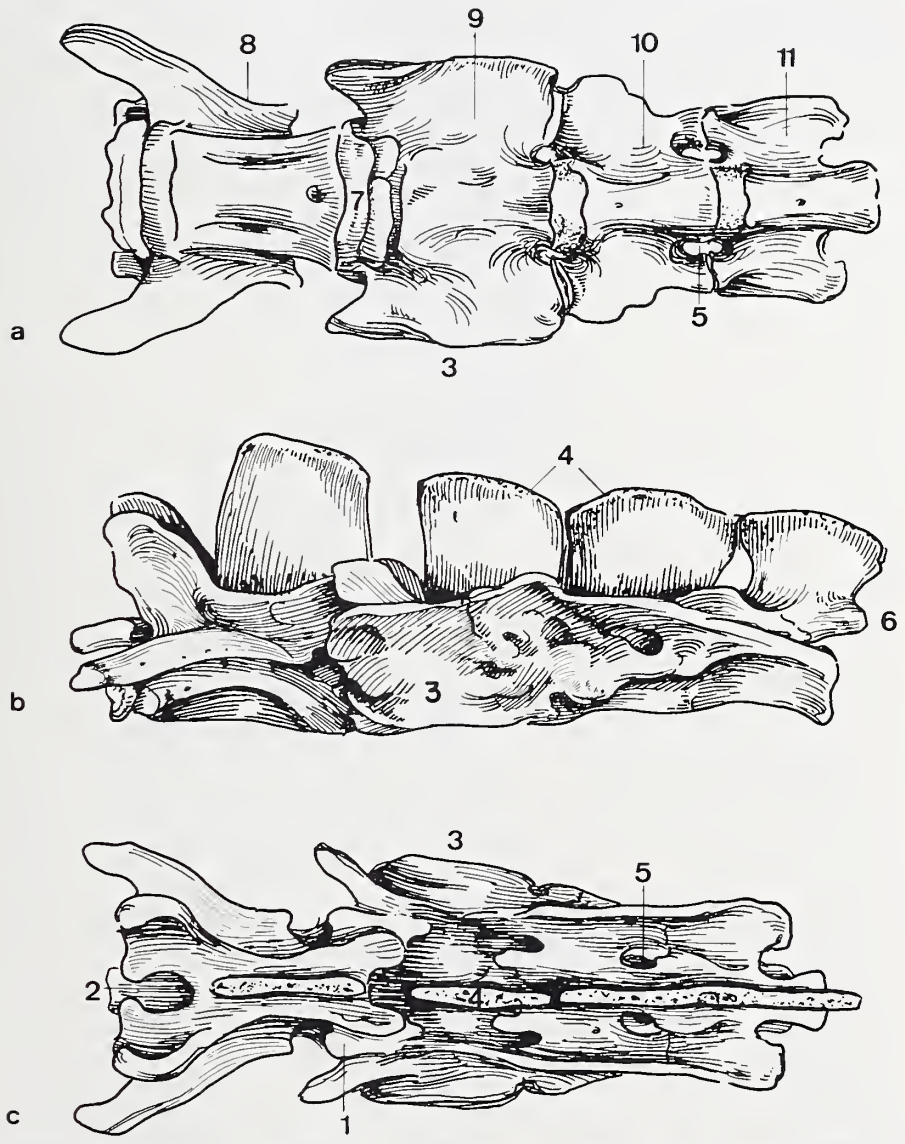

Figure 5-5: Sacrum and last lumbar vertebra. a, ventral view; b, lateral view; c, dorsal view. 1=processus articularis cranialis; 2=canalis sacralis; 3=facies auricularis; 4=processus spinosus; 5=foramina sacralia pelvina; 6=processus articularis caudalis; 7=basis ossis sacri; 8=vertebra lumbalis VI; 9=vertebra sacralis I; 10=vertebra sacralis II; 11=vertebra sacralis III.

Figure 5-6: Radiogram of pelvis and sacrum. Note articulation of auricular surface of sacrum, particularly prominent on first sacral vertebra, with wing of ilium.

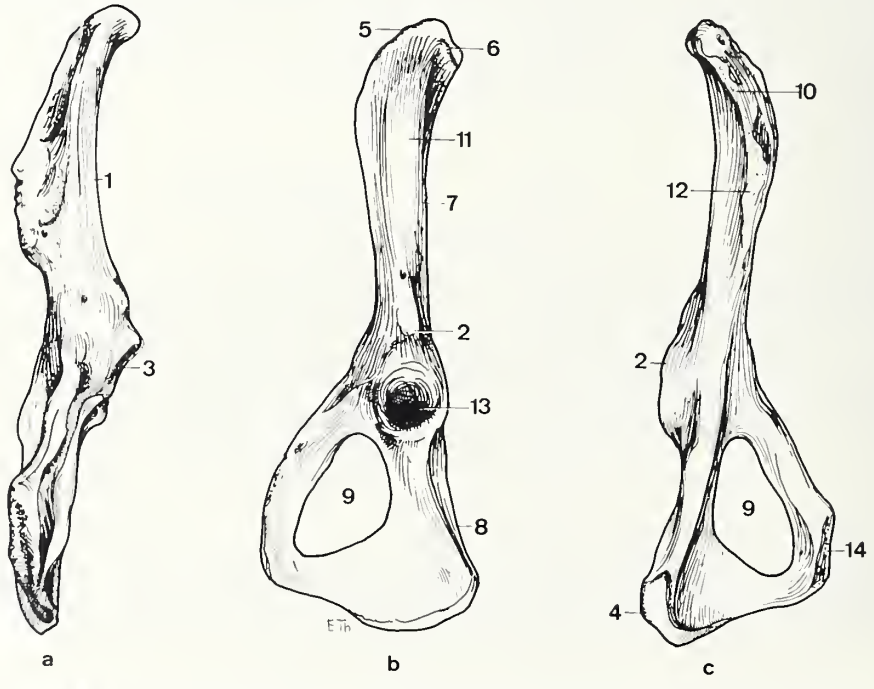

Figure 5-7: Left pelvic bone. a, ventral view; b, lateral view; c, dorsal view. 1=crista lateralis; 2=spina iliaca ventralis caudalis; 3=acetabulum; 4=tuber ischiadicum; 5=spina iliaca ventralis cranialis; 6=spina iliaca dorsalis cranialis; 7=incisura ischiadica major; 8=incisura ischiadica minor; 9=foramen obturatum; 10=tuberositas iliaca; 11=ala ossis ilii; 12=facies auricularis; 13=fossa acetabuli; 14=facies symphysialis.

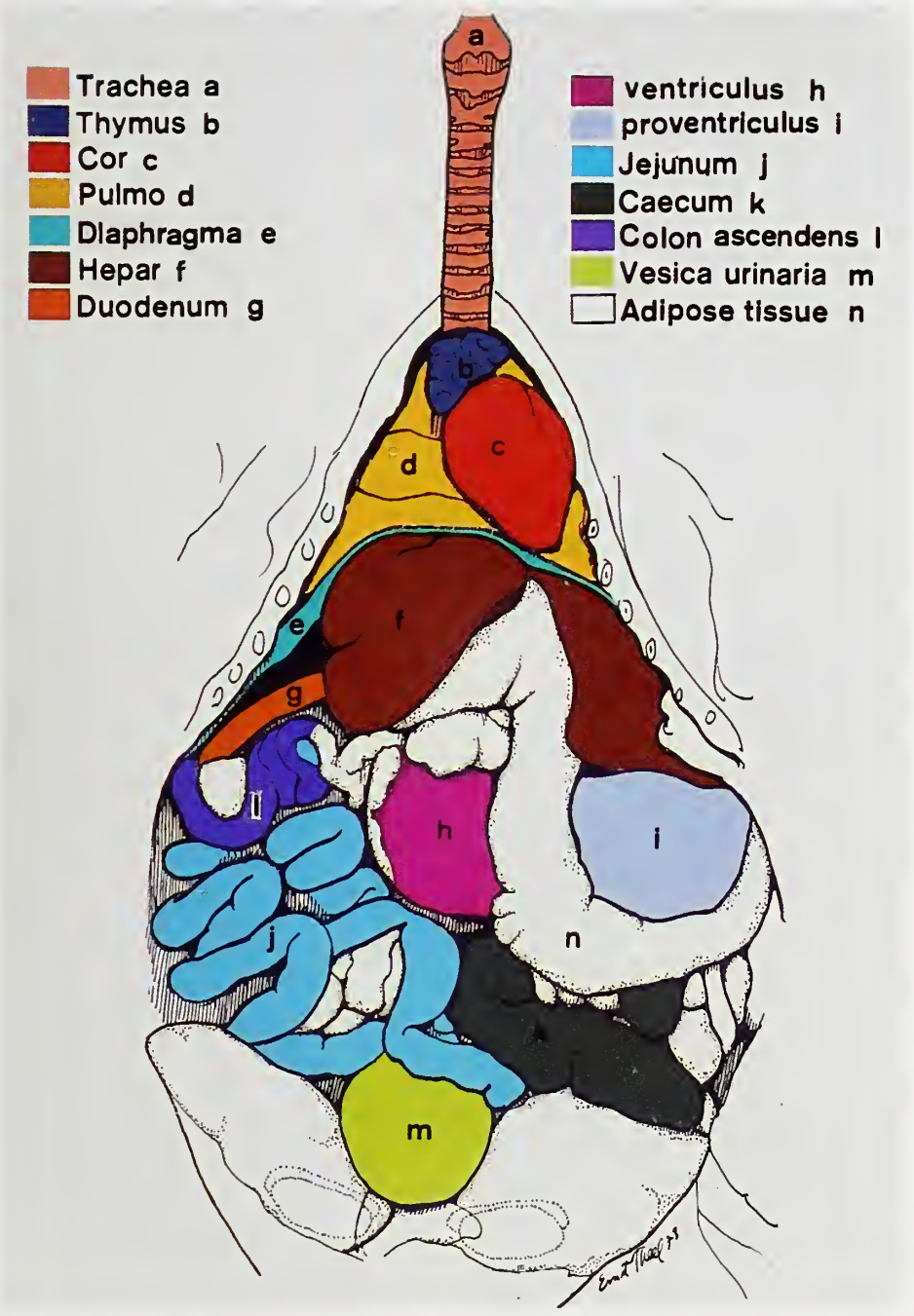

Figure 5-8: Diagram of thoracic and abdominal regions of male hamster, with positions of various organs.

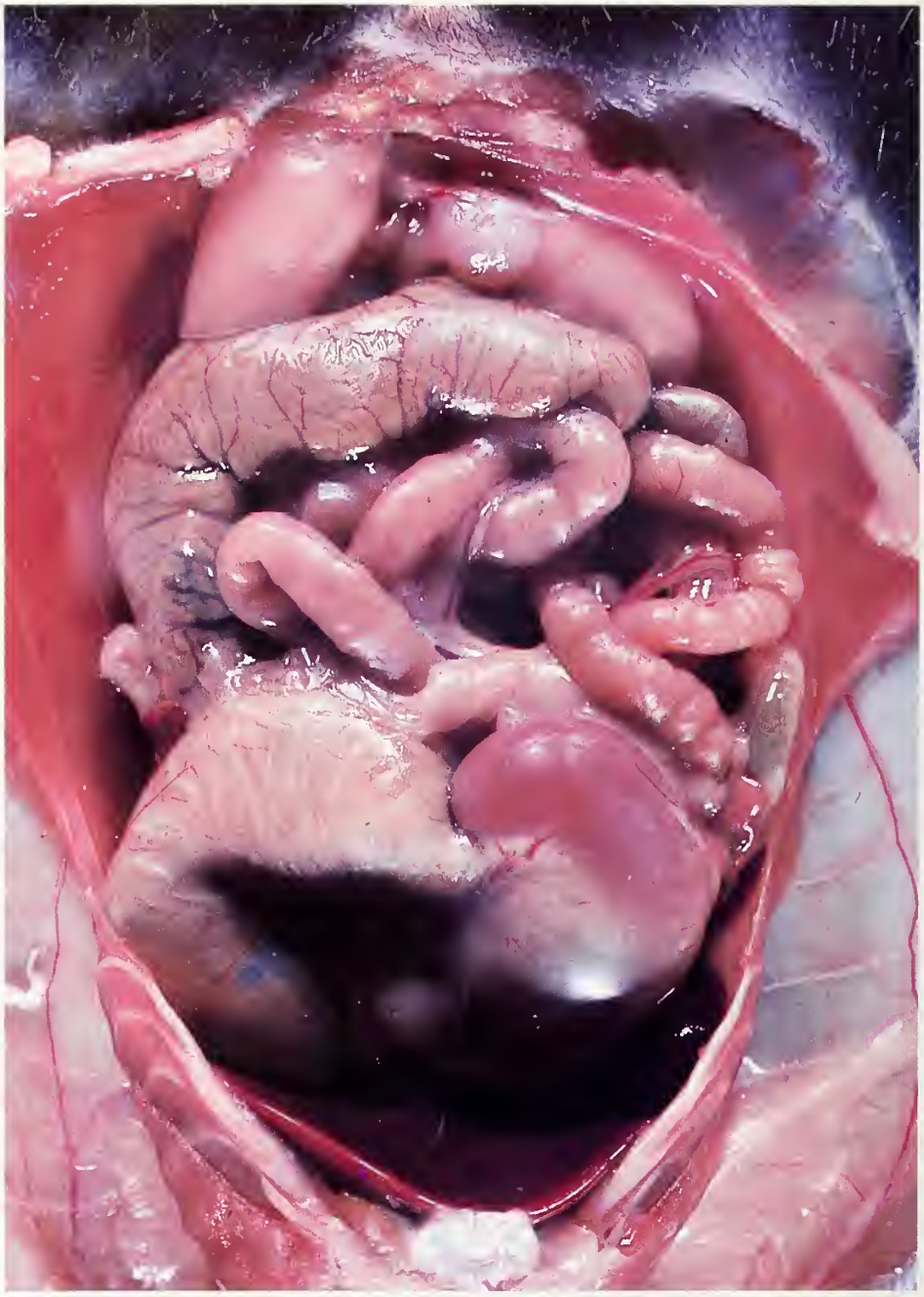

Figure 5-9: Abdominal organs *in situ*.

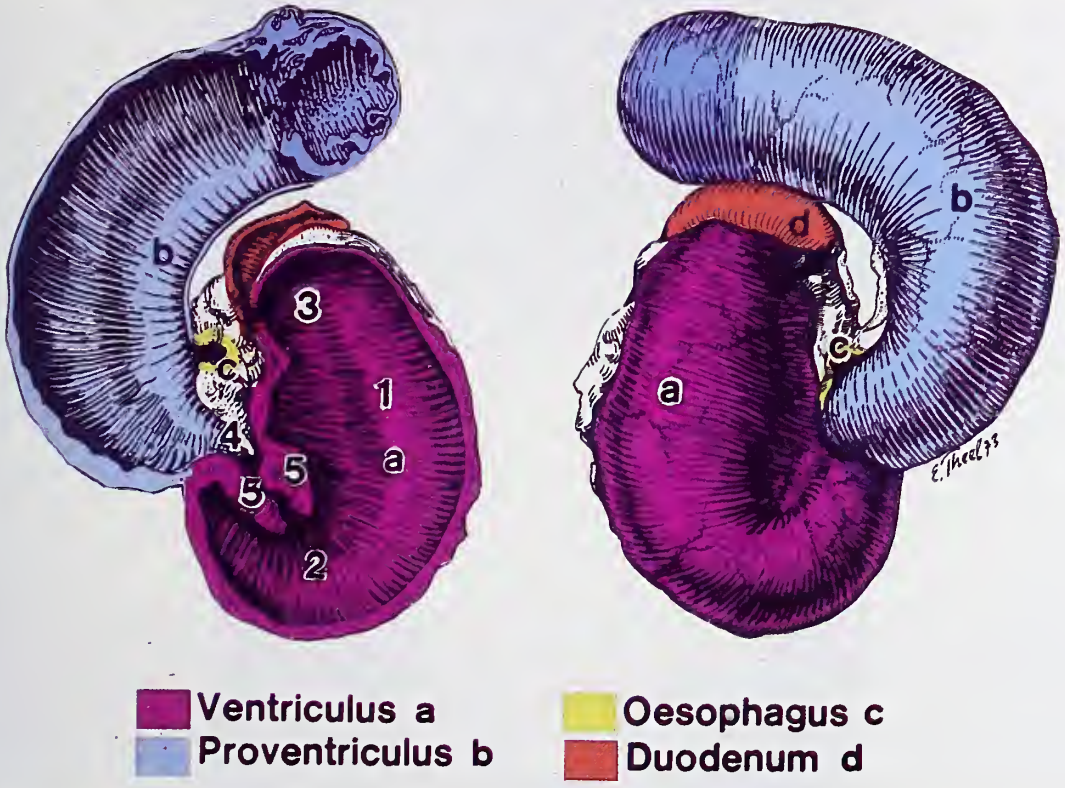

Figure 5-10: Schematic drawing of compound stomach of adult hamster, demonstrating two parts: glandular stomach (a) and forestomach (b), which are separated by deep constriction. a=ventriculus; b=proventriculus; c=duodenum; d=esophagus; 1=fundus ventriculi; 2=pars cardiaca; 3=pars pylorica; 4=sulcus ventriculi; 5=margo plicatus.

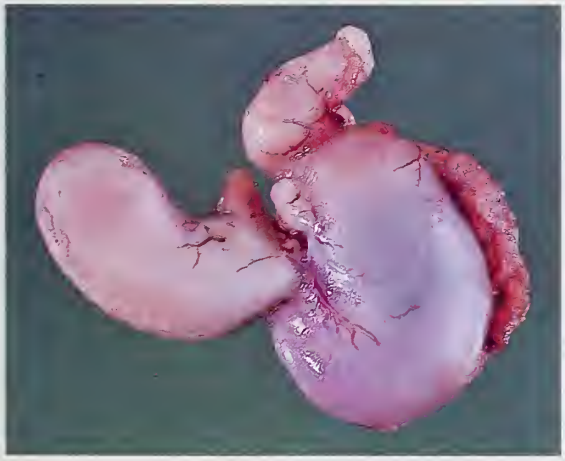

Figure 5-11: Isolated stomach. Forestomach, on right, in empty state is smaller than glandular stomach on left. At forestomach, stump of esophagus is present: at glandular stomach, pylorus is adjacent to proximal duodenum.

Figure 5-12: External surfaces of isolated stomach fixed by perfusion with glutaraldehyde. Note transparent thin walls of forestomach, which become thicker and more opaque at blind end of organ.

Figure 5-13: Radiogram of lateral aspect of abdominal region after intraesophageal instillation of Mikropaque and air. Position of abdominal part of esophagus as well as site of forestomach and glandular stomach *in vivo* are clearly shown.

Figure 5-14: Internal aspect of longitudinally bisected stomach fixed by perfusion with glutaraldehyde. Glandular stomach is coated with relatively thick velvet-like mucosa, whereas mucous membrane of forestomach is thin and glistening, except at its blind end where epithelial layer is thrown into folds. Note also well-developed margo plicatus at transition from forestomach to glandular stomach.

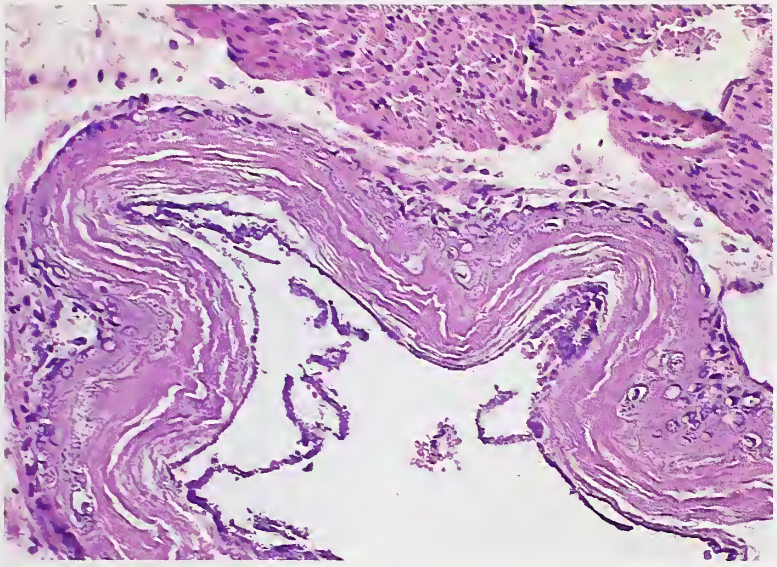

Figure 5-15: Histology of forestomach. Mucous membrane consists of simple squamous epithelium with thick layer of keratanized cells. (H & E, X73).

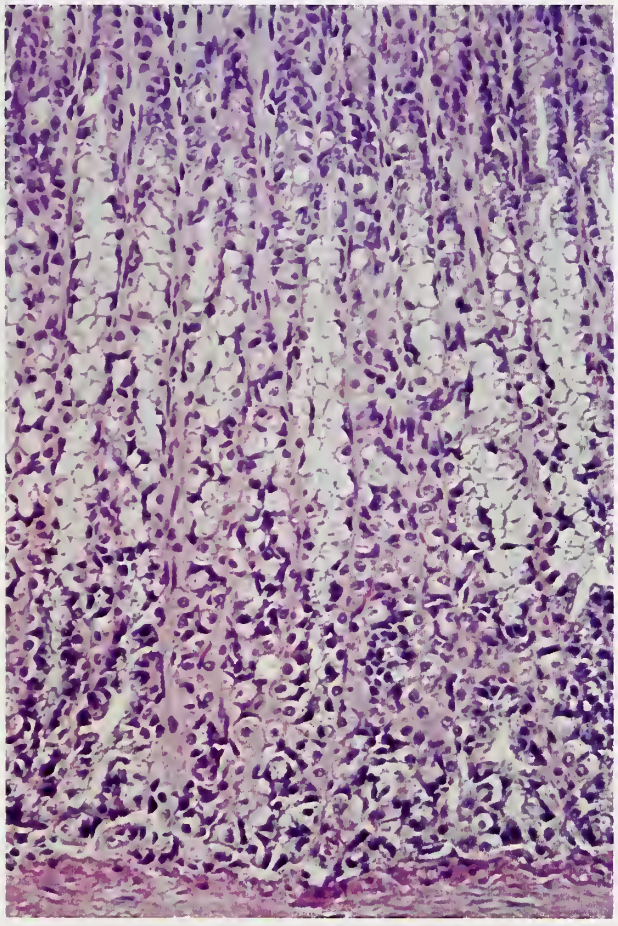

Figure 5-16: Histology of glandular stomach exhibiting gastric glands composed of tall rows of columnar epithelium. (H & E, X42).

Figure 5-17: Radiogram of forestomach, glandular stomach and duodenum *in vivo*. Double contrast with Mikropaque and air, animal in hanging position, ventral view.

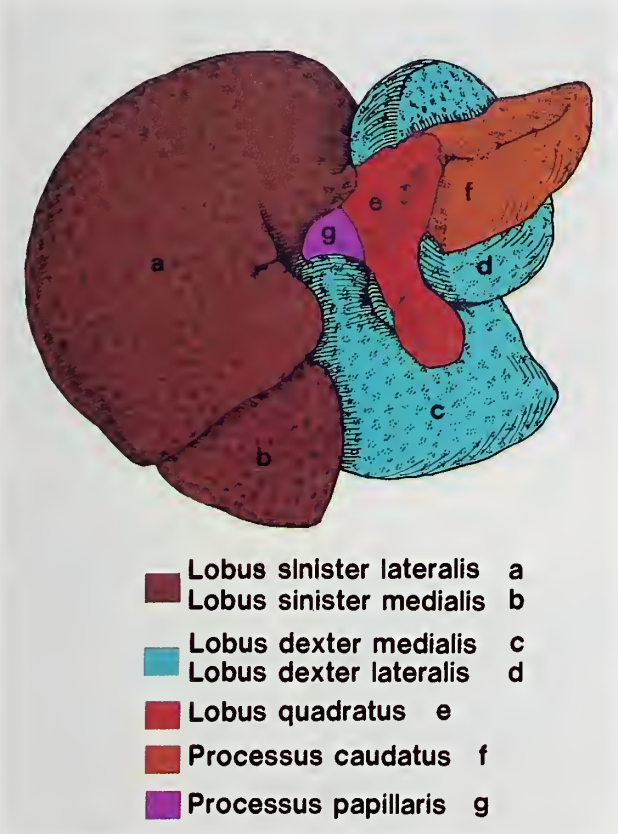

Figure 5-18: Drawing of visceral surface of liver demonstrating position of various lobes.

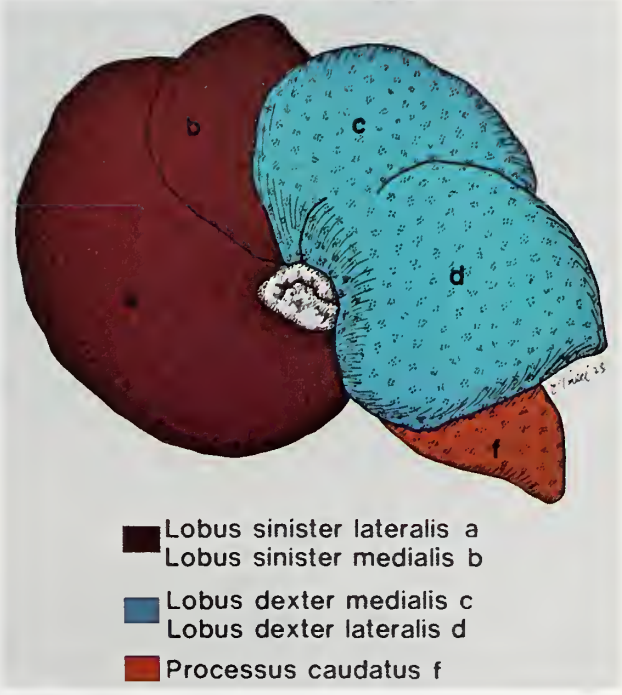

Figure 5-19: Drawing of diaphragmatic surface of liver.

Figure 5-20: Isolated fresh liver, diaphragmatic aspect. Note strongly convex shape of surface and distinct lobular structure.

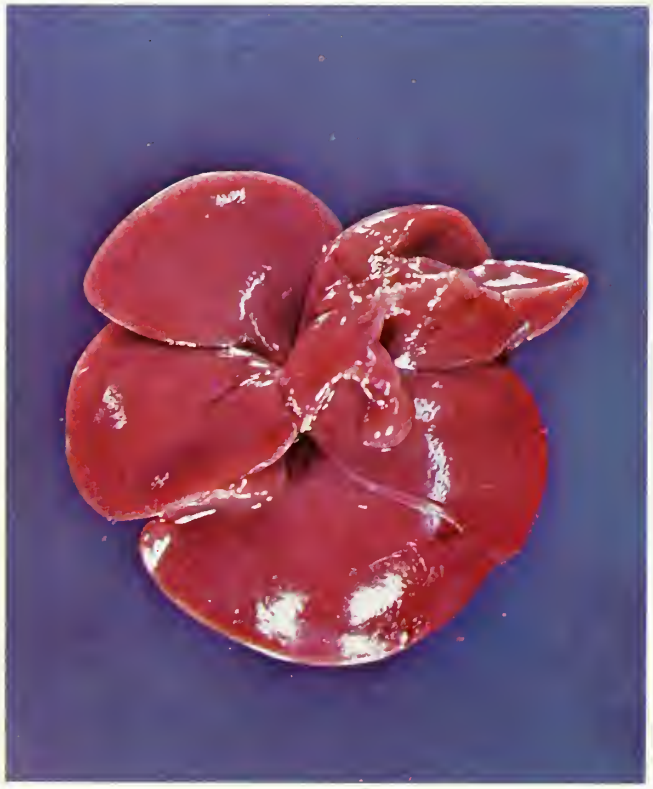

Figure 5-21: Isolated fresh liver, visceral aspect. This side is only slightly concave.

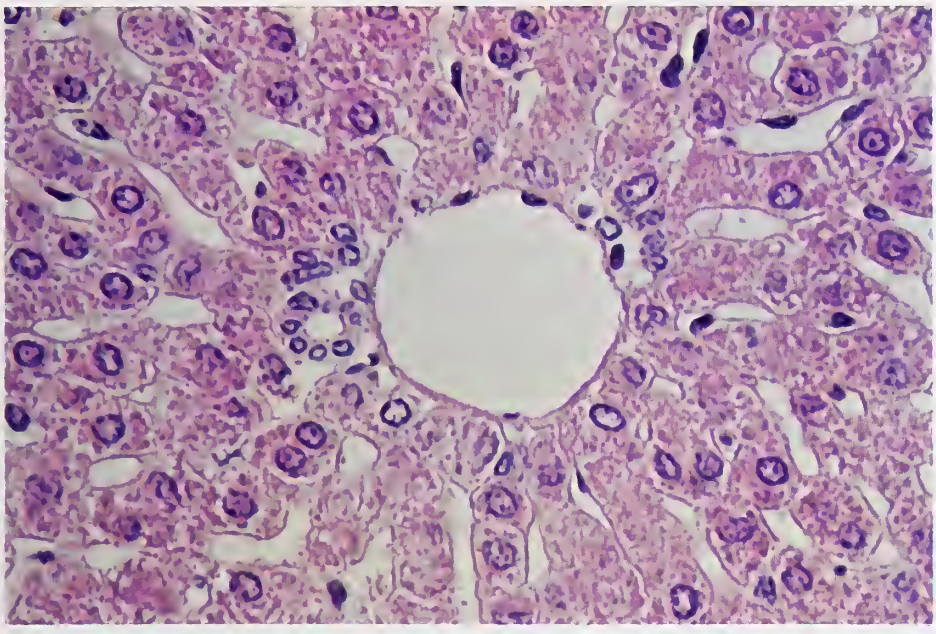

Figure 5-22: Histology of liver. Liver cells are radially arranged around central vein, and separate into cords, or "plates" (laminae hepaticae), by anastomosing sinusoids characteristic of liver lobules (lobuli hepatis). (H & E, X141).

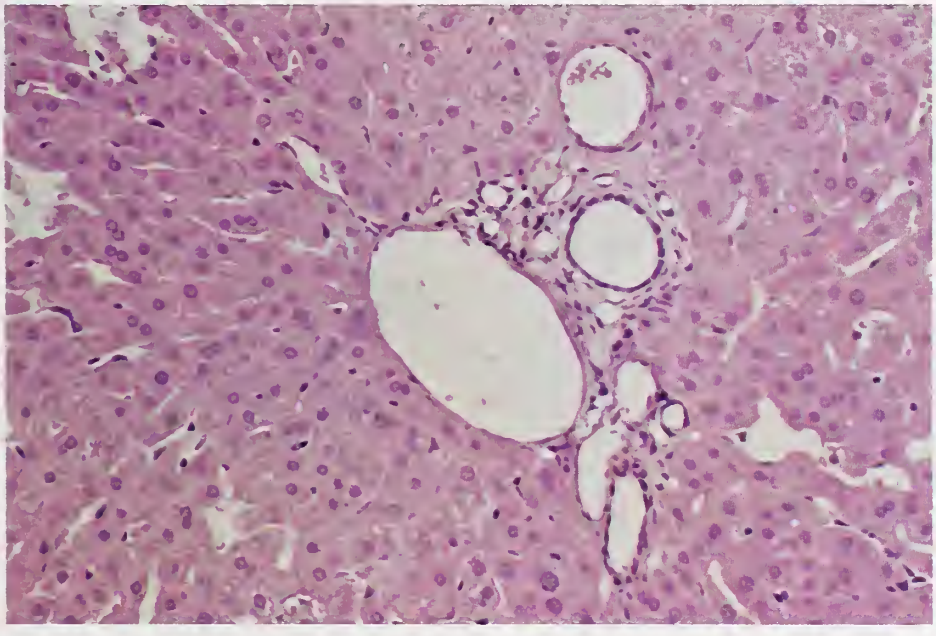

Figure 5-23: Histology of edge of liver lobule, demonstrating portal triad, which consists of branch of portal vein, branch of hepatic artery, and interlobular bile ductule. (H & E, X88).

Figure 5-24: Isolated pancreas with adipose tissue (A) and parts of the greater omentum (O). 1 = right lobe, extending between greater curvature of glandular stomach and cranial flexure of duodenum; 2 = left lobe, occupying space between spleen and descending colon; 3 = lobe, extending within duodenocolic ligament from caudal duodenal flexure to descending colon.

Figure 5-25: Ventral view of abdomen. Pancreas covered by adipose tissue (A).

Figure 5-26: Right lobe of pancreas (1), visible along dorsal aspect of greater curvature of stomach (stomach displaced ventrally).

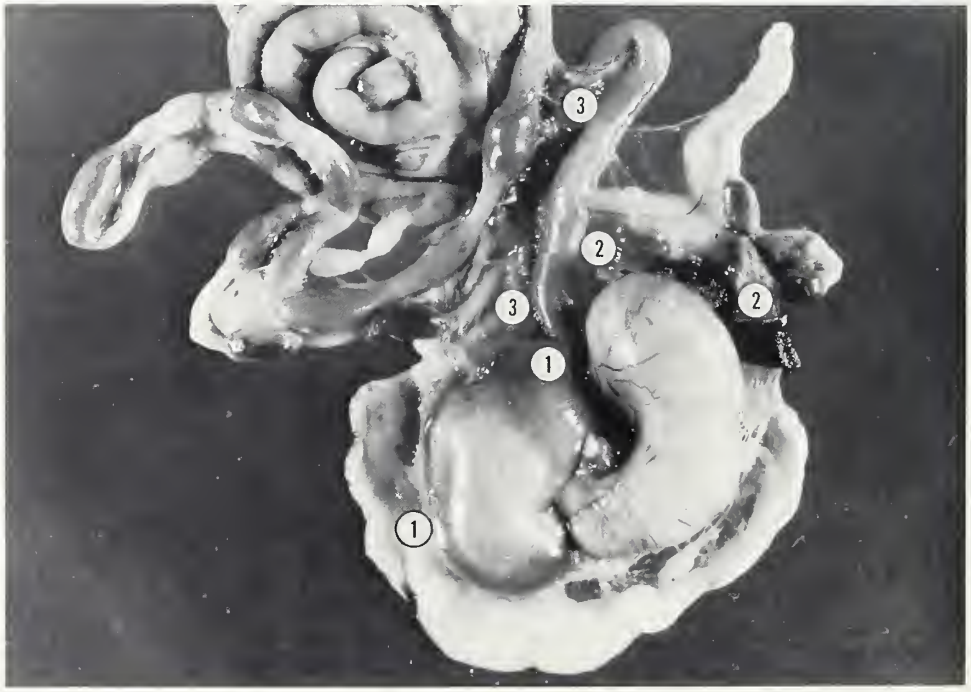

Figure 5-27: Isolated stomach and gut with spleen and pancreas, (gut displaced cranioventrally). 1=right lobe of the pancreas; 2=left lobe of pancreas occupying space between spleen and descending colon; 3=lobe within duodenocolic ligament.

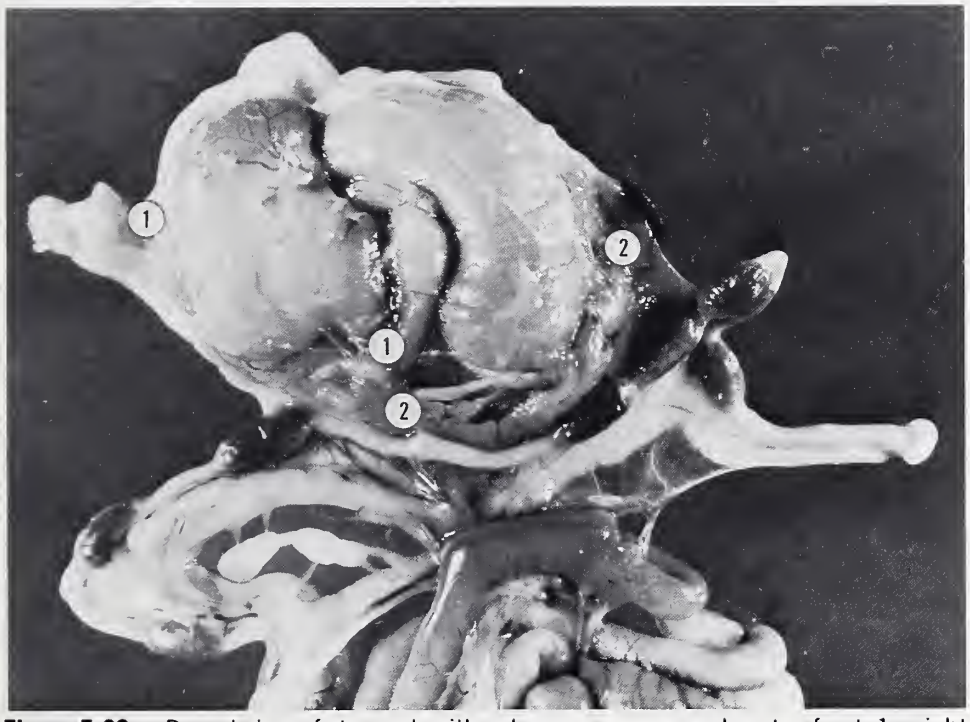

Figure 5-28: Dorsal view of stomach with spleen, pancreas, and parts of gut. 1 = right lobe of pancreas; 2 = left lobe of pancreas.

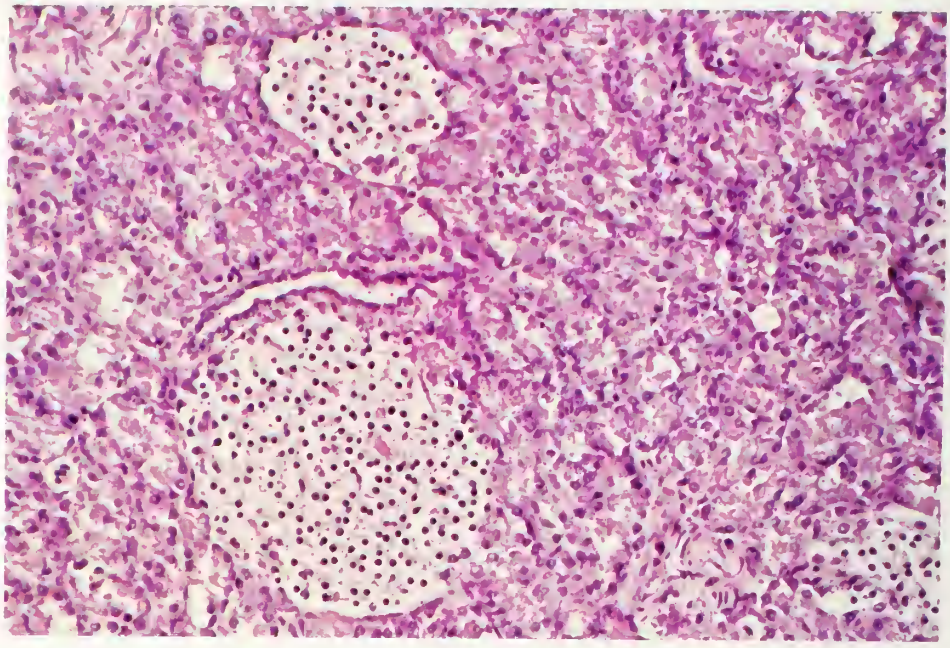

Figure 5-29: Histology of pancreas. Above. On left, two pancreatic islets of Langerhans are visible, while remaining tissue consists of glandular structures which form exocrine parts of this organ. (H & E, X88). Below. Entrance of main pancreatic duct into duodenum. (H & E, X88).

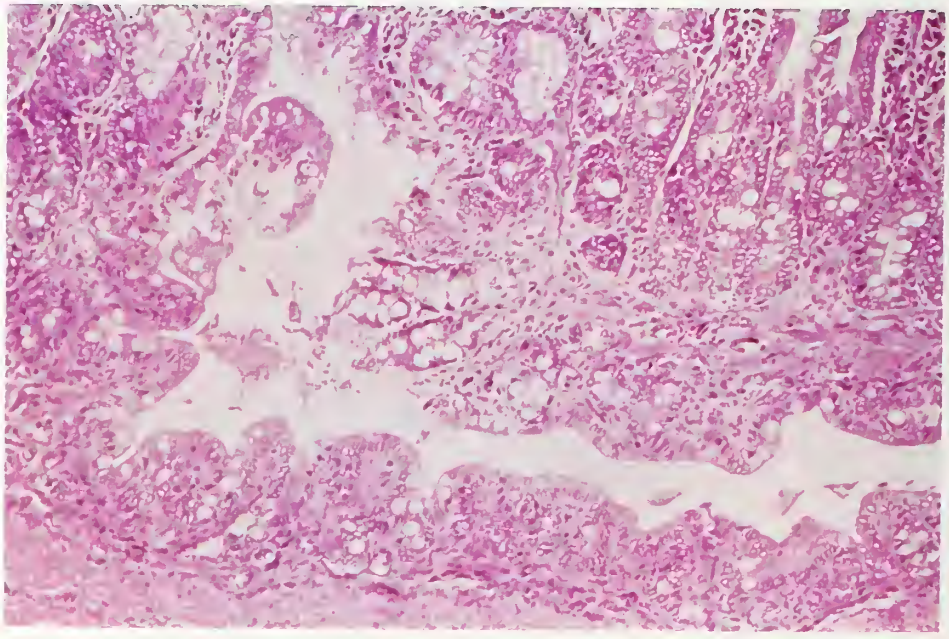

Figure 5-30: Parietal aspect of isolated lanciform spleen.

Figure 5-31: Visceral aspect of isolated spleen. Note gastrosplenic ligament attaching organ to forestomach.

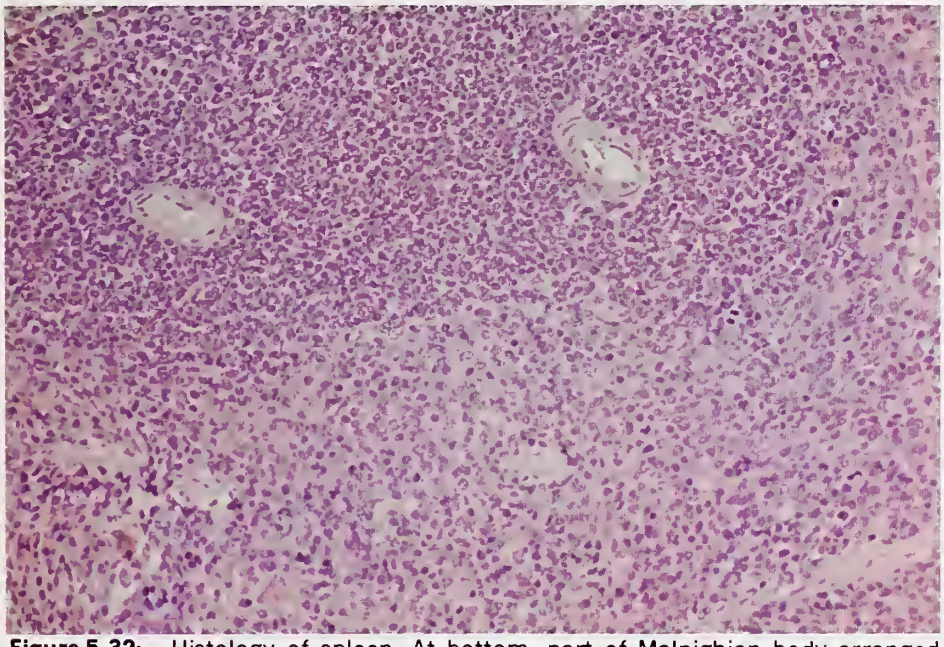

Figure 5-32: Histology of spleen. At bottom, part of Malpighian body arranged around two capillaries can be seen. (H & E, X88).

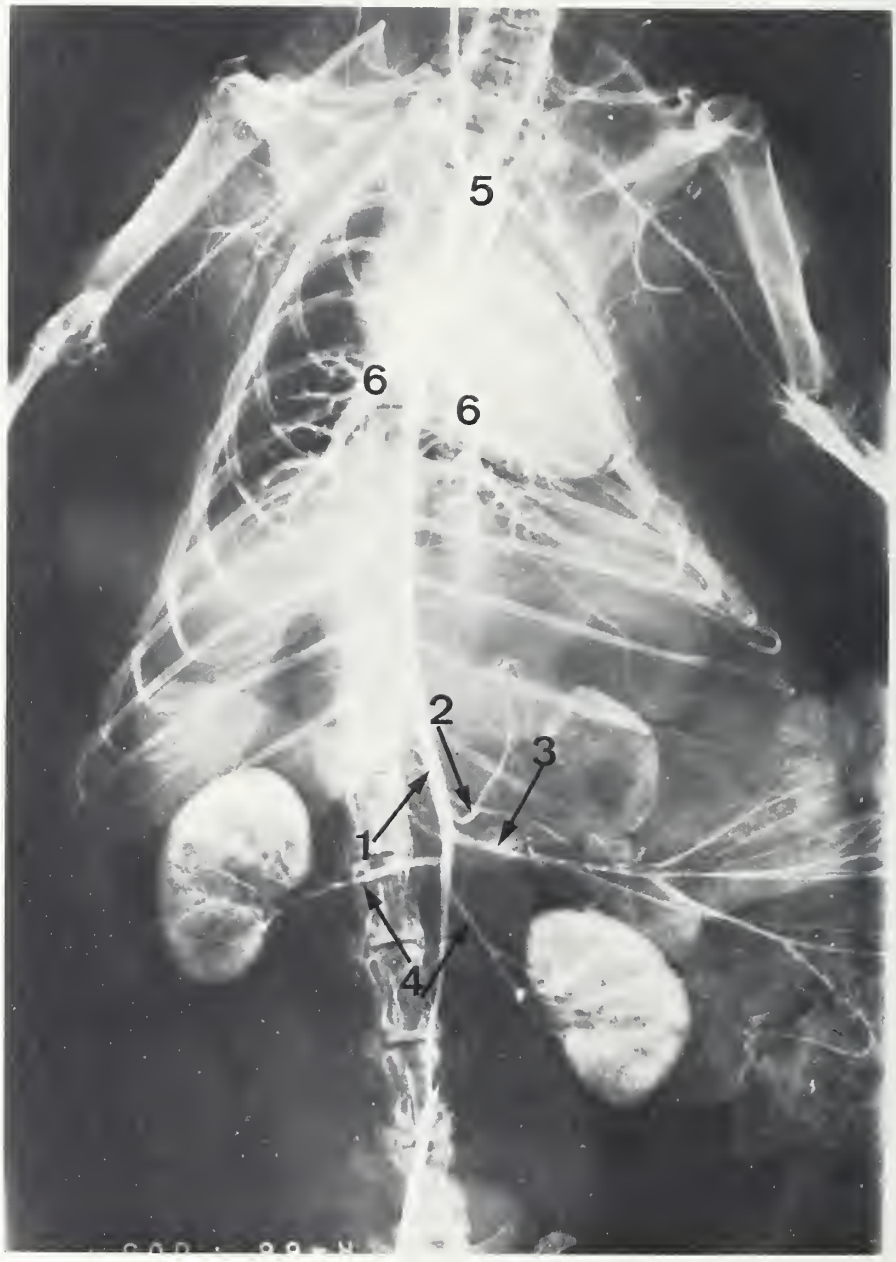

Figure 5-33: Arteriogram of thoracic and abdominal regions (gut and left kidney displaced). 1=aorta abdominalis; 2=a. coeliaca; 3=a. mesenterica cranialis; 4=aa. renales; 5=arcus aortae; 6=vv. pulmonales.

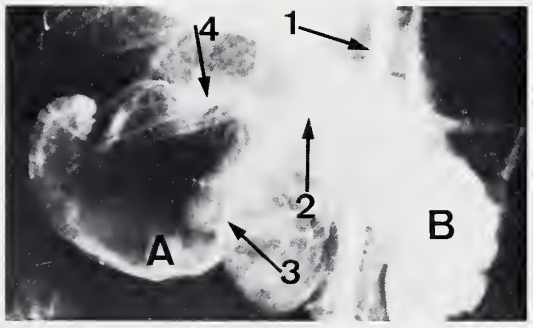

Figure 5-34: Dorsal arteriogram of abdominal region at level of spleen. 1=aorta abdominalis; 2=a. mesenterica cranialis; 3=a. pancreaticoduodenalis caudalis; 4=a. lienalis; A=lien; B=ren dexter.

Figure 5-35: Venogram of hepatic portal vein, hepatic venules, hepatic veins, and caudal vena cava. Note also small internal jugular veins.

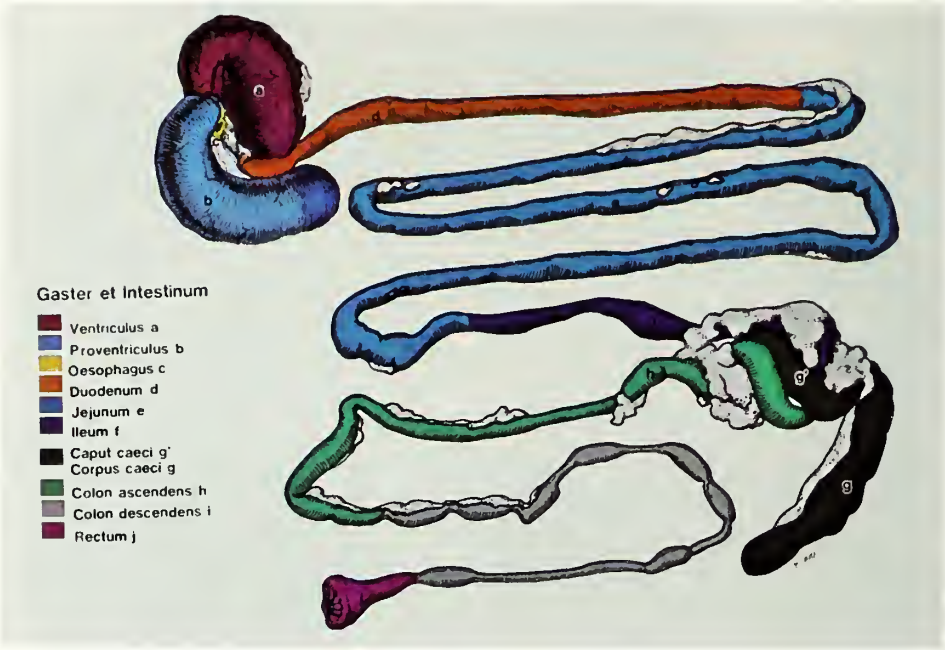

Figure 5-36: Schematic drawing of isolated stomach and intestine.

Figure 5-37: Isolated esophagus, stomach, and intestine.

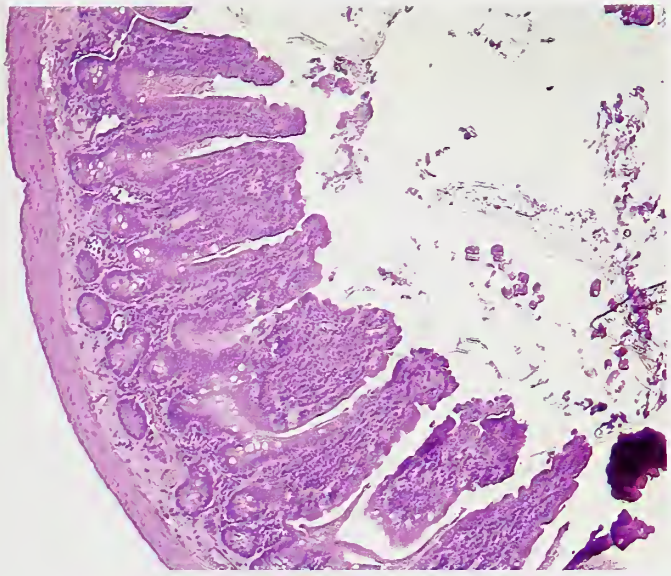

Figure 5-38: Histology of small intestine exhibiting serous, muscular, submucous, and mucous layers of wall. (H & E, X200).

Figure 5-39: Abdominal organs *in situ,* note position of jejunal loops (pink) and thick fat deposits, especially around epididymis. Also visible along right lateral abdominal wall is portion of contorted ascending colon (whitish, showing feces) and caecum (pinkish gray) in left lateral region.

Figure 5-40: Radiogram of stomach and jejunal loops *in vivo,* animal in hanging position, ventral view, double contrast with Mikropaque and air.

Figure 5-41: Isolated gut demonstrating curled jejunal loops. Broad mesojejunum allows certain change in position of this segment of intestine.

Figure 5-42: Histology of mucosal coat of jejunum; mucous membrane in this part of intestine forms tall villi. (H & E, X45).

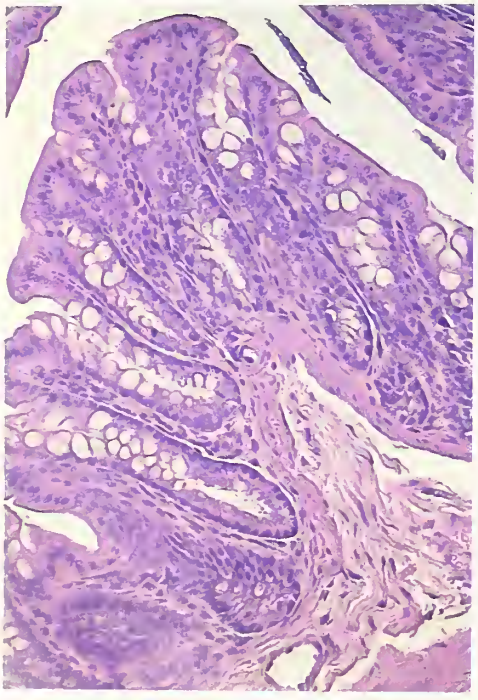

Figure 5-43: Histology of mucosal coat of colon. In this part of intestine, epithelial layer is thrown into distinct folds but does not form villi. Note abundant goblet cells. (H & E, X45).

Figure 5-44: Radiogram of colon *in vivo,* ventral view; exposure taken with animal in hanging position; double contrast with Mikropaque and air. Note beginning of fecal formation.

Figure 5-45 (left): Radiogram of descending colon and rectum of mature hamster (contrast medium, 1 ml Angiographin^{R} and 9 ml air, introduced through anus).

Figure 5-46 (right): Lateral radiogram of descending colon and rectum of mature hamster (contrast medium, 1 ml Angiographin^{R} and 9 ml air, introduced through anus). Note position of rectum relative to bony pelvis.

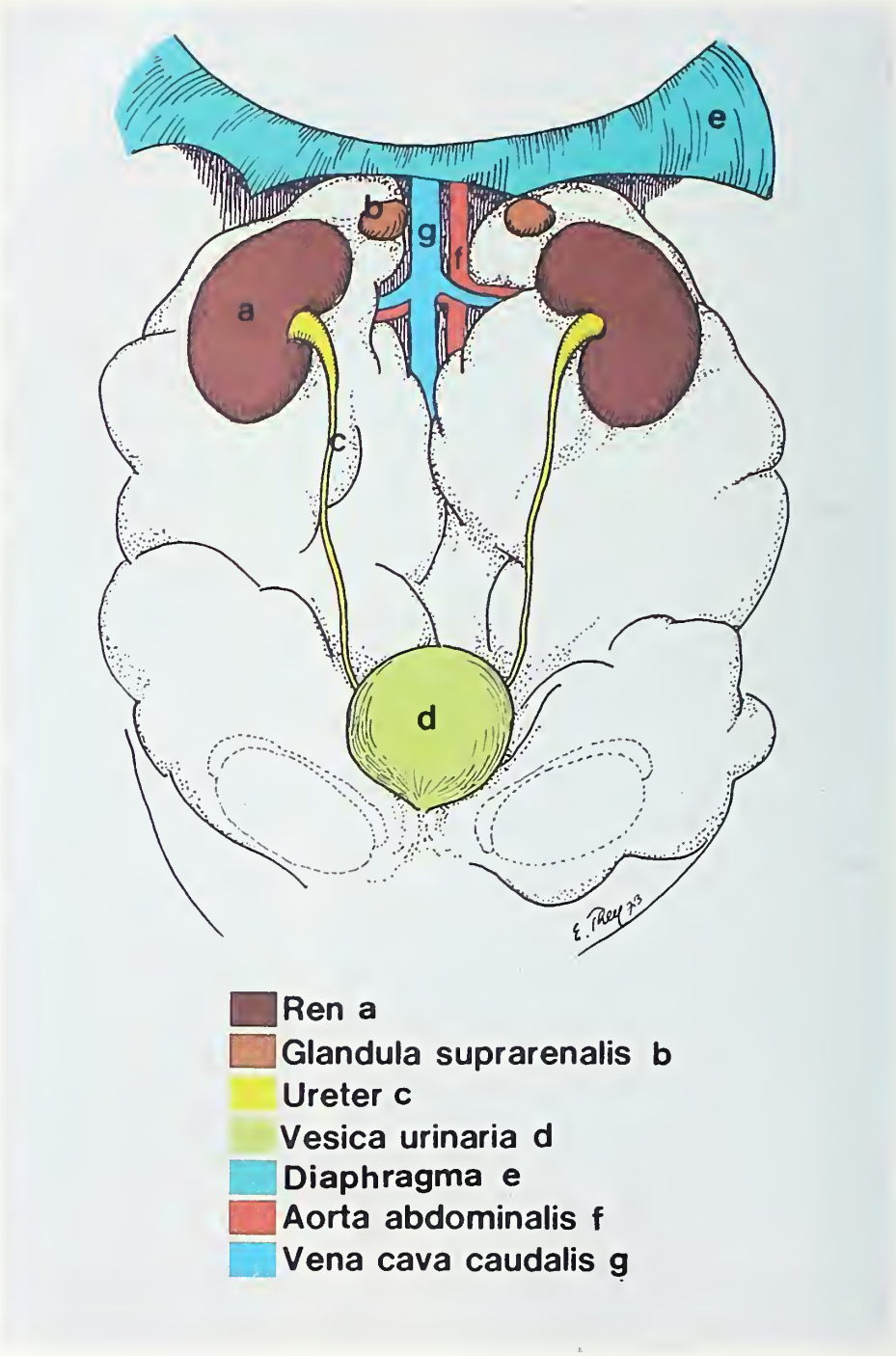

Figure 5-47: Schematic drawing of urinary organs.

Figure 5-48: Urinary organs *in situ*. These organs are embedded in well-developed adipose tissue. Urinary bladder in distended state.

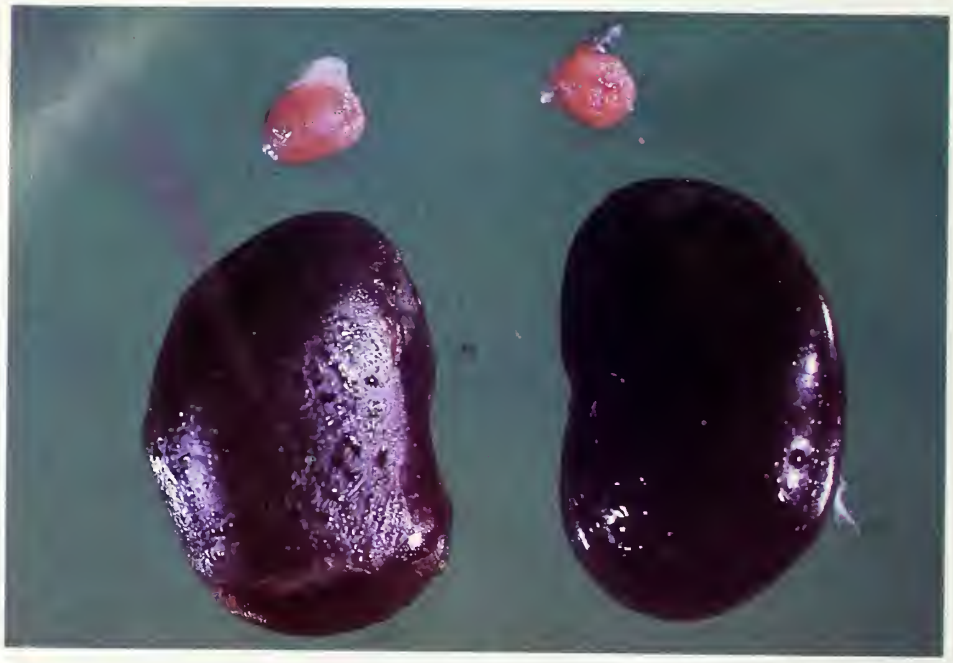

Figure 5-49: Isolated kidneys and adrenal glands.

Figure 5-50: Schematic drawing of kidney and adrenal gland, longitudinally sectioned. a=capsula fibrosa; b=cortex renis; c=zona intermedia; d=zona basalis; e=papilla renalis; 1=cortex glandulae suprarenalis; 2=medulla glandulae suprarenalis; 3=capsula adiposa glandulae suprenalis.

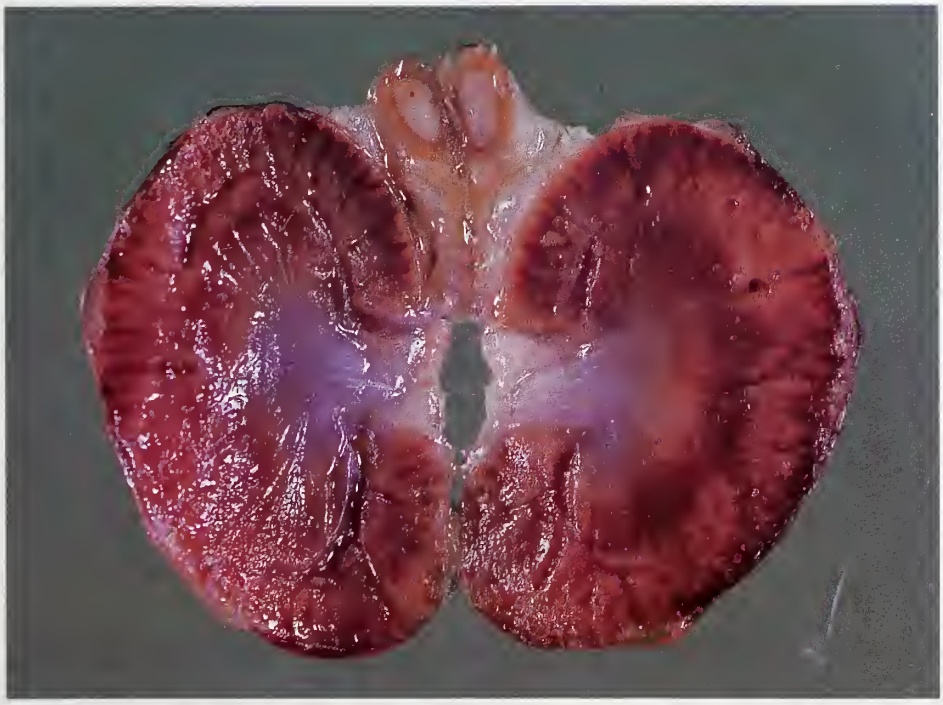

Figure 5-51: Isolated kidney with adrenal gland, cut longitudinally. Note different colors of cortical and medullary zones in adrenal gland, and clearly visible grayish-white papilla of kidney.

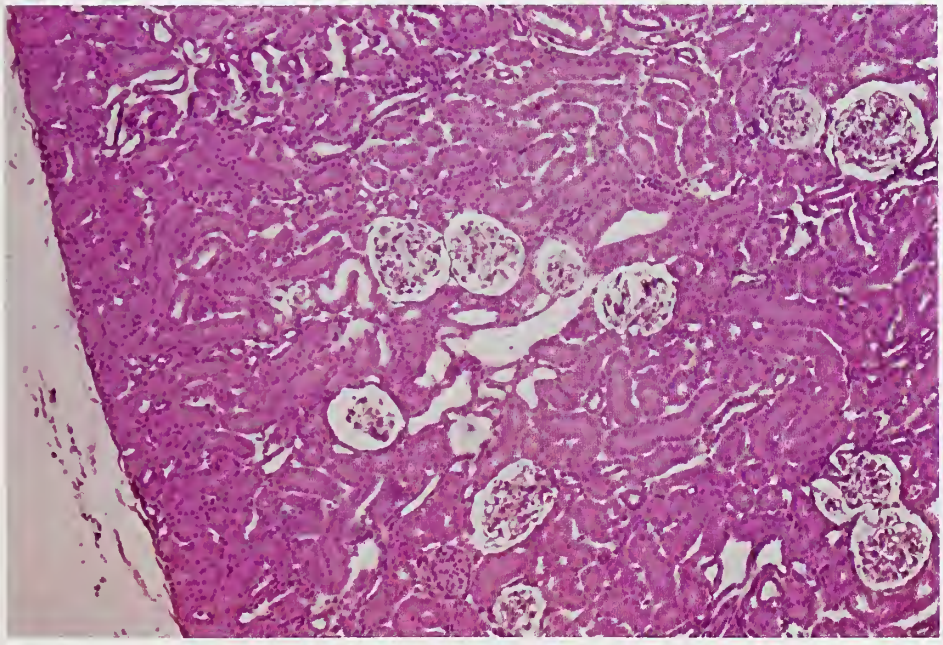

Figure 5-52: Histology of renal cortical zone. This zone consists of proximal convoluted tubules and renal corpuscles. (H & E, X22).

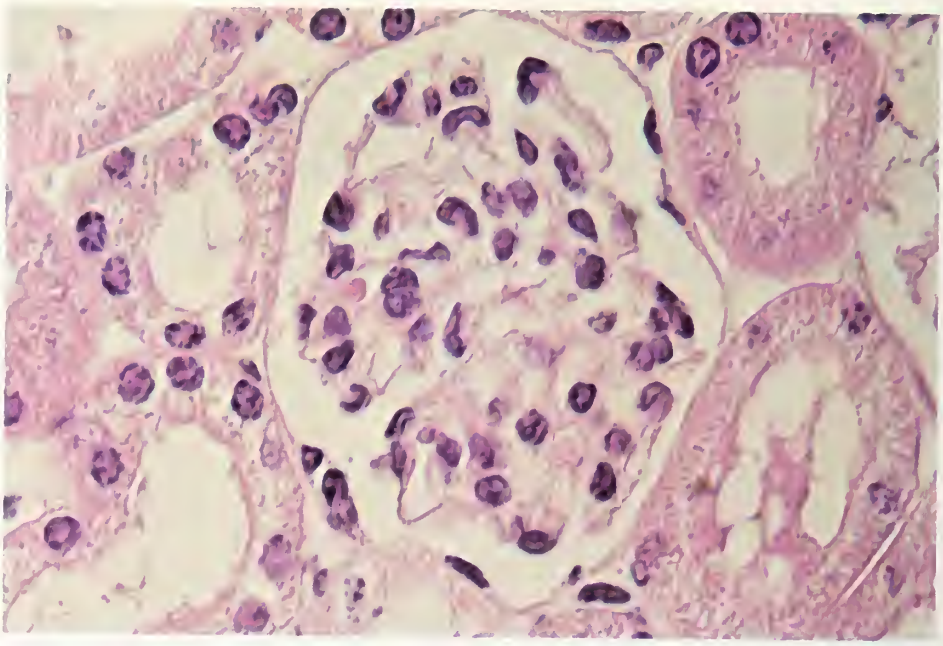

Figure 5-53: Histology of renal corpuscle demonstrating its typical elements: glomerular loops and Bowman's capsule. (H & E, X223).

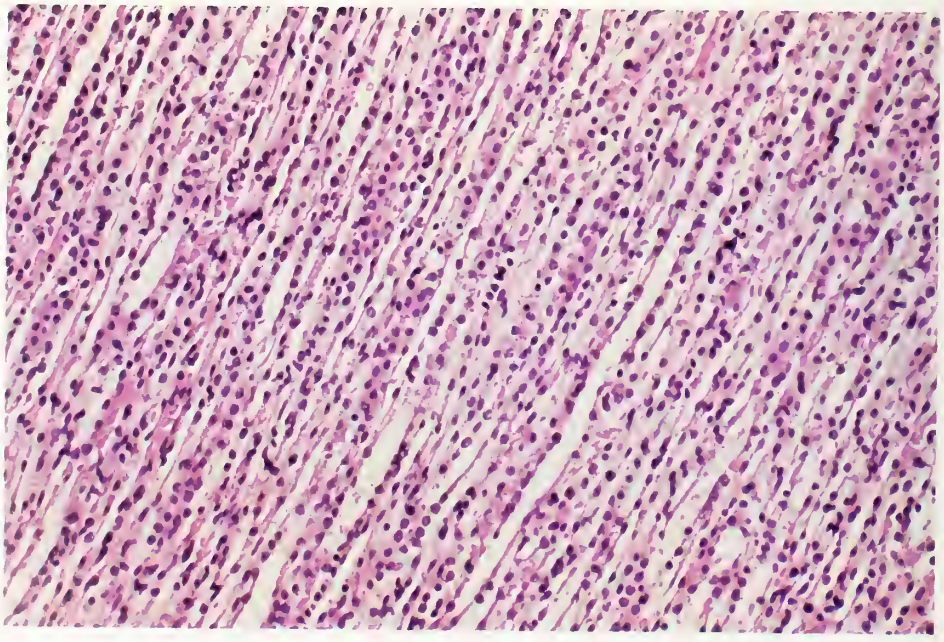

Figure 5-54: Histology of renal medulla, composed of radiating tubules. (H & E, X88).

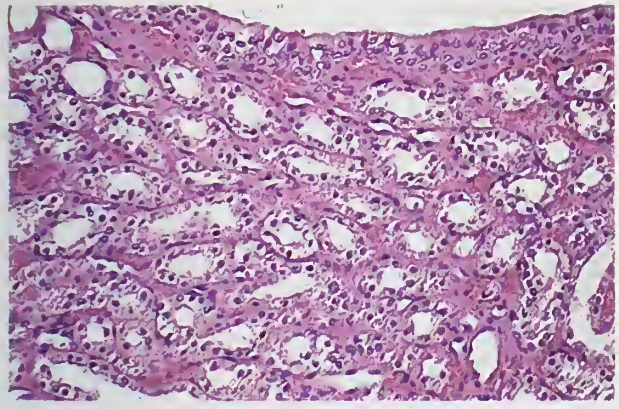

Figure 5-55: Histology of renal pelvis. Note simple epithelial coat composed of polygonal cells. (H & E, X58).

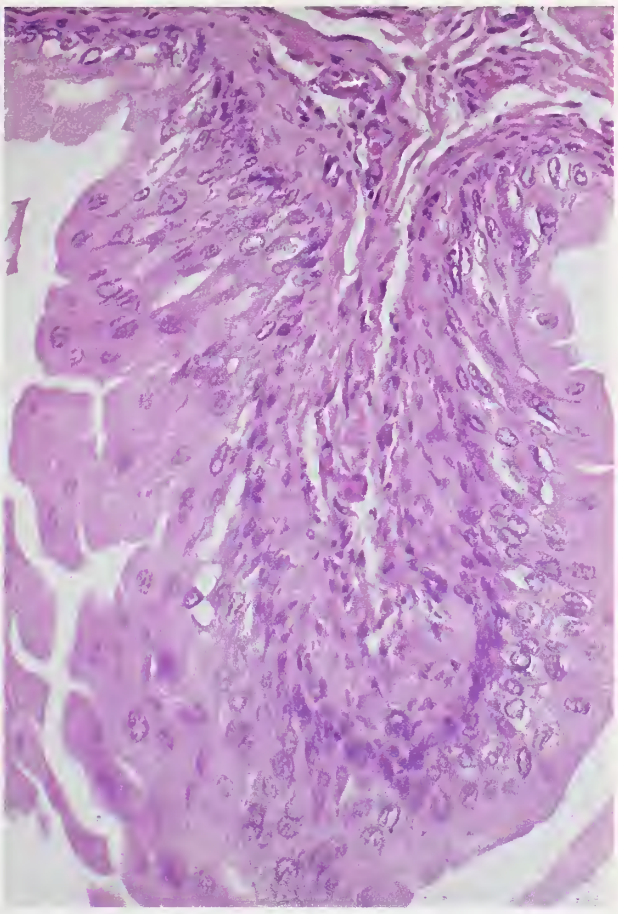

Figure 5-56: Histology of urinary bladder. Stratified transitional epithelium thrown into distinct folds when organ is empty. (H & E, X90).

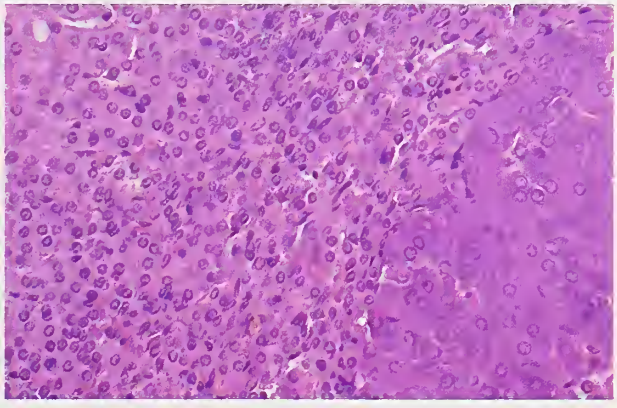

Figure 5-57: Histology of adrenal gland, demonstrating typical structure of this organ. Zona medullaris can be identified on right side, with zona fasciculata on left. (H & E, X58).

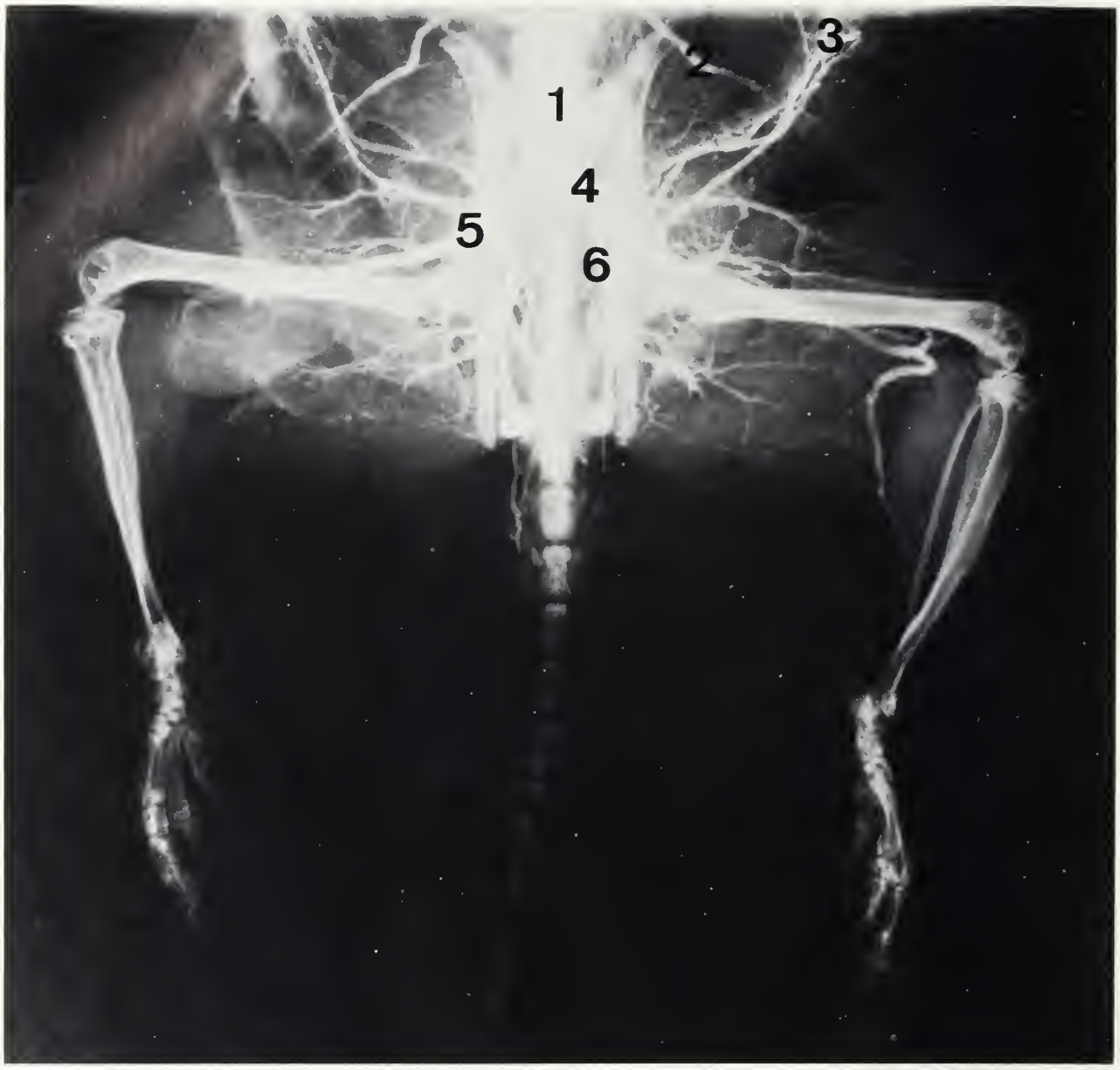

Figure 5-58: Arteriogram of pelvic region and adjacent areas in 1-year-old male European hamster. 1=aorta; 2=a. testicularis; 3=a. rectalis cranialis; 4=a. iliaca communa; 5=a. iliaca externa; 6=a. iliaca interna.

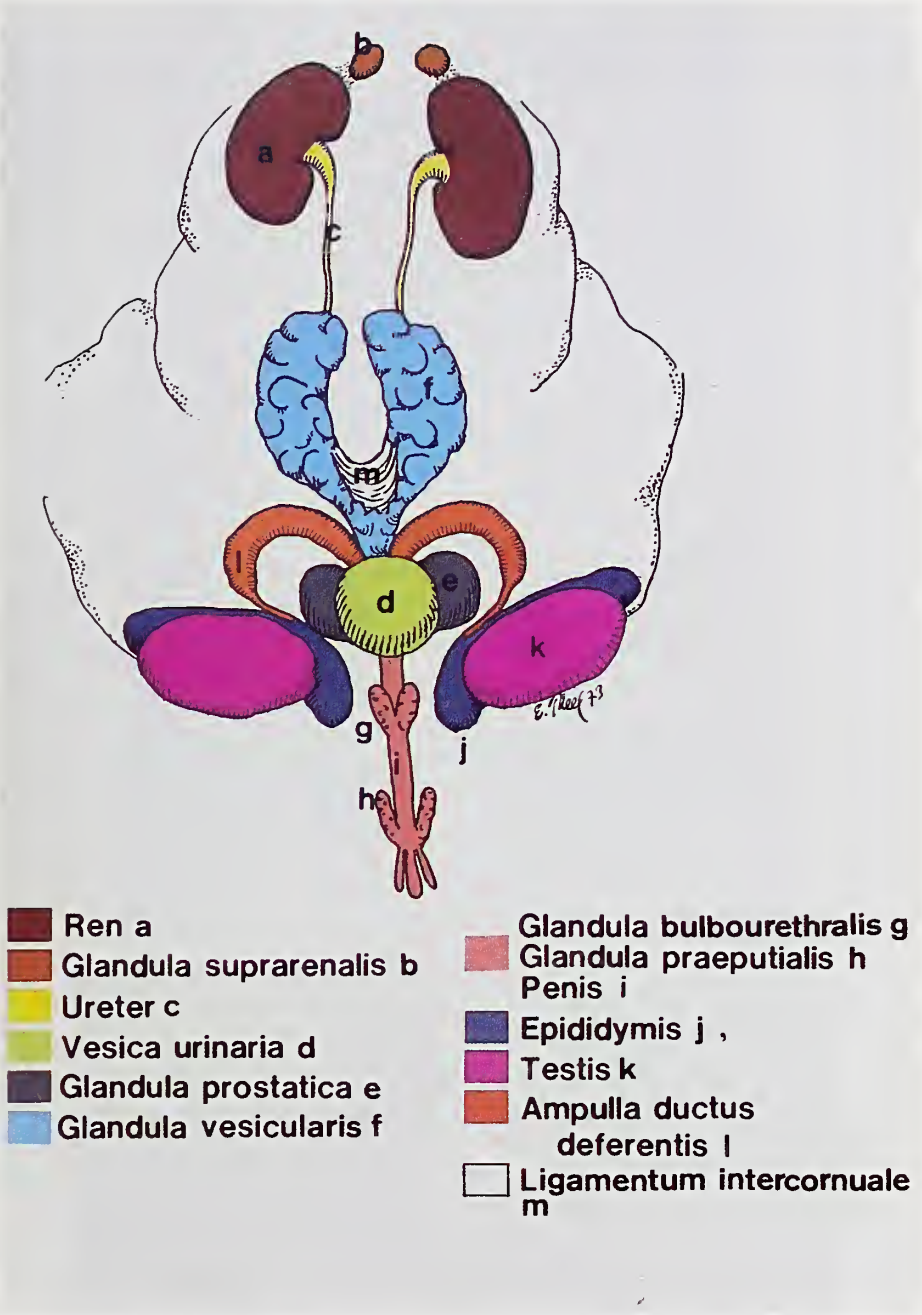

Figure 5-59: Schematic drawing of male urogenital organs.

Figure 5-60: Male urogenital organs *in situ*. Note abundant adipose tissue around kidneys and epididymides and thick ampullae of vas deferens.

Figure 5-61: Isolated formalin-fixed testes demonstrating seasonal variation in size. From left to right: testis in May; two testes in October; two testes in December during hibernation.

Figure 5-62: Isolated male reproductive organs with intestine. Note abundant fat deposits around testes.

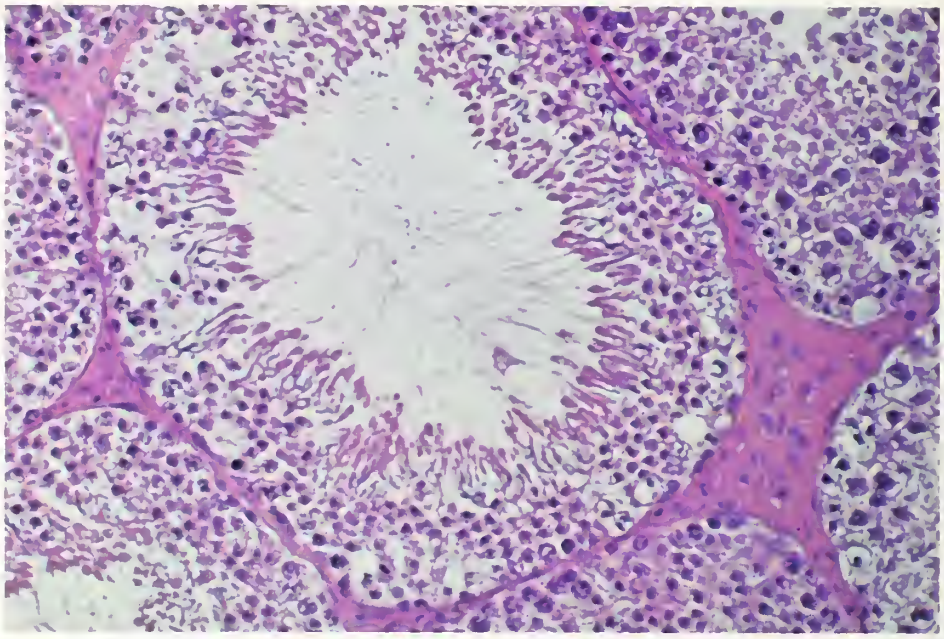

Figure 5-63: Histology of seminiferous tubule of sexually active male sacrificed in May. Note large diameter of tubule and numerous mature spermatids. (H & E, X88).

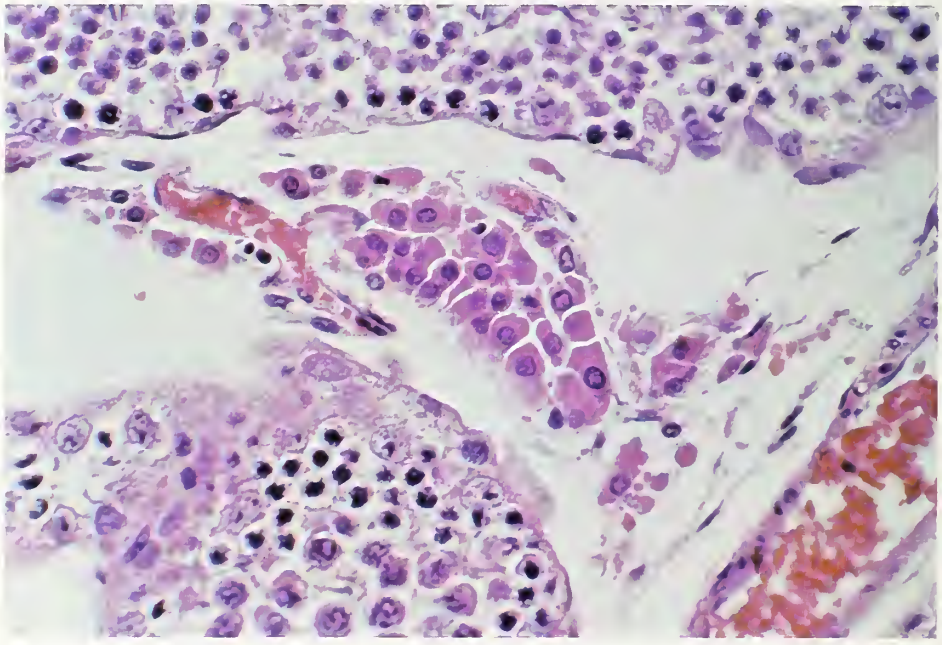

Figure 5-64: Histology of interstitial tissue in testis of sexually active male sacrificed in May. (H & E, X141).

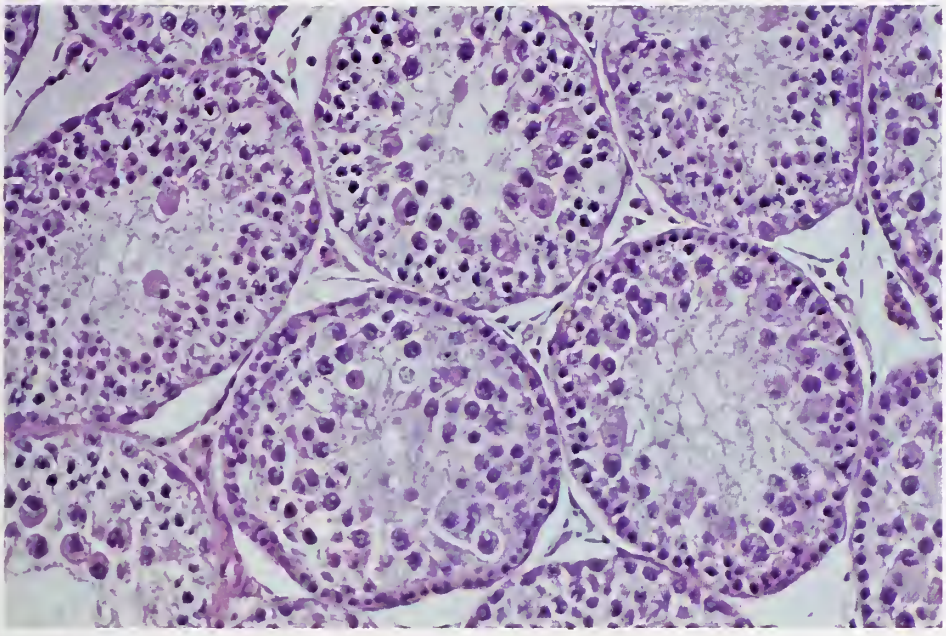

Figure 5-65: Histology of testis from male hamster during hibernation. Note small seminiferous tubules without mature spermatids and sparse interstitial tissue. (H & E, X88).

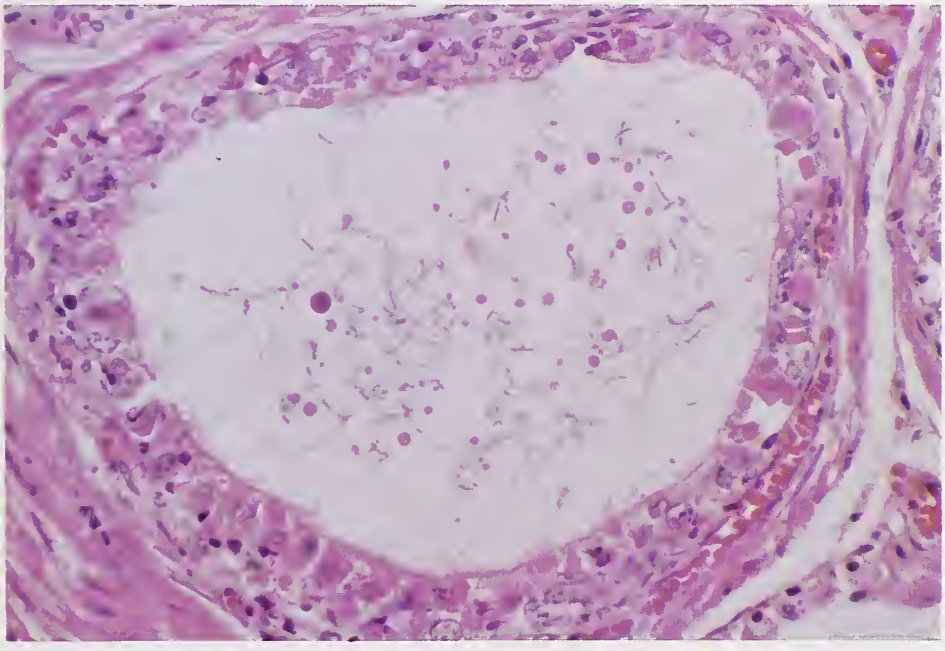

Figure 5-66: Histology of efferent ductule of head of epididymis. It is lined by columnar ciliated epithelium. (H & E, X141).

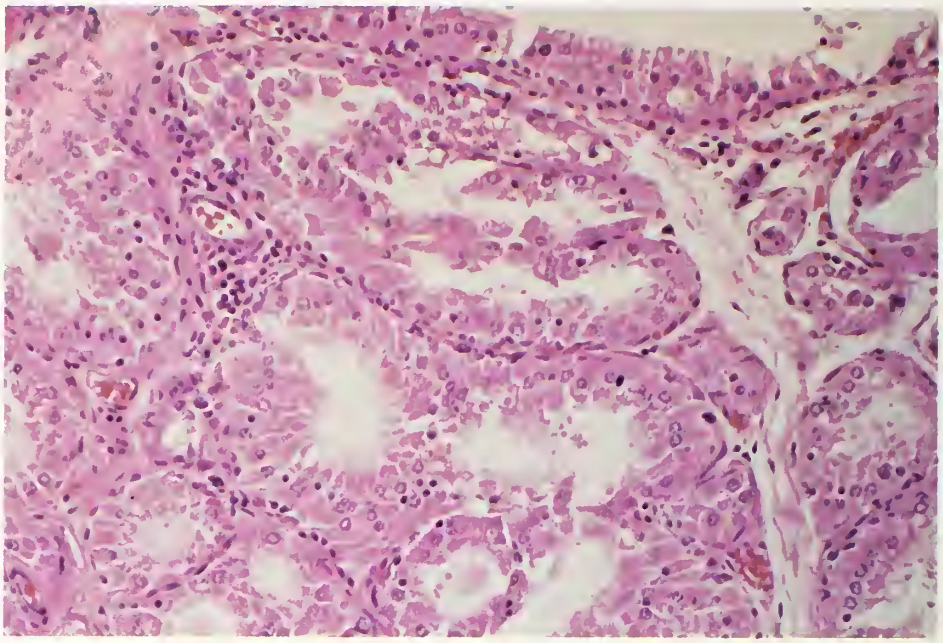

Figure 5-67: Histology of glandular part of ductus deferens. Note densely packed glands beneath pseudostratified columnar epithelium, on surface of which project long microvilli. (H & E, X88).

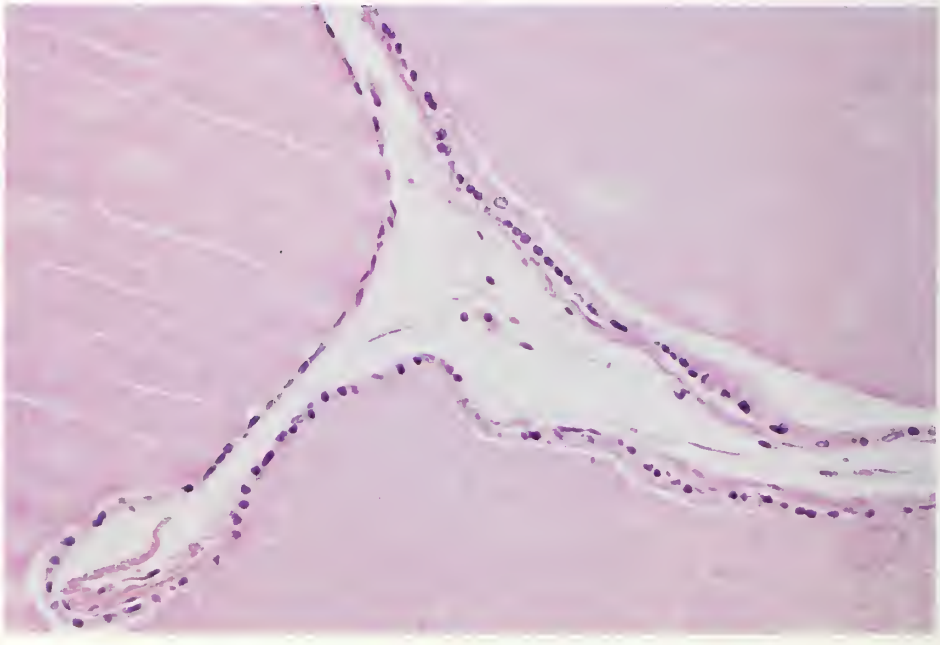

Figure 5-68: Histology of vesicular gland of sexually active male sacrificed in May. Caverns are filled with secretion, and epithelial cells of walls are flat in shape. (H & E, X35).

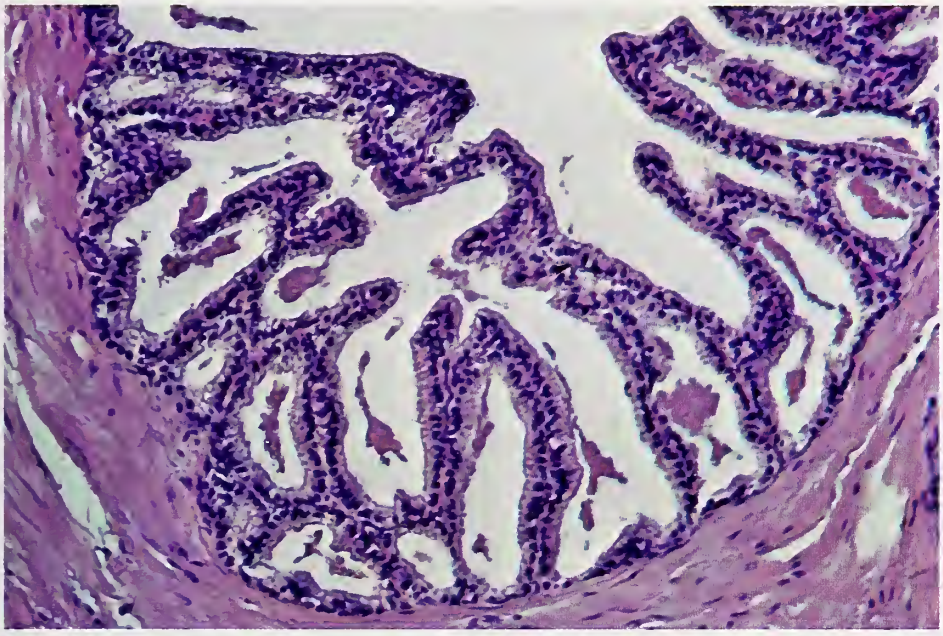

Figure 5-69: Histology of prostate gland. Note distinct papillary projections lined by simple columnar epithelium. (H & E, X88).

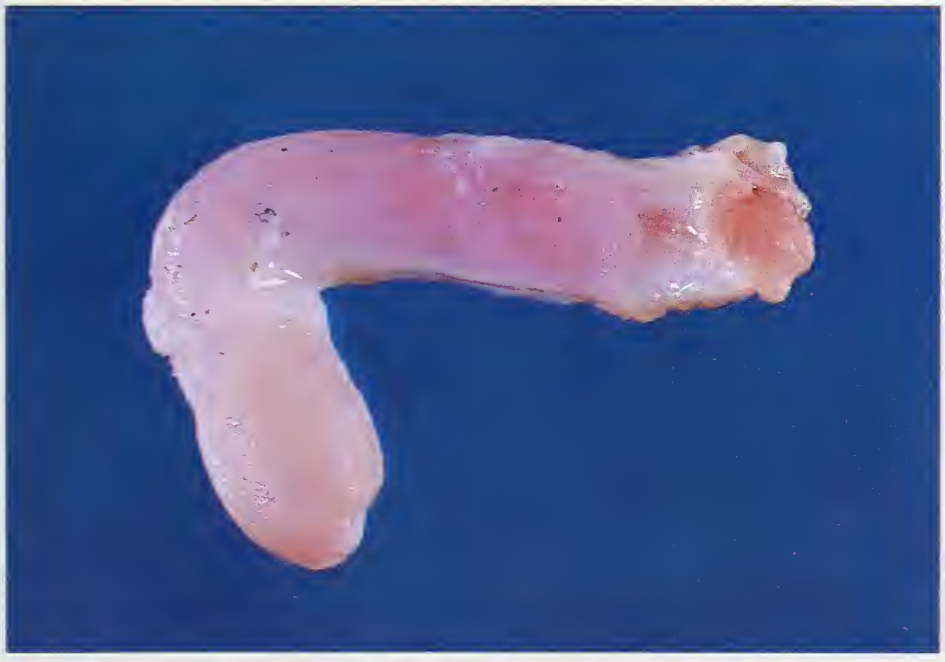

Figure 5-70: Penis of adult male. Note rectangular bend of cranial part, found when organ lies flaccid within prepuce.

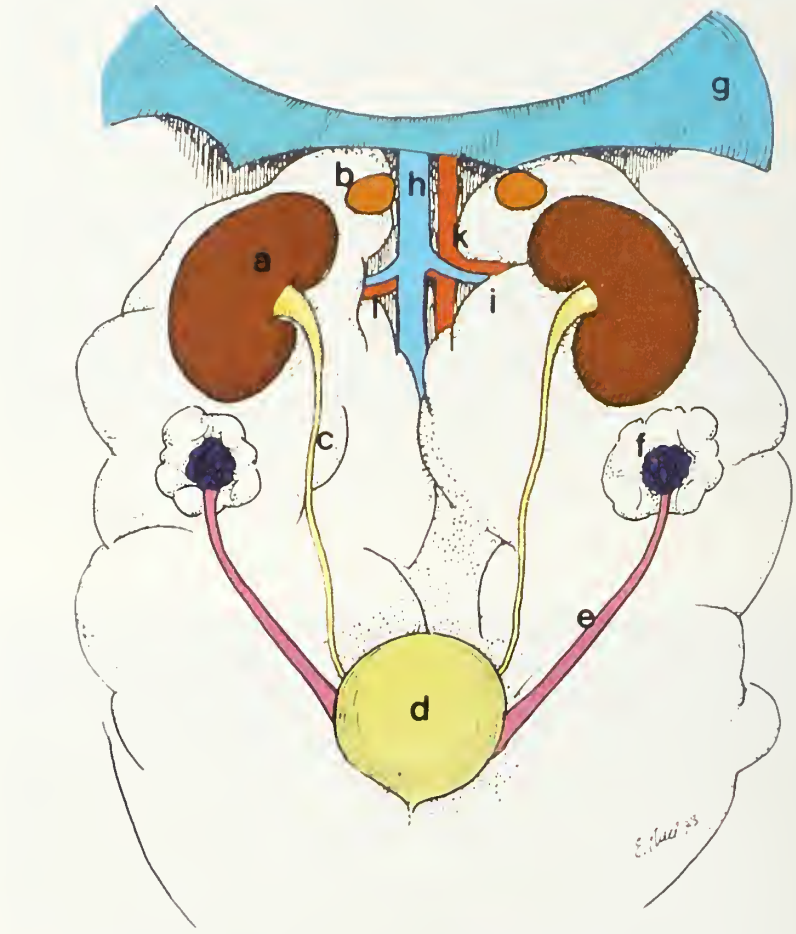

Figure 5-71: Schematic drawing of female urogenital organs.

Figure 5-72: Ventral aspect of abdomen showing female genitalia *in situ*; abdominal organs displaced. Note abundant fat deposits, which accumulate in autumn.

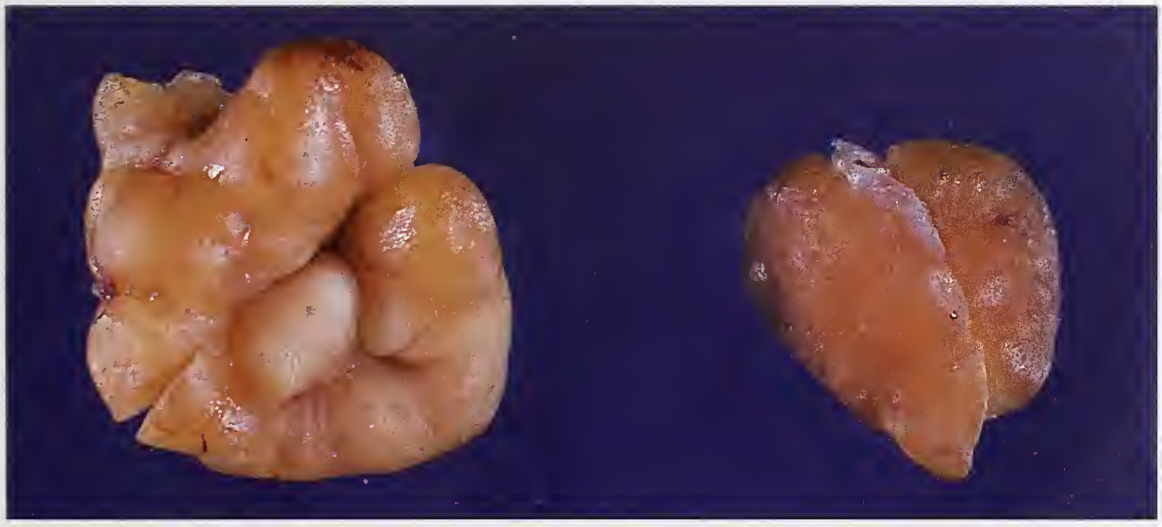

Figure 5-73: Isolated ovaries demonstrating variation in size that occurs during annual cycle. On left, organ of sexually active female sacrificed in May; on right, that of female killed during hibernation.

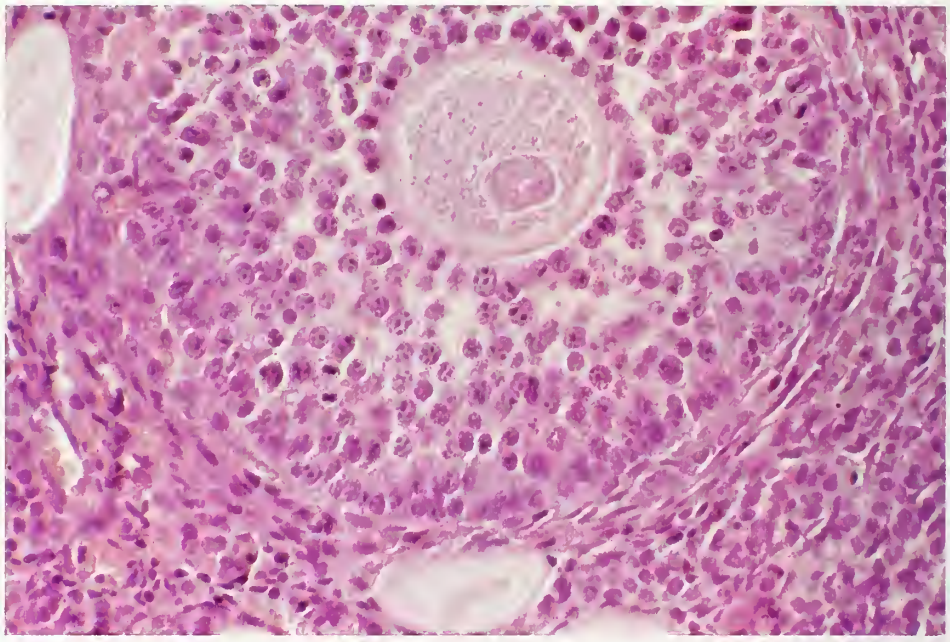

Figure 5-74: Histology of ovary taken from sexually active female in May, showing well-developed tertiary follicle. (H & E, X141).

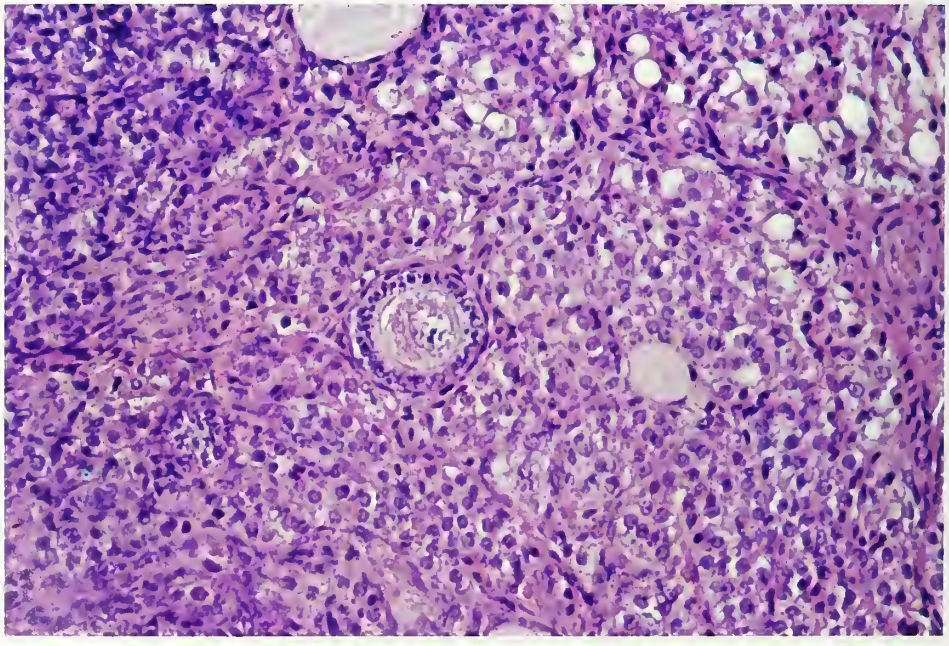

Figure 5-75: Histology of ovary from hibernating female. No mature follicles and only single small primary follicle are visible. (H & E, X141).

Figure 5-76: Isolated female reproductive organs with urinary bladder.

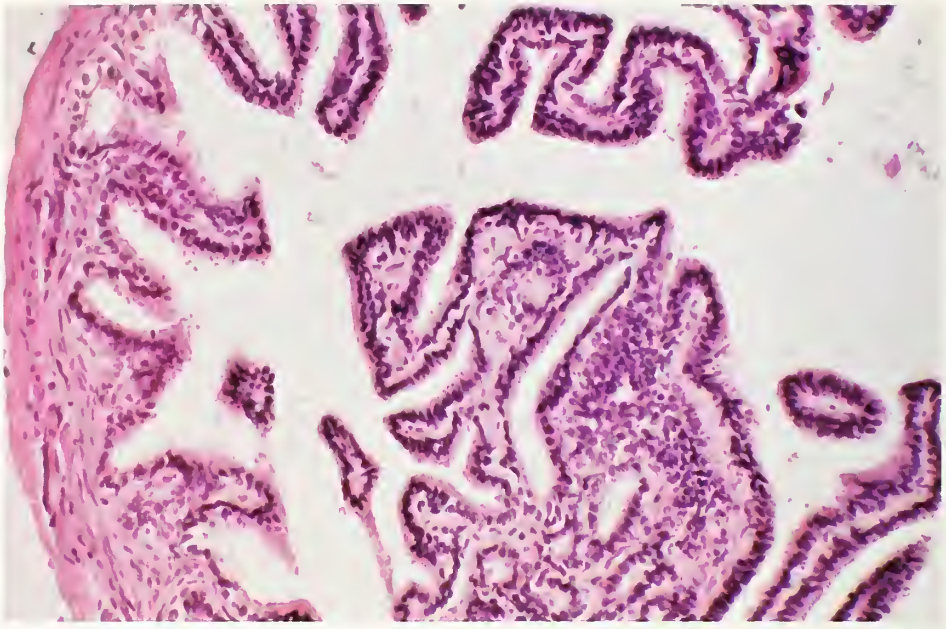

Figure 5-77: Histological view of oviduct; simple columnar epithelial lining forms papilliform folds. (H & E, X78).

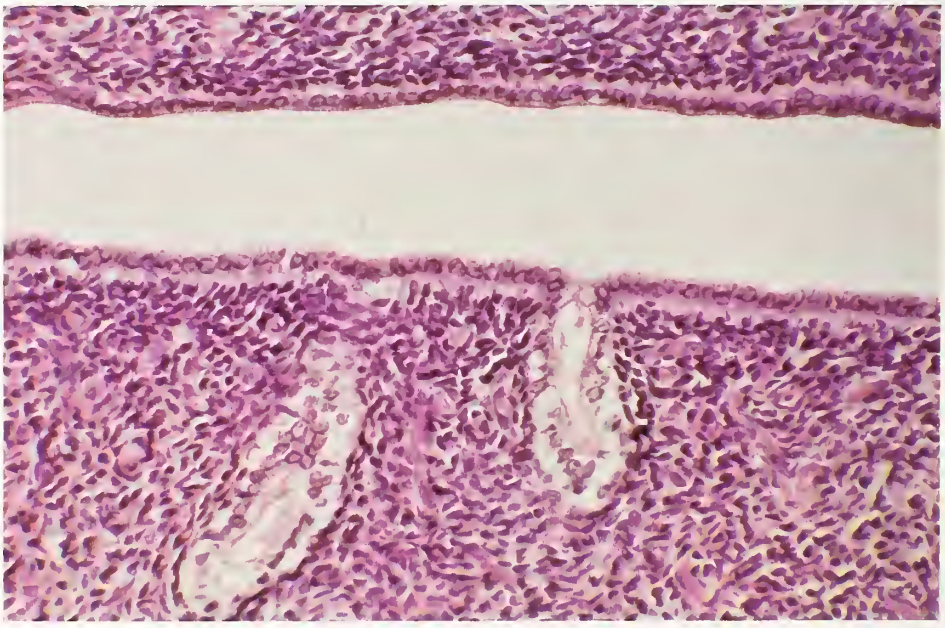

Figure 5-78: Histological aspect of uterus, with internal lining of simple cylindrical epithelium. Note two uterine glands in propria; one discharges through mucosa into uterine lumen. (H & E, X124).

TABLES

The following tables give salient statistics on the size and weight of various organs and glands of the European hamster, *Cricetus cricetus L.*

The data for Tables 9 through 22a were obtained bv examining the organs of five groups of European hamsters (five males and five females in each group) in a study of the influence of hibernation on the various endocrine (hypophysis or pituitary gland, thyroid glands, pancreatic islets, adrenal glands) and exocrine glands. The data for tables 1 through 8 were based on a sample of 10 males and 10 females.

Group January	(WH)	was killed without hibernation in January.
Group January	(H)	was killed during hibernation in January.
Group May	(WH)	was killed without hibernation in May.
Group May	(H)	was killed after awakening from hibernation in May.
Group October	(WH)	was killed before hibernation in October.

Data given for the weights and measures include the mean ($\bar{x}$) and standard deviation (s).

Table 1. Weight and size of organs

Cricetus cricetus L.		♂	♀
Body weight in g	$\bar{x}$	451.14	358.58
	s	49.00	63.42
Total length in mm	$\bar{x}$	241.06	236.48
	s	9.15	12.42
Length from neck to coccyx in mm	$\bar{x}$	190.00	184.30
	s	6.20	12.30
Length of cranium in mm	$\bar{x}$	51.06	52.14
	s	4.70	1.38
Length of trachea in *in situ* in mm	$\bar{x}$	33.69	33.34
	s	2.92	3.88
Length of isolated trachea in mm	$\bar{x}$	23.00	21.98
	s	4.30	2.70
Number of tracheal rings	$\bar{x}$	15.00	14.50
	s	0.99	0.99
Weight of trachea in mg	$\bar{x}$	86.30	67.80
	s	18.50	22.20
Weight of larynx in mg	$\bar{x}$	221.50	185.00
	s	36.00	36.00
Outer diameter of the first two tracheal rings in mm	$\bar{x}$	4.48	4.06
	s	0.27	0.30
Inner diameter of the first two tracheal rings in mm	$\bar{x}$	3.90	3.51
	s	0.41	0.36
Outer diameter of the 7th and 8th tracheal rings in mm	$\bar{x}$	3.90	3.56
	s	0.43	0.41
Inner diameter of the 7th and 8th tracheal rings in mm	$\bar{x}$	3.38	3.17
	s	0.46	0.40
Outer diameter of the last two tracheal rings in mm	$\bar{x}$	3.24	3.19
	s	0.36	0.40
Inner diameter of the last two tracheal rings in mm	$\bar{x}$	2.70	2.83
	s	0.31	0.37

Table 2. Weight and size of organs

Cricetus cricetus L.		♂	♀
Number of lobes of the lung			
Right lung		4	4
Left lung		1	1
Weight of lungs in g	$\bar{x}$	2.12	1.79
	s	0.66	0.37
Volume of lungs in ml	$\bar{x}$	2.63	2.01
	s	0.56	0.48
Weight of heart in g	$\bar{x}$	1.46	1.30
	s	0.25	0.26
Length of heart in mm	$\bar{x}$	19.31	18.04
	s	1.51	1.45
Breadth of heart in mm	$\bar{x}$	11.08	10.23
	s	1.53	0.90
Weight of liver in g	$\bar{x}$	15.25	15.34
	s	1.91	1.86
Number of lobes in liver	$\bar{x}$	5	5
	s	1	0
Weight of right kidney in mg	$\bar{x}$	926.70	922.50
	s	83.50	188.90
Weight of left kidney in mg	$\bar{x}$	930.00	910.60
	s	118.50	198.10
Length of right kidney in mm	$\bar{x}$	18.44	17.61
	s	0.84	0.10
Breadth of right kidney in mm	$\bar{x}$	8.02	7.52
	s	0.89	0.65
Height of right kidney in mm	$\bar{x}$	10.07	9.91
	s	1.05	0.72
Length of left kidney in mm	$\bar{x}$	17.89	17.18
	s	1.07	1.19
Breadth of left kidney in mm	$\bar{x}$	8.21	7.84
	s	0.83	0.94
Height of left kidney in mm	$\bar{x}$	10.65	10.17
	s	1.13	0.97

Table 3. Weight and size of organs

Cricetus cricetus L.		♂	♀
Weight of right adrenal gland in mg	$\bar{x}$	15.60	11.10
	s	4.20	5.50
Weight of left adrenal gland in mg	$\bar{x}$	16.90	21.60
	s	5.30	3.27
Length of right adrenal gland in mm	$\bar{x}$	4.13	3.64
	s	0.63	0.45
Breadth of right adrenal gland in mm	$\bar{x}$	2.15	1.82
	s	0.36	0.31
Height of right adrenal gland in mm	$\bar{x}$	2.75	2.42
	s	0.24	0.44
Length of left adrenal gland in mm	$\bar{x}$	4.34	3.92
	s	0.55	0.62
Breadth of left adrenal gland in mm	$\bar{x}$	2.23	1.87
	s	0.38	0.24
Height of left adrenal gland in mm	$\bar{x}$	2.69	2.39
	s	0.36	0.34
Weight of spleen in mg	$\bar{x}$	228.30	208.00
	s	51.60	63.80
Length of spleen in mm	$\bar{x}$	33.89	35.07
	s	4.31	3.98
Breadth of spleen in mm	$\bar{x}$	5.27	4.81
	s	0.94	1.27
Height of spleen in mm	$\bar{x}$	1.97	1.74
	s	0.54	0.52
Weight of filled stomach in g	$\bar{x}$	10.82	10.29
	s	2.70	2.85
Weight of empty stomach in g	$\bar{x}$	3.03	3.07
	s	0.45	0.65
Weight of filled intestine in g	$\bar{x}$	28.71	22.94
	s	3.96	3.99

Table 4. Weight and size of organs

Cricetus cricetus L.		♂	♀
Weight of right testis in mg	$\bar{x}$	2540.70	
	s	325.10	
Weight of left testis in mg	$\bar{x}$	2623.50	
	s	349.60	
Length of right testis in mm	$\bar{x}$	25.14	
	s	3.39	
Breadth of right testis in mm	$\bar{x}$	14.19	
	s	2.09	
Height of right testis in mm	$\bar{x}$	14.22	
	s	1.44	
Length of left testis in mm	$\bar{x}$	25.22	
	s	4.09	
Breadth of left testis in mm	$\bar{x}$	14.52	
	s	2.09	
Height of left testis in mm	$\bar{x}$	14.97	
	s	1.51	
Weight of vesicular glands in mg	$\bar{x}$	267.20	
	s	24.00	
Weight of empty urinary bladder in mg	$\bar{x}$	228.10	180.70
	s	67.80	100.90
Weight of right ovary in mg	$\bar{x}$		26.30
	s		18.60
Weight of left ovary in mg	$\bar{x}$		25.90
	s		22.40
Diameter of right ovary in mm	$\bar{x}$		4.58
	s		1.16
Diameter of left ovary in mm	$\bar{x}$		4.47
	s		0.99
Length of right uterus in mm	$\bar{x}$		58.56
	s		8.98
Length of left uterus in mm	$\bar{x}$		59.52
	s		7.63

Table 5. Proportional weight and size of organs (in %)

Cricetus cricetus L.		♂	♀
Length of cranium	$\bar{x}$	21.16	22.11
	s	1.48	1.21
Length of trachea *in situ*	$\bar{x}$	14.00	14.09
	s	1.47	1.42
Weight of trachea	$\bar{x}$	0.02	0.02
	s	0.005	0.006
Weight of larynx	$\bar{x}$	0.05	0.05
	s	0.009	0.005
Weight of lungs	$\bar{x}$	0.47	0.51
	s	0.12	0.13
Weight of heart	$\bar{x}$	0.33	0.37
	s	0.05	0.09
Weight of liver	$\bar{x}$	3.41	4.44
	s	0.52	1.59
Weight of right kidney	$\bar{x}$	0.21	0.26
	s	0.02	0.06
Weight of left kidney	$\bar{x}$	0.20	0.26
	s	0.03	0.07
Length of right kidney	$\bar{x}$	7.65	7.25
	s	0.31	0.42
Length of left kidney	$\bar{x}$	7.43	7.47
	s	0.46	0.38
Weight of right adrenal gland	$\bar{x}$	0.004	0.003
	s	0.001	0.002
Weight of left adrenal gland	$\bar{x}$	0.004	0.003
	s	0.001	0.002
Length of right adrenal gland	$\bar{x}$	1.72	1.54
	s	0.26	0.19
Length of left adrenal gland	$\bar{x}$	1.81	1.66
	s	0.23	0.27

Table 6. Proportional weight and size of organs (in %)

Cricetus cricetus L.		♂	♀
Weight of spleen	$\bar{x}$	0.05	0.06
	s	0.01	0.01
Length of spleen	$\bar{x}$	14.07	14.88
	s	1.81	1.92
Weight of filled stomach	$\bar{x}$	2.40	2.96
	s	0.60	1.05
Weight of empty stomach	$\bar{x}$	0.68	0.88
	s	0.12	0.23
Weight of filled intestine	$\bar{x}$	6.27	6.50
	s	1.07	1.30
Weight of right testis	$\bar{x}$	0.57	
	s	0.09	
Weight of left testis	$\bar{x}$	0.58	
	s	0.07	
Length of right testis	$\bar{x}$	6.89	
	s	1.42	
Length of left testis	$\bar{x}$	6.82	
	s	1.17	
Weight of vesicular gland	$\bar{x}$	0.06	
	s	0.002	
Weight of urinary bladder	$\bar{x}$	0.05	0.05
	s	0.01	0.03
Weight of right ovary	$\bar{x}$		0.007
	s		0.004
Weight of left ovary	$\bar{x}$		0.007
	s		0.006
Diameter of right ovary	$\bar{x}$		1.95
	s		0.51
Diameter of left ovary	$\bar{x}$		1.90
	s		0.45
Length of right uterus	$\bar{x}$		24.67
	s		2.79
Length of left uterus	$\bar{x}$		25.13
	s		2.53

Table 7. Absolute and relative weights of male gonads in hibernating and non hibernating animals

Group		A (H)	B (H)	C (WH)	D (WH)	E (WH)	F (H)	G (WH)
Death		February	May	February	May	October	December	December
Body weight in g	$\bar{x}$	245.06	507.24	259.00	453.68	416.92	261.32	305.30
	s	38.57	46.48	15.57	73.85	69.81	67.86	37.80
Absolute weight of right testis in g	$\bar{x}$	0.55	2.61	1.78	2.54	0.59	0.54	0.56
	s	0.12	0.39	0.48	0.32	0.11	0.08	0.30
Absolute weight of left testis in g	$\bar{x}$	0.55	2.61	1.76	2.62	0.59	0.52	0.57
	s	0.10	0.32	0.46	0.35	0.08	0.07	0.34
Relative weight of right testis in %	$\bar{x}$	0.22	0.51	0.69	0.57	0.14	0.22	0.19
	s	0.03	0.06	0.19	0.09	0.04	0.05	0.10
Relative weight of left testis in %	$\bar{x}$	0.23	0.52	0.68	0.58	0.15	0.21	0.19
	s	0.03	0.06	0.18	0.07	0.04	0.05	0.10

H = With Hibernation
WH = Without Hibernation

Table 8. Absolute and relative weights of female gonads in hibernating and nonhibernating animals

Group		A (H)	B (H)	C (WH)	D (WH)	E (WH)	F (H)	G (WH)
Death		February	May	February	May	October	December	December
Body weight in g	$\bar{x}$	174.130	165.240	295.000	356.230	336.640	278.820	310.000
	s	30.490	17.810	60.560	32.170	31.270	49.610	62.290
Absolute weight of right ovary in g	$\bar{x}$	0.032	0.025	0.139	0.154	0.019	0.029	0.066
	s	0.015	0.004	0.051	0.011	0.002	0.015	0.051
Absolute weight of left ovary in g	$\bar{x}$	0.031	0.026	0.108	0.162	0.168	0.030	0.063
	s	0.011	0.006	0.029	0.009	0.005	0.006	0.035
Relative weight of right ovary in %	$\bar{x}$	0.018	0.017	0.048	0.220	0.006	0.011	0.212
	s	0.006	0.006	0.021	0.065	0.001	0.056	0.191
Relative weight of left ovary in %	$\bar{x}$	0.018	0.016	0.038	0.218	0.005	0.007	0.209
	s	0.004	0.005	0.014	0.042	0.002	0.004	0.164

H = With Hibernation
WH = Without Hibernation

Table 9. Weight and size of hypophysis (N = 5♂, 5♀)

Time of death		Length in mm		Breadth in mm		Depth in mm		Weight in mg		Weight in %	
		♂	♀	♂	♀	♂	♀	♂	♀	♂	♀
January (WH)	$\bar{x}$	3.28	3.20	2.94	2.66	1.06	1.10	6.69	6.33	0.002	0.002
	s	0.26	0.36	0.09	0.25	0.27	0.22	0.69	0.79	0.000	0.000
January (H)	$\bar{x}$	3.24	3.38	2.86	2.68	1.38	1.10	8.45	5.88	0.002	0.003
	s	0.19	0.21	0.18	0.41	0.16	0.12	1.73	1.34	0.001	0.000
May (WH)	$\bar{x}$	3.24	3.40	2.70	2.92	1.02	1.32	8.60	7.60	0.001	0.002
	s	0.32	0.19	0.19	0.39	0.25	0.08	1.00	1.05	0.000	0.000
May (H)	$\bar{x}$	4.34	4.32	2.76	2.32	1.20	1.04	8.66	7.78	0.002	0.003
	s	0.47	0.40	0.44	0.47	0.16	0.39	1.09	1.10	0.000	0.000
October (WH)	$\bar{x}$	3.76	2.96	2.26	2.04	1.16	1.10	7.54	5.71	0.002	0.002
	s	0.57	0.47	0.21	0.23	0.23	0.28	1.44	0.94	0.000	0.000

Table 10. Weight and size of right thyroid gland (N = 5♂, 5♀)

Time of death		Length in mm		Breadth in mm		Depth in mm		Weight in mg		Weight in %	
		♂	♀	♂	♀	♂	♀	♂	♀	♂	♀
January (WH)	$\bar{x}$	6.26	7.06	2.90	2.72	1.54	1.70	20	20	0.005	0.005
	s	0.91	1.47	0.31	0.16	0.23	0.25	4	3	0.001	0.001
January (H)	$\bar{x}$	6.02	5.42	3.10	2.52	1.90	1.56	22	14	0.006	0.007
	s	0.94	0.59	0.58	0.30	0.46	0.26	9	3	0.002	0.001
May (WH)	$\bar{x}$	7.10	6.76	3.33	3.22	1.68	1.50	26	30	0.006	0.008
	s	1.00	1.48	0.59	0.70	0.05	0.34	6	11	0.001	0.003
May (H)	$\bar{x}$	6.30	5.80	3.42	2.92	1.98	1.68	30	19	0.007	0.008
	s	1.34	0.45	0.25	0.63	0.31	0.08	10	5	0.003	0.002
October (WH)	$\bar{x}$	5.50	4.54	2.64	2.20	1.30	1.44	13	11	0.004	0.004
	s	0.53	0.94	0.21	0.32	0.29	0.24	2	4	0.001	0.001

Table 10a. Weight and size of left thyroid gland (N = 5♂, 5♀)

Time of death		Length in mm		Breadth in mm		Depth in mm		Weight in mg		Weight in %	
		♂	♀	♂	♀	♂	♀	♂	♀	♂	♀
January (WH)	$\bar{x}$	5.78	6.46	2.96	2.64	1.70	1.70	19	18	0.005	0.005
	s	0.28	0.85	0.20	0.35	0.36	0.44	4	2	0.001	0.001
January (H)	$\bar{x}$	5.62	5.36	2.88	2.52	1.86	1.44	22	15	0.006	0.007
	s	0.62	0.54	0.49	0.30	0.25	0.18	7	5	0.002	0.002
May (WH)	$\bar{x}$	6.50	6.00	2.96	2.76	1.66	1.66	25	23	0.005	0.006
	s	0.40	0.73	0.39	0.33	0.50	0.39	8	5	0.001	0.001
May (H)	$\bar{x}$	6.86	5.36	3.02	2.80	1.90	1.82	30	21	0.006	0.009
	s	0.74	1.33	0.61	0.49	0.22	0.13	10	8	0.003	0.003
October	$\bar{x}$	5.08	4.44	2.30	2.08	1.44	1.54	13	9	0.004	0.004
	s	0.43	0.77	0.47	0.30	0.27	0.34	3	4	0.001	0.001

Table 11. Weight of pancreas (N = 5♂, 5♀)

Time of death		Weight in mg		Weight in %	
		♂	♀	♂	♀
January (WH)	$\bar{x}$	723	700	0.181	0.193
	s	85	74	0.029	0.025
January (H)	$\bar{x}$	867	626	0.237	0.292
	s	268	38	0.067	0.037
May (WH)	$\bar{x}$	854	915	0.190	0.257
	s	164	144	0.030	0.049
May (H)	$\bar{x}$	1045	914	0.253	0.383
	s	92	135	0.044	0.024
October (WH)	$\bar{x}$	786	574	0.237	0.242
	s	159	75	0.043	0.040

Table 11a. Size of pancreas (cranial portion) (N = 5♂, 5♀)

Time of death		Length in mm		Breadth in mm	
		♂	♀	♂	♀
January (WH)	$\bar{x}$	56.94	48.74	5.30	5.90
	s	10.25	6.20	1.75	1.12
January (H)	$\bar{x}$	62.00	49.12	6.94	4.44
	s	12.22	3.03	2.05	1.18
May (WH)	$\bar{x}$	53.40	58.18	5.52	5.20
	s	6.92	11.51	1.55	1.44
May (H)	$\bar{x}$	57.60	61.42	5.58	5.38
	s	14.95	10.09	1.15	1.39
October (WH)	$\bar{x}$	55.18	41.80	4.48	4.32
	s	19.30	7.21	1.13	1.97

Table 11b. Size of pancreas (right portion) (N = 5♂, 5♀)

Time of death		Length in mm		Breadth in mm	
		♂	♀	♂	♀
January (WH)	$\bar{x}$	37.64	37.92	4.48	4.94
	s	8.29	1.53	0.71	0.99
January (H)	$\bar{x}$	32.50	36.32	5.00	5.16
	s	8.91	8.39	0.57	1.39
May (WH)	$\bar{x}$	38.28	42.92	5.18	5.02
	s	5.76	6.33	0.55	0.94
May (H)	$\bar{x}$	60.26	44.26	5.95	4.04
	s	10.26	12.10	1.70	1.01
October (WH)	$\bar{x}$	48.76	51.32	4.88	4.64
	s	20.16	15.83	2.48	1.18

Table 11c. Size of pancreas (body) (N = 5♂, 5♀)

Time of death		Length in mm		Breadth in mm	
		♂	♀	♂	♀
January (WH)	$\bar{x}$	7.56	7.20	3.40	5.68
	s	2.07	1.87	0.89	1.67
January (H)	$\bar{x}$	6.96	5.10	5.16	5.32
	s	0.25	0.38	0.18	1.47
May (WH)	$\bar{x}$	9.90	8.54	5.90	6.18
	s	1.86	2.75	1.06	1.46
May (H)	$\bar{x}$	23.38	18.24	7.22	5.20
	s	5.99	9.54	1.57	0.90
October (WH)	$\bar{x}$	14.70	10.78	5.62	2.72
	s	3.21	2.22	2.12	0.54

Table 12. Weight and size of right adrenal gland (N = 5♂, 5♀)

Time of death		Length in mm		Breadth in mm		Depth in mm		Weight in mm		Weight in %	
		♂	♀	♂	♀	♂	♀	♂	♀	♂	♀
January (WH)	$\bar{x}$	4.42	3.96	3.04	2.84	1.96	1.98	16	16	0.004	0.005
	s	0.45	0.27	0.22	0.24	0.11	0.13	1	2	0.000	0.001
January (H)	$\bar{x}$	4.30	3.80	3.08	2.54	2.18	1.66	19	11	0.005	0.005
	s	0.63	0.20	0.34	0.39	0.25	0.13	6	2	0.002	0.000
May (WH)	$\bar{x}$	4.38	3.75	2.72	2.60	2.08	1.88	19	14	0.004	0.004
	s	0.11	0.49	0.29	0.44	0.27	0.35	2	3	0.001	0.001
May (H)	$\bar{x}$	3.98	3.44	3.00	2.52	2.12	1.76	20	11	0.004	0.005
	s	0.27	0.47	0.21	0.41	0.15	0.23	1	2	0.001	0.001
October (WH)	$\bar{x}$	3.88	3.48	2.94	2.44	1.98	1.72	13	11	0.004	0.005
	s	0.27	0.31	0.15	0.40	0.27	0.28	2	2	0.000	0.001

Table 12a. Weight and size of left adrenal gland (N = 5♂, 5♀)

Time of death		Length in mm		Breadth in mm		Depth in mm		Weight in mg		Weight in %	
		♂	♀	♂	♀	♂	♀	♂	♀	♂	♀
January (WH)	$\bar{x}$	4.76	4.00	2.86	2.74	2.22	2.36	20	18	0.005	0.005
	s	0.36	0.38	0.24	0.42	0.15	0.37	2	1	0.001	0.000
January (H)	$\bar{x}$	4.42	3.82	2.84	2.52	2.28	1.90	20	13	0.005	0.006
	s	0.55	0.43	0.32	0.24	0.45	0.22	7	3	0.002	0.001
May (WH)	$\bar{x}$	4.44	4.08	2.84	2.68	2.44	1.88	22	18	0.005	0.005
	s	0.34	0.13	0.23	0.28	0.15	0.30	4	4	0.001	0.001
May (H)	$\bar{x}$	4.34	3.82	3.06	2.68	2.26	1.42	21	13	0.005	0.005
	s	0.64	0.24	0.23	0.23	0.18	0.28	2	1	0.001	0.000
October (WH)	$\bar{x}$	4.14	3.56	2.86	2.80	2.20	1.84	15	13	0.004	0.006
	s	0.61	0.54	0.31	0.00	0.19	0.24	4	2	0.001	0.001

Table 12b. Size of right adrenal medulla (N = 5♂, 5♀)

Time of death		Length in mm		Breadth in mm	
		♂	♀	♂	♀
January (WH)	$\bar{x}$	3.18	2.86	1.60	1.68
	s	0.28	0.21	0.20	0.24
January (H)	$\bar{x}$	3.16	2.72	1.76	1.56
	s	0.84	0.31	0.65	0.19
May (WH)	$\bar{x}$	2.94	2.90	1.70	1.80
	s	0.41	0.22	0.07	0.29
May (H)	$\bar{x}$	2.82	2.48	1.36	1.04
	s	0.44	0.30	0.52	0.30
October (WH)	$\bar{x}$	2.74	2.46	1.40	1.16
	s	0.15	0.25	0.22	0.06

Table 12c. Size of right adrenal cortex (N = 5♂, 5♀)

Time of death		Length in mm	
		♂	♀
January (WH)	$\bar{x}$	0.76	0.52
	s	0.20	0.08
January (H)	$\bar{x}$	0.62	0.50
	s	0.05	0.19
May (WH)	$\bar{x}$	0.76	0.65
	s	0.18	0.17
May (H)	$\bar{x}$	0.76	0.50
	s	0.15	0.21
October (WH)	$\bar{x}$	0.70	0.64
	s	0.16	0.09

Table 12d. Size of left adrenal medulla (N = 5♂, 5♀)

Time of death		Length in mm		Breadth in mm	
		♂	♀	♂	♀
January (WH)	$\bar{x}$	2.82	3.04	1.78	1.62
	s	0.39	0.32	0.08	0.19
January (H)	$\bar{x}$	3.38	2.64	1.86	1.52
	s	0.33	0.43	0.38	0.19
May (WH)	$\bar{x}$	3.12	3.04	1.62	1.64
	s	0.59	0.41	0.26	0.31
May (H)	$\bar{x}$	2.75	2.74	1.65	1.32
	s	0.25	0.18	0.26	0.34
October (WH)	$\bar{x}$	2.86	2.64	1.46	1.32
	s	0.46	0.75	0.15	0.30

Table 12e. Size of left adrenal cortex (N = 5♂, 5♀)

Time of death		Length in mm	
		♂	♀
January (WH)	$\bar{x}$	0.70	0.62
	s	0.12	0.11
January (H)	$\bar{x}$	0.70	0.62
	s	0.10	0.14
May (WH)	$\bar{x}$	0.70	0.56
	s	0.24	0.09
May (H)	$\bar{x}$	0.70	0.56
	s	0.10	0.02
October (WH)	$\bar{x}$	0.74	0.72
	s	0.25	0.13

Table 13. Weight and size of right testis (N = 5♂)

Time of death		Length in mm	Breadth in mm	Depth in mm	Weight in mg	Weight in %
January (WH)	$\bar{x}$	12.68	6.96	6.62	354	0.088
	s	1.12	0.88	0.71	79	0.020
January (H)	$\bar{x}$	13.46	8.22	6.82	468	0.129
	s	0.98	0.99	0.96	88	0.029
May (WH)	$\bar{x}$	21.84	13.64	11.28	2109	0.468
	s	1.11	0.58	0.39	298	0.041
May (H)	$\bar{x}$	23.16	14.88	13.68	2430	0.584
	s	1.18	1.18	0.69	136	0.061
October (WH)	$\bar{x}$	9.20	5.68	4.96	145	0.044
	s	0.27	0.37	0.15	14	0.009

Table 13a. Weight and size of left testis (N = 5♂)

Time of death		Length in mm	Breadth in mm	Depth in mm	Weight in mg	Weight in %
January (WH)	$\bar{x}$	12.10	7.00	6.40	324	0.081
	s	0.91	0.71	0.58	58	0.018
January (H)	$\bar{x}$	13.32	8.06	6.38	462	0.128
	s	0.78	1.26	0.99	74	0.035
May (WH)	$\bar{x}$	21.86	13.12	11.82	2024	0.451
	s	0.79	0.92	0.49	223	0.047
May (H)	$\bar{x}$	23.54	14.98	13.38	2512	0.607
	s	0.35	0.99	1.99	199	0.109
October (WH)	$\bar{x}$	9.06	5.60	4.86	141	0.043
	s	0.22	0.40	0.52	17	0.009

Table 14. Weight and size of head of right epididymis (N = 5♂)

Time of death		Length in mm	Breadth in mm	Depth in mm	Weight in mg	Weight in %
January (WH)	$\bar{x}$	5.82	2.70	3.50	36[1]	0.009
	s	2.05	0.24	0.20	12	0.003
January (H)	$\bar{x}$	6.94	2.96	1.96	51	0.013
	s	2.67	0.84	0.46	28	0.006
May (WH)	$\bar{x}$	14.32	6.00	5.04	436	0.096
	s	2.58	0.57	0.93	85	0.013
May (H)	$\bar{x}$	14.92	6.54	5.76	470	0.112
	s	1.80	0.83	0.82	60	0.009
October (WH)	$\bar{x}$	3.92	2.12	2.80	27	0.008
	s	1.07	0.40	0.20	7	0.002

[1] These weights are for the total epididymis

Table 14a. Weight and size of head of left epididymis (N = 5♂)

Time of death		Length in mm	Breadth in mm	Depth in mm	Weight in mg	Weight in %
January (WH)	$\bar{x}$	5.33	2.88	3.20	38[1]	0.009
	s	1.87	1.02	0.20	15	0.004
January (H)	$\bar{x}$	7.88	3.08	2.23	64	0.016
	s	3.13	0.56	0.38	42	0.010
May (WH)	$\bar{x}$	15.36	6.10	4.76	449	0.100
	s	2.41	0.37	0.43	74	0.019
May (H)	$\bar{x}$	13.98	6.80	5.76	450	0.100
	s	2.37	0.91	0.52	50	0.019
October (WH)	$\bar{x}$	4.28	2.38	2.80	31	0.010
	s	0.81	0.55	0.30	5	0.002

[1] These weights are for the total epididymis

Table 14b. Size of tail of right epididymis (N = 5♂)

Time of death		Length in mm	Breadth in mm	Depth in mm
January (WH)	$\bar{x}$	5.50	2.13	1.40
	s	1.41	0.50	0.20
January (H)	$\bar{x}$	6.20	1.70	1.35
	s	1.58	0.47	0.29
May (WH)	x	13.00	4.92	3.78
	s	1.57	0.55	0.45
May (H)	$\bar{x}$	13.50	4.58	4.72
	s	1.55	0.88	0.35
October (WH)	$\bar{x}$	3.60	2.02	1.20
	s	0.72	0.59	0.15

Table 14c. Size of tail of left epididymis (N = 5♂)

Time of death		Length in mm	Breadth in mm	Depth in mm
January (WH)	$\bar{x}$	5.75	2.75	1.60
	s	1.50	0.52	0.30
January (H)	$\bar{x}$	6.78	2.40	1.62
	s	2.54	0.73	0.38
May (WH)	$\bar{x}$	14.32	4.66	3.42
	s	2.34	0.51	0.30
May (H)	$\bar{x}$	12.64	5.18	4.04
	s	1.58	0.76	0.54
October (WH)	$\bar{x}$	4.52	2.64	1.30
	s	1.11	0.43	0.20

Table 15. Weight and size of prostate gland (N = 5♂)

Time of death		Length in mm	Breadth in mm	Depth in mm	Weight in mg	Weight in %
January (WH)	$\bar{x}$	10.24	9.48	2.52	168	0.042
	s	1.83	1.26	0.25	28	0.006
January (H)	$\bar{x}$	14.32	8.80	6.30	692	0.177
	s	3.74	2.09	2.89	57	0.130
May (WH)	$\bar{x}$	15.60	9.86	9.44	1181	0.244
	s	4.33	2.82	2.13	250	0.112
May (H)	$\bar{x}$	15.58	10.50	6.80	1053	0.246
	s	2.81	1.79	1.28	487	0.090
October (WH)	$\bar{x}$	6.06	3.30	2.70	39	0.012
	s	0.86	0.26	0.25	14	0.004

Table 16. Weight and size of right vesicular gland (N = 5♂)

Time of death		Length in mm	Breadth in mm	Depth in mm	Weight in mg	Weight in %
January (WH)	$\bar{x}$	5.78	2.50	1.03	11	0.003
	s	1.67	0.85	0.17	6	0.002
January (H)	$\bar{x}$	11.72	2.76	1.20	39	0.010
	s	6.41	0.82	0.46	27	0.007
May (WH)	$\bar{x}$	21.90	8.60	3.42	455	0.099
	s	0.63	1.87	0.94	172	0.029
May (H)	$\bar{x}$	23.70	10.04	5.12	620	0.148
	s	4.01	2.19	0.63	320	0.066
October (WH)	$\bar{x}$	8.82	5.72	3.18	115	0.034
	s	1.22	1.07	0.13	38	0.008

Table 16a. Weight and size of left vesicular gland (N = 5♂)

Time of death		Length in mm	Breadth in mm	Depth in mm	Weight in mg	Weight in %
January (WH)	$\bar{x}$	5.80	2.80	1.15	14	0.003
	s	0.74	1.03	0.21	10	0.003
January (H)	$\bar{x}$	11.92	2.84	1.32	39	0.010
	s	6.34	0.87	0.78	31	0.008
May (WH)	$\bar{x}$	21.62	7.62	3.44	441	0.097
	s	4.54	1.73	0.59	40	0.034
May (H)	$\bar{x}$	24.78	9.36	5.06	670	0.159
	s	3.74	1.67	0.98	270	0.052
October (WH)	$\bar{x}$	9.04	6.12	2.94	102	0.030
	s	1.17	1.34	0.37	32	0.008

Table 17. Weight and size of bulbourethral gland (N = 5♂)

Time of death		Length in mm	Breadth in mm	Depth in mm	Weight in mg	Weight in %
January (WH)	$\bar{x}$	2.83	1.97	0.90	4	0.001
	s	0.38	0.71	0.40	3	0.001
January (H)	$\bar{x}$	5.16	2.94	1.78	31	0.007
	s	3.97	1.03	0.51	34	0.008
May (WH)	$\bar{x}$	11.18	9.10	3.66	365	0.079
	s	3.33	0.95	1.13	137	0.016
May (H)	$\bar{x}$	19.38	12.16	4.22	630	0.148
	s	5.90	3.29	0.91	150	0.024
October (WH)	$\bar{x}$	6.10	2.12	1.36	10	0.003
	s	2.04	0.49	0.56	5	0.001

Table 18. Weight and size of right ovary (N = 5♀)

Time of death		Length in mm	Breadth in mm	Depth in mm	Weight in mg	Weight in %
January (WH)	$\bar{x}$	5.00	2.82	1.64	17	0.005
	s	0.44	0.42	0.61	3	0.001
January (H)	$\bar{x}$	4.38	2.44	1.54	14	0.006
	s	0.89	0.26	0.15	5	0.001
May (WH)	$\bar{x}$	6.88	4.12	2.84	66	0.018
	s	1.16	0.61	0.78	33	0.007
May (H)	$\bar{x}$	6.66	4.44	2.78	52	0.022
	s	0.61	0.25	0.46	13	0.005
October (WH)	$\bar{x}$	3.70	2.54	1.74	9	0.004
	s	0.45	0.66	0.25	4	0.001

Table 18a. Weight and size of left ovary (N = 5♀)

Time of death		Length in mm	Breadth in mm	Depth in mm	Weight in mg	Weight in %
January (WH)	$\bar{x}$	4.82	2.76	1.66	16	0.004
	s	0.49	0.42	0.35	2	0.000
January (H)	$\bar{x}$	4.30	2.60	1.78	14	0.006
	s	0.71	0.20	0.26	4	0.001
May (WH)	$\bar{x}$	7.32	4.00	2.76	65	0.017
	s	1.23	0.81	0.84	27	0.005
May (H)	$\bar{x}$	6.18	3.96	2.48	43	0.018
	s	0.61	0.80	0.29	13	0.005
October (WH)	$\bar{x}$	3.50	2.38	1.56	9	0.004
	s	1.01	0.41	0.37	3	0.001

Table 19. Weight and size of right parotid gland (N = 5♂; 5♀)

Time of death		Length in mm		Breadth in mm		Depth in mm		Weight in mg		Weight in %	
		♂	♀	♂	♀	♂	♀	♂	♀	♂	♀
January (WH)	$\bar{x}$	38.00	32.02	4.98	5.18	2.38	1.88	210	201	0.052	0.055
	s	3.70	1.95	1.12	1.42	0.21	0.16	50	34	0.011	0.007
January (WH)	$\bar{x}$	36.50	32.58	4.30	4.06	1.86	1.84	216	171	0.059	0.079
	s	2.35	2.40	0.50	0.72	0.48	0.27	61	34	0.018	0.007
May (WH)	$\bar{x}$	39.98	35.30	4.86	4.52	2.42	1.46	262	224	0.058	0.062
	s	5.93	4.23	0.80	0.26	0.58	0.23	34	33	0.005	0.007
May (H)	$\bar{x}$	35.18	27.08	5.02	4.30	2.96	2.04	203	154	0.048	0.065
	s	3.15	4.99	1.03	0.87	0.32	0.56	26	12	0.003	0.009
October (WH)	$\bar{x}$	32.40	36.60	5.76	3.96	2.22	1.54	219	171	0.066	0.069
	s	5.79	7.65	0.95	0.91	0.28	0.52	29	55	0.001	0.006

Table 19a. Weight and size of left parotid gland (N = 5♂, 5♀)

Time of death		Length in mm		Breadth in mm		Depth in mm		Weight in mg		Weight in %	
		♂	♀	♂	♀	♂	♀	♂	♀	♂	♀
January (WH)	$\bar{x}$	34.24	30.14	5.00	5.54	1.96	2.00	216	199	0.054	0.055
	s	6.54	4.86	1.31	1.56	0.48	0.58	33	38	0.008	0.010
January (H)	$\bar{x}$	36.48	30.22	4.08	4.66	2.30	1.72	217	181	0.060	0.083
	s	3.88	5.10	0.92	0.44	0.21	0.23	31	28	0.014	0.007
May (WH)	$\bar{x}$	37.32	34.30	5.60	4.54	2.46	1.46	243	214	0.053	0.061
	s	8.41	4.43	0.91	0.67	0.80	0.34	101	33	0.016	0.016
May (H)	$\bar{x}$	33.36	30.62	4.62	4.38	2.32	1.90	216	163	0.052	0.069
	s	7.79	7.75	0.84	0.65	0.41	0.77	25	12	0.007	0.002
October (WH)	$\bar{x}$	35.08	35.38	5.40	3.68	2.42	1.56	230	163	0.069	0.068
	s	6.12	2.33	1.32	0.56	0.61	0.47	27	28	0.005	0.008

Table 20. Weight and size of right mandibular gland (N = 5♂, 5♀)

Time of death		Length in mm		Breadth in mm		Depth in mm		Weight in mg		Weight in %	
		♂	♀	♂	♀	♂	♀	♂	♀	♂	♀
January (WH)	$\bar{x}$	14.82	14.74	9.36	10.00	3.68	3.88	319	332	0.079	0.092
	s	1.05	2.03	2.30	1.04	0.55	0.90	38	50	0.003	0.015
January (H)	$\bar{x}$	15.92	15.08	9.24	8.24	3.20	2.88	315	227	0.085	0.104
	s	1.75	1.78	0.95	1.72	0.47	0.73	67	44	0.007	0.016
May (WH)	$\bar{x}$	17.26	14.44	9.30	8.80	3.94	3.44	378	343	0.085	0.097
	s	3.09	2.22	1.38	1.09	0.43	0.56	33	35	0.011	0.023
May (H)	$\bar{x}$	14.08	16.08	9.36	9.90	5.08	4.18	370	359	0.089	0.152
	s	1.33	2.08	0.95	1.25	0.68	0.93	30	41	0.012	0.024
October (WH)	$\bar{x}$	15.56	14.50	9.70	8.52	3.82	3.82	298	241	0.090	0.100
	s	2.38	2.23	0.60	1.07	0.62	0.81	34	42	0.011	0.011

Table 20a. Weight and size of left mandibular gland (N = 5♂, 5♀)

Time of death		Length in mm		Breadth in mm		Depth in mm		Weight in mg		Weight in %	
		♂	♀	♂	♀	♂	♀	♂	♀	♂	♀
January (WH)	$\bar{x}$	14.38	13.30	10.26	9.26	3.02	3.32	317	310	0.079	0.086
	s	1.03	1.83	1.15	1.05	0.35	0.15	38	50	0.006	0.015
January (H)	$\bar{x}$	16.14	15.12	9.72	7.52	3.64	3.04	309	221	0.084	0.102
	s	3.07	2.29	2.24	0.98	0.56	0.50	55	41	0.009	0.015
May (WH)	$\bar{x}$	16.78	14.14	9.32	8.32	3.24	3.14	361	346	0.080	0.097
	s	3.23	1.37	2.26	1.85	0.67	1.18	70	46	0.010	0.018
May (H)	$\bar{x}$	16.28	15.44	9.38	9.90	3.92	4.88	380	364	0.091	0.154
	s	1.45	0.31	2.04	1.04	0.87	0.59	60	35	0.013	0.023
October (WH)	$\bar{x}$	15.90	14.46	8.74	7.88	3.86	3.20	293	230	0.088	0.095
	s	1.21	3.78	1.04	0.44	0.46	0.55	34	52	0.007	0.010

Table 21. Weight and size of right sublingual gland (N = 5♂, 5♀)

Time of death		Length in mm		Breadth in mm		Depth in mm		Weight in mg		Weight in %	
		♂	♀	♂	♀	♂	♀	♂	♀	♂	♀
January (WH)	$\bar{x}$	7.98	7.66	6.72	5.86	2.84	2.50	89	76	0.022	0.021
	s	0.47	0.89	0.59	0.61	0.35	0.34	6	16	0.003	0.005
January (H)	$\bar{x}$	7.68	7.84	6.34	5.76	2.94	2.22	92	67	0.025	0.030
	s	0.89	1.67	0.62	0.95	0.15	0.70	9	33	0.004	0.010
May (WH)	$\bar{x}$	8.22	7.78	6.04	6.08	2.96	2.76	102	81	0.023	0.031
	s	0.25	0.79	0.74	0.81	0.29	0.29	15	24	0.004	0.002
May (H)	$\bar{x}$	9.62	8.14	6.42	5.94	2.90	2.80	100	85	0.025	0.036
	s	1.77	0.91	0.65	0.89	0.79	0.33	30	7	0.005	0.005
October (WH)	$\bar{x}$	7.96	7.48	6.20	5.60	3.02	2.52	81	66	0.024	0.028
	s	0.66	0.56	0.46	0.90	0.65	0.30	11	9	0.002	0.006

Table 21a. Weight and size of left sublingual gland (N = 5♂, 5♀)

Time of death		Length in mm		Breadth in mm		Depth in mm		Weight in mg		Weight in %	
		♂	♀	♂	♀	♂	♀	♂	♀	♂	♀
January (WH)	$\bar{x}$	7.76	7.42	6.58	5.64	2.58	2.18	88	73	0.022	0.020
	s	0.68	1.35	0.50	0.49	0.55	0.42	7	10	0.002	0.003
January (H)	$\bar{x}$	7.82	7.22	5.98	5.22	3.20	2.32	93	60	0.026	0.028
	s	0.49	0.84	0.82	0.66	0.56	0.39	12	10	0.005	0.002
May (WH)	$\bar{x}$	8.16	7.88	6.62	5.86	2.40	2.58	109	87	0.024	0.037
	s	0.78	0.67	0.75	0.38	0.49	0.48	24	10	0.006	0.016
May (H)	$\bar{x}$	9.38	7.68	6.84	6.02	3.18	2.36	120	82	0.028	0.035
	s	1.31	0.79	0.66	0.40	0.59	0.39	30	6	0.005	0.004
October (WH)	$\bar{x}$	7.66	7.10	5.68	5.20	2.64	2.40	78	62	0.023	0.026
	s	0.86	0.86	0.48	0.68	0.26	0.34	13	9	0.002	0.006

Table 22. Weight and size of right zygomatic gland (N = 5♂, 5♀)

Time of death		Length in mm		Breadth in mm		Depth in mm		Weight in mg		Weight in %	
		♂	♀	♂	♀	♂	♀	♂	♀	♂	♀
January (WH)	$\bar{x}$	9.18	8.78	6.30	6.36	2.30	1.98	97	81	0.024	0.022
	s	1.22	0.42	1.15	0.84	0.35	0.41	13	15	0.004	0.005
January (H)	$\bar{x}$	8.84	9.36	5.78	5.88	2.38	1.78	73	69	0.020	0.032
	s	0.54	1.29	0.75	0.68	0.48	0.32	14	8	0.006	0.002
May (WH)	$\bar{x}$	9.74	8.96	6.66	5.76	2.44	2.22	121	95	0.027	0.027
	s	0.59	2.31	0.61	0.62	0.44	0.41	8	36	0.005	0.011
May (H)	$\bar{x}$	9.80	8.88	7.50	6.38	2.64	2.70	130	103	0.030	0.043
	s	0.54	0.90	0.10	0.85	0.54	0.39	30	17	0.005	0.004
October (WH)	$\bar{x}$	9.18	8.10	6.08	5.72	2.50	2.22	85	64	0.026	0.027
	s	0.57	1.13	0.44	0.58	0.46	0.25	17	9	0.005	0.005

Table 22a. Weight and size of left zygomatic gland (N = 5♂, 5♀)

Time of death		Length in mm		Breadth in mm		Depth in mm		Weight in mg		Weight in %	
		♂	♀	♂	♀	♂	♀	♂	♀	♂	♀
January (WH)	$\bar{x}$	8.74	8.32	6.34	5.44	2.26	2.20	97	86	0.024	0.024
	s	0.71	1.68	0.64	0.76	0.57	0.33	13	14	0.004	0.004
January (WH)	$\bar{x}$	8.48	8.92	5.50	5.00	2.54	1.90	81	69	0.022	0.032
	s	0.93	1.09	0.60	1.13	0.34	0.37	14	8	0.006	0.002
May (WH)	$\bar{x}$	9.46	10.02	6.74	6.22	2.48	2.14	116	112	0.026	0.032
	s	1.22	1.37	0.80	0.58	0.46	0.34	9	4	0.003	0.006
May (H)	$\bar{x}$	8.92	8.48	7.58	7.06	2.46	2.54	110	105	0.027	0.044
	s	0.86	0.85	0.93	0.62	0.22	0.23	40	15	0.007	0.003
October (WH)	$\bar{x}$	8.14	7.70	6.38	5.84	2.34	1.80	87	63	0.026	0.027
	s	0.75	0.73	0.16	0.68	0.42	0.41	11	10	0.004	0.003

Table 23. Age dependent alterations of the skeleton in European hamsters

Age	Shoulder-joint	Elbow-joint	Hip-joint	Knee-joint	Vertebrae
18 days	Epiphysis wide	Epiphysis wide	Epiphysis wide	Epiphysis wide	Periphery not ossified
2 months	Epiphysis narrowed	Epiphysis narrowed	Epiphysis wide	Epiphysis wide	Periphery not ossified
6 months	Epiphysis narrowed	Epiphysis narrowed	Epiphysis narrowed	Epiphysis narrowed	Initial ossification of periphery
12 months	Epiphysis narrowed	Epiphysis closed	Epiphysis closed	Epiphysis narrowed	Complete ossification
20 months	Epiphysis closed	Epiphysis closed	Epiphysis closed	"Scar"	Complete ossification

BIBLIOGRAPHY

Allen, L. 1967. Lymphatics and Lymphoid tissues. Ann. Rev. Physiol. 29, 197–224.

Althoff, J., F. W. Krüger, U. Mohr, and D. Schmähl. 1971a. Dibutylnitrosamine carcinogenesis in Syrian golden and Chinese hamsters. Proc. Soc. Exp. Biol. Med. 136, 168–173.

Althoff, J., R. Wilson, and U. Mohr. 1971b. Diethylnitrosamine-induced alterations in the tracheobronchial system of Syrian golden hamsters. J. Natl. Cancer Inst. 46, 1067–1071.

Barone, R., C. Pavaux, P. C. Blim, and P. Cuq. 1973. Atlas d'Anatomie du Lapin. Masson et Cie., Paris.

Brauer, K., and W. Schober. 1970. Katalog der Säugetiergehirne. VEB Gustav Fischer Verlag, Jena, pp 11–14.

Buckingham, S. and M. E. Avery. 1962. Time of appearance of lung surfactant in the foetal mouse. Nature, 193, 688–689.

Cohrs, P., R. Jaffé, and H. Meessen. 1958. Pathologie der Laboratoriumstiere I. Band. Springer-Verlag, Berlin, pp 216–221.

Cooper, G., and A. L. Schiller. 1975. Anatomy of the Guinea Pig. Harvard University Press. Cambridge, Mass.

Creasia, D. A. and P. Nettesheim. 1975. Respiratory cocarcinogenesis studies with ferric-oxide: A test case of current experimental models, in: Experimental Lung Cancer, Carcinogenesis and Bioassays (eds. E. Karbe and J. F. Park) Springer-Verlag, Berlin.

Della Porta, G., L. Kolb, and P. Shubik. 1958. Induction of tracheobronchial carcinomas in the Syrian golden hamster, Cancer Res. 18, 592–597.

Dontenwill, W. and U. Mohr. 1961. Carcinome des Respirationstractus nach Behandlung von Goldhamstern mit Diäthylnitrosamin. Z. Krebsforsch. 64, 305–312.

Eckel, H., G. Reznik, H. Reznik-Schüller, and U. Mohr. 1974a. Bronchographic studies of the European hamster (*Cricetus cricetus* L.), the Syrian golden hamster (*Mesocricetus auratus* W.) and the Chinese hamster (*Cricetus griseus* M.). Z. Versuchstierk. 16, 322–328.

Eckel, H., G. Reznik, H. Reznik-Schüller, B. Ohse, and U. Mohr. 1974b. Radiological detection and sequential observation of experimentally induced bladder tumours in the European hamster. Br. J. Cancer, 30, 496–502.

Eckel, H., H. Reznik-Schüller, G. Reznik, J. Hilfrich, and U. Mohr. 1973. Demonstration of nitrosamine-induced tumours in the respiratory tract of the European hamster (*Cricetus cricetus* L.) by X-ray examination. Strahlentherapie 145, 600–603.

Eckel, H., H. Reznik-Schüller, G. Reznik, B. Ohse, and U. Mohr. 1975. Diagnosis of experimentally induced bronchogenic tumours in the European hamster with bronchographs. Z. Krebsforsch. 83, 207–212.

Ehard, H. 1973. Vergleichende Untersuchungen zur Anatomie der Lungen von kleinen Versuchstieren (Kaninchen, Meerschweinchen, Albino-Ratten, Syrische Goldhamster). D.V.M. Diss. Tierärztliche Hochschule Hannover.

Eibl-Eibesfeldt, I. 1953. Zur Ethologie des Hamsters (*Cricetus cricetus* L.) Z. Tierpsych. 58, 204–254.

Eickhoff, W. 1965. Die Shilddrüse—Morphologie, Funktion and Klinik, Johann Ambrosius Barth Verlag, München.

Emminger, A., G. Reznik, H. Reznik-Schüller, and U. Mohr, 1975. Differences in blood values depending on age in laboratory-bred European hamsters (*Cricetus cricetus* L.) Lab. Anim. 9, 33–42.

Fanghänel, J., E. Schultz, H. Kammel, G. H. Schumacher, and R. Fanghänel. 1972. Das Skelettsystem des syrischen Goldhamsters, *Mesocricetus auratus* (WATERHOUSE) 2. Brustkorb und obere Extremität. Thorax et ossa membri superioris. Z. Versuchstierk. 14, 320–331.

Feron, V. J., P. Emmelot, and T. Vossenaar. 1972. Lower respiratory tract tumours in Syrian golden hamsters after intratracheal instillations of diethylnitrosamine alone and with ferric oxide. Europ. J. Cancer 8, 445–449.

Freyschmidt, J., G. Reznik, H. Reznik-Schüller, H. Eckel, and W. Rippel. 1975. X-Ray enlargement modified for use in experimental animal science. Lab. Animals 9, 305–311.

Gaffrey, G. 1961. Merkmale der wildlebenden Säugetiere Mitteleuropas. Academische Verlag, Leipzig, 109–112.

Gaus, G. 1971. Die Lymphknoten der Brust- und Bauchhöhle der Ratte und ihr jeweiliges Einzugsgebiet. The VIIth International Symposium on laboratory animals. Hruba Skala 137–144.

Geyer, H. 1972. Anatomische Untersuchungen am Harn- und Geschlechtsapparat des Chinesischen Zwerghamsters (*Cricetulus griseus*) Z. Versuchstierk. 14, 107–123.

Geyer, H. 1973. Zur topographischen Anatomie der Brusthöhle und des Halses beim Chinesischen Zwerghamster (*Cricetulus griseus* MILNE EDWARDS 1867) Z. Versuchstierk. 15, 34–49.

Geyer, H., K.-H. Habermehl, H. Wissdorf, and I. Belčić. 1972. Die Topographie der Bauchorgane des Chinesischen Zwerghamsters. (*Cricetulus griseus* MILNE EDWARDS 1867). Z. Versuchtierk. 14, 50–64.

Giddens, W. E., C. K. Whitehair, and G. R. Carter. 1971. Morphologic and microbiologic features of nasal cavity and middle ear in germfree, defined-flora, conventional, and chronic respiratory disease-affected rats. Am. J. Veter. Res. 32, 99–114.

Gluck, L., M. V. Kulovich, A. I. Eidelman, L. Cordero, and A. F. Khazin. 1972. Biochemical development of surface activity in mammalian lung. IV. Pulmonary lecithin synthesis in the human fetus and newborn and etiology of the respiratory distress syndrome. Pediat. Res. 6, 81–99.

Haas, H., U. Mohr, and F. W. Krüger. 1973. Comparative studies with different doses of *N*-nitrosomorpholine, *N*-nitrosopiperidine, *N*-nitrosomethylurea, and dimethylnitrosamine in Syrian golden hamsters. J. Natl. Cancer Inst. 51, 1295–1301.

Habermehl, K. H. 1970a. Die postnatale Entwicklung von *Cricetus griseus*. Schweiz. Arch. Tierheilk. 112, 240–247.

Habermehl, K. H. 1970b. Gebissentwicklung, Backenzahnabnutzung und Zahnalterschätzung beim Chinesischen Zwerghamster. Schweiz. Arch. Tierheilk. 113, 278–286.

Hannoun, C., J.-C. Guillon, and J. Chatelain. 1974. Infection spontanée latente a papovavirus chez le hamster Européen (*Cricetus cricetus* Linné) Ann. Microbiol. (Inst. Pasteur) 125, 215–226.

Herlant, J. 1975. The identification of chromophobe cells *in*: Tixier-Vidal, A. and M. G. Farquhar. Ultrastructure in Biological Systems, Vol. 7. The Anterior Pituitary, Eds. Dalton, A. J. and F. Hageman. Academic Press, New York, 6–7.

Herrold, K. M. and L. J. Dunham. 1963. Induction of tumors in the Syrian hamster with diethylnitrosamine (*N*-nitrosodiethylamine) Cancer Res. 23, 773–777.

Hoffmann, R. A., P. F. Robinson, and H. Magalhaes. 1968. The Syrian golden hamster, its biology and use in medical research. The Iowa State University Press, Ames, Iowa.

Hoŕber, P. J., H. Geyer, and K. H. Habermehl. 1974. Topographisch-anatomische und histologische Untersuchungen am Kopf des Chinesischen Zwerghamsters mit besonderer Berücksichtigung der Blutentnahme und der Hypophysektomie. Z. Versuchstierk. 16, 214–238.

House, E. L., B. Pansky, and M. S. Jacobs. 1961. Age changes in blood of the golden hamster. Amer. J. Physiol. 200, 1018–1022.

Illman, O. 1968. The European hamster (*Cricetus cricetus*) as a laboratory animal. J. Inst. Animal Technicians 19, 52–55.

Jahn, T. 1966. Der farbige Brehm. Ein grosses Tiejbuch mit 120 Farbtafeln. Herder Verlag, Freiburg, pp. 127–129.

Jensen, A. 1977. Untersuchungen über die Strukturen der Nasen- und Nasennebenhöhlen und deren Epithelauskleidung beim Europäischen Feldhamster. D.D.M. Diss. Medizinische Hochschule, Hannover.

Kayser, C. 1961. The physiology of natural hibernation. Pergamon Press, New York.

Kayser, C. and M. Aaron. 1938. Cyclé d' activité saisonniére des glandes endocrines chez un hibernant, le hamster (*Cricetus frumentarius*). Comp. Rend. Soc. Biol. 129, 225-226.

Kelemen, G. 1950. Nasal cavity of guinea pig in experimental work. Arch. Otolaryngol. 52, 579–596.

Kelemen, G. 1953. Nonexperimental nasal and paranasal pathology in hereditarily obese mice. A.M.A. Arch. Otolaryngol. 57, 143–151.

Kelemen, G. 1955. The nasal and paranasal cavities of the rabbit in experimental work. A.M.A. Arch. Otolaryngol. 61, 497–512.

Kelemen, G. and F. Sargent. 1946. Nonexperimental pathologic nasal findings in laboratory rats. Arch. Otolaryngol. 44, 24–42.

Kittel, R. 1952–53. Die Organgewichte von *Cricetus cricetus* L. und *Mesocricetus auratus* Waterhouse. Wiss. Zeitschr. d. Martin-Luther-Univ. Halle-Wittenberg. Math. Naturwiss. Reihe, 2, Heft II 903–909.

Kittel, R. 1953. Beiträge zur topographischen Anatomie der Körperhöhlen bei *Cricetus cricetus* L. und *Mesocricetus auratus* Waterhouse. Diss. Halle. Math. u. Naturw.

Kittel, R. 1955. Beiträge zur topographischen Anatomie der Korperhohlen des Goldhamster *Mesocricetus auratus* Waterhouse. Wiss. Z.d. Martin-Luther-Univ. Halle-Wittenberg 4, 1005–1028.

Klaus, M., O. K. Reiss, W. H. Tooley, C. Piel, and J. A. Clements. 1962. Alveolar epithelial cell mitochondria as source of the surface-active lung lining. Science 137, 750–751.

Kmoch, N., G. Reznik, and U. Mohr. 1975. Inhalation experiments with ^{14}C-labelled cigarette smoke. II. The distribution of cigarette smoke particles in the hamster respiratory tract after exposure in two different smoking systems. Toxicology, 4, 373–383.

Kmoch, N., G. Reznik, and A. Schleicher. 1976. Inhalation experiments with ^{14}C-labelled cigarette smoke. III. Body size dependent distribution of particulate matter in small rodents during cigarette smoke inhalation. Toxicology 6, 219–223.

Kourist, W. 1957. Das Haarkleid des Hamsters (*Cricetus cricetus* Linné, 1758) Wiss. Z.d. Martin-Luther-Univ. Halle, Math.-Nat. 6, 413–437.

Kristal, O. 1929. New materials on the biology of the hamster (*Cricetus cricetus* L.). Visnik prirodoznavstva, 1, 42–54.

Laskin, S. and A. Sellakumar. 1975. Models in chemical respiratory carcinogenesis, in: Experimental Lung Cancer, Carcinogenesis and Bioassays (eds. E. Karbe and J. F. Park) Springer-Verlag, Berlin.

Leblond, C. P. and Y. Clermont. 1952a. Spermiogenesis of rat, mouse, hamster and guinea pig as revealed by the "periodic acid fuchsin-sulfurous acid" technique. Am. J. Anat. 90, 167–215.

Leblond, C. P. and Y. Clermont. 1952b. Definition of the stages of the cycle of the seminiferous epithelium in the rat. Ann. N.Y. Acad. Sci. 55, 548–573.

Leonhardt, H. 1971. Histologie und Zytologie des Menschen. Thieme Verlag, Stuttgart, 3. Aufl.

Lijinsky, W., A. Ferrero, R. Montesano, and C. E. M. Wenyon. 1970. Tumorigenicity of cyclic nitrosamines in Syrian golden hamsters. Z. Krebsforsch. 74, 185–189.

Matthiesen, T. and C. Messow. 1972. Histologische Befunde an Rattenschilddrüsen nach Verabreichung von Methylthiouracil im Vergleich zu klinischen Parametern. Arzneim. Forsch. 22, 2121–2123.

Messow, C., T. Matthiesen, and J. Dycka. 1973. Vergleich histometrischer Parameter an Rattenschilddrüsen nach Verabreichung von Methylthiouracil. Arzneim. Forsch. 23, 1076–1079.

Mohr, U., J. Althoff, and N. Page. 1972. Brief Communication: Tumors of the respiratory system induced in the common European hamster by *N*-diethylnitrosamine. J. Natl. Cancer Inst. 49, 595–597.

Mohr, U., J. Althoff, D. Schmähl, and F. W. Krüger. 1970. The carcinogenic effect of dibutylnitrosamine in Syrian and Chinese Hamsters. Z. Krebsforsch. 74, 112–113.

Mohr, U., J. Althoff, R. Spielhoff, and H. Bresch. 1973. The influence of hibernation upon the carcinogenic effect of *N*-diethylnitrosamine in European hamsters. Z. Krebsforsch. 80, 285–288.

Mohr, U., K. Pielsticker, O. Wieser, and V. Kinzle. 1967. Tumoren im Vormagen des chinesischen Hamsters nach Diäthylnitrosamin-Behandlung. Ein Beitrag zur Frage der Organotropie eines Karzinogens. Europ. J. Cancer 3, 139–142.

Mohr, U., G. Reznik, and H. Reznik-Schüller. 1974a. Carcinogenic effects of *N*-nitrosomorpholine and *N*-nitrosopiperidine on European hamster (*Cricetus cricetus*). J. Natl. Cancer Inst. 53, 231–237.

Mohr, U., G. Reznik, and H. Reznik-Schüller. 1974b. Urethan as a carcinogen for the European hamster. J. Natl. Cancer Inst. 53, 1359–1367.

Mohr, U., H. Schüller, G. Reznik, J. Althoff, and N. Page. 1973. Breeding of European hamsters. Lab. Animal Science 23, 799–802.

Mohr, U., O. Wieser, and K. Pielsticker. 1966. Die unterschiedliche carcinogene Wirkung von Diäthylnitrosamin beim syrischen und chinesischen Hamster. Naturwiss. 53, 437.

Montesano, R. 1970. Systemic respiratory carcinogenesis including synergistic effects. Oncology 4, 456–462.

Montesano, R. and U. Saffiotti. 1968. Carcinogenic response of the respiratory tract of Syrian golden hamsters to different doses of diethylnitrosamine. Cancer Res. 28, 2197–2210.

Montesano, R. and U. Saffiotti. 1970. Carcinogenic response of hamster respiratory tract to single subcutaneous administrations of diethylnitrosamine at birth. J. Natl. Cancer Inst. 44, 413–417.

Muschke, E. 1953. Histometrische Untersuchungen am Rattenhoden nach Hypophysektomie und nach Choriongonadotropinzufuhr. Endokrinologie 30, 281–294.

Nehring, A. 1901. Die Zahl der Zitzen und Embryonen bei *Mesocricetus* und *Cricetus*. Zool. Anz. 24, 130–131.

Nettesheim, P. 1972. Respiratory carcinogenesis studies with the Syrian golden hamster: A review, Progr. Exp. Tumor Res. 16, 185–200.

Neumann, K. 1963. Die Morphokinetik der Schilddrüse; Studie über die akuten Veränderungen im Bau eines endokrinen Organs in Abhängigkeit von seiner Leistung. Fischer Verlag, Stuttgart.

Nickel, R., A. Schummer, and E. Seiferle. 1960. Lehrbuch der Anatomie der Haustiere. Verlag Paul Parey, Berlin, Bd.I., pp. 106–174, Bd.II., pp. 207–226, 2. Aufl.

Och, R. 1959. Beitrag zur Anatomie des Respirationsapparates des Syrischen Goldhamsters (*Mesocricetus auratus*, W.) Diss. Leipzig.

Pattle, R. E., G. Gandy, C. Schock, and J. M. Creasy. 1974. Lung inclusion bodies: different ultrastructure in simian and non-simian mammals. Experientia 30, 797–798.

Petzsch, H. 1936. Beitrage zur Biologie insbesondere Fortpflauzungsbiologie des Hamsters (*Cricetus cricetus* L.). Monogr. d. Wildsäugetiere 1, 1–83.

Petzsch, H. 1937. Die Fortpflanzungsbiologie des Hamsters (*Cricetus cricetus* L.). Der Naturforscher, 13, 337–340.

Petzsch, H. 1943. Neue Beobachtungen zur Fortpflanzungsbiologie des Hamsters (*Cricetus cricetus* L.) Zool. Garten 15, 45–54.

Petzsch, H. and U. Petzsch. 1968. Neue Beobachtungen zur Fortpflanzungsbiologie von gefangengehaltenen Feldhamstern (*Cricetus cricetus* L.) und daraus ableitbare Schlussfolgerungen für die Angewandte Zoologie. Zool. Garten 35, 256–269.

Petzsch, H. and H. Petzsch. 1956. Zum Problem des Vererbungsmodus für Melanismus bei dem gemeinen Hamster (*Cricetus cricetus* L.) in Hinsicht auf die Evolution. D. Zool. Garten 22, 119–154.

Petzsch, U. and H. Petzsch. 1970. Bemerkungen über frappierende Verkehrtfärbungs- und Unterseitenzeichnungs- Analogien beim Feldhamster (*Cricetus cricetus* L.) und bei Maikäfern (*Melolontha melolontha* L. und *Melolontha hippocastani* Fabr.) Zool. Garten, 39, 15–231.

Pidoplička, J. 1928. On the biology of the hamster (*Cricetus cricetus* L.) Visnik prirodoznavstva, 1, 23–36.

Precht, H., J. Christophersen, H. Hensel, and W. Larcher. 1973. Temperature and life: Homeothermic organisms. Hensel, Brück, Raths,-Capitel XI. Hibernation and related phenomena, pp. 688–711. Springer-Verlag, Berlin, rev. ed.

Raths, P. 1953–54. Die Kerne im Hypothalamusgebiet des Hamsters (*Cricetus cricetus* L.) Wiss Zeitschr. der Martin-Luther-Univ. Halle Wittenberg, Math.-naturw. Reihe, 3, 577–590.

Reznik, G., H. Eckel, J. Freyschmidt, and H. Reznik-Schüller. 1975a. Age dependent skeletal development in the European hamster—Radiological investigations. Z. Versuchtierk. 17, 233–239.

Reznik, G., N. Kmoch, and U. Mohr. 1975b. Inhalation experiments with ^{14}C-labelled cigarette smoke. I. Determination of the effectiveness of two different smoking systems with labelled cigarettes. Toxicology 4, 363–371.

Reznik, G., U. Mohr, and N. Kmoch. 1976a. Carcinogenic effects of different nitroso-compounds in Chinese hamsters *N*-Dibutylnitrosamine and *N*-Nitrosomethylurea. Cancer Lett. 1, 183–188.

Reznik, G., U. Mohr, and N. Kmoch. 1976b. Carcinogenic effects of different nitroso-compounds in Chinese hamsters. I. Dimethylnitrosamine and *N*-diethylnitrosamine. Br. J. Cancer, 33, 411–418.

Reznik, G., U. Mohr, and N. Kmoch. 1976c. Carcinogenic effects of different nitroso-compounds in Chinese hamsters. II. *N*-nitrosomorpholine and *N*-nitrosopiperidine. Z. Krebsforsch. 86, 95–102.

Reznik, G. and H. Reznik-Schüller. 1974. Anatomical investigations of the cranium of the European hamster (*Cricetus cricetus* L.) with particular consideration to the nasal and paranasal cavities. Z. Versuchstierk. 16, 23–34.

Reznik, G., H. Reznik-Schüller, A. Emminger, and U. Mohr. 1975c. Comparative studies of blood from hibernating and nonhibernating European hamsters (*Cricetus cricetus* L.) Lab. Animal Science 25, 210–215.

Reznik, G., H. Reznik-Schüller, and U. Mohr. 1973. Comparative studies of organs in the European hamster (*Cricetus cricetus* L.) the Syrian golden hamster (*Mesocricetus auratus* W.) and the Chinese hamster (*Cricetulus griseus* M.). Z. Versuchstierk. 15, 272–282.

Reznik, G., H. Reznik-Schüller, and U. Mohr. 1977. Comparative studies concerning the carcinogenicity of *N*-diethylnitrosamine in hibernating and non-hibernating European hamsters. J. Natl. Cancer Inst. (in press).

Reznik, G., H. Reznik-Schüller, H. Schostek, K. Deppe, and U. Mohr. 1975d. Comparative studies concerning the suitability of European hamsters and Syrian golden hamsters for investigations on smoke exposure. Arzneim. Forsch. 25, 923–926.

Reznik-Schüller, H. and U. Mohr. 1975. The ultrastructure of *N*-dibutylnitrosamine induced pulmonary tumours (adenocarcinomata) in European hamsters. Br. J. Cancer 32, 230–238.

Reznik-Schüller, H. and U. Mohr. 1976a. Ultrastructure and formation of lamellated inclusion bodies in induced lung tumours of the European hamster. Am. J. Pathol., 83, 319–328.

Reznik-Schüller, H. and U. Mohr. 1976b. Ultrastructure of *N*-dibutylnitrosamine induced nasal cavity tumours in the European hamster. J. Natl. Cancer Inst. 57, 401–407.

Reznik-Schüller, H. and G. Reznik. 1973. Comparative histometric investigations of the testicular function of European hamsters (*Cricetus cricetus* L.) with and without hibernation. Fertil. Steril. 24, 698–705.

Reznik-Schüller, H. and G. Reznik. 1974. The influence of hibernation upon the ultrastructure of the Leydig cells and spermatids of the European hamster. Fertil. Steril. 25, 621–635.

Reznik-Schüller, H., G. Reznik, and U. Mohr. 1974. The European hamster (*Cricetus cricetus* L.) as an exprimental animal: Breeding methods and observations of their behavior in the laboratory. Z. Versuchstierk. 16, 48–58.

Roscher, P. 1909. Der Kopfdarm von *Cricetus frumentarius*. Hölder, Wien.

Saffiotti, U. 1969. Experimental respiratory tract carcinogenesis. Prog. Exp. Tumor. Res. 11, 302–333.

Saffiotti, U. 1974. Keynote Address: Progress carcinogenesis, in: Experimental Lung Cancer, Carcinogenesis and Bioassays (eds. E. Karbe and J. F. Park) Springer-Verlag, Berlin.

Saffiotti, U., F. Cefis, and L. H. Kolb. 1968. A method for the experimental induction of bronchogenic carcinoma. Cancer Res. 28, 104–124.

Saint Girons, M.C., W. R. van Mourik, and P. J. H. van Bree. 1968. La croissance ponderale et le cycle annuel du Hamster, *Cricetus cricetus canescens* Nehring, 1899, en captivité. Mammalia 32, 577–602.

Schlotter, W. 1976. Histometrische Untersuchungen über den Einfluss des Winterschlafes auf Adenohypophyse, Thyreoidea und Parathyreoidea beim Europäischen Feldhamster. D.D.M. Diss. Medizinische Hochschule Hannover.

Schultz, E., H. Kammel, G. H. Schumacher, J. Fänghänel, and R. Fänghanel. 1973. Das Skelett des Syrischen Goldhamsters *Mesocricetus auratus* (WATERHOUSE) 3. Beckengürtel und untere Extremität. Ossa membri inferiores. Z. Versuchstierk. 15, 96–107.

Schumacher, G. H., J. Fanghänel, E. Schultz, H. Kammel and R. Fanghänel. 1972. Das Skelettsystem des Syrischen Goldhamsters, *Mesocricetus auratus* (WATERHOUSE, 1. Wirbelsäule. Columna vertebralis. Z. Versuchstierk. 14, 233–245.

Schwarze, E. and G. Michel. 1959–60. Anatomie der Eingeweide des Syrischen Goldhamsters (*Mesocricetus auratus* W.) Wiss. Z.d. Karl-Marx Universität, Leipzig 9, 95–126.

Serebrennikov, M. K. 1930. Album einiger osteuropäischer, westsibirischer und turkestanischer Säugetiere. Z. Säugetierk. 5, 96–104.

Spit, B. J. and V. J. Feron. 1975. Comparative study of ultrastructure of tracheal and pulmonary tumours induced by multiple intratracheal instillations of diethylnitrosamine in Syrian golden hamsters. Europ. J. Cancer 11, 867–872.

Stenbäck, F. G., A. Ferrero, and P. Shubik. 1973. Synergistic effects of diethylnitrosamine and different dusts on respiratory carcinogenesis in hamsters. Cancer Res. 33, 2209–2214.

Stewart, M. O., L. Florio, and E. R. Mugrage. 1944. Hematological findings in the golden hamster (*Cricetus auratus* W.) J. Exp. Med. 80, 189–196.

Sulzer, F. G. 1774. Versuch einer Naturgeschichte des Hamsters. Dieterich, Göttingen und Gotha.

Theiler, K. 1972. The House Mouse: Development and Normal Stages from Fertilization to 4 Weeks of Age. Springer-Verlag, Berlin.

Vidič, B and H. G. Greditzer. 1971. The histochemical and microscopical differentiation of the respiratory glands around the maxillary sinus of the rat. Am. J. Anat. 132, 491–514.

Vohralik, V. 1974. Biology of the reproduction of the common hamster (*Cricetus cricetus* L.). Vest. Cs. Spol. Zool. 38, 228–240.

von Bittera, J. 1918. Einiges über die männlichen Copulationsorgane der Muriden und deren systematische Bedeutung. Zool. Jb. 41, 399–415.

Vrtiš, V. 1930. Glandular organ on the flancs of the hamster *gen. Cricetus*. Biol. Spisy 9, 1–31.

Vrtiš, V. 1932. The cutaneous umbilical glandular organ of the hamster *Cricetus cricetus* (L). Biol. Spisy 11, 16.

Warner, N. E. 1971. Basic Endocrine Pathology. Year Book Medical Publishers Inc., Chicago, 15–19.

Wauer, H. Zur Anatomie des Atmungsapparates von *Lepus timidus*. Schreb. Diss. Leipzig.

Weibel, E. R. 1973. Morphological basis of alveolar-capillary gas exchange. Physiol. Rev. 53, 419–495.

Wells, T. A. G. 1968. The Rat. A Practical Guide. Dover Publications, New York.

Wynder, E. L. and D. Hoffmann. 1964. Experimental tobacco carcinogenesis. Adv. Cancer Res. 8, 249–253.

Wynder, E. L. and D. Hoffmann. 1967. Tobacco and Tobacco Smoke. Studies in experimental carcinogenesis. Academic Press, New York.

Zimmermann, K. 1967. Taschenbuch unserer wildlebenden Säugetiere. 2. Auflage, pp. 92–93, Fackelträger-Verlag, Hannover.

Zimmermann, W. 1969. Die gegenwärtige Verbreitung melanistischer Hamster (*Cricetus cricetus* L.) in Thüringen und Bemerkungen zu deren Morphologie. Hercynia 6, 80–89.

Züchner, H. 1975. Vergleichende morphologische Untersuchungen zur Beurteilung der Ovarialfunktion beim Europäischen Feldhamster (*Cricetus cricetus* L.) unter besonderer Berücksichtigung des Winterschlafs. D.D.M. Diss., Medizinische Hochschule Hannover.

Zuckerkandl, E. 1897. Zur Muschelfrage. Monatschr. Ohrenheilk. Part 1, 321–330, Part 2, 373–386.

Zymbal, W. E. 1933. Histologische und experimentelle Untersuchungen am Epithelgewebe der Talgdrüsen (Gehörgangdrüsen der Ratte). Zeitschr. Zellforsch. Mikroskop. Anat. 18, 596–625.

INDEX

HAMSTER ATLAS

The N.A.V. standard nomenclature is given in *italic* typeface. Pages referring to illustrated structures are given in **bold** type face.

Abdomen
- bony structures of, 140, 141, 145, 146, 148, 155, 164
- cavity
  - abdominal (*cavum abdominis*), 121, 122
  - peritoneal (*cavus peritonei*), 122
- crest
  - iliac (*crista iliaca*), 121
- diaphragm, abdomen upper limit of, (*diaphragma*), 121
- *esophagus*, 124
- inlet, pelvic, abdomen lower limit of, (*apertura, pelvis cranialis*), 121
- intestines
  - large (*intestinum crassus*), 130, 131
    - *caecum*, 130
    - *colon*, 130, 131
  - small (*intestinum tenue*)
    - *duodenum*, 124, 125, 129
    - *ileum*, 129, 130
    - *jejunum*, 131, 132
- kidney (*ren*), 131, 132
- liver (*hepar*), 125–127
- lymph
  - nodes, 134
  - centers
    - coeliac, 134
    - lumbar, 135
    - mesenteric, cranial, 134, 135
- muscles
  - *m. iliacus*, 121
  - *m. obliquus internus*, 121
  - *m. psoas major*, 121
  - *m. quadratus lumborum*, 121
  - *m. rectus abdominis*, 121
- nerves, see below under abdomen, regions
- *pancreas*, 127
- portal system, 134
- regions, see also pelvis, 145
  - craniomesocolic, 122, 128
    - peritoneum, 122, 123
    - vessels, nerves, 127, 128
    - viscera, 124–127
  - caudomesocolic, 128–131
    - peritoneum, 128, 129
    - vessels, nerves, 133
    - viscera, 129–131
  - rectroperitoneal, 131–133
    - vessels, 133
    - viscera, 131–133
  - spleen (*lien*), 127
  - stomach (*gaster* or *ventriculus*), 124, 125, **147**
  - vessels, arteries and veins, see above under abdomen, regions

accessory lacrimal gland (*gl. lacrimalis accessoria*), see also gland, lacrimal, accessory, 24, 25

acetabulum (*acetabulum*), see also pelvis, 121

adhesio interthalamica, **29**

adipose tissue (*panniculus adiposus*)
- of adrenal gland, **170**
- capsule of kidneys (*capsula adiposa*), 132, **169, 170, 176**
- of epididymis, testis, 164, 176, 177
- lumbar region, **7**
- of mandibular glands, 65
- orbital (*corpus adiposum orbitae*), 24, **35, 38, 63**
- ovarian, 138, **183**
- of pancreas, 127, **154, 155**
- of parotid gland, 22
- thoracic region, **7**

aditus laryngis
- *see opening, laryngial*

aditus pharyngis
- see pharynx, entrance

adrenal gland (*gll. suprarenales*), 132, 133
- see also glands, adrenal

ala sphenodalis
- see bones, sphenoid, wing

alveolus, teeth (*alveolus dentalis*), 21

alveolus dentalis
- see alveolus, teeth

alveolar system of lungs, 94

ampulla
of ductus deferens, 136
angle
of ribs (*angulus costale*), 86
angulus costae
see angle, rib
angulus oculi medialis
see canthus, medial
angulus oris
see commissure, labial
annulus fibrosus
see ring, fibrous
anus (*anus*), 1, **10, 11,** 130, 131, 132
aorta
abdominal (*aorta abdominis*) 131, 133, **160, 161, 174**
arch of, (*arcus aortae*), 66, 88, 92, 93, **109, 160**
ascending (*aorta ascendens*), 89, 90
bifurcation, 128
descending (*aorta descendens*), 90, **111**
hiatus of, diaphragm (*hiatus aorticus*), 86, 88, 124
lumbar lymph nodes of (*lnn. lumbales aortici*), 135
nerves of, 128
thoracic (*aorta thoracica*), 89
valve (*valva aortae*)
of heart, 90
aorta abdominis
see aorta, abdominal
aorta ascendens
see aorta, ascending
aorta descendens
see aorta, descending
aorta thoracica
see aorta, thoracic
apertura nasomaxillaris
see opening, nasomaxillary
apertura pelvis caudalis
see outlet, pelvic
apertura pelvis cranialis
see inlet, pelvis, or pelvis, inlet, or abdomen, inlet
apertura thoracis caudalis
see aperture, thoracic, caudal
apertura thoracis cranialis
see aperture, thoracic, cranial
aperture
thoracic, caudal (*apertura thoracis caudalis*), 85
thoracic, cranial (*apertura thoracis cranialis*), 66, 85
vena cava (*foramen venae cavae*), of diaphragm, 87
apparatus, lacrimal (*apparatus lacrimalis*), 24
ducts, lacrimal, 24
gland, accessory lacrimal (*gl. lacrimalis accessoria*), 24
gland, lacrimal (*gl. lacrimalis*), 24
apparatus, turbinal,
see also endo/ectoturbinates, **40, 51**
apparatus lacrimalis
see apparatus, lacrimal
apex
caecal (*apex caeci*), 130, 135
epiglottic, 68
heart (*apex cordis*), 89
lung (*pulma*), 95
penis (*penis*), 137
thoracic cranial (*apertura thoracis cranialis*), 85
tongue (*apex linguae*), 21
apex caeci
see apex, caecal
apex cordis
see apex, heart
apex linguae
see tongue, tip
aquaduct, mesencephalic (*aquaeductus mesencephali*), **59**
aquaeductus mesencephali
see aquaduct, mesencephalic
arch, arches
aortic (*arcus aortae*), 66, **77,** 88, 92, 93, **109, 110, 160**
cricoid (*arcus cricoideus*), 67
lumbocostal (*arcua lumbocostales*), 86
palatopharyngeal (*arcus palatopharyngeus*), 66
soft palate (*palatum molle*), 66
vertebral (*arcus vertebrae*)
of cervical vertebrae (*vertebrae cervicales*), 65
zygomatic, 24
arcua lumbocostales
see arches, lumbocostal

arcus aortae
see arch, aortic
arcus cricoideus
see arch, cricoideum
arcus palatopharyngeus
see arch, palatopharyngeal
arcus vertebral
see arch, vertebral
aa. auricularis caudalis et rostralis
see arteries, auricular
a. basilaris
see artery, basilar
a. bursa baccalis
see artery, cheek pouch
a. carotis communis
see artery, carotid, common
a. carotis communis dextra
see artery, carotid, common, right
a. carotis externa
see artery, carotid, common, external
a. carotis interna
see artery, carotid, common, internal
a. caudalis mediana
see artery, caudal median
aa. cerebelli caudalis
see arteries, cerebellar, caudal
aa. cerebelli rostralis
see arteries, cerebellar, rostral
a. coeliac
see artery, coeliac
a. colica dextra
see artery, colic, right
a. colica media
see artery, colic, middle
a. facialis
see artery, facial
a. gastrica dextra
see artery, gastric, right
a. gastrica sinistra
see artery, gastric, left
a. gastroduodenalis
see artery, gastroduodenal
a. hepatica
see artery, liver
aa. ilei
see arteries, ileal
a. ileocolica
see artery, ileocolic
aa. iliacae communes
see arteries, iliac, common
aa. iliacae externae
see arteries, iliac, external
aa. iliacae internal
see arteries, iliac, internal
aa. intercarotica caudalis
see arteries, carotid, internal, dorsal branch
aa. intercarotica rostralis
see arteries, carotid, internal, ventral branch
aa. interlobularis
see arteries, interlobular
aa. jejunales
see arteries, jejunal
a. lienalis
see artery, splenic
a. lingualis
see artery, lingual
a. masseterica
see artery, masseter
a. maxillaris
see artery, maxillary
a. maxillaris interna
see artery, maxillary, internal
a. mesenterica caudalis
see artery, mesenteric, caudal
a. mesenterica cranialis
see artery, mesenteric, cranial
a. occipitalis
see artery, occipital
a. ophthalmica interna
see artery, ophthalmic, internal
aa. ovaricae
see arteries, ovarian
a. pancreatoduodenalis caudalis
see artery, pancreatoduodenal, caudal
a. pulmonalis
see artery, pulmonary
a. renalis
see artery, renal
a. sacralis mediana
see artery, sacral, median
a. subclavia
see artery, subclavian
a. subclavia dextra
see artery, subclavian, right
aa. suprarenales
see arteries, suprarenal (or adrenal)

a. temporalis superficialis
see artery, temporal, superficial
aa. testiculares
see arteries, testicular
a. thoracica interna
see artery, thoracic, internal
a. transversa faciei
see artery, facial, transverse
a. vertebralis
see artery, vertebral
artery, arteries
adrenals
see artery, suprarenal
aorta
abdominal, 133, **160, 161**
ascending (*aorta ascendens*), 90
descending (*aorta descendens*), 90
aortic arch (*arcus aortae*), **77,** 90, **110, 160**
see also aorta, and arch, aorta
auricular (*caudal and rostral*) (*aa. auricularis caudalis et rostrales*), 25
basilar (*a. basilaris*), 25, **61**
brachial (*a. brachiales*), 110
brachiocephalic trunk (*truncus brachiocephalicus*), **77,** 90, **109, 110, 111**
of bronchus, 94
carotid, common (*a. carotis communis*), 25, 66, 88, 90, 93
external (*a. carotis externa*), 25, 66
internal (*a. carotis interna*), 25, **61,** 66
dorsal branch (*a. intercarotica caudalis*), 25
ventral branch (*a. intercarotica rostralis*), 25
left (*a. carotis communis sinistra*), **77,** 93, **109, 110, 111**
right (*a. carotis communis dextra*), **77,** 90, 93, **109, 110, 111**
caudal, median (*a. caudalis mediana*), 133
cerebellar, caudal (*a. cerebelli caudalis*), 25, **61**
cerebellar, rostral (*a. cerebelli rostralis*), 25, **61**
cerebral
caudal (*a. cerebri caudalis*), **61**
medial (*a. cerebri media*), **61**
rostral (*a. cerebri rostralis*), **61**
cheek pouch (*a. bursa buccalis*), 25
coeliac (*a. coeliaca*), 128, **160**
colic, middle (*a. colica media*), 133
colic, right (*a. colica dextra*), 133
facial (*a. facialis*), 25
transverse (*a. transversa faciei*), 25
gastric
left (*a. gastrica sinistra*), 128
right (*a. gastrica dextra*), 128
gastroduodenal (*a. gastroduodenalis*), 128
hepatic (*a. hepatica*), 124, 127, 128
ileal (*aa. ilei*), 133
ileocolic (*a. ileocolica*), 133
iliac
common (*aa. iliacae communes*), 133, **174**
external (*aa. iliacae externae*), 133, **174**
internal (*aa. iliacae internae*), 133, **174**
incisura vasorum, 25
interlobular (*aa. interlobulares*), 131
jejunal (*aa. jejunales*), 133
of kidneys, 133
lingual (*a. lingualis*), 25
masseter (*a. masseterica*), 25
maxillary, internal (*a. maxillaris interna*), 25
mesenteric
caudal (*a. mesenterica caudalis*), 128, 133
cranial (*a. mesenterica cranialis*), 128, **160, 161**
occipital (*a. occipitalis*), 25
ophthalmic, internal (*a. ophthalmica interna*), 25
ovarian (*aa. ovaricae*), 133
pancreatoduodenal, caudal (*a. pancreatoduodenalis caudalis*), 128, **161**
pulmonary (*a. pulmonalis*), 90, 91, 94–96, **109, 111**
rectal, 133
cranial (*rectalis cranialis*), **174**
renal, 131, 133, **160**
sacral, median (*a. sacralis mediana*), 133
splenic (*a. linealis*), 128, **161**
subclavian (*a. subclavia*), 66, 87, 90
left (*a. subclavia sinistra*), **77,** 93, **109, 110**
right (*a. subclavia dextra*), **77,** 88, 90, **109, 110, 111**
suprarenal (*aa. subrarenales*), 133
temporal, superficial (*a. temporalis superficialis*), 25
testicular (*aa. testiculares*), 133, **174**

artery, arteries—*continued*
thoracic (*a. thoracica*),
internal (*a. thoracica interna*), 90
trachea, 90
vertebral (*a. vertebralis*), 25, **61**
articulatio intermandibularis
see joint, intermandibular
articulatio temporomandibulares
see joint, temporomandibular
atlas (*atlas*)
of cervical vertebrae, 65
atrium
left (*atrium sinistrum*)
of heart, 88, 90
right (*atrium dextrum*)
of heart, 89
atrium dextrum
see atrium, right
atrium sinistrum
see atrium, left
auditory bulla (*bulla tympanica*), 18, **31**
auriculae
see auricles
auricles (*auriculae*)
of heart, 89
auris externa
see ears, external
axis (*axis*) of cervical vertebra, 65
articular processes (*processus articularis*), 65
body (*corpus*), 65
odontoid process (*dens*), 65
spinous process (*processus spinosus*), 65
transverse processes (*processus transversi*), 65
vertebral arch (*arcus vertebrae*), 65
base (*basis*)
caecal (*basis caeci*), 129, 130
of heart (*basis cordis*), 89
sacral (*basis ossis sacri*), 14
basis
see base
basis caeci
see base, caecal
basis cordis
see base, heart
basis ossis sacri
see base, sacral
basophils
of pituitary, 24
behavior, social and dominance, **14, 15**
bifurcatio tracheae
see bifurcation, tracheal
bifurcation
aortic
craniomesocolic vascularization, 125
tracheal (*bifurcatio tracheae*), 88, 92, 93
bladder
gall (*vesica fellea*),
lacking in this species
urinary (*vesica urinaria*), 132, **173, 185**
body (*corpus*)
caecum (*corpus caeci*), 130
cervical vertebrae (*vertebrae cervicales*)
axis (*axis*), 65
epididymis (*corpus epididymidis*), 136
Malpighian, of spleen, **159**
mamillary (*corpus mamillare*), 23, **59**
penis (*corpus penis*), 137
sternum (*corpus sterni*), 85
uterus (*corpus uteri*), 128, 131, 138
bone(s), see also skeleton
basisphenoid (*os basisphenoidale*), 36, 62
clavicle (*clavicula*), see also clavicle, **71, 111**
ethmoid (*os ethmoides*), 17, **30**
cribriform plate of (*lamina cribrosa*), 18
frontal (*os frontales*), 17, **29, 30, 31, 34**
hyoid (*os hyoideum*), 17
ilium (*os ilium*), 121
incisive (premaxillary) (*dens incisivum*), 17, **29, 30, 31, 51**
interparietal (*os interparietale*), **29, 30, 31**
ischium (*os oschium*), 121
mandible (*mandibula*), **29, 34, 35, 44, 62, 73, 118**
maxillary (*maxilla*), 17, **30, 31, 32, 33, 51**
nasal (*os nasales*), 17, **29, 30, 31, 32, 33**
occipital (*os occipitale*), 23, **31**
palatine (*os palatinum*), 17, **31, 51**
parietal (*os parietale*), 23, **29, 30, 31**
pelvic (*os coxae*), see also pelvis, 121
penis (*os penis*), 137
premaxillary (incisive) (*os incisivum*), 17
presphenoid (*os praesphenoidale*), 18, **62**
pubic (*os pubis*), 121
sacrum (*os sacrum*), see also sacrum and vertebrae, sacral, 121, 131, **143, 144**
scapula, see scapula, **71**
of skull, 17
sphenoid (*os spehenoidale*), 23, **29, 31, 62**

bone(s), see also skeleton—*continued*
sternum, (see sternum)
temporal, **31**
mastoid process (*os temporale, pars mastoidea*), 25
petrous portion (*os temporalis, pars petrosa*), 23
tympanic portion (*os temporalis, pars tympanica*), 23
vomer (*vomer*), **31**
nasopharynx (*pharynx, pars nasalis*), **18, 32, 33**
zygomatic (*os zygomaticum*), **31**
brain (*encephalon*)
bony case of, (*cranium*), 23
cerebellum (*cerebellum*), 23
lobi paramediani, 23
paraflocculi, 23
vermis cerebelli, 23
cerebral hemispheres (*hemispheria cerebri*), 23
neurocranium or *cranium*, 23
olfactory bulbs (*bulbi olfactorii*), 23
optic chiasma (*chiasma opticum*), 23
branch
coeliac (*ramus coeliacus*)
nerves, 128
gastric (*ramus gastricus visceralis*)
nerves, 128
breeding
see also mating, pregnancy, **14**
effect of laboratory on, *vi*
bronci lobares
see bronchus, lobar
bronchi principales
see bronchus, main
bronchi segmentales
see bronchus, segmented
bronchi terminales
see bronchioles, terminal
bronchioles
terminal (*bronchi terminales*), 23, 94, **117**
bronchus(i), 93, 94, **116, 117**
lobar (*bronchi lobares*), 93, 94, **102, 115**
main (*bronchi principales*), 93, **102**
left (*bronchus principales sinister*), **114, 115**
right (*bronchus principales dexter*), **114**
sagital spur (*carina*), 93
segmental (*bronchi segmentales*), 94, **102, 115**
buccae
see cheeks
bulbi oculi
see eye(s)
bulbi olfactorii
see bulbs, olfactory
bulbourethral gland
see gland, bulbourethral
bulbs, olfactory (*bulbi olfactorii*), **29, 34, 35, 38, 57, 58, 59, 60, 61**
bulla tympanica
see auditory bulla
bursa
omental (*bursa omentalis*), 123
ovarian (*bursa ovarica*), 138
bursa omentalis
see bursa, omental
bursa ovarica
see bursa, ovarian
bursae buccales
see cheek pouches
caecum, 130, **164**
apex (*apex caeci*), 130
base (*basis caeci*), 130
body (*corpus caeci*), 130
cage
bony thorax (*ossa cavi thoracis*), 85
calices renales
see calyces, renal
calyces
renal (*calices renales*), 132
canal(s)
infraorbital (*canalis infraorbitalis*), 25
sacral (*canalis sacralis*), 121
tear (*canaliculi lacrimales*), 25
vertebral (*canalis vertebralis*), **103,** 121
canaliculi lacrimales
see canals, tear
canalis infraorbitalis
see canal, infraorbital
canalis sacralis
see canal, sacral
canalis vertebralis
see canal, vertebral
canthus, medial (*angulus oculi medialis*), 25
capsula adiposa
see capsule, adipose

capsula fibrosa
see capsule, fibrous
capsule(s)
adipose (*capsula adiposa*)
of kidney, 132
fibrous (*capsula fibrosa*)
of kidney, 132
of liver, 126
caput epididymidis, 136
cardia (*pars cardiaca*)
of stomach, 125
carina
see spur, sagital, or bronchus, main
cartilage(s)
arytenoid (*cartilago arytenoidea*), **29,** 67, **80, 81**
corniculate (*cartilago corniculata*), 67
cricoid (*cartilago cricoidea*), 67, 69, **80, 81**
cuneiform (*cartilago cuneiformis*), 67
of epiglottis (*cartilago epiglottica*), **29,** 67, **80, 81**
of manubrium (*cartilago manubrii*), 85
thyroid (*cartilago thyreoidea*), 67, **80, 81**
tracheal (*cartiligines tracheales*), 69
xiphoid (*cartilago xiphoidea*), 85
cartilagines tracheales
see cartilages, tracheal
cartilago arytenoidea
see cartilage, arytenoid
cartilago corniculata
see cartilage, corniculate
cartilago cricoidea
see cartilage, cricoid
cartilago cuneiformis
see cartilage, cuneiform
cartilago epiglottica
see cartilage, epiglottis
cartilago manubrii
see cartilage, manubrium
cartilago thyreoidea
see cartilage, thyroid
cartilago xiphoidea
see cartilage, xiphoid
carunculae sublinguales
see carunculae, sublingual
carunculae
sublingual, 21, 22
cauda epididymidis
see tail, epididymis
caudomesocolic region, 128–134
arteries, 133
caecum, 129
circulation, portal, 134
colon, 129
duodenum, 129
gland, adrenal, 132, 133
ileum, 129
intestine
large, 130, 131
small, 129, 130
jejunum, 129
kidneys, 131, 132
lymph, system of, 134, 135
peritoneum, 128, 129
ureter, 131, 132
urinary organs, 131
veins, 133, 134
cavity(ies)
abdominal (*cavum abdominis*), 122
see also abdomen, cavity
infundibular (*pars cava infundibuli*)
of pituitary gland, posterior lobe (*neurohypophysis*), 24
laryngeal
caudal (*cavum laryngis caudalis*), 80
intermediate (*cavum laryngis intermedium*), 80
nasal (*cavum nasi*), 17, 18
oral (*cavum oris*), 19, 20, **29, 32, 33, 34, 45**
proper (*cavum oris proprium*), 19
paranasal (*sinus paranasalis*), 19
pelvic (*cavum pelvis*), 121, 128
peritoneal (*cavum peritonei*), 122
pleural
intermediate (*cavum pleurae intermedium*), 87
left (*cavum pleurae sinistrum*), 87
right (*cavum pleurae dextrum*), 87
thoracic (*cavum thoracis*), 87–93
cavum abdominis
see cavity, abdominal
cavum hypophysis
see cleft, interhypophyseal
cavus infraglotticum
see infraglottis
cavum laryngis caudale
see cavity, laryngeal
cavum laryngis intermedium
see cavity, *laryngeal*

cavum nasi
see cavity, nasal
cavum oris
see cavity, oral
cavum oris proprium
see cavity, oral, proper
cavum pelvis
see cavity, pelvic
cavum peritonei
see cavity, peritoneal
cavum pleurae dextrum
see cavity, pleural, right
cavum pleurae intermedium
see cavity, pleural, intermediate
cavum pleurae sinistrum
see cavity, pleural, left
cavum thoracis
see cavity, thoracic
centrum tendineum
see tendon, central
cerebellum, 23, **29**
fissures (*fissura cerebelli*), **57, 58, 59**
hemisphere of (*hemispherium cerebelli*), **61**
lobules (*lobuli cerebelli*), **57, 58, 59, 60**
cerebrum, **29, 35, 36**
cervical region, 65–69, **71, 97**
hemisphere of (*hemispherium cerebri*), 61
cervix (*cervix uteri*), 138, 139
cervix uteri
see cervix
cheek pouches (*bursae buccales*), 19, 20, **45, 46, 47, 52, 53, 64, 73, 77, 109**
cheeks (*buccae*), 19, 20
mastication in, 20
retractor bursae buccalis et retractor buccinator of, 20
chiasma, optic (*chiasma opticum*), 23, **59, 60, 61**
chiasma opticum
see chiasma, optic
choana (*choana*), 17, 18, **29, 30, 35**
cisterna chyli, 134
clavicle (*clavicula*), 65, 66
extremitas acromialis, **76**
extremitas sternalis, **76**
clavicula
see clavicle
claws (*ungues*), **9**
cleft
interhypophyseal (*cavum hypophysis*) of pituitary gland, anterior lobe (*adenophysis*), 24
clitoris (*clitoris*), 138
coelic lymph center, 134
colliculus rostralis, **59**
colon, **166**
ascending (*colon ascendens*), **164**
caecum, apex (*apex caeci*), 130
caecum, body (*corpus caeci*), 130
descending (*colon descendens*), 130, 131, **167**
lymph centers, 135
mesocolon, 130
mucosa, **166**
transverse (*colon transversum*), 123, 128, 130, 131
colon ascendens
see colon, ascending
colon descendens
see colon, descending
colon transversum
see colon, transverse
coloring
summer vs. winter, 1, **6**
column
spinal (*columna vertebralis*), **70, 72,** 85, 88, 93, 123, 125, 128, **141**
columna vertebralis
see column, spinal, and vertebra
commissure, labial (*angulus oris*), 19, 20
commissure, rostral (*commissura rostralis*), **59**
concha
nasal
dorsal (*concha nasalis dorsalis*), 17, 18, **29, 32, 37, 41**
ventral (*concha nasalis ventralis*), 17, 18, **29, 32, 37**
concha nasalis dorsalis
see concha, nasal, dorsal
concha nasalis ventralis
see concha, nasal, ventral
condyle, occipital (*condylus occipitalis*), **30, 31**
cor
see heart
corona dentis
see teeth, crowns of
cornua uteri
see horns, uterine
cornu caudale
see horn, caudal

cornu dorsale
see horn, dorsal
cornu rostrale
see horn, rostral
corpora
albicantia, 138
atretica, 138
cavernosa, 137
lutea, 138
corpus
see body
corpus adiposum orbitae
see orbit, adipose tissue of
corpus caeci
see body, caecal
corpus callosum, **59**
corpus epididymidis
see body, epididymis
corpus linguae
see tongue, body
corpus mamillare
see body, mamillary
corpus penis
see body, penis
corpus sterni
see body, sternum
corpus trapezoides, **60**
corpus uteri
see body, uterine
corpuscles
renal (*corpuscula renis*), 132
corpuscula renis
see corpuscles, renal
cortex
of adrenal glands (*gll. suprarenales*), 133
of ovary (*zona parenchymatosa*), 138
renal (*cortex renis*), 132
cortex renis
see cortex, renal
costae
see ribs
costae spuriae
see ribs, asternal ("false" ribs)
costae verae
see ribs, sternal ("true" ribs)
cranial and facial vascularization, 25, 26
arteries, 25
ophthalmic plexus (*plexus ophthalmicus*), 25, 26
venous drainage of, 25, 26
cranial lymph center, 134, 135
craniomesocolic region, 124–128
arteries, 127, 128
duodenum, proximal, 125
esophagus, 124
liver, 125–127
nerves, 128
pancreas, 127
peritoneum, 122–124
spleen, 127
stomach, 124, 125
veins, 128
cranium
see neurocranium
crest
iliac (*crista iliaca*), 121, 132
cribriform plate (*lamina cribrosa*), 18, 23
Cricetus cricetus Lineé
see hamster, European
crista iliaca
see crest, iliac
crista mediana
see ridge, median
crurae, cerebral (*pedunculi cerebri*), 23
cupula pleurae
see pleura, cervical
curvatura ventriculi major
see curvature, greater
curvatura ventriculi minor
see curvature, lesser
curvature
greater (*curvatura ventriculi major*)
of stomach (*ventriculus*), 125
lesser (*curvatura ventriculi minor*)
of stomach (*ventriculus*), 125
cuspis angularis
see cusps, angular
cuspis parietalis
see cusps, parietal
cuspis septalis
see cusps, septal
cusps
angular (*cuspis angularis*), 90
parietal (*cuspis parietalis*), 90
septal (*cuspis septalis*), 90
cutis, **32, 33, 34**
decussation, pyramidal (*decussatio pyramidum*), **60**

dens
see process, odontoid, of axis
dens incisivium
see teeth, incisor
dentes
see teeth
dentes incisivi
see teeth, incisors
dentes molares
see teeth, molars
dentes permanentes
see teeth, permanent
dentes premolares
see teeth, premolars
dentition (*dentes*), 21
see also teeth
diaphragm (*diaphragma*), **77**, 86, 87, **99, 104, 105, 109**
foramen, vena cava (*foramen venae cavae*), 87, **105**
hiatus
aortic (*hiatus aorticus*), 86, **105**
esophageal (*hiatus esophageus*), 86, **104, 105**
muscle of (*diaphragma, pars muscularis*), 86
parts
rostral (*pars rostralis*), **105**
sternal (*pars sternalis*), **105**
lumbar (*pars lumbalis*), **105**
peritineum on, 123
tendon of, central (*centrum tendineum*), 86, **104, 105**
vessels of, 127, 128
diaphragma, pars muscularis
see diaphragm, muscle of
diploë, **34, 35**
disc
intervertebral (*discus intervertebrales*), 85
discus intervertebralis
see disc, intervertebral
distribution, of species, 2, **16**
dorsal mediastinum, 92, 93
dorsum nasi, **8**, 17
dorsum penis
see penis surface, dorsal
duct(s), ductule(s)
bile (*ductus choledochus*), 126, 127
bulbourethral gland (*ductus gl. bulbourethralis*), 137
ductus deferens, 132, 135, 136, 137, **180**
efferent, of prostate (*ductuli prostatici*), 137
ejaculatory (*ductus ejaculatorius*), 137
epididymis (*ductus epididymidis*), 136
excretory
of accessory lacrimal gland (*ductuli excretorii*), 24
of vesicular gland (*ductus excretorius*), 137
incisive (*ductus incisivius*), 17
interlobular, bile (*ductulus biliferus*), 127
mandibular (*ductus mandibularis*)
of sublingual gland, 22
nasolacrimal (*ductus nasolacrimalis*), 17, 25
pancreatic (*ductus pancreaticus*), 127
parotid (*ductus parotideus*), 22, **73**
prostatic (*ductuli prostatici*), 13, 7
sublingual (*ductus sublingualis*), 22
thoracic (*ductus thoracicus*)
see lymph trunks, thoracic
ductuli excretorii
see ducts, excretory, of accessory lacrimal gland
ductuli prostatici
see ducts, prostatic
ductulus biliferus
see duct, interlobular, bile
ductus choledochus
see duct, bile
ductus deferens
see duct, deferens and vas deferens
ductus ejaculatorius
see duct, ejaculatory
ductus epididymidis
see duct, epididymis
ductus excretorius
see duct, excretory, of vesicular gland
ductus incisivius
see duct, incisive
ductus mandibularis
see duct, mandibular
ductus nasolacrimalis
see duct, nasolacrimal
ductus pancreaticus
see duct, pancreatic
ductus parotideus
see duct, parotid
ductus sublingualis
see duct, sublingual

ductus thoracicus
see lymph trunks, thoracic
duodenum, 125, 129, **147, 150**
flexures
caudal (*flexura duodeni caudalis*), 129
cranial (*flexura duodeni cranialis*), 129
ligaments, duodenocolic, 129
parts
ascending (*duodenum, pars ascendens*), 129
cranial (*duodenum, pars cranialis*), 129
see also duodenum, proximal
descending (*duodenum, pars descendens*), 129
peritoneum of, craniomesocolic, 123
proximal, 125
vascularization of, craniomesocolic, 128
duodenum pars ascendens
see duodenum, ascending
duodenum pars cranialis
see duodenum, cranial and proximal
duodenum pars descendens
see duodenum, descending
ear, external (*auris externa*), 1, **8**
ear, internal (*auris interna*), **52**
ear, middle (*auris media*), **36, 39**
ectoturbinalia
see ectoturbinals
ectoturbinals (*ectoturbinalia*), 17, 18, **33, 34, 38**
edge(s)
sharp, of lung (*margo acutus*), 95
of soft palate (*velum palatinum*), 66
encephalon
see brain
end
dorsal, of spleen (*extremitas dorsalis*), 127
ventral, of spleen (*extremitas ventralis*), 127
endocardium, 90
endocrine system, see glands
endoturbinalia
see endoturbinals
endoturbinals (*endoturbinalia*), 17, 18, **29, 30, 33, 34, 35, 38, 40**
entrance
of epiglottis (*vallecula epiglottica*), 66
of pharynx (*aditus pharyngis*), 66
epicardium, 90
epididymis (*epididymidis*), 135, 136, **176**
body (*corpus epididymidis*), 136
caudal extremity (*cauda epididymidis*), 136
duct (*ductus epididymidis*), 136
head (*caput epididymidis*), 136
vascular cones of (*coni vasculosi*), 136
epiglottis (*epiglottis* or *valecula epiglottis*), 18, **29,** 66, 68
base (*basis*), 68
cartilage of (*cartilago epiglottica*), 67
soft palate, caudal edge (*velum palatinum*), 66
tip (*apex*), 68
episternum, 85
see also sternum
esophagus, **29, 80,** 86, 92, 93, **109, 111, 112, 113, 119,** 124, **147, 162**
foramen of
see hiatus, below
hiatus (*hiatus esphageus*), 93, 124
estrus cycle
wild vs. laboratory bred, 2
ethmoturbinalia
see ethmoturbinals
ethmoturbinals
ectoturbinals, 17, 18
endoturbinals, 17, 18
eustachean tube (*tuba auditiva*), 18
excavationes rectogenitalis et vesicogenitalis
see pouches, rectogenital and vesicogenital
external anatomy & features
body weight
dependence on hibernation, 1
male vs. female, 1, **6**
summer vs. winter, 1
coloring
summer vs. winter, 1, **6**
length
male vs. female, 1, **6**
extremitas caudata
see poles, caudal
extremitas dorsalis
see end, dorsal
extremitas tubaria
see extremity, ovarian
extremitas uterina
see extremity, uterine
extremitas ventralis
see end, ventral
extremitates caudales
see poles, caudal

extremitates craniales
see poles, cranial
extremity(ies)
ovarian (*extremitas tubaria*), 138
uterine (*extremitas uterina*), 138
eye(s) (*oculi* or *bulbi oculi*), 1, **8,** 24, 26, **34, 35, 52, 61, 64**
eyelid(s), **8, 34**
lower (*palpebra inferior*), 25
upper (*palpebra superior*), 25
facies
see skeleton, facial
facies auricularis ossis sacri, 121
facies diaphragmatica
see surface, diaphragmatic
facies mediales
see surface, medial
facies parietalis
see surface, parietal
facies pulmonales
see surface, pulmonary
facies sternocostalis
see surface, sternocostal
facies visceralis
see surface, visceral
fascia, lumbodorsal (*fascia lumbodorsalis*), 20
fascia lumbodorsalis
see fascia, lumbodorsal
feet
see forefeet and hindfeet
female genital organs, **10, 11,** 138, 139, **182, 183, 185**
in active period, **183, 184**
in hibernation, **183, 184**
cervix, 138, 139
clitoris, 138, 139
ovaries, 138, **183**
oviducts, 138, **186**
uterine horns, 138, 139
uterus, 138, 139, **186**
vagina, 138, 139
fissura lig. teretis
see fissure, ligamentum teres
fissura palatina
see fissure, palatine
fissurae interlobares
see fissures, interlobar
fissure(s)
interlobar (*fissurae interlobares*)
of lung, 95
ligamentum teres (*fissura lig. teretis*)
of liver, 126
palatine (*fissura palatina*), 17, 19
transverse
of craniomesocolic peritoneum, 128
flank organs
see organs, flank
flexura duodeni caudalis
see flexure, duodenal, caudal
flexura duodeni cranialis
see flexure, duodenal, cranial
flexure(s)
duodenal
caudal (*flexura duodeni caudalis*), 129
cranial (*flexura duodeni cranialis*), 125, 129
fold(s)
aryepiglottic (*plica aryepiglottica*), 66
oral, mucosa (*tunica mucosa oris*), 19
pleural, investing the vena cava (*plica venae cavae*), 88
vocal (*plica vocalis*), **80**
follicles
ovarian (*folliculi ovarici*), 138
folliculi ovarici
see follicles, ovarian
foramen
epiploic (*foramen epiploicum*)
of craniomesocolic peritoneum, 123
esophageal, 124
jugular (*foramen jugulare*), 25, **31**
mandibular (*foramen mandibulae*), **44**
mental (*foramen mentale*), **44**
optic (*foramen opticum*), 24
transverse (*foramen transversarium*), 65
vena cava (*foramen venae cavae*), 128
foramen epiploicum
see foramen, epiploic
foramen incisivum, **31**
foramen jugulare
see foramen, jugular
foramen lacerum, **31**
foramen magnum, **31**
foramen mandibulae
see foramen, mandibular
foramen mentale
see foramen, mental

foramen obturatum
see opening obturator
foramen opticum
see foramen, optic
foramen ovale, 25, **31**
foramen transversarium
see foramen, transverse
foramen venae cavae
see aperture, vena cava and foramen, vena cava
forestomach (*proventriculus*), 93, 124, 126, 127, 134
see also stomach
forefeet
pads (*tori*), 1, 9
palms or soles (*palma manus*), 1, 9
fornix, 59
fossa masseterica, 44
fossa pterygoidea, 44
fovea costalis caudalis
see ribs, fovea
fovea costalis cranialis
see ribs, fovea
frenulum(a)
labial
mandibular (*frenulum labii mandibularis*), 19
maxillary (*frenulum labii maxillaris*), 19
lingual (*frenulum linguae*), 20–22
frenulum labii mandibularis
see frenulum, labial, mandibular
frenulum labii maxillaris
see frenulum, labial, maxillary
frenulum linguae
see frenulum, lingual
fundus
of stomach (*fundus ventriculi*), 125
fundus ventriculi
see fundus, of stomach
gall bladder: lacking in this species (*vesica fellea*)
ganglia coeliaca
see ganglia, coeliac
ganglia trunci sympathici
see ganglia, sympathetic
ganglion(a)
cervical cranial (*ganglion cervicale craniale*), 66
cervical middle (*ganglion cervicale medium*), 66
coeliac (*ganglia coeliaca*), 128
stellate (*ganglion stellatum*), 66
sympathetic (*ganglia trunci sympathici*), 128
ganglion cervicale craniale
see ganglion, cervical, cranial
ganglion cervicale medium
see ganglion, cervical, middle
ganglion stellatum
see ganglion, stellate
gingivae
see gums
girdle, pectoral
see bones, clavicle, ribs, scapula, and sternum
gland(s)
adrenal, 132, 133, **170**
cortex, **170, 171**
medulla, **170, 171**
nerves, 128
suprarenal arteries (*aa. suprarenales*), 133
suprarenal veins (*vv. suprarenales*), 133
zona fasciculata, **173**
zona glomerulosa, 133
zona medullaris, **173**
zona reticularis, 133
bronchial, 95
bulbourethral (*gll. bulbourethrales*), 134, 137
duct (*ductus gl. bulbourethralis*), 137
cardiac (*gll. cardiacae*)
of stomach, 125
duodenal (*gll. duodenales*), 129
genital, accessory (*gll. genitales accessoriae*), 136
intestinal (*gll. intestinales*), 129
lacrimal apparatus (*apparatus lacrimalis*), 24, 25, **52**
accessory lacrimal gl. (*gl. lacrimalis accessoria*), 24
canals
infraorbital (*canalis infraorbital*), 25
tear (*canaliculi lacrimales*), 25
duct(s)
excretory (*ductuli excretorii*), 24
nasolacrimal (*ductus nasolacrimalis*), 25
lacrimal gl. (*gl. lacrimalis*), 24, **33, 34, 35**
sac(s)
conjunctival (*saccus conjunctivae*), 24

lacrimal (*saccus lacrimalis*), 24
mandibular (*gl. mandibularis*), 21, 22, 65, 66, **77, 109**
orbital, external
see gland, zygomatic
parathyroid (*gl. parathyreoidea*), 69, **79**
parotid (*parotis*), 22, **73**
lymph node (*ln. parotideus*), 67
parotid duct (*ductus parotideus*), 22
salivary papilla (*papilla parotidea*), 22
pituitary (*hypophysis*), 23, 24, **61, 62**
anterior lobe (*adenohypophysis*) distal part of, (*pars distalis*), 24, **62**
acidophils, 24
somatotropes, 24
mammotropes, 24
basophils, 24
gonadotropes, 24
thyrotropes, 24
corticotropes, 24
chromophobes, 24
cavity, infundibular (*pars cava infundibuli*), 24, **62**
cleft, interhypophyseal (*cavum hypophysis*), 24, **62**
middle or intermediate lobe (*pars intermedia*), 24, **62**
posterior lobe (*neurohypophysis*), 24, **62**
sella turcica, 23
tuber cinereum, 23
praeputial (*gll. praeputiales*)
of penis, 137
prostate (*prostata*), 135, 137, **181**
pyloric (*gll. pyloricae*), 125
salivary (*gll. oris*), see also under individual glands, 21, 22, **52, 53, 54, 55**
mandibular (*glandula mandibularis*), 22, **52, 53, 54, 55**
parotid (*parotis*), 22, 23, **52, 53, 55, 56**
sublingual (*glandula sublingualis*), 22, **52, 53, 54, 55**
zygomatic (*glandula zygomatica*), 23, **52, 53**
sebaceous
gland, Zymbal gland analogue, **56**
umbilical glandular organ, 2, **12**
sublingual (*gl. sublingualis*), 22
mandibular duct (*ductus mandibularis*), 22
sublingual caruncles, 22
sublingual duct (*ductus sublingualis*), 22
thymus, 88, 92, 93, **111**
left (*thymus sinister*), **77**
right (*thymus dexter*), **77**
thyroid (*gl. thyreoidea*), 67, 69, **79, 80, 83**
uterine, **186**
vesicular (*gll. vesiculares*), 136, 137, **181**
duct, excretory (*ductus excretorius*), 137
sheaths
external areolar (*tunica adventitia*), 137
internal mucous (*tunica mucosa*), 137
muscular (*tunica musculosa*), 137
zygomatic (*gl. zygomatica*), 23
gll. bulbourethrales
see glands, bulbourethral
gll. cardiacae
see glands, cardiac
gll. duodenales
see glands, duodenal
gll. genitales accessoriae
see glands, genital accessory
gll. intestinales
see glands, intestinal
gl. lacrimalis
see gland, lacrimal
gl. lacrimalis accessoria
see gland, lacrimal, accessory
gl. mandibularis
see gland, mandibular
gl. parathyreoidea
see gland, parathyroid
gll. praeputiales
see glands, praeputial
gll. pyloricae
see glands, pyloric
gl. suprarenalis
see gland, adrenal
gl. sublingualis
see gland, sublingual
gl. thyreoidea
see gland, thyroid
gll. vesiculares
see glands, vesicular

gl. zygomatica
see gland, zygomatic
glans penis, 137
glottis
of larynx, 68
groove(s)
interventricular (*sulcus interventricularis*)
of heart, 89
urethral (*sulcus urethralis*)
of penis, 137
vena cava (*sulcus venae cavae*)
of lung, 96
gums (*gingivae*), 20, 21
hairs (*pili*)
length of, 1, **6**
tail and scrotum
length of, 1, **6**
hamster, European (*Cricetus cricetus Lineé*)
comparison with Syrian golden hamster, **4**
haustra
of caecum, 130
head
of epididymis (*caput epididymidis*), 136
head, region, 17–26
heart (*cor*), 82, 89, 90, 107, 111, 118, 120
aorta, ascending, 89
apex (*apex cordis*), 89
atrium
left (*atrium sinistrum*), 89, 90, 106
right (*atrium dextrum*), 89, 90, 106
auricles, 89
left (*auricula dextra*), 77, 109
right (*auricula sinistra*), 77, 109, 111
base (*basis cordis*), 89
cusp
angular (*cuspis angularis*), 90
parietal (*cuspis parietalis*), 90
septal (*cuspis septalis*), 90
endocardium, 90
epicardium, 90
ligament
phrenicopericardial (*ligamentum phrenicopericardiacum*), 89
mediastinum, ventral, 89, 90
muscles, papillary (*mm. papillares*), 90
myocardium, 90, 106, 107
nerves, 89, 92
pericardium
parietal portion (*lamina parietalis*), 89
visceral portion (*lamina visceralis*), 89
ring, fibrous (*annulus fibrosa*), 90
septum
interventricular (*septum interventriculare*), 106
sulcus
coronary (*sulcus coronarius*), 89
interventricular (*sulcus interventricularis*), 89
surface
left pulmonary (*facies pulmonales sinistra*), 89
right pulmonary (*facies pulmonales dextra*), 89
sternocostal (*facies sternocostalis*), 89
trabecula septomarginalis, 106, 108
valve
aortic (*valva aortae*), 90
bicuspid (*valva bicuspidalis*), 90
pulmonary (*valva truncae pulmonis*), 90
semilunar (*valvulae semilunares*), 90
tricuspid (*valva tricuspidalis*), 90
ventricle
left (*ventricle sinister*), 77, 89, 90, 106, 109, 111
right (*ventricle dexter*), 77, 89, 90, 106, 107, 108, 111
hepar (see liver)
hemisphere, cerebellar (*hemispherium cerebelli*)
see cerebellum, hemisphere of
hemisphere, cerebral (*hemispherium cerebri*)
see cerebrum, hemisphere of
hiatus (see also opening, aperture)
aortic (*hiatus aorticus*), 86, 124, 127
esophageal (*hiatus esophagus*), 86, 88, 93, 104
hiatus aorticus
see opening, aortic
hiatus esophageus
see hiatus, esophageal
hibernation
deposits, fat, 1, **7**
glands, in
ovaries, 138
parathyroid (*gl. parathyreoidea*), 69
pituitary (*hypophysis*), 24
prostate (*prostata*), 137
thyroid (*gl. thyreoidea*), 69
testis, 136

hibernation—*continued*
laboratory effects in
artificial induction, **5**
lifespan changes, *v*
reproduction, 2
sex determination, 1, 2
vagina, 2, 139
weight, body, 1
hilus
kidney (*hilus renalis*), 131
liver (see portal, hepatic)
lung, 95, 96
ovary (*hilus ovarici*), 138
spleen (*hilus lienis*), 127
hilus lienis
see hilus, spleen
hilus ovarici
see hilus, ovary
hilus renalis
see hilus, kidney
hindfeet
claws (*ungues*), **9**
pads (*tori*), 1, **9**
soles (*planta*), 1, **9**
horn(s)
caudal (*cornu caudale*), 67
cranial (*cornu rostrale*), 67
dorsal (*cornu dorsale*), 67
uterine (*cornua uteri*), 131, 138, 139
humerus
xiphoid process, 65
hypophysis
see gland, pituitary
hypothalamus
length of, 23
illeum, 129, 130
ligament, ileocaecal (*plica ileocaecalis*), 129, 130
lymph
centers, 135
nodes, ileocaecal (*lnn. ileocaecales*), 135
"valve, ileocaecal" (*papilla ilealis*), 130
impressio cardiaca dextra
see impression, of lung
impressio esophagea
see impression, of liver, gastric
impressio gastrica
see impression, of liver, esophageal
impressio renales
see impression, of liver, renal
impression
of liver
esophageal (*impressio esophagea*), 126
gastric (*impressio gastrica*), 126
renal (*impressio renalis*), 126
of lung
cardiac, left (*impressio cardiaca sinistra*), 96
cardiac, right (*impressio cardiaca dextra*), 96
incisura clavicularis
see notch, clavicular
incisivus ductus
see duct, incisive
incisura vasorum facialium, 25, **44**
incisura vertebralis caudalis
see ribs, incisura
incisura vertebralis cranialis
see ribs, incisura
infraglottis (*cavum infraglotticus*), 68
infundibulum,
of the oviducts (*infundibulum tubae uterinae*), 138
of pituitary (*pars cava infundibuli*), 24, **60, 61**
infundibulum tubae uterinae
see infundibulum, of the oviducts
intrapulmonary system, 94, 95
bronchioles, 94
segmental bronchi (*bronchi segmentales*), 94
intestine, see also under separate terms, **162**
large (*intestinum crassum*), 130
anus (*anus*), 130
caecum (*caecum*), 130
colon (*colon*), 130
lymph centers (*lymphocentrum*), 135
mucous membrane, 130
rectum (*rectum*), 130
small (*intestinum tenue*), 129
duodenum, 129
glands
duodenal (*gll. duodenales*), 129
intestinal (*gll. intestinales*), 129
illeum, 129
jejunum, 129
junction, ileocaecal (*ostium ileale*), 129
layers, **163**
lymph centers (*lymphocentrum*), 135

intestine—*continued*
mucous membrane of, 129, **163**
peritoneum of
caudomesocolic, 128
craniomesocolic, 123
pylorus, 125
intestinum crassum
see intestine, large
intestinum tenue
see intestine, small
jaws
see also bone, mandible, maxilla, **50**
jejunum (*jejunum*), 129, **164, 165, 166**
lymph centers (*lymphocentrum*), 135
lymph nodes (*lnn. jejunales*), 135
mucosa, **166**
joint(s)
intermandibular (*articulatio intermandibularis*), **44, 62**
temporomandibular (*articulatio temporomandibularis*), **44**
junction,
esophageal, with stomach, 125
ileocaecal (*ostium ileale*), 129
kidney (*ren*), 131, 132, **161, 168, 169, 170, 171**
arteries
interlobular (*aa. interlobulares*), 131
renal (*a. renalis*), 131
calyces (*calices renales*), 132
capsule, connective tissue (*capsula fibrosa*), 132
capsule, perirenal fat (*capsula adiposa*), 132, **170**
corpuscles (*corpuscula renis*), 132, **172**
cortex (*cortex renis*), 132, **170, 171**
hibernation, in, 132
hilus (*hilus renalis*), 131
lymph nodes (*lnn. renales*), 135
medulla (*medulla renis*), 132, **172**
nerves, 128
papilla (*papilla renalis*), 131, **170**
pelvis (*pelvis renalis*), 132, **173**
pole, caudal (*extremitates caudales*), 131
pole, cranial (*extremitates craniales*), 131
tubules, convoluted (*tubuli renales contorti*), 132
tubules, straight (*tubuli renales recti*), 132
veins
interlobular (*vv. interlobulares*), 131
renal (*v. renalis*), 131
zona intermedia, **170**
zona basalis, **170**
labium mandibulare
see lip, lower
labium maxillare
see lip, upper
labia oris
see lips
lacrimal apparatus, 24
lacrimal gland, 24
see gland, lacrimal
lactation, **11**
lamina
cricoid, of larynx (*lamina cricoidea*), 67, **80**
external (*lamina externa*) of prepuce, 137
internal (*lamina interna*) of prepuce, 137
thyroid (*laminae thyreoideae*) of larynx, 67
lamina cribrosa
see cribriform plate
lamina cricoidea
see lamina, cricoid
lamina perpendicularis, **30**
lamina tecti, 57
laminae externa et internae
see lamina, external and internal
laminae thyreoideae
see lamina, thyroid
Langerhans, islets of, **158**
larynx, **29**, 67, 68, **73, 75, 79, 82, 118**
cartilages
arytenoid (*cartilago arytenoidea*), **29**, 67, **80, 81**
muscular process (*processus muscularis*), 68
vocal process (*processus vocalis*), 68
corniculate (*cartilago corniculata*), 67
cricoid (*cartilago cricoidea*), 67, **80, 81**
arch (*arcus cricoideus*), 67
lamina (*lamina cricoidea*), 67, **80**
ridge (*crista mediana*), 67
cuneiform (*cartilago cuneiformis*), 67
epiglottis (*cartilago epiglottica*), **29**, 67, **80, 81**
thyroid (*cartilago thyreoidea*), 67, **80, 81**
plates (*laminae thyreoideae*), 67
cranial horn (*cornu rostrae*), 67
caudal horn (*cornu caudale*), 67
dorsal horn (*cornu dorsale*), 67

larynx—*continued*
cavities
caudal (*cavum laryngis caudale*), **80**
intermediate (*cavum laryngis intermedium*), **80**
epiglottis, 68
folds
aryepiglottic (*plicae aryepiglotticae*), 68
vestibular (*plica vestibularis*), 68
vocal (*plica vocales*), 68, **80**
glottis, 68
infraglottis (*cavum infraglotticum*), 68
muscles
arytaenoideus transversus (*m. arytaenoideus transversus*), 68
cricoarytaenoideus dorsalis muscle (*m. cricoarytaenoideus dorsalis*), 68
cricoarytaenoideus lateralis muscle (*m. cricoarytaenoideus lateralis*), 68
cricothyreoideus (*m. cricothyreoideus*), 68
cricotrachealis muscle (*m. cricotrachealis*), 68
hyoepiglotticus (*m. hyoepiglotticus*), 68
sternohyoideus (*m. sternohyoideus*), 68
thyreoarytaenoideus muscle (*m. thyreoarytaenoideus*), 68
thyreohyoideus muscle (*m. thyreohyoideus*), 68
vocalis muscle (*m. vocalis*), 68
opening (*aditus laryngis*), 61
ligaments
cricothyroid (*lig. cricothyreoideum*), 67, 68
cricotracheal (*lig. cricotracheale*), 68
thyreoepiglottic (*lig. thyreoepiglotticum*), 68
vocal (*lig. vocale*), 68
rima glottidis, 68
ventricles, **80**
lateral (*ventriculus laryngis lateralis*), 68, **80**
median (*ventriculus laryngis medianus*), 68
latissimus dorsi
see muscle, latissimus dorsi
layers
fibrous (*tunica adventitia*) of ureter, 132
mucous (*tunica mucosa*)
of ureter, 132
of vesicular glands, 137
muscular (*tunica muscularis*)
of ureter, 132
of vesicular glands, 137
sheath, external areolar (*tunica adventitia*) of vesicular glands, 137
length
male vs. female, 1
lien
see spleen
lifespan
under laboratory conditions, *vi*
ligament(s)
annular, (*ligg. annularia*) of trachea, 69
broad, of ovary (*lig. latum uteri*), 138
coronary, of liver (*lig. coronarium hepatis*), 123, 126
cricothyroid (*lig. cricothyreoideum*), 67
cricotracheal (*lig. cricotracheale*), 68
duodenocolic (*plica duodenocolica*), 129, **156**
falciform, of liver (*lig. falciforme*), 126, 128
gastrophrenic (*lig. gastrophrenicum*), 124
gastrosplenic (*lig. gastrolienale*), 127, **159**
hepatoduodenal, (*lig. hepatoduodenale*) of lesser omentum, 125
hepatogastric (*lig. hepatogastricum*), 123, 125
ileocaecal (*plica ileocaecalis*), 129, 130
lateral, of urinary bladder (*lig. vesicae laterales*), 132
lienoreal (*lig. lienorenale*), 124, 127
middle, of urinary bladder (*lig. vesicae medianum*), 132
ovarian (*lig. ovarii*), 138
phrenicopericardical (*lig. phrenicopericardiacum*), 89
pulmonary (*lig. pulmonale*), 95
sternopericardial (*lig. sternopericardiaca*), 88
teres, of liver (*lig. teres hepatis*), 126
thyroepiglottic (*lig. thyreopiglotticum*), 68
triangular, left, of peritoneum (*lig. triangularia sinistrum*), 123, 126
triangular, right, of peritoneum (*lig. triangularia dextrum*), 123, 126
vocal (*lig. vocale*), 68
ligg. annularia
see ligaments, annular
lig. coronarium sinistrum hepatis
see ligament, coronary, left
lig. cricothyreoideum
see ligament, cricothyroid

lig. cricotracheale
see ligament, cricotracheal
lig. falciforme hepatis
see ligament, falciform, of liver
lig. gastrolienale
see ligament, gastrosplenic
lig. gastrophrenicum
see ligament, gastrophrenic
lig. hepatoduodenale
see ligament, hepatoduodenal
lig. hepatogastricum
see ligament, hepatogastric
lig. latum uteri
see ligament, broad, of uterus
lig. lienorenale
see ligament, lienorenal
lig. ovarii
see ligament, ovarian
lig. phrenicopericardiacum
see ligament, phrenicopericardial
lig. pulmonale
see ligament, pulmonary
lig. sternopericardiaca
see ligament, sternopericardial
lig. teres hepatis
see ligament, teres, of liver
lig. thyreopiglotticum
see larynx, ligaments
lig. triangulare dextrum
see ligament, triangular, right
lig. triangulare sinistrum
see ligament, triangular, left
lig. vesicae lateralis
see ligament, lateral, of urinary bladder
lig. vesicae medianum
see ligament, middle, of urinary bladder
lig. vocale
see ligament, vocal and larynx, ligaments
lingua
see tongue
lips (*labia oris*), 19
lower, (*labium mandibulare*), 19
upper, (*labium maxillare*), 19
liver (*hepar*), 125–127, **152**
artery (*a. hepatica*), 127
capsule, fibrous (*capsula fibrosa*), 126–127
ducts
bile (*ductus choledochus*), 126
ductules
interlobular (*ductulus biliferus*), 127
fissure, ligamentum teres (*fissura lig. teretis*), 126
impressions
esophageal (*impressio esophagea*), 126
gastric (*impressio gastrica*), 126
renal (*impressio renalis*), 126
ligaments
coronary (*lig. coronarium*), 126
falciform (*lig. falciforme*), 126
teres (*lig. teres hepatis*), 126
triangular (*ligg. triangularia*), 126
lobes, **151**
caudate (*lobus caudatus*), 125, 126
lateral, left (*lobus hepatis sinister lateralis*), 125
lateral, right (*lobus hepatis dexter lateralis*), 126
medial, left (*lobus hepatis sinister medialis*), 125
medial, right (*lobus hepatis dexter medialis*), 125
quadrate (*lobus quadratus*), 126
lobules, 127, **153**
portal (*porta hepatis*), 126
processes, of caudate lobe
caudate (*processus caudatus*), 126
papillary (*processus papillaris*), 126
surfaces
convex parietal (*facies diaphragmatica*), 126, 151
visceral (*facies visceralis*), 126, 151
veins
central (*v. centralis*), 127
hepatic (*v. hepatica*), 127
lobes (*lobi*)
of brain, 23
of liver, 125–128
of lung, 95, 96
of pancreas, 127, 154
lobi paramediani
of brain, 23, 60
lobules
of liver, 127
lobus accessorius
see lung, lobes
lobus cranialis
see lung, lobes

lobus caudalis
see lung, lobes
lobus caudatus
see liver, lobes
lobus hepatis dexter lateralis
see liver, lobes
lobus hepatis dexter medialis
see liver, lobes
lobus hepatis sinister lateralis
see liver, lobes
lobus hepatis sinister medialis
see liver, lobes
lobus intermedius accessorius
see lung, lobes
lobus medius
see lung, lobes
lobus pancreatis dexter
see pancreas, lobes
lobus piriformis, 61
lobus quadratus
see liver, lobes
lobus sinister
see liver, lobes
lordosis
of cervical vertebrae, 65
lumbar
fat deposits of, 7
lobi
see lobes
lungs (*pulmo*), **77,** 94–96, **111, 114, 115, 118, 119, 120**
alveoli, 94
arteries
pulmonary (*a. pulmonalis*), 94, 96
bronchioles, 94
ducts
alveolar, 94
edge, of left lung (*margo acutus*), 95
fissures
interlobar, 95
groove
vena cava (*sulcus venae cavae*), 96
hilum
pulmonary, 95
impressions, cardiac
left lobe, 96
intermedial lobe, 96
ligaments
pulmonary (*lig. pulmonale*), 95
lobes
accessory (*lobus accessorius*), **77,** 95, **109, 111, 114, 119**
cranial (*lobus cranialis*), **77,** 95, **109, 115, 119**
diaphragmatic (*lobus caudalis*), **77,** 95, **109, 114**
intermediate accessory (*lobus intermedius accessorius*), 95, **114, 120**
left (*lobus sinister*), **77,** 95, **109, 111, 114**
middle (*lobus medius*), **77,** 95, **109, 114, 119**
lobules, 94, **109**
lymph nodes, bronchial (*lnn. bronchioles*), 95
nerves of, 92
pleura, 95
segments, bronchopulmonary, 94
root (*radix pulmonis*), 95
surfaces
diaphragmatic (*facies diaphragmatica*), 96, **104**
veins
pulmonary, 96
lymph
centers
coeliac (*lymphocentrum coeliacum*), 134
cranial mesenteric (*lymphocentrum mesentericum craniale*), 134
ilofemoral (*lymphocentrum iliofemorale*), 135
ilosacral (*lymphocentrum iliosacrale*), 135
inguinofemoral (*lymphocentrum inguinofemorale*), 135
mandibular (*lymphocentrum mandibulare*), **52,** 66, 67
popliteal (*lymphocentrum popliteum*), 135
retropharyngeal (*lymphocentrum retropharyngeum*), 67
duct, right (*ductus lymphaticus dexter*), 92
lymph nodes
accessory hepatic (*lnn. hepatici accessorii*), **78,** 134
accessory axillary (*lnn. axillaris accessorius*), 67, **78**
aortic lumbar (*lnn. lumbales aortici*), 135
axillary (*ln. axillaris*), 67, **78**
bronchial (*lnn. bronchiales*), 95

lymph nodes—*continued*
cervical, caudal, deep (*lnn. cervicalis profundus cranialis*), 67, **78**
colic or colonic (*lnn. colici*), 135
gastric (*lnn. gastrici*), 134
hepatic (*lnn. hepatica*), **78,** 134
iliac, lateral (*lnn. iliaci laterales*), **78,** 135
iliac, medial (*lnn. iliaci mediales*), **78,** 135
iliocaecal (*lnn. iliocaecales*), 135
inguinal, deep (*lnn. inguinales profundi*), **78,** 135
inguinal, superficial (*lnn. inguinales superficales*), **78,** 135
jejunal (*lnn. jejunales*), 135
mandibular (*lnn. mandibulares*), 66, 67
caudal (*lnn. mandibulares caudalis*), **78**
rostral (*lnn. mandibulares rostralis*), **78**
mesenteric, cranial (*lnn. mesenterici craniales*), 135
pancreaticoduodenal (*lnn. pancreaticoduodenales*), 134
parotid (*lnn. parotideus*), **52,** 67, **78**
popliteal (*ln. popliteus*), **78,** 135
renal (*lnn. renales*), **78,** 135
retropharyngeal (*lnn. retropharyngei*), 67
lateral (*lnn. retropharyngeus lateralis*), **78**
medial (*lnn. retropharyngeus medialis*), **78**
sacral (*lnn. sacrales*), **78,** 135
tracheobronchial (*lnn. trachiobronchales*), 92
left dorsal (*ln. tracheobronchales sinister dorsalis*), **144**
left ventral (*lnn. tracheobronchales sinistri ventrales*), **114**
right dorsal (*lnn. tracheobronchales dextri dorsales*), **114**
right ventral (*lnn. tracheobronchales dextri ventrales*), **114**
lymph trunks
coeliac (*truncus coeliacus*), 134
intestinal (*truncus intestinales*), 134
lumbar (*truncus lumbalis*), 134
thoracic (*truncus thoracicus* or *ductus thoracicus*), 92, **114**
lymphocentrum coeliacum
see lymph centers, coeliac
lymphocentrum mandibulare
see lymph centers, mandibular
lymphocentrum mesentericum craniale
see lymph centers, mesenteric, cranial
lymphocentrum retropharyngeum
see lymph centers, retropharyngeal
male
genital organs of, **10, 11, 175, 176, 177**
ampullae, of *vas deferens,* 135, **176, 179, 180**
ductus deferens, 135
epididymis, 135, **176**
penis, **181**
glands
accessory genital (*gll. genitales accessoriae*), 135
bulbourethral (*gll. bulbourethrales*), 135
prostate (*prostata*), 135, **181**
vesicular (*gll. vesiculares*), 135, **180**
scrotum, 135
testes, 135, **176**
urethra, pelvic part (*pars pelvina*), 135
vas deferens, 135
mammillae
see teat
mandibles
see bones, mandible, 19
mandibular gland, 22
see glands, mandibular
manubrium
of sternum, 65, 88, 93
margo acutus
see lungs, edge
margo plicatus
of esophagus, 124
massa intermedia, **59**
mastication
cheeks (*buccae*), 20
mating
wild vs. laboratory bred, 2
maxilla
see bones, maxillary
maxilloturbinal
see concha, nasal, ventral
meatus, auditory, external (*meatus acusticus externus*), 8, **31, 36, 73**
meatus, auditory, internal (*meatus acusticus internus*), **30**
meatus
nasal
dorsal (*meatus nasi dorsalis*), 18, **29, 32, 33**

meatus, nasal—*continued*
middle (*meatus nasi medius*), 18, **29, 32,** 33
ventral (*meatus nasi ventralis*), 18, **29,** 32, 33, **34**
mediastinum
dorsal, 92–93
ventral, 88–92
medulla
of brain (*medulla oblongata*), 23, **29, 58, 59, 61**
of gland, adrenal, 133
of kidney, 132
of ovary (*zona vasculosa*), 138
of spinal cord (*medulla spinalis*), **29**
melanin, 2
membrane, mucous
of hard palate, 20
of large intestine, 130
of small intestine, 129
mesocolon, 122, 123, 130
mesogastrium, 129
mesojejunum, 129, **165**
mesovarium, 138
mucosa
of oral cavity (*tunica mucosa oris*), 19, 20
muscle(s)
arytaenoideus transversus, 68
biceps femoris, 135
brachiocephalic (*m. brachiocephalicus*), 65
cleidobrachial (*m. cleidobrachialis*), 65
cleidocephalic (*m. cleidocephalicus*), 65, 66, **73**
cricoarytaenoideus
dorsalis, 68, **80**
lateralis, 68
cricothyreoideus, 68
cricotrachealis, 68
digastric (*m. digastricus*), **53,** 65, **73, 74**
gastrocnemius, 135
hyoepiglotticus, 68
iliac (*m. iliacus*), 121
intercostals
external (*mm. intercostales externi*), 86
internal (*mm. intercostales interni*), 86
ischiourethralis, 137
laryngeal, 68
latissimus dorsi, 67
levatores costarum, 86
longus colli, 63, 66
masseter, 22, **53, 74**
medialis, pars rostralis, **73**
pars superficialis, **73**
oblique, external (*m. obliquus externus*), **53, 74**
oblique, internal (*m. obliquus internus*), 121
omohyoid (*m. omohyoideus*), 65
omotransversarius (*m. omotransversarius*), 65
papillary, of heart (*mm. papillares*), 90
pectorals, deep (*m. pectoralis profundus*), 66
pectorals, superficial (*m. pectoralis superficiales*), **53**
caudal transverse (*pars transversus*), 66
clavicular (*pars clavicularis*), **53, 74**
cranial descending (*pars descendens*), 66
sternocostal (*pars sternocostalis*), **53, 74**
psoas major (*m. psoas major*), 121, 128
quadrate (*m. quadratus lumborum*), 121
rectus abdominis, 121
retractor
buccinator, 20
bursae buccalis, 20, **47**
scalene
dorsal (*m. scalenus dorsalis*), 65
middle (*m. scalenus medius*), 65
semitendinosus, 135
sphincter
pyloric (*m. sphincter pylori*), 125
sternocephalic (*m. sternocephalicus*), 66
sternohyoid (*m. sternohyoideus*), **53, 77, 109**
sternothyreoideus, 68, **77, 109**
temporal (*m. temporalis*), **73**
terres major, 67
thyreoarytaenoideus, 68
thyreohyoideus, 68, **73**
tracheales, 69
transversus tracheae, **80**
triceps brachii, 67, **74**
vocalis, 68
m. brachiocephalicus
see muscle, brachiocephalic
m. cleidobrachialis
see muscle, cleidobrachial
m. cleidocephalicus
see muscle, cleidocephalic
m. digastricus
see muscle, digastric

m. iliacus
see muscle, iliac
mm. intercostales externi
see muscles, intercostals, external
mm. intercostales interni
see muscles, intercostals, internal
m. obliquus internus
see muscle, oblique, internal
m. omohyoideus
see muscle, omohyoid
mm. papillares
see muscles, papillary
m. pectoralis superficialis pars descendens
see muscle, pectoral, superficial, descending
m. pectoralis superficialis pars transversus
see muscle, pectoral, superficial, transverse
m. quadratus lumborum
see muscle, quadrate
m. scalenus dorsalis
see muscle, scalene, dorsal
m. scalenus medius
see muscle, scalene, middle
m. sternocephalicus
see muscle, sternocephalic
myocardium, 90
nares
see nostrils
nasal cavity
see cavity, nasal, 17, 18
nasolacrimal duct (*ductus nasolacrimalis*), 25
see also duct, nasolacrimal
nasopharynx (*pharynx, pars nasalis*), 17, 18, 24, **29, 36,** 66
nasoturbinal
see concha, nasal
neck
see cervical region
neopallium, **57, 58, 59**
neurocranium or brain case (*cranium*), 17, 23
ethmoid bone (*os ethmoides*), 17, 23
cribriform plate of (*lamina cribrosa*), 23
frontal bone (*os frontale*), 17, 23
interparietal bone (*os interparietale*), 23
occipital bone (*os occipitale*), 23
parietal bone (*os parietale*), 23
sphenoid bone (*os sphenoidale*), 23
neurohypophysis
see gland, pituitary, posterior lobe
nerves
cervical, 92
cranial, 23
facial (*n. facialis*), **60**
genitofemoral nerve (*n. genitofemoralis*), 128
hypoglossal (*n. hypoglossis*), **60**
iliohypogastric nerve (*n. iliohypogastricus*), 128
laryngeal, recurrent, left (*n. laryngeus recurrens sinister*), 92
laryngeal, recurrent, right (*n. laryngeus recurrens dexter*), 92
mandibular (*n. mandibularis*), **61**
maxillary (*n. maxillaris*), **61**
of mediastinum, ventral, 92
oculomotor (*n. oculomotorius*), 23, **60**
olfactory, 19
optic, 23, 26, **61**
phrenic (*nn. phrenici*), 88, 92
splanchnic (*nn. splanchnici*), 128
major (*n. splanchnici major*), 128
minor (*n. splanchnici minor*), 128
thoracic, 92
trigeminal (*n. trigeminus*), 23, **60, 61**
trochlear (*n. trochlearis*), 23
trunk, sympathetic (*truncus sympatheticus*), 88, 92, 93, 128
trunk, vagosympathetic (*truncus vagosympatheticus*), 66
vagus nerves (*nn. vagii*), 88, 89, 92, 128
left (*n. vagus sinister*), **77,** 92, **109,** 128
right (*n. vagus dexter*), **77,** 92, **109,** 128
coeliac branch (*ramus coeliacus*), 128
gastric branch (*ramus gastricus visceralis*), 128
n. genitofemoralis
see nerve, genitofemoral
n. iliohypogastricus
see nerve, iliohypogastric
n. laryngeus recurrens dexter
see nerve, laryngeal, recurrent, right
n. laryngeus recurrens sinister
see nerve, laryngeal, recurrent, left
n. oculomotorius
see nerve, oculomotor

nn. phrenici
see nerves, phrenic
nn. splanchnic
see nerves, splanchnic
n. trigeminus
see nerve, trigeminal
n. trochlearis
see nerve, trochlear
nn. vagi
see nerves, vagus
n. vagus dexter
see nerve, vagus, right
n. vagus sinister
see nerve, vagus, left
nostrils (*nares*), 1, **8, 32**
notch, clavicular, 85
see also *sulcus*
oculi
see eyes
olfactory nerve
see nerve, olfactory
omentum
greater (*omentum majus*), 123, 124, 127
lesser (*omentum minus*), 125
omentum majus
see omentum, greater
omentum minus
see omentum, lesser
opening
aortic
mediastinum, 88
laryngeal (*aditus laryngis*), 67, 68
nasomaxillary
of paranasal cavity, 19
obturator
of pelvis, 121
preputial (*ostinum praeputiale*), 1
urinary (*orificium urethrae externum*), 2
urogenital, **11**
ophthalmic plexus, 25, 26, **64**
oral cavity, 19
see cavity, oral
orbit (*orbita*), **31**
adipose tissue of (*corpus adiposum orbitae*), 24
organa uropoetica, **168, 169**
see separate urinary organs
organ(s)
flank, 2, **13**
umbilical glandular, 2, **12, 32, 33,** 37
vomeronasal (*organum vomeronasale*), 18–19, **32, 33, 34, 41**
organum vomeronasale
see organs, vomeronasal
oropharynx (*pharynx, pars oralis*), 17, 19, 66
orifice(s)
external, of uterus (*ostium uteri externum*), 139
internal, of uterus (*ostia uteri interna*), 139
vaginal (*ostium vaginae*), **1,** 139
orificium urethrae externum
see opening, urinary
os coxae
see bone, pelvic
os ethmoidale
see bone, ethmoid
os frontale
see bone, frontal
os hyoideum
see bone, hyoid
os ilium
see bone, ilium
os incisivum
see bone, premaxillary
os interparietale
see bone, interparietal
os ischium
see bone, ischium
os nasale
see bone, nasal
os occipitale
see bone, occipital
os palatinum
see bone, palatine
os parietale
see bone, parietal
os praesphenoidale
see bone, presphenoid
os pubis
see bone, pubic
os sacrum
see bone, *sacrum*
os sphenoidales
see bone, sphenoid
os temporalis, pars mastoidea
see bone, temporal, mastoid process
os temporalis, pars petrosa
see bone, temporal, petrous portion

os temporalis, pars tympanica
see bone, temporal, tympanic portion
ossa cavi thoracis
see cage, bony thorax
ostinum ileale
see junction, iliocaecal
ostium praeputiale
see opening, preputial
ostium urethrae externum
see opening, urinary
ostium uteri externum
see orifice, external, of uterus
ostia uteri interna
see orifice, internal, of uterus
ostium vaginae
see orifice, vagina
outlet, pelvic (*apertura pelvis caudales*), 121
ovaries (*ovaria*), 138
bursa of (*bursa ovarica*), 138, **183**
corpora albicantia, 138
corpora atretica, 138
corpora lutea, 138
cortex (*zona parenchymatosa*), 138
extremity, tubal (*extremitas tubana*), 138
extremity, uterine (*extremitas uterina*), 138
follicles (*folliculi ovarici*), 138
hibernation, in, 138
hilus (*hilus ovarici*), 138
ligament (*lig. ovarii proprium*), 138
medulla (*zona vasculosa*), 138
tunica albuginea, 138
oviducts (*tuba uterina*), 138, **186**
fimbriae tubae, 138
infundibulum (*infundibulum tubae uterinae*), 138
pads (*tori*)
of forefeet, hindfeet, 1, **9**
palate
hard (*palatum durum*), 19, 20, **29, 32, 33, 34, 45, 48**
rugae of (*rugae palatinae*), 20
soft (*palatum molle*), 17–20, **29, 45,** 66, 68
palatum durum
see palate, hard
palatum molle
see palate, soft
palaeopallium, **60**
palma manus
see forefeet, soles
palpebra
see eyelid(s)
palpebrae inferior
see eyelids, lower
palpebrae superior
see eyelids, upper
pancreas, 122, 127, **154, 156, 157**
islets of Langerhans, **158**
lobes
left, 127, **154, 156, 157**
right, 127, **154, 156, 157**
within duodenocolic ligament, 127, **154, 156**
panniculus adiposus
see adipose
papilla
of kidney (*papilla renalis*), 131
salivary, of parotid (*papilla parotidea*), 22
papilla renalis
see kidney, papilla
papilla ilealis
see valve, ileocaecal
papilla parotidea
see papilla, salivary
papillae incisivae
of incisive ducts, 20
papillae linguales
see tongue, papillae
papillae mammae
see teats
paraflocculi
of brain, 23, **60, 61**
paranasal cavity (*sinus paranasales*)
see cavity, paranasal, 17, 19
parathormone, 69
parotid gland
see gland, parotid
parotis
see gland, parotid
pars cardiaca
see cardia, of stomach
pars cava infundibuli
of pituitary, 24
pars distalis
of pituitary, 24
pars intermedia
of pituitary, 24
pars pylorica
see pylorus, of stomach

pedunculi cerebri
see crurae, cerebral
pelvis, 121, 130–139, **144, 167**
acetabulum, **144**
ala ossis ilii, **144**
crista lateralis, **144**
facies auricularis, **144**
facies symphysialis, **144**
foramen obturatum, **144**
fossa acetabuli, **144**
incisura ischiadica major, **144**
incisura ischiadica minor, **144**
spina iliaca dorsalis cranialis, **144**
spina iliaca ventralis caudalis, **144**
spina iliaca ventralis cranialis, **144**
tuber ischiadicum, **144**
tuberositas iliaca, **144**
penis, **10, 11,** 137
body of (*corpus penis*), 137
corpora cavernosa, 137
sheath of (*tunica albuginea corporum cavernosum*), 137
glans (*glans penis*), 137
opening, urethral (*ostium urethrae externum*), 137
os penis, 137
prepuce (*praeputium*), 137
glands of (*gll. praeputiales*), 137
laminae of, external (*laminae externa*), 137
laminae of, internal (*laminae internal*), 137
root (*radix penis*), 137
surfaces
dorsal (*dorsum penis*), 137
ventral, urethral groove (*sulcus urethralis*), 137
pericardium
parietal portion (*lamina parietalis*), 89
visceral portion (*lamina visceralis*), 87, 88, 89, 92, 95
peritoneum, 122–124, 128, 129
bursa, omental (*bursa omentalis*), 123
caudomesocolic region, 128, 129
cavity (*cavum peritonei*), 122
craniomesocolic region, 122–124
foramen of
epiploic (*foramen epiploicum*), 123
ligaments of
coronary, left (*lig. coronarium sinistrum hepatis*), 123
falciform (*lig. falciforme hepatis*), 123
gastrolienic (*lig. gastrolineale*), 127
gastrophrenic (*lig. gastrophrenicum*), 124
hepatoduodenal (*lig. hepatoduodenale*), 123
hepatogastric (*lig. hepatogastricum*), 123
lienorenal (*lig. lienorenale*), 124
ligamentum teres (*lig. teres hepatis*), 123
triangular, left (*lig. triangularia sinistrum*), 123
triangular, right (*lig. triangularia dextrum*), 123
mesentery, 122
mesocolon, 122
mesovarium, 138
omentum
greater (*omentum majus*), 123
lesser (*omentum minus*), 123
parietal part (*peritoneum parietale*), 122
rectogenital pouch (*excavationes rectogenitales*), 122, 128
vesicogenital pouch (*excavationes vesicogenitales*), 122, 128, 129
visceral part (*peritoneum viscerale*), 122
pharynx, 66, **80**
arch, palatopharyngeal (*arcus palatopharyngeus*), 66
entrance, lower limit (*vallecula epiglottica*), 66
entrance, upper limit (*aditus pharyngis*), 66
fold, aryepiglottic (*plica aryepiglottica*), 66
palate, soft, caudal edge of (*velum palatinum*), 66
parts of
laryngeal (*pars laryngea*), 66
nasal (*pars nasalis*), 66
oral (*pars oralis*), 66
philtrum, 1, **8, 32**
pharynx, pars nasalis
see nasopharynx, pharynx
pharynx, pars oralis
see oropharynx, pharynx
pili
see hairs
planta
see hindfeet, soles
planum nasale, **32**

plates
of thyroid cartilage (*laminae thyreoideae*), 67
pleura
cervical portion (*pleura cervicalis* or *cupula pleurae*), 87
costal portion (*pleura costalis*), 87, **99**
diaphragmatic portion (*pleura diaphragmatica*), 87
folds of
vena cava (*plica venae cavae*), 88
intermediate sac, of (*cavum pleurae intermedium*), 87
left sac of (*cavum pleurae sinistrum*), 87
mediastinal portion (*pleura mediastinalis*), 87
parietal layer (*pleura parietalis*), 87
recesses of
recessus mediastini sive cavum pleurae intermedium, 88
costodiaphragmatic (*recessus costodiaphragmaticus*), 88
costomediastinal (*recessus costomediastinalis*), 88
right, sac of (*cavum pleurae dextrum*), 87
sinuses of, 87
visceral surface, investing lung (*pleura pulmonalis*), 87
pleura cervicalis
see pleura, cervical portion of
pleura costalis
see pleura, costal portion of
pleura diaphragmatica
see pleura, diaphragmatic portion of
pleura mediastinalis
see pleura, mediastinal portion of
pleura parietalis
see pleural, parietal surface
pleura pulmonalis
see pleura, visceral surface
plexus
brachial (*plexus brachialis*), 92, **99**
lumbar (*plexus lumbalis*), 128
ophthalmic (*plexus ophthalmicus*), 26
plexus brachialis
see plexus, brachial
plexus lumbalis
see plexus, lumbar
plexus ophthalmicus
see plexus, ophthalmic
plica aryepiglottica
see folds, aryepiglottic
plica duodenocolica
see ligaments, duodenocolic
plica ileocaecalis
see ligaments, ileocaecal
plica venae cavae
see pleura, folds
plica vocalis
see folds, vocal
plica vestibularis
see folds, vestibular
poles
cranial (*extremitates craniales*)
of kidney, 130, 131
caudal (*extremitates caudales*)
of epididymis, 135
of kidney, 131
pons, 22, **29, 58, 59, 61**
portal
hepatic (*porta hepatis*), 126
porta hepatis
see portal, hepatic
portal circulation, 134
colic
left vein (*v. colica sinistra*), 134
middle vein (*v. colica media*), 134
right vein (*v. colica dextra*), 134
gastroduodenal v. (*v. gastroduodenalis*), 134
iliocolic vein (*v. ileocolica*), 134
ilial veins (*vv. ilei*), 134
jejunal veins (*vv. jejunales*), 134
mesenteric
caudal vein (*v. mesenterica caudalis*), 134
cranial vein (*v. mesenterica cranialis*), 134
portal vein (*v. porta*), 134
rectal, cranial (*v. rectalis cranialis*), 134
splenic vein (*v. lienalis*), 134
pouch
rectogenital (*excavationes rectogenitalis*), 122
vesicogenital (*excavatio vesicogenitalis*), 128, 129
praeputium
see prepuce
pregnancy (see also reproduction)
duration
wild vs. laboratory-bred, 2

prepuce (*praeputium*)
of penis, 1, 137, **10, 11**
preputial opening (*ostium praeputiale*)
see opening, preputial
process
acromion
of scapula, 65
alveolar (*processus alveolaris*), **32, 33**
angular (*processus angularis*), **44**
articular
of vertebra (*processus articulares*), 65, 86, **103**, 121
of mandible (*processus condylaris*), 21
caudate
of liver (*processus caudatus*), 126
condylar (*processus condylaris*), **44**
coronoid (*processus coronoideus*), **44**
muscular (*processus muscularis*)
of arytenoid cartilage, 68
odontoid (*dens*)
of axis, 65
papillary
of liver (*processus papillaris*), 126
pterygoid (*processus pterygoideus*), **31**
spinous
of vertebra (*processus spinosus*), 65, **86, 103**, 121
transverse
of vertebra (*processus transversi*), 65, **103**, 121
vocal (*processus vocalis*)
of arytenoid cartilage, 68
xiphoid (*processus xiphoideus*)
of sternum, 86, 121
processus articulares
see process, articular
processus caudatus
see process, caudate
processus condylaris
see process, articular, of mandible
processus muscularis
see process, muscular
processus papillaris
see process, papillary
processus spinosus
see process, spinous
processus transversi
see process, transverse
processus vocalis
see process, vocal
processus xiphoideus
see process, xiphoid
prominence (*promontorium*)
sacral
of pelvis, 121
promontorium
see prominence
prostata
see gland, prostate
proventriculus
see forestomach
proximal duodenum, 125
pulmo
see lung
pulvini buccales
see pads, buccal
pulp, of teeth (*pulpa dentis*), **34, 35**
pylorus, 125, 126, 129, 134
pyramis, **60**
quadrate lobe (*lobus quadratus*)
see liver, lobes
radices dentes
see teeth, roots
radix incisivis
see root, incisor
radix linguae
see tongue, root
radix mesenterii
see root, mesentery
radix molaris
see root, molar
radix penis
see root, penis
radix pulmonis
see root, pulmonary
ramus coeliacus
see branch, coeliac
ramus gastricus visceralis
see branch, gastric
recessus cavi nasi, **33**
recessus costodiaphragmaticus
see pleura, recesses of
recessus costomediastinalis
see pleura, recesses of
recessus mediastini sive cavum pleurae intermedium
see pleura, recesses of
rectum, 131, **167**

regio abdominis lateralis sinister
see region, abdominal, lateral, left
regio hypochondriaca
see region, hypochondrium
regio inguinalis
see region, inguinal
regio pubica
see region, pubic
regio umbilicalis
see region, umbilical
regio xiphoidea
see region, xiphoid
region
abdominal, lateral, left (*regio abdominis lateralis sinister*), 130
caudomesocolic, 128
cervical, ventral, 65, 66
hypochondriac (*regio hypochondriaca*), 124
inguinal (*regio inguinalis*), 122
pubic (*regio pubica*), 132
renal, 122
umbilical (*regio umbilicalis*), 124, 129, 130
xiphoid (*regio xiphoidea*), 126
ren
see kidney
reproduction
see breeding, pregnancy, mating, 2
behavior, 2, **14**
breeding, laboratory, 2, **14**
estrus, 2
organs
female genital, 138, 139
male genital, 135–138
respiratory system, 93–96
extrapulmonary bronchi, 93, 94
intrapulmonary system, 94, 95
lungs and pulmonary topography, 95, 96
trachea, 93, 94
rete testes, 136
retractor bursae buccalis et retractor buccinator, 20
retroperitoneal viscera and relations, 131, 132
rhombencephalon, 23
ribs (*costae*), **99, 100, 141**
angle of (*angulus costae*), 86
asternal, see ribs, false
false (*costae spuriae*), 85
head of (*caput costae*), **100**
space, intercostal (*spatium intercostale*), 86
sternal, see ribs, true
true (*costae verae*), 85
muscles of
intercostal
external (*mm. intercostales externi*), 86
internal (*mm. intercostales interni*), 86
levatores costarum, 86
tuberculum costae, **100**
ridge
cricoid
of larynx, 67
dorsal median
of larynx, 67
rima oris
see cavity, oral
rings, of trachea
see trachea, cartilages of
root
incisor (*radix incisivi*), **49, 51**
mesentery (*radix mesenteri*), 135
molar (*radix molaris*), **34**
pulmonary (*radix pulmonis*), 95, 96
penis (*radix penis*), 137
rugae palatinae
see rugae, palatine
rugae, palatine (*rugae palatinae*), 20, **33, 45**
sac
conjunctival (*saccus conjunctivae*), 24
lacrimal (*saccus lacrimalis*), 25
sacculi
of large intestine, 130
saccus conjunctivae
see sac, conjunctival
saccus lacrimalis
see sac, lacrimal
sacrum (*os sacrum*), 121, **144**
salivary glands (*gll. oris*), 21, 22
see also glands, salivary
scapula (*scapula*), 65
acromion, **72**
angulus caudalis, **72**
angulus cranialis, **72**
facies articularis, **72**
fossa infraspinata, **72**
fossa supraspinata, **72**
margo caudalis, **72**
margo cranialis, **72**
margo dorsalis, **72**

scapula (*scapula*)—*continued*
processus coracoideus, **72**
processus suprahamatus, **72**
spina scapulae, **72**
scrolls, turbinal
see turbinals (*turbinala*), 17
scrotum, 135
sella turcica
of pituitary gland, 23
seminal fluid
of vesicular glands, 137
septum
interventricular
see heart, septum
nasal (*septum nasi*), 17, 19, **29, 42**
septum nasi
see septum, nasal
sex differentiation
external, 1, 2, **6, 11**
sinus
maxillary (*sinus maxillaris*), **33, 34, 38, 42, 43**
paranasal (*sinus paranasales*), 19
sinus maxillaris
see sinus, maxillary
sinus paranasales
see cavity, paranasal and sinus, paranasal
skeleton, **27**
abdominal and pelvic, 121
adult European hamster, **27**
cervical
see also vertebrae, cervical (*vertebrae cervicales*), 65
facial (*facies*), 17, **28, 29, 30**
skull, 17, **28, 29, 30, 31, 40, 49, 51, 61, 71**
thoracic, 85, 86
smell
vomeronasal organs (*organum vomeronasale*), 19
soles (*planta*)
of hindfeet, 1, **9**
space
intercostal (*spatium intercostale*), 86
spatium intercostale
see space, intercostal
sperm, 13
spermatids, **178, 179**
spinal column, **70**
spleen (*lien*), 127, **156, 157, 159, 161**
body, Malpighian, 159
ends
dorsal (*extremitas dorsalis*), 127
ventral (*extremitas ventralis*), 127
hilus (*hilus lienus*), 127
ligaments
gastrosplenic (*lig. gastrolienale*), 127, **159**
pulp
red (*pulpa lienis rubra*), 127
white (*pulpa lienis alba*), 127
surface
parietal (*facies parietalis*), 127
sternum (*sternum*)
angle of (*angulus sternae*), 85
body (*corpus sterni*), 85, **101, 105**
cartilages of
episternum, 85
cartilago manubrii, 85
cartilago xiphoidea, 85, **100**
manubrium (*manubrium sterni*), 85, **100**
process
xiphoid (*processus xiphoideus*), 85, 86, **100**
sternebrae, **98, 100, 101**
stomach (*gaster* or *ventriculus*), 124, 125, **147, 156, 157, 162, 165**
cardia (*pars cardiaca*), 125, **147**
curvature, of
greater (*curvatura ventriculi major*), 125, **156**
lesser (*curvatura ventriculi minor*), 125
forestomach (*proventriculus*), **112**, 124, 125, **147, 148, 149, 150, 159**
fundus (*fundus ventriculi*), 125, **147**
glands of
cardiac (*gll. cardiacae*), 125
pyloric (*gll. pyloricae*), 125
glandular stomach (*ventriculus glandularis*), 124, 125, **147, 148, 150**
labia, 125
ligaments of
gastrophrenic, 124
gastrosplenic, **159**
hepatogastric, 125
margo plicatus, 124, **147, 148, 149**
pylorus (*pars pylorica*), 125, **147**
regions of
abdominal, cranial (*regio abdominis cranialis*), 122, 124
hypochondrium, left (*regio hypochondri-*

stomach (*gaster* or *ventriculus*)—*continued*
aca sinistra), 124
sphincter (*m. sphincter pylori*), 125
sulcus (*sulcus ventriculi*), **147**
sublingual glands
see glands, sublingual
sulcus
coronary (*sulcus coronarius*), 89
sulcus coronarius
see sulcus, coronary
sulcus interventricularis
see groove, interventricular
sulcus medianus linguae
see tongue, sulcus, median
sulcus rhinalis lateralis (*fissura palaeo-neocorticalis*), **58, 60**
sulcus urethralis
see urethra, surface, ventral
sulcus venae cavae
see groove, vena cava
surface
diaphragmatic (*facies diaphragmatica*)
of liver, 126
of lung, 96
dorsal, penis (*dorsum penis*), 137
ear (*facies auriculares*), 121
lateral (*facies lateralis*)
of sacrum, 121
medial (*facies mediales*)
of lung, 96
parietal
of peritoneum, 121
of spleen, 127
of stomach, 125
pulmonary
left (*facies pulmonales sinistra*)
of heart, 89
right (*facies pulmonales dextra*)
of heart, 89
sternocostal (*facies sternocostalis*)
of heart, 89
visceral (*facies visceralis*)
of peritoneum, 122
symphysis
mandibular (*symphysis intermandibularis*), 21
pubic (*symphysis pubica*), 121
symphysis intermandibularis
see symphysis, mandibular
symphysis pubica
see symphysis, pubic
synchondrosis sphenooccipitalis, 23, **31**
taeniae
caecum, lack of, 130
tail, 1, 6
teats (*papillae mammae*), 1, 2, **10, 11**
teeth (*dentes*) see also dentition
alveolus of (*alveolus dentalis*), 21
canines (*dentes canini*), 21
crowns of (*corona dentis*), 21
incisors (*dentes incisivi*), 19, 21, **29, 30, 31, 32, 33, 44**
molars (*dentes molares*), 21, **30, 31, 34, 35, 44, 50, 51**
gums of (*gingivae*), 21
permanent (*dentes permanentes*), 21
premolar (*dentes premolares*), 21
pulp of (*pulpa dentis*), 34, 35
roots of (*radices dentes*), 21
incisor (*radix incisivi*), **49, 51**
molar (*radix molaris*), **34**
telencephalon, 23
tendon
central (*centrum tendineum*)
of diaphragm, 86
teres major muscle
see muscle, teres major
testes (*testes*)
in active periods, 178
in hibernation, 135, 136, **176, 179**
Leydig cells, 136, **176**
scrotum, 136
Sertoli cells, 136
sex differentiation, **10, 11**
sperm, 136
spermatocytes, 136
spermatogonia, 136
tubules, seminiferous (*tubuli seminiferi*), 136, **179**
tunica albuginea, 136
tunica vaginalis, 136
thorax, 85–96, **145**
cage, bony (*ossa cavi thoracis*), 85, **97, 98, 99, 140, 141**
cavity (*cavum thoracis*), 85, 87–93
diaphragm (*diaphragma*), 85
fat deposits in, **7**
ligament, sternopericardial (*lig. sternoperi-*

thorax—*continued*
cardiaca), 88
limits of
apex, cranial (*apertura cranialis*), 85
opening, caudal (*apertura thoracis caudalis*), 85
lungs (*pulmo*), 94–96
mediastinum, 88–93
dorsal, 92, 93
esophagus, 93
lymphatic tissue, 92, 93
ventral
great vessels, 90, 91
heart (*cor*), 89, 90
nerves, 92
thymus and lymphatic tissue, 91, 92
muscles, 86
intercostal
external (*mm. intercostales externi*), 86
internal (*mm. intercostales interni*), 86
levatores costarum, 86
pectoral
deep (*m. pectoralis profundis*), 86
caudal transverse (*pars transversus*), 86
cranial descending (*pars descendens*), 86
superficial (*m. pectoralis superficialis*), 86
pericardum, sac (*cavum pericardium*), 87, 88
pleura, 87, 88
cervical (*pleura cervicalis* or *cupula pleurae*), 87
costal (*pleura costalis*), 87
cupula pleurae, see pleura, cervical
diaphragmatic (*pleura diaphragmatica*), 87
mediastinal (*pleura mediastinalis*), 87
parietal (*pleura parietalis*), 87
visceral (*pleura visceralis*), 87
pleural sacs, 87
intermediate (*cavum pleurae intermedium*), 87
left (*cavum pleurae sinistrum*), 87
right (*cavum pleurae dextrum*), 87
pleural sinuses
costodiaphragmatic (*recessus costodiaphragmaticus*), 88
costomediastinal (*recessus costomediastinalis*), 88
respiration, 85
ribs, (*costae*), 85
angle of (*angulus costae*), 86
spinal column (*columna vertebralis*), 85
sternum, 85
xiphoid process of (*processus xiphoideus*), 85
thymus, 91
vertebrae (*vertebrae thoracicae*), 86
kyphosis of, 86
processes
articular (*processus articularis*), 86
spinous (*processus spinosus*), 86
thymus and related lymphatic tissue, 91, 92
see also gland, thymus
thyroid and parathyroid glands
see gland, thyroid and gland, parathyroid
thyroxin, 69
tissue, adipose, orbital (*corpus adiposum orbitae*), 24
tongue (*lingua*), 20, 21, **29, 45**
body of (*corpus linguae*), 21
frenulum (*frenulum linguae*), 20, 21, 22
median sulcus (*sulcus medianus linguae*), 21
papillae (*papillae linguales*), 21, **48**
root (*radix linguae*), 21, 22
sublingual carunculae (*carunculae sublinguales*), 21
sublingual gland (*gl. sublingualis*), 21
tip (*apex linguae*), 21
tonsils, 66
tori
see pads, forefeet, and hindfeet
toruli
see tongue, sublingual carunculae
trabeculae
of penis, 131
septomarginalis, of heart,
see heart, trabecula
trachea, **29,** 68, 69, **73, 74, 79, 82, 83,** 93, 94, **109, 111, 114, 118**
bifurcation (*bifurcatio tracheae*), **79, 80,** 93, **102**
cartilages of (*cartilagines tracheales*), 69, **75, 79, 80**
ligaments, annular (*ligg. annularia*), 69

trachea—*continued*
muscles (*mm. tracheales*), 69, **80**
nerves, 92
rings of, see trachea, cartilages
tractus olfactorius laterus, **60**
triceps brachii
see muscle, *triceps brachii*
truncus brachiocephalicus
see trunk, arterial, brachiocephalic and artery, brachiocephalic
truncus coeliacus
see trunk, lymphatic, coeliac
truncus intestinalis
see trunk, lymphatic, intestinal
truncus lumbalis
see trunk, lymphatic lumbar
truncus sympathicus
see trunk, nerves, sympathetic
truncus thoracicus
see trunk, lymphatic, thoracic
truncus sympathicus
see trunk, nerve, sympathetic
truncus vagosympathicus
see trunk, nerve, vagosympathetic
trunk
arterial
brachiocephalic (*truncus brachiocephalicus*), 66, 93, **109, 110, 111**
lymphatic
coeliac (*truncus coeliacus*), 128, 131
cranialmesocolic vascularization, 128
intestinal (*truncus intestinalis*), 134
lumbar (*truncus lumbalis*), 134
lymph nodes, 134
thoracic (*truncus thoracicus*), 92
nerve, sympathetic (*truncus sympathicus*), 92
cranial cervical ganglion (*ganglion cervicale*), 66
middle cervical ganglion (*ganglion cervicale medium*), 66
stellate ganglion (*ganglion stellatum*), 66
vagosympathetic (*truncus vagosympathicus*), 66
tuba auditiva
see Eustachian tube
tuba uterina
see oviducts
tuber ischiadicum
see tuberosity, ischial
tuber cinereum
of pituitary gland, 23, **61**
tuberculum olfactorium, **60**
tuberosity
ischial (*tuber ischiadicum*), 137
tubules
convoluted
of kidney (*tubuli renales contorti*), 132
efferent, of epididymis, 179
seminiferous (*tubuli seminiferi*), 136, **178, 179**
straight
of kidney (*tubuli renales recti*), 132
tubuli renales contorti
see tubules, convoluted
tubuli renales recti
see tubules, straight
tubuli seminiferi
see tubules, seminiferous
tunica adventitia, of ureter
see layer, fibrous
tunica adventitia, of vesicular glands
see layer, sheath, external areolar
tunica albuginea
see testes, tunica
tunica mucosa
see layers, mucous
tunica mucosa oris
see mucosa, oral
tunica muscularis
see layers, muscular
tunica vaginalis
see testis, tunica
umbilical glandular organ
see organ, umbilical glandular
umbilicus, **11**
unguis
see claws
ureter, 132
layers
fibrous (*tunica adventitia*), 132
mucous (*tunica mucosa*), 132
muscular (*tunica muscularis*), 132
location of, 132
renal pelvis, 132
urinary bladder (*vesica urinaria*), 132
urethra
external orifice of (*ostium urethrae externum*), 132

urethra—*continued*
female (*urethra feminina*), 132
male (*urethra masculina*), 132, 137
pelvic part (*pars pelvica*), 135
urethra feminina
see urethra, female
urethra masculina
see urethra, male
urethra pars pelvina
see urethra, pelvic part
urinary bladder (*vesica urinaria*), 132
ligaments
lateral (*lig. vesicae laterales*), 132
middle (*lig. vesicae medianum*), 132
muscles
m. pubovesicalis, 132
m. rectourethralis, 132
ureter, 132
vesicular glands (*gll. vesiculares*), 132, 136, 137
urinary organs (*organa uropoëtica*)
kidneys (*ren*), 131
urethra, 131, 132, 135, 137
ureters (*ureter*), 131
urinary bladder (*vesica urinaria*), 132
uterus, 138, 139, **186**
body (*corpus uteri*), 138
cervix, 139
external orifice (*ostium uteri externa*), 139
glands of, 139
horns (*cornua uteri*), 138
internal orifices (*ostia uteri internum*), 139
septum (*velum uteri*), 139
vagina, 2, 139
orifice (*ostium vaginae*), 139
vallecula epiglottica
see epiglottis
valva aortae
see valve, aortic
valva bicuspidalis
see valve, bicuspid
valva tricuspidalis
see valve, tricuspid
valva truncae pulmonis
see valve, pulmonary
valve
aortic, of heart (*valva aortae*), 90
bicuspid (*valva bicuspidalis*)
of heart, 90
ileocaecal (*papilla ilealis*)
of colon, 130
pulmonary (*valva truncae pulmonis*)
of heart, 90
semilunar (*valvulae semilunares*)
of heart, 90
tricuspid (*valva bicuspidalis*)
of heart, 90
valvulae semilunares
see valves, semilunar
vas deferens, 135, **174**
vein(s)
auricular, caudal (*v. auricularis caudalis*), 26, **52, 64**
auricular, rostral (*v. auricularis rostralis*), 26, **52, 64**
azygos (*vena azygos*), 91
brachiocephalic (*truncus brachiocephalicus*), 93
of brain, 26
central (*v. centralis*)
of liver, 127
cervical, superficial (*v. cervicalis superficialis*), **64**
colic
left (*v. colica sinistra*), 134
middle (*v. colica media*), 134
right (*v. colica dextra*), 134
of eye, 26
medial angle of (*v. angularis oculi*), 26, 52, **64**
facial (*v. facialis*), 25, **64**
facial, transverse (*v. transversa faciei*), 26, **52, 64**
gastroduodenal (*v. gastroduodenalis*), 134
of heart (*v. cordis magna*), **111**
hepatic (*v. hepaticae*), 127, 134, **161**
of portal circulation, 134
ileocolic (*v. ileocolica*), 134
of ileum (*v. ilei*), 134
iliac
common (*v. iliacae communis*), 133
external (*v. iliacae externae*), 133
internal (*v. iliacae internae*), 133
interlobular (*vv. interlobulares*)
of kidney, 131
of jejunum (*vv. jejunales*), 134
jugular
external (*v. jugularis externa*), 25, **52, 64,** 66, **76,** 90, 91
internal (*v. jugularis interna*), **76,** 91,

vein(s)—*continued*
161
lingual (*v. lingualis*), 26, **52, 64**
lingofacial (*v. linguofacialis*), 25, **52, 64**
lips
upper (*v. labialis maxillaris*), 26, **64**
lower (*v. labialis mandibularis*), 26, **64**
of manubrium, 91
masseteric (*v. masseterica*), 26, **52, 64**
maxillary (*v. maxillaris*), 25, **52, 64**
mesenteric, 134
nasal, dorsal (*v. lateralis nasi*), 26, **52, 64**
ophthalmic plexus (*plexus ophthalmicus*), 25, **52, 64**
of orbit, 26
ovarian (*vv. ovaricae*), 133
phrenic, cranial (*vv. phrenicae cranialis*), 128
portal (*v. porta*), 134, **161**
portal shunt—hepatic vein system, 134
pulmonary (*vv. pulmonales*), **76,** 91, 95, 96, **110, 160**
rectal, cranial (*v. rectalis craniales*), 134
renal (*v. renales*), 131, 133, 134
splenic (*v. lienalis*), 134
subclavian (*v. subclavia*), 66
suprarenal (*vv. suprarenales*), 133
temporal, superficial (*v. temporalis superficialis*), 26, **52, 69**
testicular (*v. testicularis*), 133
trachea, 91

velum palatinum
see edge, palate

velum uteri
see uterus, septum

vena cava
caudal (*vena cava caudalis*), **77,** 91, **119,** 131, 133, **161**
cranial (*vena cava cranialis*), 88, 91

v. angularis oculi
see vein, eye, angle

v. auricularis caudalis
see vein, auricular caudal

v. auricularis rostralis
see vein, auricular, rostral

v. azygos
see vein, azygos

vena cava caudalis
see vena cava, caudal

vena cava craniales
see vena cava, cranial

v. centralis
see vein, central

v. colica dextra
see vein, colic, right

v. colica media
see vein, colic, middle

v. colica sinistra
see vein, colic, left

v. cordis magna
see vein, of heart

v. facialis
see vein, facial

v. gastroduodenalis
see vein, gastroduodenal

vv. hepaticae
see veins, hepatic

vv. ilei
see veins, ileum

v. ileocolica
see vein, ileocolic

v. iliaca communis
see vein, iliac, common

vv. interlobulares
see veins, interlobular

vv. jejunales
see veins, jejunum

v. jugularis externa
see vein, jugular, external

v. jugularis interna
see vein, jugular, internal

v. labialis mandibularis
see vein, lip, lower

v. labialis maxillaris
see vein, lip, upper

v. lateralis nasi
see vein, nasal, dorsal part

v. lienalis
see vein, splenic

v. lingualis
see vein, lingual

v. linguofacialis
see vein, linguofacial

v. masseterica
see vein, masseteric

v. maxillaris
see vein, maxillary

vv. ovaricae
see veins, ovarian
vv. phrenicae craniales
see veins, phrenic, cranial
v. porta
see vein, portal
vv. pulmonales
see veins, pulmonary
v. rectalis cranialis
see vein, rectal, cranial
v. subclavia
see vein, subclavian
vv. suprarenales
see veins, suprarenal
v. temporalis superficialis
see vein, temporal, superficial
v. testicularis
see vein, testicular
v. transversa faciei
see vein, facial, transverse
venous drainage
of skull, 25, 26
venous plexus, ophthalmic, 26, **64**
(*plexus ophthalmicus*), 26, **64**
ventral mediastinum, 88–92
great vessels, 90, 91
heart, 89, 90
nerves, 92
thymus and lymphatic tissue, 91, 92
ventricle(s)
of brain
fourth (*ventriculus quartus*), 59
third (*ventriculus tertius*), 59, 62
of heart
left (*ventriculus sinister*), 89
right (*ventriculus dexter*), 89
of larynx
lateral (*ventriculus laryngis lateralis*), 68
median (*ventriculus laryngis medianus*), 68
ventriculus dexter
see ventricle, of heart, right
ventriculus sinister
see ventricle, of heart, left
ventriculus glandularis
see stomach, glandular
ventriculus laryngis lateralis
see ventricle, laryngeal, lateral
ventriculus laryngis medianus
see ventricle, laryngeal, median
ventriculus quartus
see ventricle, of brain
ventriculus tertius
see ventricle, of brain
venules, hepatic, **161**
vermis cerebelli
of brain, 23
vertebrae
caudal, **70,** 121, 131
cervical, **29,** 65, **70**
arcus caudalis, **72**
articular process (*processus articularis*), 65
atlas (*atlas*), 65, **72**
axis (*axis*), 65, **72**
body (*corpus*), 65
foramen alare, **72**
fovea articularis caudalis, **72**
fovea articularis cranialis, **72**
massa lateralis, **72**
odontoid process (*dens*), 65, **72**
spinous process (*processus spinosus*), 65
transverse foramen (*foramen transversarium*), 65
transverse process (*processus transversii*), 65, **72**
tuberculum dorsale, **72**
tuberculum ventrale, **72**
vetebral arch (*arcus vertebrae*), 65
lumbar (*vertebrae lumbales*), **70,** 121, 122, 130, **141**
centrum
surface, caudal articular, **142**
surface, cranial articular, **142**
process
accessory (*processus accessorius*), **142**
articular, caudal (*processus articularis caudalis*), **142**
articular, cranial (*processus articularis cranialis*), **142**
mamillary (*processus mamillaris*), **142**
spinous (*processus spinosus*), **142**
sacral (*vertebrae sacrales* or *sacrum*), **70,** 121, **131**
base (*basis ossis sacri*), **143**
canal of (*canalis sacralis*), **143**

vertebrae—*continued*
foramen (*foramina sacralia pelvina*), **143**
process
articular, caudal (*processus articularis caudalis*), **143**
articular, cranial (*processus articularis cranialis*), **143**
spinous (*processus spinosus*), **143**
surface, auricular (*facies auricularis*), **143**
thoracic (*vertebrae thoracicae*), **70**, 92, **99**, **112**, **141**
canal (*canalis vertebralis*), **103**
fovea costalis caudalis, **103**
fovea costalis cranialis, **103**
fovea costalis transversus, **103**
incisura vertebralis caudalis, **103**
incisura vertebralis cranialis, **103**
process
articular
caudal (*processus articularis caudalis*), **103**
cranial (*processus articularis cranialis*), **103**
spinous (*processus spinosus*), **103**
transverse (*processus transversus*), **103**
vertebrae caudales
see vertebrae, caudal
vertebrae cervicales
see vertebrae, cervical
vertebrae lumbales
see vertebrae, lumbar
vertebrae sacrales
see vertebrae, sacral
vertebrae, thoracicae
see vertebrae, thoracic
vesica fellea
see bladder, gall
vesica urinaria
see bladder, urinary
vestibule
buccal (*vestibulum buccale*), 19
labial (*vestibulum labiale*), 19
laryngeal (*vestibulum laryngis*), 68, **80**
lateral (*vestibulum laryngis lateralis*), **80**
nasal (*vestibulum nasi*), 19, 25
oral (*vestibulum oris*), 19
vestibulum buccale
see vestibule, buccal
vestibulum labiale
see vestibule, labial
vestibulum laryngis
see vestibule, laryngeal
vestibulum nasi
see vestibule, nasal
vestibulum oris
see vestibule, oral
vibrissae, 1, **8**
villi
of small intestine, 129
vomer
see bone, vomer
vomeronasal organs
see organs, vomeronasal
weight, 1, 6
zona fasciculata
see gland, adrenal
zona glomerulosa
see gland, adrenal
zona medullaris
see gland, adrenal
zona parenchymatosa
see cortex, ovary
zona reticularis
see gland, adrenal
zona vasculosa
see medulla, ovary
zygomatic gland, 23

☆ U.S. GOVERNMENT PRINTING OFFICE: 1978 O-215-023

NIH Library, Building 10
National Institutes of Health
Bethesda, Md. 20892

http://nihlibrary.nih.gov

10 Center Drive
Bethesda, MD 20892-1150
301-496-1080

NIH LIBRARY
3 1496 00527 9677

JUL 17 1996
SEP - 6
MAR 14 2001
NOV 1
MAY 11 2002

DHEW Publication No. (NIH) 76-1184
U.S. DEPARTMENT OF HEALTH, EDUCATION, AND WELFARE
Public Health Service
National Institutes of Health